



---

Publicly Accessible Penn Dissertations

---


1-1-2014

# Role of cytoskeletal remodeling in T cell receptor signaling and integrin activation at the immunological synapse

Alexander Babich

University of Pennsylvania, babich@mail.med.upenn.edu

Follow this and additional works at: <http://repository.upenn.edu/edissertations>

 Part of the [Allergy and Immunology Commons](#), [Cell Biology Commons](#), [Immunology and Infectious Disease Commons](#), [Medical Immunology Commons](#), and the [Molecular Biology Commons](#)

---

## Recommended Citation

Babich, Alexander, "Role of cytoskeletal remodeling in T cell receptor signaling and integrin activation at the immunological synapse" (2014). *Publicly Accessible Penn Dissertations*. 1197.  
<http://repository.upenn.edu/edissertations/1197>

This paper is posted at ScholarlyCommons. <http://repository.upenn.edu/edissertations/1197>  
For more information, please contact [libraryrepository@pobox.upenn.edu](mailto:libraryrepository@pobox.upenn.edu).

---

# Role of cytoskeletal remodeling in T cell receptor signaling and integrin activation at the immunological synapse

## **Abstract**

The efficiency of an immune response critically depends on the ability of T cells to respond to antigens. Upon encountering cognate antigenic peptides on the surface of antigen-presenting cells, T cells form a specialized interface, termed the immunological synapse (IS), which serves as the site of information transfer between the cells. This contact zone is characterized by the enrichment of signaling receptors, kinases and adaptor proteins, and is the site of extensive cytoskeletal remodeling. The versatile nature and spatio-temporal regulation of signaling cascades at the IS has long been recognized but the exact mechanisms that coordinate these processes remain poorly understood. In this work we have investigated the role of cytoskeletal remodeling in propagation of signaling events that lead to T cell activation. Using human T cell lines and primary T cells, we demonstrate that F-actin flow is largely driven by actin polymerization, rather than by myosin IIA contraction. While myosin IIA is able to exert forces on the cytoskeleton, it is dispensable for bulk network flow. Conversely, myosin IIA controls the extent of cell spreading and synaptic symmetry. We have also found that ongoing retrograde flow of F-actin sustains calcium mobilization at the level of release from endoplasmic reticulum stores. This defect is likely due to loss of PLCgamma1 activity at the IS, since the concentration of phosphorylated PLCgamma1 plummets upon F-actin immobilization. Furthermore, we have examined whether F-actin remodeling is required for integrin LFA-1 activation, which in turn strengthens conjugate formation and costimulation. Taking advantage of stimulatory planar lipid bilayers and cell-cell conjugates, we show that F-actin flow drives affinity maturation and spatial organization of LFA-1 at the IS. These observations are in line with a mechanotransduction model, in which F-actin-derived force induces integrin conformational change, thereby modulating binding affinity for ligand. The net inward movement of F-actin also recruits LFA-1 to the interface, thereby increasing its effective concentration. Taken together, these findings indicate that ongoing remodeling of actin cytoskeleton is required to sustain signaling and to choreograph spatio-temporal organization of receptors and their associated complexes at the IS during early phases of T cell activation.

## **Degree Type**

Dissertation

## **Degree Name**

Doctor of Philosophy (PhD)

## **Graduate Group**

Cell & Molecular Biology

## **First Advisor**

Janis K. Burkhardt

## **Keywords**

F-actin, Immunological Synapse, Integrin LFA-1, Mechanotransduction, T cell activation, T cell receptor

---

**Subject Categories**

Allergy and Immunology | Cell Biology | Immunology and Infectious Disease | Medical Immunology |  
Molecular Biology

**ROLE OF CYTOSKELETAL REMODELING IN T CELL  
RECEPTOR SIGNALING AND INTEGRIN ACTIVATION AT THE  
IMMUNOLOGICAL SYNAPSE**

**Alexander Babich**

A DISSERTATION

in

Cell and Molecular Biology

Presented to the Faculties of the University of Pennsylvania

in

Partial Fulfillment of the Requirements for the

Degree of Doctor of Philosophy

2014

Supervisor of Dissertation

---

Janis K. Burkhardt, PhD, Associate Professor of Pathology and Laboratory Medicine

Graduate Group Chairperson

---

Daniel S. Kessler, PhD, Associate Professor of Cell and Developmental Biology

Dissertation Committee

E. Michael Ostap, PhD, Professor of Physiology

Gary A. Koretzky, MD, PhD, Professor of Pathology and Laboratory Medicine

Michael C. Milone, MD, PhD, Assistant Professor of Pathology and Laboratory Medicine

Tobias Baumgart, PhD, Associate Professor of Physical and Biological Chemistry

ROLE OF CYTOSKELETAL REMODELING IN T CELL RECEPTOR SIGNALING  
AND INTEGRIN ACTIVATION AT THE IMMUNOLOGICAL SYNAPSE  
COPYRIGHT

2014

Alexander Babich

This work is licensed under the Creative Commons  
Attribution-NonCommercial-ShareAlike 3.0 License

To view a copy of this license, visit

<http://creativecommons.org/licenses/by-nc-sa/3.0/>

This work was supported in part by NIH T32-AR7442-25

## **DEDICATION**

I dedicate this thesis to my wife and friend, Oksana, who has selflessly sacrificed much of herself to enable me to spend many hours of research and contemplation. Her love and encouragement are instrumental in my success. Through many challenges on our journey I can confidently say that she is that kind of wife who is “far more precious than jewels.”

## ACKNOWLEDGEMENTS

I would like to extend my sincere gratitude my mentor Janis Burkhardt. Your enthusiasm has been a continual source of my inspiration. Your helping hand was always there for me when I was in need. Your keen eye has kept me in check to achieve my best in lab and in life. I have very much enjoyed the liberty to “play in the sandbox” and discover a few things along with you. It has been a true privilege to be your student.

I also wish to thank my committee members, Drs. Michael Ostap, Gary Koretzky, Michael Milone and Tobias Baumgart, who have offered invaluable advice and constructive conversations to help me navigate the course. Your guidance is much appreciated.

I am indebted to the members of the Burkhardt lab, both past and present; a more welcoming group of people I have seldom experienced. I wish to acknowledge Dr. Shuixing Li for his simple and kind heart that made for many pleasant conversations. I also would like to thank Fiona Clarke, who has been the most punctual and diligent lab technician I have ever met. I especially want to recognize William Comrie for his intellectual rigor in countless scientific discussions which have expanded my horizons and pushed the quality of my research to higher levels.

Words cannot express the appreciation I have for my family. My dear parents, Vladimir and Lyudmila, who have given me and my siblings the best life they could, and who continue to serve us with devoted hearts. My loving wife, Oksana, who had boldly ventured with me into the unknown, and whose unwavering resolve to help me succeed has been the cornerstone on which I rest. And my little children, whose innocent smiles make all my worries vanish into thin air.

Above all, I thank my Lord and Savior Jesus Christ for His gracious providence in all of my life. Whatever glory this thesis may deserve, let it be attributed to God alone.



## ABSTRACT

### ROLE OF CYTOSKELETAL REMODELING IN T CELL RECEPTOR SIGNALING AND INTEGRIN ACTIVATION AT THE IMMUNOLOGICAL SYNAPSE

Alexander Babich

Dr. Janis K. Burkhardt

The efficiency of an immune response critically depends on the ability of T cells to respond to antigens. Upon encountering cognate antigenic peptides on the surface of antigen-presenting cells, T cells form a specialized interface, termed the immunological synapse (IS), which serves as the site of information transfer between the cells. This contact zone is characterized by the enrichment of signaling receptors, kinases and adaptor proteins, and is the site of extensive cytoskeletal remodeling. The versatile nature and spatio-temporal regulation of signaling cascades at the IS has long been recognized but the exact mechanisms that coordinate these processes remain poorly understood. In this work we have investigated the role of cytoskeletal remodeling in propagation of signaling events that lead to T cell activation. Using human T cell lines and primary T cells, we demonstrate that F-actin flow is largely driven by actin polymerization, rather than by myosin IIA contraction. While myosin IIA is able to exert forces on the cytoskeleton, it is dispensable for bulk network flow. Conversely, myosin IIA controls the extent of cell spreading and synaptic symmetry. We have also found that ongoing retrograde flow of F-actin sustains calcium mobilization at the level of release from endoplasmic reticulum stores. This defect is likely due to loss of PLC $\gamma$ 1 activity at the IS,

since the concentration of phosphorylated PLC $\gamma$ 1 plummets upon F-actin immobilization. Furthermore, we have examined whether F-actin remodeling is required for integrin LFA-1 activation, which in turn strengthens conjugate formation and costimulation. Taking advantage of stimulatory planar lipid bilayers and cell-cell conjugates, we show that F-actin flow drives affinity maturation and spatial organization of LFA-1 at the IS. These observations are in line with a mechanotransduction model, in which F-actin-derived force induces integrin conformational change, thereby modulating binding affinity for ligand. The net inward movement of F-actin also recruits LFA-1 to the interface, thereby increasing its effective concentration. Taken together, these findings indicate that ongoing remodeling of actin cytoskeleton is required to sustain signaling and to choreograph spatio-temporal organization of receptors and their associated complexes at the IS during early phases of T cell activation.

# TABLE OF CONTENTS

<b>ACKNOWLEDGEMENTS .....</b>	<b>V</b>
<b>ABSTRACT.....</b>	<b>VI</b>
<b>LIST OF FIGURES .....</b>	<b>XI</b>
<b>LIST OF ABBREVIATIONS .....</b>	<b>XIII</b>
<b>LIST OF ELECTRONIC FILES .....</b>	<b>XV</b>
<b>CHAPTER 1: INTRODUCTION.....</b>	<b>1</b>
<b>I. Summary .....</b>	<b>1</b>
<b>II. Cytoskeletal control of calcium mobilization downstream of the TCR.....</b>	<b>2</b>
General features of Ca <sup>2+</sup> signaling.....	3
Actin function in TCR signaling.....	7
Calcium-regulatory roles of individual actin-regulatory proteins .....	11
Calcium mobilization via cytoskeletal control of organelle positioning .....	18
Regulation of cytoskeletal dynamics by Ca <sup>2+</sup> signaling .....	21
Higher level complexity: the transition from migration to activation .....	28
F-actin function in TCR-induced Ca <sup>2+</sup> mobilization .....	30
<b>III. Mechanotransduction and signaling of the integrin LFA-1 at the IS .....</b>	<b>31</b>
Integrins in T cell biology.....	31
Structural features of LFA-1 .....	31
TCR-dependent activation of LFA-1 .....	34
Costimulation through “outside-in” signaling .....	36
LFA-1 activation and organization at the IS.....	37
<b>CHAPTER 2: F-ACTIN POLYMERIZATION AND RETROGRADE FLOW DRIVE SUSTAINED PLCT1 SIGNALING DURING T CELL ACTIVATION.....</b>	<b>39</b>
<b>I. Summary .....</b>	<b>39</b>
<b>II. Introduction.....</b>	<b>40</b>
<b>III. Results .....</b>	<b>43</b>
Quantitative analysis of actomyosin distribution and dynamics at the IS .....	43

Myosin IIA exerts contractile force on the F-actin network, but is dispensable for F-actin flow .....	49
Inhibition of myosin IIA and F-actin turnover arrests cytoskeletal retrograde flow .....	55
Depletion of actin-capping protein IQGAP1 accelerates the F-actin network flow .....	58
F-actin retrograde flow governs SLP-76 MC centralization.....	60
SLP-76 MC dynamics do not correlate with F-actin behavior .....	62
Dynamic microtubule network translocates to the IS in close proximity to SLP-76 MCs.....	64
Dynamic F-actin network maintains microtubules close to the PM.....	67
F-actin dynamics are necessary for sustained Ca <sup>2+</sup> signaling .....	69
F-actin retrograde flow maintains activation of PLC $\gamma$ 1 in MCs.....	71
<b>IV. Discussion .....</b>	<b>74</b>
 <b>CHAPTER 3: ONGOING FLOW OF THE F-ACTIN NETWORK DRIVES AFFINITY MATURATION AND SPATIAL ORGANIZATION OF LFA-1 AT THE IMMUNOLOGICAL SYNAPSE .....</b>	<b>83</b>
<b>I. Summary .....</b>	<b>83</b>
<b>II. Introduction.....</b>	<b>84</b>
<b>III. Results .....</b>	<b>89</b>
Extended and extended open conformations of LFA-1 display distinct patterns of organization at the IS .....	89
High affinity, extended open conformation of LFA-1 is enriched in areas of low F-actin dynamics .....	94
Ligand mobility influences the magnitude of the retrograde flow rate of F-actin.....	98
LFA-1 engagement by immobilized ICAM-1 retains high affinity LFA-1 in the periphery of the IS.....	100
F-actin flow regulates the valency of LFA-1 at the IS.....	104
Myosin II contraction and F-actin flow regulate affinity maturation of LFA-1 at the IS .....	106
F-actin dynamics regulate the localization and distribution of extended open conformation LFA-1 .....	111
Co-ligation of $\beta$ 1 integrins slows the F-actin network and dampens LFA-1 activation.....	115
<b>IV. Discussion .....</b>	<b>118</b>
 <b>CHAPTER 4: DISCUSSION .....</b>	<b>128</b>
<b>Summary.....</b>	<b>128</b>

<b>The architecture of actomyosin and microtubule networks at the IS.....</b>	<b>129</b>
<b>The function (or lack thereof) of myosin IIA at the IS.....</b>	<b>132</b>
<b>What role do F-actin dynamics play in T cell signaling? .....</b>	<b>135</b>
<b>Mechanotransduction at the IS.....</b>	<b>139</b>
<b>What are the clutch molecules that couple signaling molecules to cytoskeletal flow? .....</b>	<b>149</b>
<b>Cross-talk between TCR and integrin signaling complexes .....</b>	<b>150</b>
<b>Actin-microtubule cross-talk in synaptic organization and dynamics .....</b>	<b>151</b>
<b>Concluding comments – the big picture of the IS .....</b>	<b>154</b>
<b>CHAPTER 5: MATERIALS AND METHODS .....</b>	<b>156</b>
Reagents and Antibodies.....	156
Plasmids and RNAi.....	157
Transfection of Jurkat and primary T cells .....	158
Lentiviral transduction of primary T cells .....	159
Production and purification of His-tagged ICAM-1 .....	160
Cell Culture and T cell-B cell conjugation .....	161
Western blotting.....	161
Preparation of supported planar lipid bilayers .....	162
Single-cell Ca <sup>2+</sup> assays.....	163
Fixed-cell fluorescence microscopy .....	164
Live-cell fluorescence microscopy .....	165
Image processing and quantitative analysis .....	166
Statistical evaluation .....	169
<b>APPENDIX A: PREPARATION OF MIXED-MOBILITY SURFACES.....</b>	<b>170</b>
Preparation of glass surfaces.....	170
Preparation of small unilamellar vesicles .....	172
Preparation of supported planar bilayers .....	173
Preparation of the PDMS stamps.....	174
Micro-contact printing .....	176
Preparation of mixed-mobility surfaces.....	177
<b>APPENDIX B: SUPPLEMENTAL MOVIE LEGENDS.....</b>	<b>181</b>
<b>REFERENCES.....</b>	<b>189</b>

## LIST OF FIGURES

<b>Figure 1.1.</b> F-actin remodeling and Ca <sup>2+</sup> mobilization downstream of TCR signaling.....	<b>4</b>
<b>Figure 1.2.</b> Morphological changes and organelle remodeling associated with T cell polarization in response to TCR triggering.....	<b>22</b>
<b>Figure 1.3.</b> Parallel control of cytoskeletal remodeling and calcium signaling via lipid metabolism.....	<b>27</b>
<b>Figure 1.4.</b> Integrin activation through conformational intermediates.....	<b>33</b>
<b>Figure 2.1.</b> Distribution and dynamics of the T cell actomyosin network.....	<b>45</b>
<b>Figure 2.2.</b> Measurement of F-actin dynamics at the IS.....	<b>48</b>
<b>Figure 2.3.</b> Potential mechanisms that can drive actomyosin retrograde flow in symmetrically spreading cells.....	<b>50</b>
<b>Figure 2.4.</b> F-actin stabilization leads to contraction of the actomyosin network.....	<b>51</b>
<b>Figure 2.5.</b> Myosin IIA is not required for F-actin flow but is necessary for long-term maintenance of the IS.....	<b>53</b>
<b>Figure 2.6.</b> Inhibition of myosin IIA and F-actin stabilization arrests retrograde flow....	<b>56</b>
<b>Figure 2.7.</b> Assessment of F-actin dynamics in response to Jas treatment of cells suppressed for myosin IIA.....	<b>57</b>
<b>Figure 2.8.</b> IQGAP1 knockdown in Jurkat T cells accelerates F-actin dynamics.....	<b>59</b>
<b>Figure 2.9.</b> F-actin governs MC dynamics but has different velocity distribution across the IS.....	<b>61</b>
<b>Figure 2.10.</b> Measurement of SLP-76 MC velocities at the IS.....	<b>63</b>
<b>Figure 2.11.</b> Dynamic microtubule network translocates to the IS proximally to SLP-76 MCs.....	<b>65</b>
<b>Figure 2.12.</b> Dynamic F-actin network presses microtubules against plasma membrane at the IS.....	<b>68</b>
<b>Figure 2.13.</b> Loss of F-actin dynamics abrogates sustained Ca <sup>2+</sup> signaling by perturbing Ca <sup>2+</sup> release from ER stores.....	<b>70</b>
<b>Figure 2.14.</b> F-actin immobilization selectively inhibits PLCγ1 phosphorylation.....	<b>72</b>
<b>Figure 2.15.</b> Assessment of SLP-76 phosphorylation in response to F-actin immobilization.....	<b>73</b>
<b>Figure 3.1.</b> LFA-1 conformational change at the IS is organized into a concentric array via a T-cell intrinsic mechanism.....	<b>90</b>
<b>Figure 3.2.</b> LFA-1 conformational change at the IS is organized into a concentric array regardless of CD3 accumulation in the cSMAC or function type.....	<b>93</b>
<b>Figure 3.3.</b> Active LFA-1 is excluded from the zones of high F-actin dynamics.....	<b>96</b>
<b>Figure 3.4.</b> Ligand mobility modulates F-actin retrograde flow rate.....	<b>99</b>
<b>Figure 3.5.</b> ICAM-1 binding retains the pool of activated LFA-1 in the IS periphery...	<b>101</b>
<b>Figure 3.6.</b> Actin dynamics persist in the under myosin II inhibition alone but cease completely after abrogating F-actin turnover.....	<b>105</b>
<b>Figure 3.7.</b> Centripetal flow of the actomyosin II network regulates valency and affinity of LFA-1.....	<b>107</b>
<b>Figure 3.8.</b> Data from individual conjugates from a single donor in Figure 3.7.....	<b>109</b>
<b>Figure 3.9.</b> F-actin dynamics regulates the localization and distribution of extended open conformation of LFA-1.....	<b>112</b>

<b>Figure 3.10.</b> Myosin IIA contraction and F-actin flow maintain high affinity conformation of LFA-1 and its localization at the IS.....	<b>114</b>
<b>Figure 3.11.</b> Co-ligation of VLA-4 slows F-actin flow and dampens LFA-1 activation.....	<b>117</b>
<b>Figure 3.12.</b> Comparative analysis of F-actin dynamics of T cells responding to various combinations of stimulatory and adhesive ligands.....	<b>119</b>
<b>Figure 3.13.</b> Model of avidity regulation of LFA-1 at the IS.....	<b>122</b>
<b>Figure 4.1.</b> Cytoskeleton-dependent organization of signaling machinery at the T cell immunological synapse.....	<b>131</b>
<b>Figure X.1.</b> Characterization of supported planar lipid bilayer mobility.....	<b>178</b>
<b>Figure X.2.</b> Various patterns that are appropriate for studies of T cell signaling dynamics at the IS.....	<b>179</b>
<b>Figure X.3.</b> Combination of supported lipid bilayers and patterned surfaces provides stimulatory substrates with mixed-mobility ligands.....	<b>180</b>

## LIST OF ABBREVIATIONS

<b>Abbreviation</b>	<b>Full Name</b>
APC	antigen-presenting cell
Arp2/3	actin related protein 2 and 3
Bleb	blebbistatin
Ca <sup>2+</sup>	calcium
CaMK	calmodulin kinase
CB	cell body
CRAC	Calcium Release-Activated Calcium
cSMAC	central supramolecular activating cluster
DAG	diacylglycerol
DMSO	dimethyl sulfoxide
dSMAC	distal supramolecular activating cluster
EGFP	enhanced green fluorescent protein
ER	endoplasmic reticulum
F-actin	filamentous actin
GADS	Grb2-related adaptor downstream of Shc
GAPDH	glyceraldehyde 3-phosphate dehydrogenase
GFP	green fluorescent protein
ICAM-1	intracellular adhesion molecule 1
IL-2	interleukin 2
IP <sub>3</sub>	inositol triphosphate
IS	immunological synapse
ITAM	inducible tyrosine activation motif
Jas	jasplakinolide
LAT	linker for activation of T cell
Lck	lymphocyte specific protein tyrosine kinase
LFA-1	lymphocyte function-associated antigen 1
LM	lamellum
LP	lamellipodium
MC	microcluster
MLCK	myosin light chain kinase
MTOC	microtubule organizing center
Myh9	myosin IIA heavy chain
Nck	non-catalytic region of tyrosine kinase
NFAT	nuclear factor of activated T cells
NPF	nucleation-promoting factor
PALM	Photo-activation localization microscopy



## LIST OF ABBREVIATIONS (CONT.)

<b>Abbreviation</b>	<b>Full Name</b>
PIP <sub>2</sub>	phosphatidylinositide 4,5-bisphosphate
PKC $\theta$	protein kinase C $\theta$
PLC $\gamma$ 1	phospholipase C-gamma 1
PM	plasma membrane
pMHC	peptide-loaded major histocompatibility complex
pSMAC	peripheral supramolecular activating cluster
RNAi	RNA interference
ROCK	Rho kinase
RIAM	Rap1-interacting adaptor molecule
RPMI	Roswell Park Memorial Institute
SD	standard deviation
SEE	staphylococcal enterotoxin E
SEM	standard error of mean
SERCA	sarco/endoplasmic reticulum Ca <sup>2+</sup> -ATPase
shRNA	short hairpin RNA
siRNA	small interfering RNA
SLP-76	SH2 domain-containing leukocyte protein of 76 kDa
SOCE	Store-Operated Calcium Entry
STEDM	Stimulated emission depletion microscopy
STIM1	stromal interacting molecule 1
Syk	spleen tyrosine kinase
TCR	T cell receptor
Tg	thapsigargin
TIRF	total internal reflection fluorescence
VCAM-1	vascular cell adhesion molecule 1
VLA-4	very late antigen 4
WASp	Wiskott Aldrich syndrome protein
WAVE	WASp family verprolin homologous protein
WIP	WASp interacting protein
WT	wild-type
Y-27	Y-27632
Zap70	zeta chain-associated protein of 70 kDa

## LIST OF ELECTRONIC FILES<sup>1</sup>

<b>File</b>	<b>Format</b>	<b>Size</b>	<b>Reference</b>
Movie 2A	QuickTime Movie	8.9 MB	p. 44
Movie 2B	QuickTime Movie	26.1 MB	p. 47
Movie 2C	QuickTime Movie	0.5 MB	p. 47
Movie 2D	QuickTime Movie	4.8 MB	p. 49
Movie 2E	QuickTime Movie	2.2 MB	p. 49
Movie 2F	QuickTime Movie	3.2 MB	p. 49
Movie 2G	QuickTime Movie	2.0 MB	p. 52
Movie 2H	QuickTime Movie	1.6 MB	p. 52
Movie 2I	QuickTime Movie	2.0 MB	p. 55
Movie 2J	QuickTime Movie	1.8 MB	p. 55
Movie 2K	QuickTime Movie	0.8 MB	p. 55
Movie 2L	QuickTime Movie	2.1 MB	p. 58
Movie 2M	QuickTime Movie	1.6 MB	p. 60
Movie 2N	QuickTime Movie	1.0 MB	p. 62
Movie 2O	QuickTime Movie	1.6 MB	p. 67
Movie 3A	QuickTime Movie	0.2 MB	p. 89
Movie 3B	QuickTime Movie	2.1 MB	p.94
Movie 3C	QuickTime Movie	1.2 MB	p. 98
Movie 3D	QuickTime Movie	0.4 MB	p. 103
Movie 3E	QuickTime Movie	0.4 MB	p. 103
Movie 3F	QuickTime Movie	1.6 MB	p. 104
Movie 3G	QuickTime Movie	0.9 MB	p. 116
Movie XA	QuickTime Movie	0.3 MB	p. 177

---

<sup>1</sup> For movie titles and legends refer to Appendix B

## CHAPTER 1: INTRODUCTION<sup>2</sup>

### I. Summary

Cytoskeletal remodeling plays an essential role in coordinating molecular rearrangements in T cells interacting with antigen-presenting cells (APCs). Recent advances in the field have demonstrated that the actomyosin and microtubule networks are intertwined in many ways and provide a dynamic milieu for signaling cascades downstream of T cell receptor (TCR) and integrins in the context of polarized stimulation (Bunnell et al., 2001; Lasserre et al., 2010). Two major tasks converge on the T cell cytoskeleton during early stages of immunological synapse (IS) formation. First, the engaged TCR and the associated molecules must be assembled into signaling complexes, known as microclusters (MCs), which further must be organized in space and time to fine-tune signaling (Yokosuka and Saito, 2010). Second, the cell–cell interface must develop shortly after stimulation and remain firmly adhered through integrins for a number of hours for optimal immune response (Beemiller and Krummel, 2010). TCR and integrins associate with the cytoskeleton and cooperatively initiate sustained calcium ( $\text{Ca}^{2+}$ ) mobilization and firm adhesion, which ultimately drive transcriptional reprogramming of T cell functions. This thesis addresses the organization and dynamics

---

<sup>2</sup> Parts of this chapter have been published as:

Babich A, Burkhardt JK  
Coordinate control of cytoskeletal remodeling and calcium mobilization during T-cell activation.  
Immunological Reviews. November 2013; Volume 256, pp. 80-94.

of T cell cytoskeleton and its role in maintenance of synaptic architecture and transduction of signaling downstream of surface receptors.

## **II. Cytoskeletal control of calcium mobilization downstream of the TCR**

Cytoskeletal responses and  $\text{Ca}^{2+}$  signaling in T cells are functionally integrated in complex ways, creating feedback loops that promote T cell activation and direct effector functions. Correlative evidence for a linkage between cytoskeletal remodeling and  $\text{Ca}^{2+}$  mobilization dates back to the earliest single-cell studies of T cell activation. In the 70's and 80's, it was noted that target cell lysis required extracellular  $\text{Ca}^{2+}$ , and entailed a programmed series of cell shape changes (reviewed in (Kupfer and Singer, 1989)). Soon thereafter, TCR engagement was shown to induce an increase in intracellular  $\text{Ca}^{2+}$  levels (Ostergaard and Clark, 1987). Moreover, two distinct sets of cytoskeletal rearrangements were observed: first, APC binding-induced polymerization of F-actin and recruitment of cytoskeletal proteins such as talin to the cell-cell contact site, and second, the T cell microtubule organizing center (MTOC), associated Golgi complex, and lytic granules reoriented to face the APC. Causal linkage between  $\text{Ca}^{2+}$  mobilization and cytoskeletal remodeling was established by subsequent pharmacological studies. Using pharmacological agents to disrupt actin turnover, several groups showed that TCR-induced polymerization of actin is needed for  $\text{Ca}^{2+}$  mobilization (Delon et al., 1998; Liu et al., 1995; Valitutti et al., 1995). Reciprocal experiments showed that  $\text{Ca}^{2+}$  responses are needed for cytoskeletal remodeling as well. Although initial studies showed that chelation of extracellular  $\text{Ca}^{2+}$  using EGTA does not inhibit TCR-induced polymerization of actin or recruitment of talin to the immunological synapse (IS) (Kupfer and Singer, 1989; Phatak and Packman, 1994), treatment of T cells with a combination of EGTA and

BAPTA-AM to deplete both extracellular and intracellular  $\text{Ca}^{2+}$  showed that  $\text{Ca}^{2+}$  elevation is required for actin-dependent spreading (Bunnell et al., 2001). In addition, elevated intracellular  $\text{Ca}^{2+}$  was also found to be required for MTOC reorientation toward the APC (Kupfer et al., 1985).

Recent years have seen considerable progress in our understanding of the mutual regulation of cytoskeletal remodeling and  $\text{Ca}^{2+}$  signaling during T cell activation. Many of the key proteins that control both actin dynamics and  $\text{Ca}^{2+}$  mobilization have been identified, making it possible to define specific points where the two pathways intersect. Moreover, as we begin to grasp how the cytoskeletal network functions as a unit, we are gaining new insights into the role of cell shape changes, mechanotransduction and other higher order signaling events (Quintana et al., 2009). In this section I will address the mechanisms underlying the complex interaction between cytoskeletal reorganization and  $\text{Ca}^{2+}$  signaling in T cells, and highlight important areas for future investigation.

### *General features of $\text{Ca}^{2+}$ signaling*

In order to understand the interplay between cytoskeletal dynamics and  $\text{Ca}^{2+}$  signaling, it is important to review the mechanisms by which TCR engagement leads to  $\text{Ca}^{2+}$  mobilization. Broadly speaking, T cell  $\text{Ca}^{2+}$  signals reflect two distinct but interrelated processes: triggering  $\text{Ca}^{2+}$  release from ER stores, and activation of calcium release-activated calcium (CRAC) channels (Orai1) in the plasma membrane (PM) (Figure 1.1). Release of  $\text{Ca}^{2+}$  from the ER by TCR engagement results from the formation of sub-micron scale signaling MCs, enriched in TCRs as well as kinases and adaptor proteins (Yokosuka and Saito, 2010). The early tyrosine phosphorylation events that take

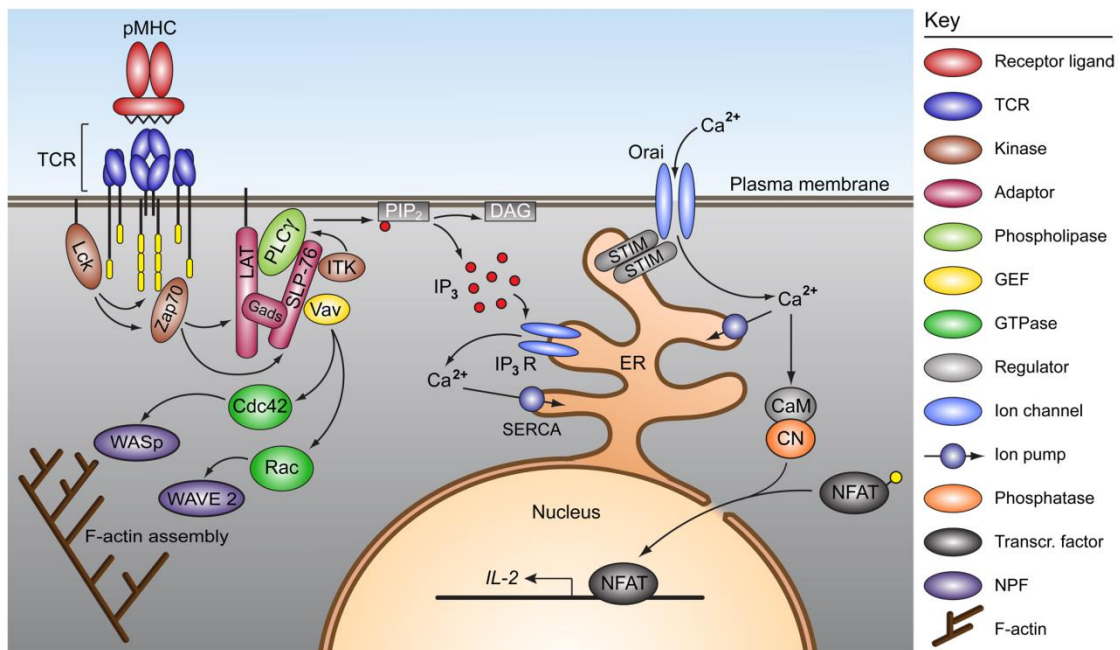


**Figure 1.1. F-actin remodeling and Ca<sup>2+</sup> mobilization downstream of TCR signaling**

TCR stimulation by peptide-loaded MHC triggers Lck-mediated phosphorylation of ITAM motifs in the intracellular regions of the TCR complex. Once phosphorylated, these sites recruit Zap70, which phosphorylates LAT and subsequently SLP-76. These adaptor proteins cooperatively serve as a docking site for PLCγ1. SLP-76 also recruits two other key regulators of downstream signaling – Vav1 and Itk. Vav1 promotes F-actin polymerization by activating Rac and Cdc42, which in turn activate WAVE and WASp. Itk phosphorylates and activates PLCγ1, which then cleaves PIP<sub>2</sub>, generating DAG and IP<sub>3</sub>. IP<sub>3</sub> binds to IP<sub>3</sub> receptors on the ER membrane, inducing the release of Ca<sup>2+</sup> from ER stores. This process is opposed by SERCA pumps, which refill ER stores on an ongoing basis. ER store depletion triggers oligomerization of STIM 1 in the ER membrane, which facilitates STIM 1 delivery to PM at specialized sites of ER-PM apposition. There, STIM 1 interacts with and activates the CRAC channel Orai1 to allow the influx of extracellular Ca<sup>2+</sup> into the cytosol. Sustained Ca<sup>2+</sup> mobilization activates the phosphatase calcineurin, which then activates NFAT and allows its shuttling into the nucleus to initiate T cell reprogramming at the level of gene expression.

place within MCs have been reviewed extensively elsewhere (Dustin and Groves, 2012; Fuller et al., 2003). Briefly, the Src kinase Lck phosphorylates inducible tyrosine activation motifs (ITAMs) on the  $\zeta$  chains of the receptor complex, which serve as docking sites for the Syk kinase  $\zeta$ -chain associated protein of 70 kDa (Zap70). Zap70 then phosphorylates Linker for Activation of T cells (LAT) and SH2 domain-containing Leukocyte Protein of 76 kDa (SLP-76). Cooperative assembly of these and other MC components culminates in the recruitment and subsequent activation of phospholipase C  $\gamma$ 1 (PLC $\gamma$ 1). Upon activation, PLC $\gamma$ 1 cleaves phosphatidylinositol 4,5-bisphosphate (PIP<sub>2</sub>) into diacylglycerol (DAG) and inositol 1,4,5-trisphosphate (IP<sub>3</sub>). DAG activates the Ras pathway, while IP<sub>3</sub> triggers its receptors in the ER membrane, leading to Ca<sup>2+</sup> release from ER stores. This early phase of Ca<sup>2+</sup> mobilization ensues within seconds of TCR engagement and requires engagement of only a few TCRs (Irvine et al., 2002). ER stores are emptied within seconds, and sarco/endoplasmic reticulum Ca<sup>2+</sup>-ATPase (SERCA) pumps in the ER membrane immediately begin to return cytoplasmic Ca<sup>2+</sup> to the ER. Thus, on its own, this phase represents a transient and relatively small rise in intracellular Ca<sup>2+</sup>, lasting on the order of minutes.

Release of Ca<sup>2+</sup> from the ER initiates events that lead to a more prolonged increase in cytoplasmic Ca<sup>2+</sup> levels. IP<sub>3</sub>-induced depletion of Ca<sup>2+</sup> from ER stores and the resulting decrease in ER Ca<sup>2+</sup> concentration leads to dissociation of Ca<sup>2+</sup> from N-terminal EF hand domains of Stromal Interaction Molecule 1 (STIM 1), a Ca<sup>2+</sup> sensor that spans the ER membrane (Luik et al., 2008). A subsequent conformational change in STIM 1 leads to its oligomerization and subsequent delivery to the sites of ER-PM apposition, probably through its interaction with microtubule +TIP tracking proteins (Barr et al., 2008;

Grigoriev et al., 2008). There, STIM 1 associates with trans-membrane Orai1 (CRAC) channels and activates them. This allows the entry of  $\text{Ca}^{2+}$  from the extracellular space via a process termed store-operated calcium entry (SOCE) (Reviewed in Hogan, 2010). The resulting sustained elevation of cytoplasmic  $\text{Ca}^{2+}$  is responsible for the activation of T cell transcriptional machinery. A key target of elevated intracellular  $\text{Ca}^{2+}$  is calcineurin, which dephosphorylates the transcription factor NF-AT, allowing its translocation to the nucleus (Rao, 2009). Once in the nucleus, NF-AT promotes transcription of interleukin-2 (IL-2) and other proteins that lead to T cell activation.

Importantly, the two phases of T cell  $\text{Ca}^{2+}$  mobilization are not temporally segregated. Thus, during the initial rise in  $\text{Ca}^{2+}$  due to release from the ER, extracellular  $\text{Ca}^{2+}$  enters via Orai1 and “floods” the cytoplasm. Without ongoing TCR signaling leading to continued  $\text{IP}_3$  receptor activation, SERCA pumps in the ER membrane quickly replenish ER stores, STIM 1 disengages Orai1 and relocates away from the PM, and Orai1 channels close (Alonso et al., 2012; Smyth et al., 2008). In support of the requirement for ongoing signaling leading to ER store release, disruption of  $\text{PLC}\gamma 1$  activation during the sustained phase of signaling correlates with a concomitant drop in intracellular  $\text{Ca}^{2+}$  levels (Babich et al., 2012). The finely-tuned nature of this 2-phase system becomes apparent when one considers the magnitude of changes in the intracellular  $\text{Ca}^{2+}$  concentration upon TCR triggering. In resting T cells, the cytosolic  $\text{Ca}^{2+}$  concentration is 50-100 nM, while  $\text{Ca}^{2+}$  concentrations in the ER and the extracellular space are 800-1000  $\mu\text{M}$  and 2 mM, respectively. Upon TCR engagement, cytoplasmic  $\text{Ca}^{2+}$  levels rise by an order of magnitude, to  $\sim 1 \mu\text{M}$ . Efficient  $\text{Ca}^{2+}$  influx is facilitated by the steep concentration gradient across the PM (Robert et al., 2012). As discussed below,



cytoskeletal dynamics have an important function in positioning signaling molecules and organelles to modulate this process.

### *Actin function in TCR signaling*

Actin dynamics are intimately involved in basic mechanical interactions and spatio-temporal control of signaling events leading to  $\text{Ca}^{2+}$  mobilization. Actin promotes early steps of TCR signaling at two levels: via effects on the TCR itself, and via the assembly of MCs, which transduce and amplify TCR signals. In both cases, the actin cytoskeleton is not just a static scaffold or a conventional link in a chain of signaling events. Instead, actin exerts forces and orchestrates molecular movements needed for  $\text{Ca}^{2+}$  signaling.

### Initial TCR triggering

In mature T cells, TCR engagement leads to association of phosphorylated ITAM motifs in the TCR complex with the actin cytoskeleton (Rozdzial et al., 1995; Rozdzial et al., 1998). Moreover, the CD3 complex reportedly binds to Nck, a component of a protein complex that drives actin polymerization (Kesti et al., 2007). Linkage of the TCR complex to actin filaments is almost certainly indirect, and the exact molecular mechanisms remain controversial. Nonetheless, there is broad consensus that centripetal TCR movement at the IS is orchestrated by F-actin dynamics (Barda-Saad et al., 2005; DeMond et al., 2008; Hartman et al., 2009). The dynamic association of the TCR complex with the actin cytoskeleton has two important implications for signaling events leading to  $\text{Ca}^{2+}$  mobilization. First, the actin-dependent movement of the TCR impacts the kinetics of TCR-pMHC interactions. Recent studies have shown that the outcome of TCR engagement is controlled by receptor-ligand kinetics, rather than by  $t_{1/2}$  or  $K_D$  of

antigen/TCR binding alone (Govern et al., 2010; Huang et al., 2010), and ligands with fast on-rates can bind and rebind the same TCR several times. Thus, depending on the particular TCR-pMHC interaction, continuous movement of the TCR at the IS may either facilitate serial receptor encounters with rare agonist pMHC or minimize opportunities for pMHC rebinding. Huppa *et al.* (2010), demonstrated that the synaptic TCR-pMHC dissociation rate is decreased significantly upon treatment of T cells with actin depolymerizing agents, consistent with idea that actin-driven TCR movement promotes its dissociation from pMHC complexes. Since ligand mobility is an important variable in this model, it is important to point out that these experiments were done using stimulatory planar lipid bilayers where pMHC mobility is essentially unrestricted. Mobility of pMHC complexes and costimulatory ligands on the APC membrane is modulated by the APC cytoskeleton (our unpublished data). Thus, it will be important to determine to what extent this affects TCR-pMHC binding kinetics.

Another mechanism through which the actin cytoskeleton may directly affect TCR signaling involves mechanotransduction. Recent studies indicate that the TCR is a mechano-receptor that depends on physical force in order to propagate signals across the membrane (Kim et al., 2012; Kim et al., 2009). Thus, interaction of the TCR complex with the actin cytoskeleton could promote TCR signaling through mechanical tension, produced by active cytoskeletal flow on the one side and ligand binding on the other (Feigelson et al., 2010; Hsu et al., 2012; Tseng et al., 2005). To account for the role of the F-actin flow in TCR signaling, Ma and Finkel have proposed the receptor deformation model (Ma and Finkel, 2010; Ma et al., 2008a). Building upon the earlier work showing that TCR stimulation is greatly increased by the immobilization of agonist pMHCs, they

showed that effective TCR triggering depends on T cell adhesion to the stimulatory surfaces and an intact T cell cytoskeleton; lack of either of those factors precludes efficient  $\text{Ca}^{2+}$  mobilization. Based on this evidence, the authors postulated that actin flow at the T cell IS provides a force that is counteracted by molecular interactions at the T cell–APC interface. The resulting tension on the TCR elicits structural changes within the complex to facilitate downstream signaling. The specific mechanism of TCR triggering is not fully understood (Dushek, 2011; van der Merwe and Dushek, 2011), and the contribution of force-induced TCR deformation is controversial. Arguably, ITAM motifs in the TCR complex are fully exposed without applied force, such that any role for mechanotransduction must lie downstream of the TCR itself. Nonetheless, the involvement of mechanical tension at some stage in TCR signaling is supported by evidence that depletion of F-actin abrogates signaling (Kaizuka et al., 2007; Varma et al., 2006). Moreover, investigation in Chapter 2 reveals that a static F-actin network is insufficient to sustain TCR-induced  $\text{Ca}^{2+}$  signaling, pointing to the necessity for ongoing actin polymerization and/or centripetal flow of the branched actin network at the IS. Additional support for mechanical tension in T cell signaling comes from studies of T cells interacting with TCR stimulatory beads, where  $\text{Ca}^{2+}$  mobilization is enhanced by moving the attached bead away from the IS (Li et al., 2010).

One important and understudied question in this arena is the role played by the stimulatory APC. Ligand mobility and surface stiffness have both been implicated in modulating TCR signaling (Hsu et al., 2012; Judokusumo et al., 2012; O'Connor et al., 2012; Tseng et al., 2005). Consequently, determinants of these variables on APCs could significantly impact both receptor-ligand binding kinetics and mechanotransduction

(Govern et al., 2010). Since there is evidence that actin is recruited to the dendritic cell side of the IS (Al-Alwan et al., 2003), it will be important to understand how the APC cytoskeleton impacts these aspects of T cell activation.

### TCR microcluster assembly and maintenance

In addition to its role in TCR triggering, the actin cytoskeleton regulates the assembly of TCR-proximal signaling complexes at the T cell–APC contact site. These complexes form MCs containing receptors, kinases and adaptor molecules, many of which contain actin-binding and actin-regulatory domains. Studies of the IS using surrogate planar stimulatory surfaces have greatly advanced our understanding of cytoskeletal function in the assembly and maintenance of signaling MCs. TCR MCs arise at initial sites of T cell contact with stimulatory surfaces, concomitant with the initiation of intracellular  $\text{Ca}^{2+}$  signaling (Bunnell et al., 2002; Campi et al., 2005; Yokosuka et al., 2005). Multiple actin-regulatory molecules are also recruited to these earliest sites of TCR signaling (Barda-Saad et al., 2005; Singleton et al., 2011). This process, in turn, induces T cell spreading and formation of a well-defined lamellipodial region rich in branched actin filaments, and an inner lamellar region that contains prominent actomyosin II bundles (Babich et al., 2012; Hammer and Burkhardt, 2013; Yi et al., 2012). The ongoing polymerization of actin at the cell periphery, coupled with the organizing forces generated by myosin II contraction, results in persistent actin centripetal flow at the IS. After maximal spreading has been achieved, nucleation of TCR MCs persists in the lamellar region and they are swept inward in parallel with the cytoskeletal flow (Bunnell et al., 2002; Nguyen et al., 2008; Varma et al., 2006; Yokosuka et al., 2005).

The actin cytoskeleton is essential for stabilizing newly-formed MCs. Key evidence from the Dustin lab showed that the integration of signaling molecules into the cytoskeletal scaffold greatly increases the lifetime of nascent MCs and promotes T cell stimulation (Varma et al., 2006). When fully spread T cells were treated with actin destabilizing agent, Latrunculin A, the newly-formed peripheral MCs dissolved, while the mature central MCs persisted for more than 10 minutes after drug treatment, presumably because they were stabilized by higher order interactions among MC components.

#### *Calcium-regulatory roles of individual actin-regulatory proteins*

In view of the multiple levels at which cytoskeletal remodeling affects  $\text{Ca}^{2+}$  signaling in T cells, one would expect that loss of important actin-regulatory molecules would affect  $\text{Ca}^{2+}$  mobilization; indeed, this is the case. As in other cell types, the formation of a branched F-actin network in T cells is driven by the seven subunit Arp2/3 complex, which directs the formation of new actin filaments on the sides of pre-existing filaments. The Arp2/3 complex is activated by one or more nucleation-promoting factors (NPFs), including WASp, WAVE2 and HS1 (Higgs and Pollard, 1999). WASp and WAVE2 function downstream of the Rho GTPases Cdc42 and Rac1, which are, in turn, activated by guanine exchange factors such as Vav1. Superimposed on this branched actin network is a higher level of organization; myosin II induces bundling and sliding of filaments within lamellar regions of the IS. Analysis of signaling defects in cells lacking individual actin-regulatory proteins is instructive in defining the mechanisms through which cytoskeletal dynamics influence  $\text{Ca}^{2+}$  mobilization.

### Nucleation-promoting factors

WASp: The first actin-regulatory molecule to be carefully studied in T cells was WASp, the protein defective in the immunodeficiency disorder Wiskott-Aldrich syndrome. T cells lacking WASp exhibit defects in actin dynamics, although the magnitude of such defects is variable (Badour et al., 2003; Cannon and Burkhardt, 2004; Nolz et al., 2006), possibly due to overlapping function of the closely related protein N-WASp (Cotta-de-Almeida et al., 2007), or even more distantly related proteins such as WAVE2. However, WASp deficient T cells show a significant reduction in  $\text{Ca}^{2+}$  influx, which is associated with defective nuclear translocation of NF-AT and diminished T cell activation (Cannon and Burkhardt, 2004; Dupre et al., 2002; Zhang et al., 1999). Conversely, mutations that perturb ubiquitin-dependent degradation of WASp lead to increased  $\text{Ca}^{2+}$  influx (Reicher et al., 2012). In a recent study, Calvez *et al.* (2011) explored the relationship between WASp function and T cell  $\text{Ca}^{2+}$  responses. They showed that T cells from WAS patients formed conjugates with APCs at normal frequency, but exhibited disorganized actin responses and asymmetric polarization of the MTOC, culminating in reduced proliferation in response to superantigen-pulsed APCs. In keeping with the idea that WASp manages signaling dynamics at the IS, the authors show that in comparison with control T cells, WAS T cells show diminished focusing of phospho-tyrosine at the IS. Interestingly,  $\text{Ca}^{2+}$  mobilization during the sustained phase of signaling was erratic and sometimes pulsatory, a phenotype that the authors attribute to the unstable nature of the T cell–APC interaction. While this study does not directly test whether the  $\text{Ca}^{2+}$  defects in these cells occur at the level of ER store release or CRAC channel function, the observed alterations in tyrosine phosphorylation patterns suggest

that early signaling steps leading to IP<sub>3</sub> generation and ER Ca<sup>2+</sup> release are perturbed. These findings showing that WASp is important for synapse organization are consistent with a model proposed by Dustin and coworkers in which WASp controls synapse symmetry by opposing the activity of PKCθ (Sims et al., 2007). According to this view, synapse stabilization and symmetry may be required for efficient integration of TCR (and possibly also costimulatory) signals.

HS1: Signaling defects similar to those observed in WASp-deficient T cells are seen in T cells lacking HS1, the hematopoietic homologue of cortactin. Like WASp, HS1 can activate Arp2/3 complex-dependent formation of branched actin filaments, and additionally, it can stabilize F-actin by binding to it. The Billadeau lab showed that T cells lacking HS1 exhibit defects in TCR engagement-induced actin dynamics as well as Ca<sup>2+</sup> mobilization and NF-AT dependent transcriptional activation (Gomez et al., 2006). In cell spreading assays, HS1-deficient T cells exhibit unstable lamellipodial protrusions, and in conjugates, they show loss of F-actin accumulation at the IS within a few minutes of cell-cell contact. Although the researchers did not observe destabilization of adhesion in HS1-deficient T cells, defects in integrin-dependent adhesion and signaling were noted in conjugates formed with HS1-deficient NK cells (Butler et al., 2008). Single cell analysis of T cell Ca<sup>2+</sup> responses showed that release from ER stores is inhibited. Moreover, defects in Ca<sup>2+</sup> signaling are rescued by treatment with the SERCA pump inhibitor thapsigargin, indicating that CRAC channel activity is intact (Carrizosa et al., 2009). Further analysis of TCR signaling pathways revealed that PLCγ1 phosphorylation and recruitment to the IS is intact, but that dynamics of PLCγ1 MCs and cytoskeletal association of phospho-PLCγ1 was perturbed (Carrizosa et al., 2009). Thus, in the case

of HS1, it seems clear that defects in stabilization of branched actin filaments lead to unstable lamellipodial protrusions and aberrant dynamics of TCR-induced signaling MCs, resulting in defective induction of ER store release. Numerous technical differences in the analysis of T cells deficient for HS1 and WASp make it hard to make direct comparisons. Nonetheless, there are many phenotypic similarities, consistent with the observation that these two proteins frequently work together to generate and stabilize branched actin networks.

WAVE 2: Like WASp and HS1, WAVE2 functions together with WAVE complex components to activate Arp2/3 complex-dependent formation of branched actin filaments in response to TCR engagement (Nolz et al., 2006). In comparison with T cells lacking WASp or HS1, T cells lacking WAVE2 show much more profound defects in TCR-induced actin polymerization and lamellipodial protrusion. WAVE2 deficiency abrogates spreading and T cell–APC conjugates show virtually no actin polymerization at the IS. Similar defects are observed in T cells lacking Abi proteins, components of the WAVE complex that are needed for translocation of WAVE to the IS (Zipfel et al., 2006). As with loss of other Arp2/3 complex activators, loss of WAVE2 leads to significant blunting of Ca<sup>2+</sup> mobilization. Surprisingly, however, WAVE2 deficient cells differ from cells lacking HS1 in that the initial release of Ca<sup>2+</sup> from ER stores is intact. Moreover, defects are not bypassed by thapsigargin treatment. This phenotype points clearly to a requirement for WAVE2 in signaling for extracellular Ca<sup>2+</sup> influx. Whether WAVE2 is needed for Orai1 function *per se*, or for facilitating STIM 1/Orai1 interactions remains to be determined. In other cell types, WAVE2 has been shown to be targeted to sites of lamellipodial protrusion via interactions with proteins that control microtubule dynamics



such as EB1 and stathmin (Takahashi, 2012), raising the possibility that WAVE2 promotes microtubule-dependent dynamics of STIM 1.

### Upstream regulators of actin nucleation

As one might expect, molecules that regulate activation of WASp, WAVE2 and HS1 downstream of the TCR are required for both actin responses and  $\text{Ca}^{2+}$  mobilization. For example, Rac GTPases, which activate WAVE2, are needed for both processes (Arrieumerlou et al., 2000; Yu et al., 2001). Often, however the relevant signaling proteins are large, modular molecules with several interdependent functions. Thus, it can be difficult to distinguish the extent to which they affect  $\text{Ca}^{2+}$  signaling by regulating actin dynamics. Several recent reviews address T cell signaling pathways leading to actin polymerization in detail (Burkhardt et al., 2008; Fooksman et al., 2010; Gomez and Billadeau, 2008). Here, I will discuss key molecules that illustrate the complexities associated with upstream regulation of actin and  $\text{Ca}^{2+}$  responses.

Vav1: A good example of this type of functional complexity is Vav1. Upon TCR engagement, Vav1 is recruited to the IS and behaves as a guanine exchange factor (GEF) for the Rho family GTPases Rac1 and Cdc42 (Dumont et al., 2009), which activate WAVE2 and WASp, respectively. Vav1 function is essential for actin polymerization at the IS (Bustelo, 2001; Turner and Billadeau, 2002; Tybulewicz et al., 2003). Other Vav family members are ubiquitously expressed and participate redundantly in the activation of small GTPases (Cao et al., 2002; Zakaria et al., 2004). T cells lacking Vav1 show profound defects in  $\text{Ca}^{2+}$  mobilization. Interestingly, however, Vav1's role in regulating actin and  $\text{Ca}^{2+}$  responses may be distinct. In particular, the GEF activity of Vav1 seems to be dispensable for  $\text{Ca}^{2+}$  mobilization, since T cells from knock-in mice bearing a Vav1

mutant lacking GEF activity display normal  $\text{Ca}^{2+}$  and proliferative responses. Furthermore, Vav2 and Vav3 cannot mediate  $\text{Ca}^{2+}$  elevation in stimulated T cells, indicating that the isoforms are not completely redundant. In a recent study, Li *et al.* (2013) isolated a 20 amino acid region in the N-terminus of Vav1 that is indispensable for  $\text{Ca}^{2+}$  mobilization independently of GEF activity. The authors argue that this sequence within the calponin homology domain is essential for calmodulin binding and recruitment to the sites of active signaling (Li *et al.*, 2013; Zhou *et al.*, 2007), highlighting the scaffolding function of Vav1 in TCR-induced  $\text{Ca}^{2+}$  mobilization.

**Itk:** A second example of multidomain complexity is seen in the Tec family kinase Itk. Like Vav1, Itk is a component of the TCR signalosome. Itk phosphorylates PLC $\gamma$ 1, and so plays a critical role in signaling  $\text{Ca}^{2+}$  release from ER stores. Through its SH2 domain, Itk interacts with HS1 and recruits it to the IS (Carrizosa *et al.*, 2009), and T cells deficient for Itk show defective actin responses similar to those of HS1-deficient T cells (Dombroski *et al.*, 2005; Grasis *et al.*, 2003; Labno *et al.*, 2003). Via HS1, Itk also promotes Vav1 recruitment to the IS, so that Itk-deficient T cells also have defects in TCR engagement-induced activation of Cdc42 and WASp (Labno *et al.*, 2003). Interestingly, it appears that the domains of Itk responsible for regulating actin and  $\text{Ca}^{2+}$  responses are largely distinct. PLC $\gamma$ 1 activation requires kinase activity, while actin regulation requires the SH2 domain, and is unaffected by mutations that abrogate kinase activity (Dombroski *et al.*, 2005). Even so, this separation may not be complete. Binding of SLP-76 to the SH2 domain of Itk has been shown to activate Itk kinase activity (Bogin *et al.*, 2007), and the same may be true for interactions with HS1. Thus, there could be a

direct linkage between  $\text{Ca}^{2+}$  signaling and actin-regulatory pathways, even though actual actin remodeling is not involved.

In addition to the complexities introduced by multi-domain signaling molecules, higher order molecular organization intertwines actin polymerization and  $\text{Ca}^{2+}$  signaling. Signalosome components are held together by multiple low affinity molecular interactions, such that loss of any one component disrupts interactions among the others and perturbs T cell signaling (Barda-Saad et al., 2010; Hartgroves et al., 2003; Houtman et al., 2006). As part of this process, actin scaffolds generated by these signaling molecules stabilize newly formed signaling complexes (Campi et al., 2005), thereby generating a positive feedback loop to facilitate T cell activation. As discussed further below, there is evidence that this process requires ongoing actin polymerization, rather than a static actin scaffold (Babich et al., 2012). Interestingly, PLC $\gamma$ 1 activation appears to be an important control point for this higher order cytoskeletal control of  $\text{Ca}^{2+}$  signaling (Babich et al., 2012; Carrizosa et al., 2009).

#### Myosin IIA function in the T cell $\text{Ca}^{2+}$ response

Another actin interacting protein that has gained recent interest in the field is myosin IIA. This motor protein is the sole representative of non-muscle myosin II family in mouse primary T cells (Jacobelli et al., 2004). Jurkat T cells of human origin also express myosin IIB (Jbireal et al., 2010). The results of multiple studies are conflicting as to the exact role that myosin IIA plays at the IS both in terms of actin dynamics and  $\text{Ca}^{2+}$  signaling (Hammer and Burkhardt, 2013). Initial work by Ilani *et al.* (2009) concluded that myosin IIA is indispensable for centripetal movement of TCR microclusters at the IS (presumably driven by the actomyosin retrograde flow), as well as for both initial and

sustained  $\text{Ca}^{2+}$  signaling. However, subsequent detailed studies yielded disparate results. In studies of murine TCR transgenic T cells responding to stimulatory planar bilayers, Yu *et al.* (2012) found that inhibition of myosin light chain kinase with ML-7 resulted in a profound decrease in  $\text{Ca}^{2+}$  mobilization, while Kumari *et al.* (2012) observed only a modest dampening of the  $\text{Ca}^{2+}$  response upon RNAi-mediated suppression of myosin IIA. Recent report from the Krummel lab confirms their original conclusion that myosin IIA is dispensable for IS formation and F-actin flow (Beemiller et al., 2012). However, the researchers did not provide any experiments testing the role of myosin IIA in  $\text{Ca}^{2+}$  mobilization. Our investigation in Chapter 2 deals in depth with the role of myosin IIA in signaling and dynamics at the IS.

#### *Calcium mobilization via cytoskeletal control of organelle positioning*

In addition to promoting the immediate signaling events that take place downstream of TCR, the cytoskeleton directs the higher order organization of cellular organelles; this also contributes to prolong  $\text{Ca}^{2+}$  signaling. Organelles known to modulate  $\text{Ca}^{2+}$  signaling in a cytoskeleton-dependent fashion include the ER, mitochondria, and the PM.

#### Remodeling of the endoplasmic reticulum

The ER is distributed throughout the cytoplasm via its interactions with the cytoskeleton. While comparatively little is known about ER remodeling in T cells, analysis in other cell types has shown that ER organization is determined by the balance between movement toward the cell periphery driven by microtubule motors and attachment to growing microtubule tips, and movement toward the cell body driven by actomyosin (Terasaki et al., 1986; Waterman-Storer et al., 1998). The net result of these

processes is the formation of specialized sites where the ER membrane comes in close proximity to the PM, and it is at these sites where the ER protein STIM 1 engages Orai1 in the PM, promoting  $\text{Ca}^{2+}$  influx (Shen et al., 2011). STIM 1 associates with the MT tip tracking protein EB1, which directs the accumulation of Stim1 to sites where the ER interacts with microtubule plus ends. Indeed, Grigoriev *et al.* (2008) investigated the role of Stim1 in ER remodeling in HeLa cells and MRC5 fibroblasts, and found that the interaction between Stim1 and EB3 (and to lesser extent EB1) promotes ER tubule extension. Upon depletion of ER  $\text{Ca}^{2+}$  stores, Stim1 oligomerizes and moves within the plane of the ER, triggering the formation of Stim1-ORAI1 clusters at ER-PM junctions. Consistent with the notion that the microtubule cytoskeleton positions the ER to promote Stim1-Orai1 interactions, depolymerization of microtubules with nocodazole inhibits SOCE (Smyth et al., 2007).

#### Recruitment of mitochondria to the immunological synapse

Mitochondria are delivered to the IS along microtubules by kinesin-1 (Pilling et al., 2006). Besides their canonical role as “cellular powerhouses”, mitochondria are well-adapted for  $\text{Ca}^{2+}$  buffering in their immediate vicinity. This turns out to be important for the function of the Orai1 channel, which becomes auto-inhibited if the local concentration of  $\text{Ca}^{2+}$  reaches high levels (Hoth et al., 1997). Mitochondria at the IS buffer  $\text{Ca}^{2+}$ , preventing its accumulation at the channel mouth, thereby ensuring that the CRAC channels remain active. Mitochondria then release  $\text{Ca}^{2+}$  away from the IS so that it can propagate the signaling cascade (Quintana et al., 2009). In this way, mitochondria set up a narrow gradient of  $\text{Ca}^{2+}$  ions near the sites of TCR signaling (Schwindling et al., 2010).

Polarization of mitochondria to the IS is microtubule-dependent. Contento *et al.* (2010) reported that MTOC and mitochondrial polarization to the IS occurs via outside-in LFA-1 signaling, providing a potential costimulatory mechanism. However, microtubule tracks by themselves are not sufficient for the delivery of mitochondria to the IS. Mitochondria are large organelles that are fused into intricate networks, which impedes their navigation through intracellular space. Thus, regulated remodeling of mitochondria by fusion and fission proteins facilitates their delivery to the IS and promotes their interaction with CRAC channels, as well as delivery of ATP to the TCR signaling machinery.

TCR stimulation triggers activation of dynamin-related protein 1 (Drp1), a GTPase essential for mitochondrial fission (Smirnova *et al.*, 2001). Depletion of Drp1 in T cells interacting with APCs leads to defects in mitochondrial polarization and TCR dynamics (Baixauli *et al.*, 2011). Once at the IS, mitochondrial fragments are fused into large structures by mitofusin, and become enriched at the pSMAC region (Figure 1.2). This localization is most likely regulated by the interplay between microtubule- and actin-dependent motors; cytoplasmic dynein binding to mitochondria would drive centripetal movement, as would pushing by actin retrograde flow. Centripetal movement of mitochondria at the IS may be opposed by kinesin-1 and myosin V, which have been shown to bind to mitochondria and direct their migration toward the cell periphery in other cell types (Pathak *et al.*, 2010; Saxton and Hollenbeck, 2012). Interestingly, kinesin-1 binding to the mitochondrial surface is regulated by  $\text{Ca}^{2+}$  (Wang and Schwarz, 2009). This provides a potential feedback mechanism that could couple mitochondrial to CRAC activity at the IS.

### Plasma membrane flattening

Because the  $\text{Ca}^{2+}$  buffering efficiency of mitochondria is limited to short distances, it is essential that these organelles be juxtaposed against the IS within 200 nm of the PM (Quintana et al., 2009). Therefore, flattening of the T cell PM at the IS is important to facilitate signaling. The Hoth lab investigated the importance of cell morphology during T cell activation (Quintana et al., 2009). They discovered that  $\text{Ca}^{2+}$  signaling was augmented in cells that underwent actin-dependent PM flattening upon TCR signaling and that these changes promoted mitochondrial delivery to the peripheral contact zone (Figure 1.2). Furthermore, they demonstrated that pre-incubation of T cells with non-stimulatory adhesive beads (a process that deforms the PM) greatly increased their ability to respond to soluble TCR ligands.

### *Regulation of cytoskeletal dynamics by $\text{Ca}^{2+}$ signaling*

Although most of the available literature focuses on cytoskeletal control of  $\text{Ca}^{2+}$  mobilization, it is clear that  $\text{Ca}^{2+}$  signaling also impacts remodeling of both actin filaments and microtubules. Perhaps more importantly, cytoskeletal dynamics and  $\text{Ca}^{2+}$  signaling are inextricably linked at the level of inositol metabolism (Figure 1.3).

### $\text{Ca}^{2+}$ control of the actin cytoskeleton

With respect to the actin cytoskeleton, Bunnell *et al.* (2001) showed that chelation of extracellular and intracellular  $\text{Ca}^{2+}$  blocked actin-dependent T cell spreading on TCR-stimulatory surfaces. The defect was profound and mirrored that of blocking Src kinase activity. This observation revealed the necessity for elevated intracellular  $\text{Ca}^{2+}$  early in the sequence of events leading to actin polymerization and cell spreading. Although

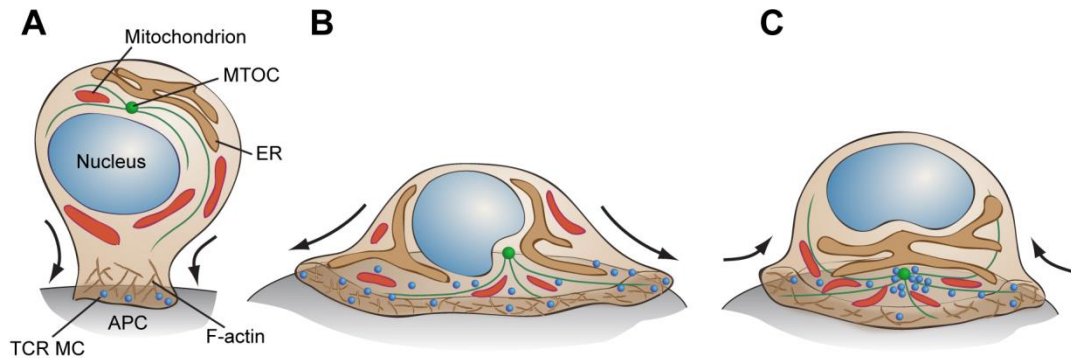


**Figure 1.2. Morphological changes and organelle remodeling associated with T cell polarization in response to TCR triggering**

(A) Upon encountering an APC bearing cognate pMHC, a T cell undergoes polarization towards the site of antigen presentation. Actin polymerization at sites of TCR engagement stabilizes newly-formed signaling MCs, and lamellipodial F-actin polymerization induces T cell spreading on the APC surface. (B) TCR MCs form in the actin-rich periphery of the IS and are continuously delivered to the central region in parallel with actin retrograde flow, a process that involves actin polymerization at the cell periphery coupled with contraction of the actomyosin network. For at least some MC components, microtubule-dependent motor activity also contributes to centripetal movement. Concomitant with T cell spreading, the MTOC is recruited to the cell-cell contact zone, which establishes tracks for retrograde traffic of signaling molecules to the cSMAC region, and anterograde movement of the ER and mitochondria to the IS. Mitochondria undergo fission and fusion to enhance their trafficking to the sites of active TCR signaling. (C) Once the machinery is set in place, T cells undergo partial actomyosin-dependent contraction to focus receptors and develop a mature IS.



the mechanisms involved have not been elucidated in detail, many actin-regulatory proteins are  $\text{Ca}^{2+}$ -sensitive. These include proteins such as myosin II, L-plastin and gelsolin that are regulated directly by  $\text{Ca}^{2+}$ , as well as proteins such as talin, ezrin and WASp that are sensitive to cleavage by the  $\text{Ca}^{2+}$ -dependent protease calpain.

One proposed mechanism by which  $\text{Ca}^{2+}$  signaling may modulate T cell cytoskeletal function involves cleavage of key actin regulatory proteins by the  $\text{Ca}^{2+}$ -activated proteases calpain 1 and 2. Such a mechanism has been proposed to explain seemingly unique functions of ezrin, which is calpain sensitive, vs. the closely homologous protein moesin, which lacks a calpain cleavage site (Ilani et al., 2007; Shcherbina et al., 1999). Similarly, calpain has been implicated in degradation of WASp under conditions where it is not assembled with WIP (de la Fuente et al., 2007). Finally, calpain has been proposed to regulate LFA-1 activation and consequent adhesion and migration via cleavage of talin or other proteins such as  $\alpha$ -actinin and filamin A (Bleijis et al., 2001; Cairo et al., 2006; Stewart et al., 1998). However, while these proteins are calpain substrates, recent work has cast doubt about the physiological significance of these cleavage events for T cell function. In the case of ezrin, our lab recently generated mice with conditional deletion of ezrin in mature T cells, in hopes of uncovering ezrin-specific aspects of T cell function. Shaffer and colleagues found minimal ezrin-specific defects in these cells; instead, our results pointed to overlapping, dose-dependent function of ezrin and moesin in T cell activation, adhesion and migration (Chen et al., 2013; Shaffer et al., 2009). With respect to WASp,  $\text{Ca}^{2+}$  influx downstream of TCR stimulation leads to calpain-dependent cleavage of WASp followed by proteasomal degradation, and treatment with the calpain inhibitor calpeptin reportedly prolonged high F-actin content post TCR

stimulation (de la Fuente et al., 2007; Watanabe et al., 2013). However only a minor fraction of WASp is cleaved in WT cells, and significant cleavage was shown only in activated T cells from patients with destabilizing WASp mutations (de la Fuente et al., 2007; Watanabe et al., 2013). Lastly, the Huttenlocher lab looked closely at calpain-dependent activation of LFA-1 in T cells. Unlike previous studies that relied on pharmacological inhibition of calpain, this group generated mice with deletion of calpain 4 in mature T cells (Wernimont et al., 2010). Though T cells from these mice expressed very low levels of both calpain 1 and 2 (both of which rely on assembly with calpain 4 for stabilization) and exhibited diminished talin proteolysis, the T cells showed normal LFA-1-dependent adhesion and migration. Binding to APCs, recruitment of F-actin to the IS, and proliferation were also unperturbed. This study provides strong evidence that calpain-dependent proteolysis is not a major mechanism by which  $\text{Ca}^{2+}$  levels affect actin remodeling in T cells.

While the role of calpain is in question, other cytoskeletal regulatory proteins are clearly  $\text{Ca}^{2+}$ -dependent. One of the best examples is the actin bundling protein L-plastin (reviewed in (Morley, 2013)). Although multiple plastin isoforms are expressed throughout the body, L-plastin is the sole isoform expressed in T cells (Heng et al., 2008) and seems to be the only one that is  $\text{Ca}^{2+}$ -dependent (Namba et al., 1992). All plastin isoforms contain two N-terminal  $\text{Ca}^{2+}$ -binding sites and two C-terminal actin-binding sites, which enable plastins to bundle actin filaments. Actin-bundling activity is thought to be negatively regulated by  $\text{Ca}^{2+}$  (Namba et al., 1992). Thus, in low  $\text{Ca}^{2+}$  concentrations (~ 100 nM), L-plastin is able to bundle actin, while  $\text{Ca}^{2+}$  concentrations in the micromolar range perturb its bundling activity. Given the  $\text{Ca}^{2+}$  concentrations associated

with T cell activation, it seems that L-plastin would be active prior to TCR signaling, when intracellular  $\text{Ca}^{2+}$  levels are low, and would be inactivated upon  $\text{Ca}^{2+}$  elevation during early TCR signaling. This hypothesis is in line with evidence that early TCR-dependent phosphorylation events and  $\text{Ca}^{2+}$  influx are intact in T cells lacking L-plastin (Wabnitz et al., 2010). However, L-plastin-deficient T cells have defects in IS maturation and polarization, indicating that L-plastin promotes later stages of T cell activation, perhaps by regaining activity as cytoplasmic  $\text{Ca}^{2+}$  levels decay. Finally, as discussed below,  $\text{Ca}^{2+}$  signaling regulates the balance between T cell migration and stopping, and L-plastin is poised to play an important role in that context. In keeping with that idea, L-plastin-deficient T cells exhibit migration defects (Freeley et al., 2012).

#### $\text{Ca}^{2+}$ control of microtubule dynamics

$\text{Ca}^{2+}$  signaling also plays a role in MTOC reorientation to the IS interface. Early work by the Kupfer lab demonstrated that the MTOC polarization is  $\text{Ca}^{2+}$ -dependent (Kupfer et al., 1985). This finding was confirmed by the Weiss lab (Kuhne et al., 2003; Lowinkropf et al., 1998), who showed that MTOC reorientation is dependent on signaling through  $\text{PLC}\gamma 1$ , and on the presence of extracellular  $\text{Ca}^{2+}$ . The relevant  $\text{Ca}^{2+}$ -dependent molecules were not identified, although involvement of calcineurin and CaMK was ruled out. More recently, however, the Huse laboratory found that MTOC reorientation is  $\text{Ca}^{2+}$ -independent, and depends instead on local production of DAG (thereby explaining the dependence on  $\text{PLC}\gamma 1$ ) (Quann et al., 2009). In that study, T cells pretreated with  $\text{Ca}^{2+}$  blockade solution (EGTA plus BAPTA-AM) polarized their MTOCs to the IS just as efficiently as control cells and maintained a high degree of polarization for the first 10

minutes of stimulation. One explanation that could reconcile these conflicting findings is the temporal differences in the experimental conditions. While the earlier work concentrated on prolonged T cell–APC contact (15–60 min.), the Huse lab analyzed MTOC reorientation by live-cell microscopy immediately post TCR stimulation. Thus, it may be that  $\text{Ca}^{2+}$  is not needed for initial MTOC recruitment to the IS, but is required for retention at later times. Finally, it is worth noting that MTOC reorientation requires both pulling forces provided by cytoplasmic dynein as well as pushing forces produced by myosin II (Combs et al., 2006; Liu et al., 2013); (Huse et al., 2013). Thus, the requirement for myosin II function could explain the  $\text{Ca}^{2+}$  dependence of MTOC reorientation in some experimental settings.

#### Parallel control via inositol metabolism

While one tends to think about serial signaling pathways in which cytoskeletal dynamics regulate  $\text{Ca}^{2+}$  mobilization or *vice versa*, it is important to point out that these two processes can be signaled in parallel, via a common mediator,  $\text{PIP}_2$  (Figure 1.3). Thus, the observed coordinate control is at least partially attributable to mutual dependence on inositol metabolism, since cytoskeletal regulatory pathways are highly sensitive to inositol lipids, especially  $\text{PIP}_2$  and its metabolite, diacylglycerol. Many actin-regulatory proteins including WASp, WAVE 2, moesin, cofilin and Vav1 interact with and are activated by  $\text{PIP}_2$  in the PM (Ben-Aissa et al., 2012; Han et al., 1998; Higgs and Pollard, 2000; Sun et al., 2011; Yonezawa et al., 1990).  $\text{PLC}\gamma 1$ -dependent cleavage of  $\text{PIP}_2$  simultaneously stimulates ER store release by generating  $\text{IP}_3$  and consumes a key upstream regulator of actin dynamics. For example, the actin tethering protein moesin binds to  $\text{PIP}_2$  (Hirao et al., 1996), which activates its ability to link PM proteins to the

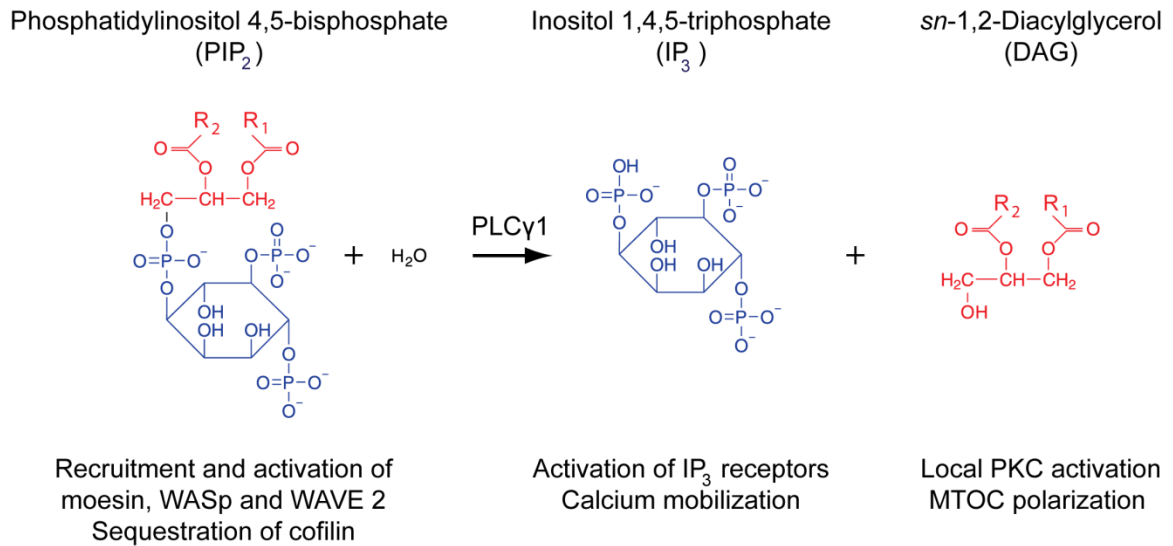


**Figure 1.3. Parallel control of cytoskeletal remodeling and calcium signaling via lipid metabolism**

Phosphatidylinositol 4,5-bisphosphate (PIP<sub>2</sub>) is required for recruitment and regulation of key actin-regulatory proteins, such as moesin, WASp, WAVE 2, and cofilin. PLCγ1 activity cleaves PIP<sub>2</sub> at the IS to generate Inositol 1,4,5-triphosphate (IP<sub>3</sub>) and sn-1,2-Diacylglycerol (DAG). The release of IP<sub>3</sub> triggers receptors on the ER membrane, resulting in release of stored Ca<sup>2+</sup>. The release of DAG stimulates local protein kinase C activation, defining the site for MTOC polarization, as well as enhancing Ras signaling and other processes. PLCγ1 also affects F-actin remodeling at the IS by transiently consuming PIP<sub>2</sub>. This leads to release and inactivation of moesin and down-regulates activity of WASp and WAVE2, as well as other signaling proteins including Vav1 and Itk. The actin severing protein cofilin is sequestered by binding to PIP<sub>2</sub>, and is released in an active form by PLCγ1 activity.

actin cytoskeleton. Cleavage of PIP<sub>2</sub> leads to moesin inactivation, resulting in diminished cortical stiffness, and allowing redistribution of moesin-linked PM proteins (Ben-Aissa et al., 2012; Delon et al., 2001). On the other hand, cleavage of PIP<sub>2</sub> by PLC $\gamma$ 1 releases and activates cofilin, leading to enhanced severing activity and providing free monomer and uncapped barbed ends for new filament growth (van Rheenen et al., 2007). In the case of WASp and WAVE2, which are activated by both Rho GTPases and PIP<sub>2</sub> binding, consumption of PIP<sub>2</sub> may serve to attenuate or terminate the response that was initially activated by TCR-dependent activation of Rho GTPases. The interplay between inositol metabolism, Ca<sup>2+</sup> signaling and cytoskeletal reorganization is even clearer in the case of microtubule reorganization. Here, local accumulation of DAG produced by PIP<sub>2</sub> cleavage activates protein kinase C-dependent events leading to MTOC reorientation. Details of that pathway are reviewed in depth in Huse et al. (2013).

*Higher level complexity: the transition from migration to activation*

The complex interplay between cytoskeletal dynamics and Ca<sup>2+</sup> signaling sets the stage for finely-tuned changes in response to environmental cues. For example, since Ca<sup>2+</sup> signaling also controls migratory responses downstream of chemokine receptors, it is poised to coordinate the “stop” signal that occurs when T cells migrating within lymphoid organs encounter APCs bearing rare agonist pMHCs. In migrating T cells, extrinsic factors such as chemokines and integrin ligands induce F-actin polymerization in the leading edge of the cell, and myosin II contraction to form a trailing uropod (Barreiro et al., 2004). The MTOC localizes behind the nucleus, stabilizing the uropod and establishing directional persistence (Ratner et al., 1997; Takesono et al., 2010). Upon

encounter with an APC, intracellular  $\text{Ca}^{2+}$  levels rise, and the T cell stops migrating, rounds up, and polarizes actin filaments and the MTOC toward the APC. This series of events occurs in mature T cells encountering antigen in peripheral lymphoid organs (Wei et al., 2007), and also during thymic development. Using two-photon microscopy Bhakta *et al.* (2005) showed that naïve thymocytes are highly mobile when intracellular  $\text{Ca}^{2+}$  concentration are low. However, upon an increase in intracellular  $\text{Ca}^{2+}$  levels, thymocytes become immobile and eventually undergo positive selection. By artificially manipulating  $\text{Ca}^{2+}$  levels, the group could show that elevation of intracellular  $\text{Ca}^{2+}$  is sufficient to inhibit cell migration, prolonging interaction with antigen-bearing stromal cells and promoting genetic reprogramming and positive selection. This study highlights the importance of crosstalk between  $\text{Ca}^{2+}$  signaling and cytoskeletal dynamics for T cell development. Subsequent work from the Krummel lab (Beemiller et al., 2012) extended the investigation of the relationship between  $\text{Ca}^{2+}$  and cell migration using stimulatory planar lipid bilayers. Their findings showed that the amplitude of the  $\text{Ca}^{2+}$  response is dependent on the density of the presented antigen. Consistent with previous *in vivo* observations (Friedman et al., 2010; Skokos et al., 2007), the lab found that TCR stimulation slowed the T cells but did not strictly halt their migration. T cell migration was inversely proportional to  $\text{Ca}^{2+}$  spikes. Thus, while T cells with high intracellular  $\text{Ca}^{2+}$  concentrations stopped migration, cells with intermediate  $\text{Ca}^{2+}$  signaling showed a graded response in motility. Furthermore, the average speed of migrating T cells underwent step changes between high, intermediate and low motile cells. In a related study, Marangoni et al. (2013) compared the  $\text{Ca}^{2+}$  responses required for diminished T cell motility with those required for translocation of NFAT to the nucleus, and found that NFAT translocation

requires high intracellular  $\text{Ca}^{2+}$  levels associated with migratory arrest. In tumor-infiltrating T cells, nuclear NFAT was maintained for several minutes in cells with diminished intracellular  $\text{Ca}^{2+}$  and unstable APC contacts, a condition that was associated with induction of T cell tolerance. Taken together, these studies demonstrate the integration of  $\text{Ca}^{2+}$  mobilization and T cell migration during TCR signaling, and emphasize the importance of these events for T cell development and effector function.

#### *F-actin function in TCR-induced $\text{Ca}^{2+}$ mobilization*

The interdependence of  $\text{Ca}^{2+}$  signaling and cytoskeletal remodeling has been evident since the earliest single studies of T cell activation. Over the past several years, researchers have identified many of the molecules that control these two processes, and placed them into major regulatory pathways. This has revealed key points of intersection within the signaling network. Cytoskeletal influence on  $\text{Ca}^{2+}$  signaling is simultaneously exerted at various scales, ranging from single molecule conformational changes to changes in cell morphology. The tight association between  $\text{Ca}^{2+}$  signaling and the cytoskeleton provides mechanisms by which environmental cues can tune the T cell response, such as when the presence of cognate antigen induces stopping of T cells trafficking through lymphoid organs. In addition, the complex interplay between  $\text{Ca}^{2+}$  and the cytoskeleton provides a basis for positive and negative feedback loops. For example, minute bursts of actin polymerization may promote early TCR signaling. The resulting rise in cytoplasmic  $\text{Ca}^{2+}$  may then sustain actin remodeling during T cell spreading. Finally, cell shape changes or forces generated by T cell spreading may, in turn, promote sustained  $\text{Ca}^{2+}$  elevation.



### **III. Mechanotransduction and signaling of the integrin LFA-1 at the IS**

#### *Integrins in T cell biology*

Physiological milieus that require efficient T cell responses often present substantial challenges, both in terms of mechanical stresses associated with biological processes and availability of activating stimuli. To overcome these obstacles, T cells must be able to modulate their adhesiveness and signaling efficiency. These tasks converge on adhesion receptors known as integrins, first characterized in the late 80's (Tamkun et al., 1986). These proteins, as the name suggests, integrate the chemical and mechanical properties of external environments with the cell interior. Integrins are a large family of transmembrane proteins, comprised of 24 known members. Each integrin molecule is assembled as a dimer of one  $\alpha$  and one  $\beta$  subunit. Lymphocyte function-associated antigen-1 (LFA-1) is  $\alpha$ L $\beta$ 2 integrin. It is expressed only in leukocytes and has been implicated in T cell migration and adhesion. Recent findings also show that LFA-1 is a potent costimulatory molecule that lowers the threshold of T cell activation. CD4<sup>+</sup> T cells deficient for LFA-1 exhibit priming defects at the level of IL-2 production and proliferation (Kandula and Abraham, 2004; Varga et al., 2010). Furthermore, malfunctions in LFA-1-dependent adhesion and tethering results in a profound immunodeficiency disorder known as leukocyte adhesion deficiency (LAD) (Bunting et al., 2002). Therefore, LFA-1 activation and its function in T cell adhesion and signaling are important areas of investigation that may lead to new therapeutic targets.

#### *Structural features of LFA-1*

The  $\alpha$ L and the  $\beta$ 2 subunits of LFA-1 are non-covalently associated in the PM with large N-terminal extracellular head regions and relatively short C-terminal cytoplasmic

tails. Their single-span transmembrane domains convey information across the cell membrane in both directions. LFA-1 contains an  $\alpha I$  (inserted) domain in the headpiece region that binds to ligand, ICAM-1, with high specificity (Springer and Dustin, 2011). In  $\alpha I$ -less integrins, e.g.  $\alpha V\beta 3$ , ligand specificity is determined by the  $\beta I$  domain in the  $\beta$  subunit, which is homologous to  $\alpha I$  and is also present in the  $\beta 2$  chain of LFA-1. The two  $I$  domains are positioned closely to each other and undergo analogous alterations in structure to modulate binding affinity for ICAM-1 (Springer and Dustin, 2011).

On naïve T cells, resting LFA-1 exists in a bent conformation that has low affinity for ICAM-1. Signaling downstream of TCR (or other cell sensors, such as chemokine and selectin receptors) stimulates talin binding to the  $\beta$  tail, which induces jack knife-like extension of the LFA-1 headpiece and promotes intermediate affinity for ligand (Kim et al., 2003; Luo et al., 2005; Partridge et al., 2005). This first step in LFA-1 activation is known as “inside-out” signaling (Hogg et al., 2011). Multiple studies have investigated the subsequent conformational changes that fully activate LFA-1 (Weitz-Schmidt et al., 2011; Zhu et al., 2008). The extended open, high-affinity LFA-1 requires lateral swing-out of the hybrid domain which pulls on the  $\alpha 7$  helix in the  $\beta I$  domain and eventually opens the  $\alpha I$  domain (Figure 1.4). The allosteric opening of the  $\alpha I$  domain increases integrin’s affinity for ICAM-1 by three orders of magnitude (Schurpf and Springer, 2011). Current models propose that cytoskeletal forces can segregate the  $\alpha$  and  $\beta$  tails and induce the high affinity state of LFA-1 (Zhu et al., 2008). Tracking of individual LFA1–ICAM-1 pairs at the IS indicates that bond lifetimes last for seconds, which is consistent with participation of cytoskeletal dynamics in this process (Shimaoka et al., 2003; Springer and Dustin, 2011). The  $\beta$  chain of LFA-1 is primarily responsible for talin-

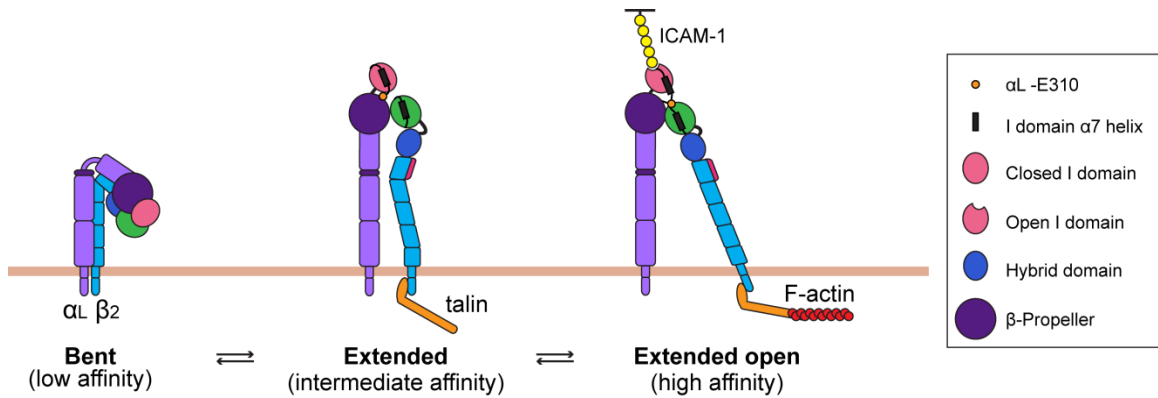


**Figure 1.4. Integrin activation through conformational intermediates**

On the surface of T cells the integrin LFA-1 exists mainly in three interdependent conformational states. Inactive LFA-1 is present in the bent conformation on the surface of T cells and exhibits low affinity for ligand. Inside-out signaling induces talin binding to the  $\beta$  chain of LFA-1, which leads to a switchblade-like extension of the integrin away from plasma membrane. This step increases affinity for ligand by a factor of four and results in the intermediate affinity state. Subsequent cytoskeletal engagement results in a lateral swing-out of the hybrid domain, resulting in a downward movement of the  $\alpha_7$  helix in the  $\beta I$  domain, which allosterically opens it for substrate binding. Binding of glutamate 310 to the open  $\beta I$  domain pulls on the  $\alpha_7$  helix of the  $\alpha I$  domain, in turn increasing the affinity of that domain for ICAM-1 by 1000-fold. This extended open conformation of LFA-1 is capable of strong adhesion and outside-in signaling.

mediated interactions with the cytoskeleton and transduction of tension. In agreement with this, immobilization of ICAM-1 was found to be critical for triggering of the high-affinity state (Feigelson et al., 2010).

### *TCR-dependent activation of LFA-1*

In order to interact with its ligand, LFA-1 must undergo preliminary activation by inside-out signaling downstream of stimulatory receptors. Unlike chemokine- or selectin-induced activation, TCR-induced inside-out signaling occurs in the absence of shear flow. Therefore, cytoskeletal dynamics are expected to play an important role in the generation of forces, which facilitate LFA-1 activation (Alon and Dustin, 2007). Besides establishing cytoskeletal dynamics, TCR signaling induces recruitment of certain adaptor molecules that facilitate LFA-1 clustering and conformational changes at the IS. Some of the fundamental understanding of the integrin activating machinery comes from reductionist studies in platelets, where it has been shown that the process requires the small GTPase RAP1, the adaptor protein RIAM and the cytoskeletal protein talin. Furthermore, the membrane-targeting sequence of RAP1 fused to the talin-binding fragment of Lamellipodin (a homolog of RIAM) was shown to be sufficient for integrin activation (Lee et al., 2009). This finding indicated that the association with the PM and activation of RAP1 and RIAM-mediated recruitment of talin with the integrin  $\beta$  tail represent the functional core of inside-out signaling. I will briefly describe these events below.

A crucial component of integrin activation is localization of activated RAP1 GTPase at the PM (Katagiri and Kinashi, 2012). This process must be tightly regulated since

expression of a constitutively active mutant of RAP1 induces hyper-activation of  $\beta 2$  and  $\beta 1$  integrins and stabilizes T cell–APC interactions (Sebzda et al., 2002). The active GTP-loaded form of RAP1 is maintained by guanine exchange factors such as C3G. Recent studies in Jurkat T cells demonstrated that C3G associates with CrkL and participates in T cell adhesion to ICAM-1–coated surfaces. This report also implicated WAVE2 and cAbl kinase in recruitment and activation of C3G at the IS (Nolz et al., 2008). Once at the PM, active Rap1 modulates functions of adaptor molecules such as RapL and RIAM to trigger the activation of LFA-1. The mechanisms that regulate RAP1 delivery to the IS remain to be established; while RAP1 localizes to secretory vesicles (Bivona et al., 2004), it is also reported to reside constitutively in the PM (Raab et al., 2010). However, since inhibition of recycling machinery inhibits RAP1 recruitment to the PM, it seems likely that RAP1 localization continuously depends on exocytosis. To determine whether activation of RAP1 occurs on recycling vesicles or in the PM, Bivona and colleagues studied the localization of GFP-tagged Ras binding domain of RalGDS, a reporter of GTP-bound RAP1. They observed signal only on the PM, which suggests that RAP1 activation is PM-specific (Bivona et al., 2004).

RAP1-dependent localization of RapL and RIAM to the PM is a critical part of inside–out signaling, which subsequently facilitates recruitment of talin to integrin  $\beta$  tail. Optimal activation of LFA-1 requires talin binding to facilitate the transition into the active conformation. In resting T cells, talin exists in the cytosol as an auto-inhibited head-to-tail dimer. The FERM domain of talin has affinity for  $\text{PIP}_2$  and this interaction partially releases the auto-inhibited conformation (Goksoy et al., 2008). Furthermore, the FERM domain binds to membrane-proximal NPXY site in the  $\beta$ -subunit tail of LFA-1

(Calderwood et al., 2002). Kindlin 3 also binds the  $\beta$ -subunit tail but at a membrane-distal NPLF sequence (Feigelson et al., 2011). It is thought that kindlin 3 facilitates the interaction of talin with LFA-1 and thus orchestrates integrin activation because loss of kindlin 3 results in loss of adhesion and immune responses in T cells (Moser et al., 2009). These binding events are critical for induction of the LFA-1 extended conformation and subsequent activation of the high-affinity form.

#### *Costimulation through “outside-in” signaling*

The costimulatory properties of LFA-1 have been appreciated since the early 90's, when it was shown that ICAM-1 binding can tune the sensitivity of T cells for activating stimuli (Van Severter et al., 1990). “Outside-in” signaling pertains to ligand-induced molecular rearrangements that strengthen adhesion and enhance signaling downstream of LFA-1. Engagement of LFA-1 heightens the sensitivity of T cells for agonist peptides by two orders of magnitude (Bachmann et al., 1997) and augments IL-2 gene transcription (Abraham and Miller, 2001). One of the ways in which LFA-1 can aid in costimulation at the IS, is production of an F-actin cloud that facilitates delivery of TCR-associated molecules and may generate forces required for TCR triggering (Porter et al., 2002; Suzuki et al., 2007). LFA-1 accumulates in the peripheral activating cluster at the IS (Monks et al., 1998), which is the site of ongoing TCR signaling (Yokosuka et al., 2005). While TCR and LFA-1 clusters accumulate in the same general area of the IS, they never completely colocalize but rather reside in distinct membrane domains (Kaizuka et al., 2007), suggesting that the interactions between these receptors must be mediated by cytosolic activators and adaptor proteins.

Many molecules from the TCR signaling pathway have been detected downstream of LFA-1 activation. Lck and Zap70 kinases associate with the cytoplasmic tails of LFA-1 and undergo activation upon integrin ligation (Evans et al., 2011). Phosphorylated Zap70 colocalizes with SLP-76 MCs at the PM upon integrin stimulation (Baker et al., 2009). SLP-76 is one of the key players at the IS since it serves as a docking site for many accessory protein modules involved in TCR signaling (GADS–LAT–PLC $\gamma$ 1 axis), integrin activation (ADAP–SKAP55 axis), and actin polymerization (VAV1/Nck–WAVE2 axis). Thus, SLP-76 may integrate signaling downstream of LFA-1 and TCR in a single molecular complex. Interestingly, both RIAM and RapL have been implicated in bringing the SKAP55–ADAP module to the  $\alpha$  chain of LFA-1 revealing a physical link between integrins and SLP-76 MCs (Katagiri et al., 2003; Menasche et al., 2007). Experiments with the  $\beta$ 1 integrin VLA-4 demonstrate that engagement of immobilized integrin ligands can attenuate the dynamics of signaling molecules at the IS and concentrate F-actin-dependent tension (Nguyen et al., 2008); however, whether this mechanism applies to LFA-1 signaling remains to be investigated.

#### *LFA-1 activation and organization at the IS*

LFA-1 is an important adhesion protein that stabilizes cell-cell interactions and provides costimulatory cues to enhance T cell activation. By virtue of their structure, integrins rely on mechanical stresses for activation and signaling. Protein crystallography and electron microscopy have revealed precise conformational changes that take place upon inside-out and outside-in signaling. Usage of monoclonal antibodies that recognize different conformations of human LFA-1 has greatly accelerated our understanding of the

molecular rearrangements that direct LFA-1 activation. However, there are still many unknown factors that coordinate affinity maturation and valency at the cellular level. For example, to date, it is still unclear how integrins are organized into the micron-scale supramolecular activation cluster at the IS. Furthermore, which integrin molecules in the IS-associated pool are activated also remains unanswered in the field. This work aspires to answer these pending questions.



## **CHAPTER 2: F-ACTIN POLYMERIZATION AND RETROGRADE FLOW DRIVE SUSTAINED PLC $\gamma$ 1 SIGNALING DURING T CELL ACTIVATION<sup>34</sup>**

### **I. Summary**

Activation of T cells by APCs involves assembly of signaling molecules into dynamic MCs within the IS. Actin and myosin IIA localize to the IS, and depletion of F-actin abrogates MC movement and T cell activation. However, the mechanisms that coordinate actomyosin dynamics and T-cell receptor signaling are poorly understood. Using pharmacological inhibitors that perturb individual aspects of actomyosin dynamics without dismantling the network, we demonstrate that F-actin polymerization is the primary driver of actin retrograde flow, whereas myosin IIA promotes long-term integrity of the IS. F-actin arrest led to a complete immobilization of SLP-76-containing MCs even in the regions, where the network was sparse. Furthermore, rate analysis indicated MCs exhibit a fundamentally different mode of translocation than the F-actin network. In line with this, microtubules were enriched at the IS and localized in close proximity to MCs. Confocal and TIRF microscopy imaging revealed that although F-actin flow is dispensable for microtubule turnover, the forces associated with F-actin polymerization

---

<sup>3</sup> Parts of this chapter have been published as:

Babich A, Li S, O'Connor RS, Milone MC, Freedman BD, and Burkhardt JK. F-actin polymerization and retrograde flow drive sustained PLC $\gamma$ 1 signaling during T cell activation. *Journal of Cell Biology*. June 2012; Volume 197, pp. 775-787.

<sup>4</sup> AB designed and conducted the experiments, SL performed molecular cloning, and RO provided primary T cells expressing fluorescent actin. MM, BF and JB oversaw the work in their respective labs, conducted discussions and provided critical reading and revision of the manuscript.

are required to press microtubule filaments to PM, where MCs originate. Additionally, disruption of F-actin retrograde flow, but not myosin IIA contraction, inhibited sustained  $\text{Ca}^{2+}$  signaling at the level of ER store release. Loss of F-actin dynamics inhibited PLC $\gamma$ 1 phosphorylation within MCs but left Zap70 activity intact. These studies highlight the importance of ongoing actin polymerization as a central driver of actomyosin retrograde flow, MC centralization, microtubule positioning and sustained  $\text{Ca}^{2+}$  signaling in T cells during the early stages of activation.

## II. Introduction

T cell activation by APCs requires the formation of a specialized cell-cell interface, known as the IS. This process involves extensive spatial and temporal regulation of protein complexes to coordinate and tune signaling events. Initial TCR engagement triggers the formation of sub-micron scale signaling MCs enriched in receptors, kinases and adaptor proteins that propagate downstream signaling events. In the MCs, the Src kinase Lck phosphorylates the  $\zeta$  chains of the TCR complex.  $\zeta$ -chain Associated Protein of 70 kDa (Zap70), a kinase crucial in MC assembly, associates with the TCR and phosphorylates LAT and SLP-76. Cooperative assembly of these and other MC components culminates in the recruitment and subsequent activation of phospholipase C (PLC) $\gamma$ 1 at the PM (Bunnell et al., 2006; Houtman et al., 2004; Sherman et al., 2011). Upon activation, PLC $\gamma$ 1 cleaves PIP<sub>2</sub> into diacylglycerol and inositol 1,4,5-trisphosphate (IP<sub>3</sub>). Subsequently, IP<sub>3</sub> stimulates the release of  $\text{Ca}^{2+}$  from ER stores, which in turn leads to opening of Orail channels in the PM (Zhang et al., 1999). The resulting sustained  $\text{Ca}^{2+}$  mobilization is required for initiation of gene transcription.

Newly generated MCs arise in the periphery of the IS, and are the predominant sites for active signaling (Bunnell et al., 2002; Lee et al., 2002; Yokosuka et al., 2005). These structures undergo continuous translocation to the center of the IS, the central supramolecular activation cluster (cSMAC), where signaling is extinguished. This provides a clock for MC lifetime, and is thought to modulate response to antigens (Valitutti et al., 2010). MC dynamics are dependent on the actin cytoskeleton in complex ways. Treatment of spreading T cells with the F-actin depolymerizing agent Latrunculin A inhibits formation of new MCs, indicating that actin filaments promote MC assembly. Once formed, however, MCs are stable in the absence of F-actin, although their centripetal movement ceases with F-actin depletion. In keeping with the close association between signaling MCs and the actin cytoskeleton, T cell activation is highly dependent on maintenance of an intact F-actin network. Treatment of T cells with actin depolymerizing agents or disruption of key actin regulatory proteins leads to loss of  $Ca^{2+}$  mobilization and downstream transcriptional activation (Nolz et al., 2006; Varma et al., 2006).

Recent studies have shown that TCR-induced F-actin polymerization depends on activation of Arp2/3 complex by multiple nucleation promoting factors, including WAVE2, HS1 and WASp (Gomez et al., 2006; Nolz et al., 2006; Zhang et al., 1999). However, the mechanisms that coordinate F-actin retrograde flow and disassembly of the F-actin network are largely unexplored, and the role of myosin II contraction is poorly understood and controversial. Jacobelli et al. (2004) showed that non-muscle myosin IIA is recruited to the IS, but found that activity of this motor protein was dispensable for conjugate formation and for recruitment of signaling molecules to the IS.

In contrast, Ilani et al. (2009) found that inhibition or knockdown of myosin IIA disrupts T cell–APC conjugates and inhibits multiple aspects of TCR signaling. In that study, centripetal TCR MC movement was shown to be myosin II-dependent. Since myosin II contraction is known to contribute to actin retrograde flow in non-hematopoietic cells (Cai et al., 2006), this could reflect a linkage between myosin II function, F-actin retrograde flow, and MC centralization. Understanding this process will require detailed analysis of actomyosin dynamics with respect to distinct MC components.

The mechanisms that link the actin cytoskeleton to T cell signaling in general are largely unknown. F-actin could promote signaling in multiple ways, including maintenance of cell-cell contact, organization of gross cell polarity, and providing a nano-scale scaffold for assembly of signaling complexes (Kaizuka et al., 2007; Wulfiging and Davis, 1998). Recent studies also point to the exciting possibility that F-actin dynamics could actively promote signaling by exerting force on receptors or signaling molecules (Alon and Dustin, 2007; Beemiller and Krummel, 2010). These possibilities are not mutually exclusive, but cannot be distinguished based upon manipulations that globally deplete actin filaments.

In this chapter, we have systematically studied the roles of actin polymerization and myosin II contraction in controlling protein dynamics and signaling during T cell activation. We found that F-actin and myosin IIA exhibit distinct but overlapping distributions at the IS. Using a panel of cytoskeletal inhibitors together with an RNAi approach, we found that actin polymerization is the primary driver of actomyosin retrograde flow, while myosin IIA exerts contractile forces on the network and helps maintain its radial symmetry. We show that simultaneous inhibition of both F-actin

turnover and myosin IIA contraction leads to arrest of retrograde flow without disassembling the actin network. Under these conditions, centralization of SLP-76 MCs is also arrested, likely because microtubules, which provide tracks for MC translocation, move away from the PM in the absence of pushing forces generated by F-actin polymerization. Functionally,  $\text{Ca}^{2+}$  elevation is abrogated at the level of release from stores and phosphorylation of PLC $\gamma$ 1 but not Zap70 is inhibited after F-actin immobilization. This highlights that cytoskeletal dynamics selectively affect specific signaling molecules at the IS. Our studies demonstrate a requirement for F-actin polymerization-driven flow in promoting T cell activation.

### **III. Results**

#### *Quantitative analysis of actomyosin distribution and dynamics at the IS*

Numerous studies have shown the importance of actin for T cell activation, but the mechanics of actin movement at the IS have not been carefully addressed. Moreover, myosin II function at the IS is poorly understood, and results are conflicting (Ilani et al., 2009; Jacobelli et al., 2004). To investigate the actomyosin network as a functional unit, we used Jurkat T cells stably expressing low levels of GFP-actin (Gomez et al., 2006), and transfected with mKate2-tagged heavy chain of non-muscle myosin IIA (NMHC II-A). When these cells were allowed to spread on anti-CD3-coated coverglasses, they formed characteristic actin-rich lamellipodial protrusions. Consistent with previous observations (Bunnell et al., 2001; Gomez et al., 2006), cell spreading reached a maximum within 2-4 minutes, and was maintained for 15-20 minutes before partial contraction. We concentrated our studies on the fully spread cells, representing the sustained phase of TCR signaling. Myosin IIA localized to the IS (Figure 2.1 A), as

reported previously in T cell–APC conjugates (Jacobelli et al., 2004) and formed characteristic arcs, as seen by others (Yi et al., 2012). Intensity profile analysis showed that myosin IIA was present throughout the actin-rich region, but accumulated most prominently behind the lamellipodium (Figure 2.1 B). Importantly, while the distribution of F-actin and myosin IIA are distinct, they are overlapping; F-actin was detectable throughout the myosin-rich region, albeit at lower levels than in the lamellipodium. Indeed, the presence of myosin IIA within the lamellum region highlights a pool of F-actin that is not readily appreciated in images contrasted for optimal observation of the more abundant actin filaments in the lamellipodium. Similar distributions were observed using antibody and phalloidin labeling of F-actin and endogenous myosin IIA in fixed cells (Figures 2.1 D and 2.5 E), although endogenous pool of myosin IIA did not form the prominent arcs, suggesting that the features seen in cells transfected with mKate2-NMHC IIA may be partially attributed to over-expression artifacts.

Live-cell microscopy revealed that myosin IIA undergoes continuous retrograde flow comparable to that of F-actin (Movie 2A). Interestingly, both actin and myosin IIA were nearly undetectable in the central region of the IS. This was not due to an artifact of cell shape and shallow focal plane, since 3D reconstructions showed that the network exhibits a planar organization only about 1  $\mu\text{m}$  in thickness, and since we could readily detect other structures within this region (e.g. SLP-76 MCs in Figure 2.1 D, and the MTOC in Figure 2.11 B). Based on these studies, we define three regions with distinct cytoskeletal topology: the actin-rich lamellipodium (LP), the myosin IIA-rich lamellum (LM), and the cell body (CB), a perinuclear region largely devoid of actomyosin filaments.

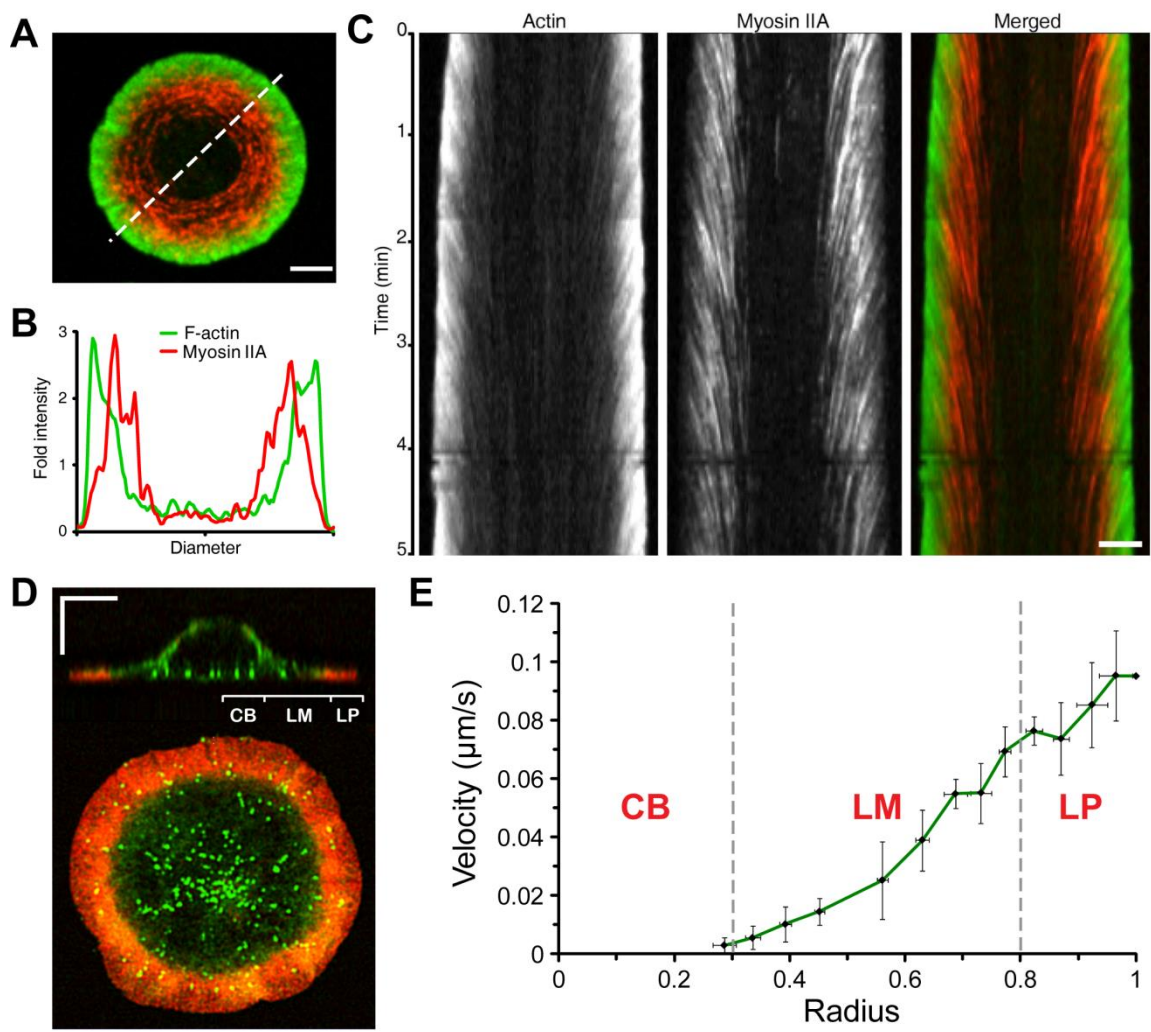


**Figure 2.1. Distribution and dynamics of the T cell actomyosin network**

(A) mKate2-NMHC II-A was transiently expressed in Jurkat T cells stably expressing GFP-actin. The cells were dropped on OKT3-coated coverglass and imaged at a single focal plane every 3 s. An image from a sequence is shown and is representative of four independent experiments. Scale bar represents 5  $\mu\text{m}$ . (B) The intensity profile of F-actin and myosin IIA was acquired along the dashed line in (A). (C) Composite kymograph of actomyosin dynamics was acquired along the dashed line in (A). Scale bar represents 5  $\mu\text{m}$ . (D) Jurkat T cells stably expressing GFP-SLP-76 (green) were stimulated as in (A), fixed after 5 minutes and stained for F-actin with phalloidin (red). Z-stacks of whole cells were collected with 0.25- $\mu\text{m}$  step size and deconvolved using calculated Point Spread Function in Volocity. A representative cell is shown in XZ and XY planes; CB – cell body, LM – lamellum, LP – lamellipodium. Scale bars represent 5  $\mu\text{m} \times 5 \mu\text{m}$ . (E) Kymography analysis of F-actin features was compiled into a single graph to show the distribution of F-actin velocity across the IS radius. Abbreviations are same as in (D). Mean  $\pm$  SD are shown for each point ( $n = 13$  cells). Similar results were obtained from three independent experiments.



We next quantified the velocity of the F-actin retrograde flow in two complementary ways. First, movies were digitally sharpened to amplify signal-to-noise, and fiduciary features with  $\sim 1\text{-}2\ \mu\text{m}$  spacing along the radius were tracked by kymography (Figure 2.2 A and B and Movie 2B). Alternatively, a region was photo-bleached to induce synchronous incorporation of bleached GFP-actin into the network, generating a high-contrast wave that is easily identified by kymography (Figure 2.2 C and Movie 2C). Results using both approaches were in agreement, and showed that F-actin flow at the very edge of the IS proceeds at  $0.095 \pm 0.028\ \mu\text{m/s}$ . Upon closer examination of these kymographs, however, we noted that actin velocity depended on position along the radius of the IS. This is evident in Figure 2.2 B, where the deflection of the red line drawn near the periphery is more pronounced than that of the blue line drawn in the LM region, indicating a slowing of movement toward the IS center. Features within the central CB region track vertically (yellow line), indicating that they are immobile. Similar behavior is evident in kymographs generated from myosin IIA movies (Figure 2.1 C). The distribution of actomyosin dynamics across the IS in a population of cells is shown in Figure 2.1 E, with the three respective regions of the IS are indicated for comparison. Centripetal flow decelerates gradually from the periphery through the LM. The occasional features that show movement within the CB region appear to be diffusive.

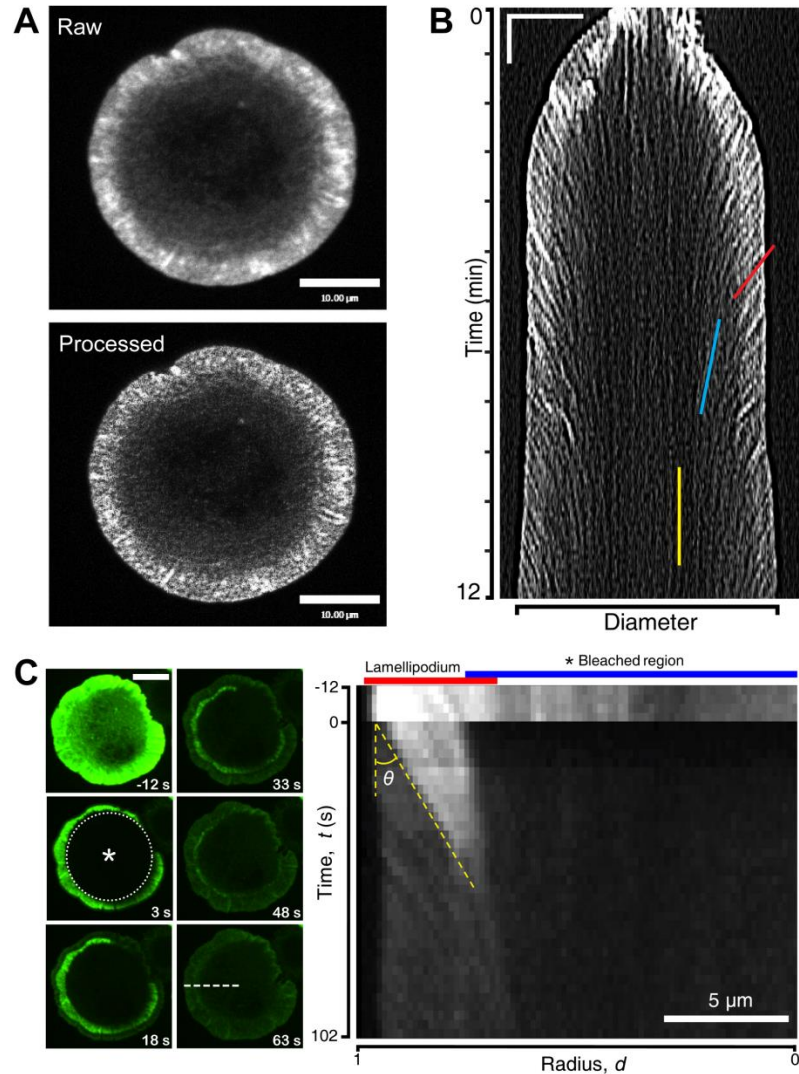


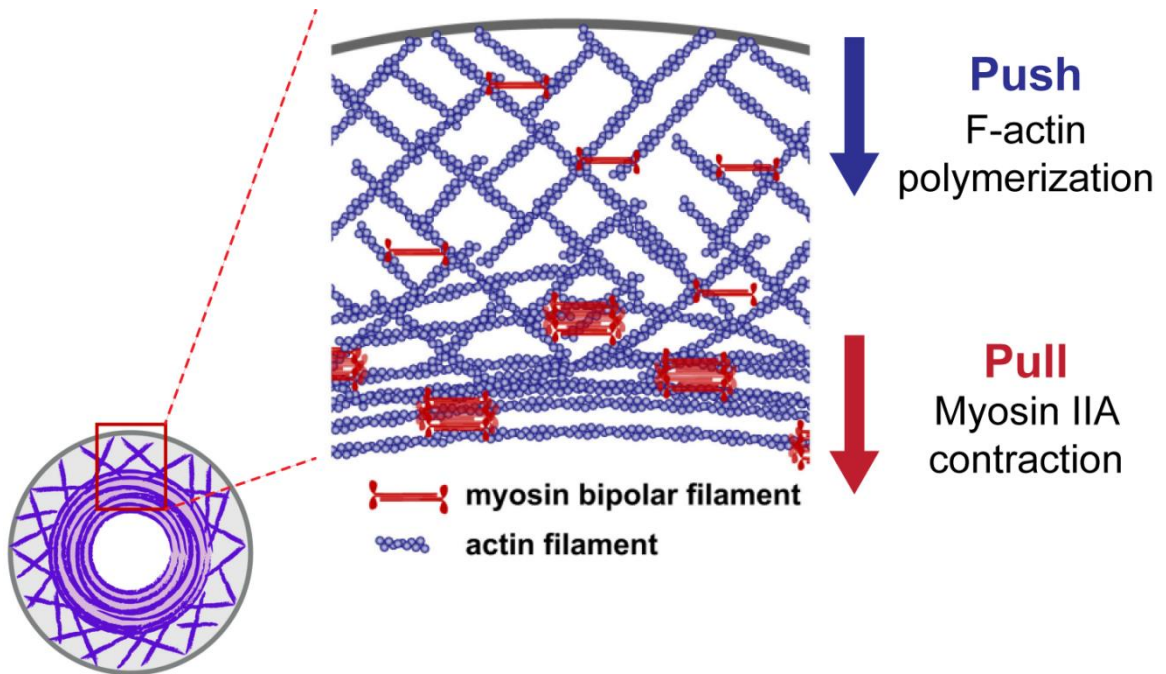
**Figure 2.2. Measurement of F-actin dynamics at the IS**

(A) Top: “Raw” image of a fully spread IS of a Jurkat T cell expressing GFP-actin. Bottom: Same image digitally “processed” in Adobe Photoshop using a filter with 300% intensity increase for local maxima within 3 pixel radius. Scale bars represent 10 μm. (B) Kymograph generated from the video sequence and along the diameter of the cell depicted in (A) and processed as above. Scale bars represent 10 μm × 1 min. (C) Left: Image series of a spreading GFP-actin Jurkat T cell subjected to photo-bleaching in the region marked with an asterisk (\*). Scale bar, 10 μm. Right: Kymograph generated along the dashed line from the sequence on the left.  $\theta$  represents the angle of deflection from the vertical position.

*Myosin IIA exerts contractile force on the F-actin network, but is dispensable for F-actin flow*

The observed centripetal flow could be driven by F-actin polymerization pushing against the membrane edge (Pollard and Berro, 2009) or myosin II contraction pulling against the branched F-actin network (Cai et al., 2006; Wilson et al., 2010) (Figure 2.3). To uncouple these components, we used a panel of well-defined pharmacological inhibitors. Initially, we tested the effects of jasplakinolide (Jas), an F-actin stabilizing agent that perturbs actin turnover (Bubb et al., 1994). T cells pretreated with Jas were not useful for analysis, since this abrogated cell spreading and induced cytoplasmic F-actin aggregates (data not shown). We therefore allowed cells to contact a stimulatory coverglass for 3 minutes before addition of the drug. Acute addition of Jas collapsed the F-actin network toward the center of the IS. This was true in both Jurkat T cells (Figure 2.4 A and Movie 2D) and human primary T cell blasts (Figure 2.4 B and Movie 2E). Myosin IIA behaved similarly (Figure 2.4 C and Movie 2F), with two important differences. First, the collapse of myosin IIA was more rapid. This is evident in the kymography analysis of F-actin and myosin IIA dynamics (Figures 2.4 D and E, respectively). Second, unlike F-actin, which accumulated in an irregular ring around the CB, myosin IIA transiently formed a tight symmetrical ring that subsequently disappeared as large aggregates accumulated in the periphery. Thus, myosin IIA is able to exert centripetal force on the T cell cytoskeleton, which is revealed upon stabilization of the F-actin network.

We next analyzed retrograde flow under conditions where myosin II activity is perturbed. The Rho kinase inhibitor, Y-27632, blocks phosphorylation of myosin light

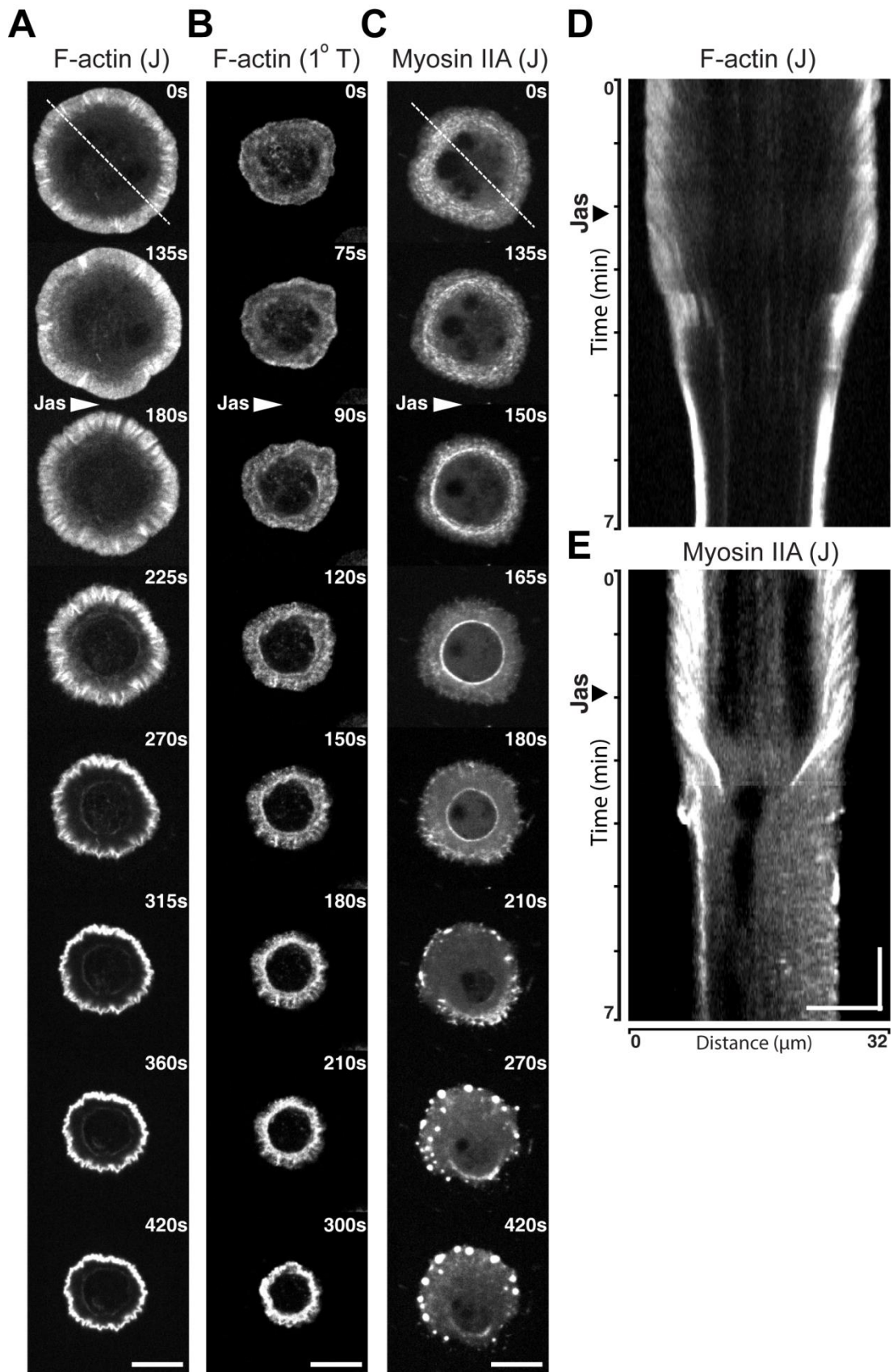


### Spreading cell

**Figure 2.3. Potential mechanisms that can drive actomyosin retrograde flow in symmetrically spreading cells\***

In the lamellipodium, ongoing F-actin polymerization generates pushing forces against the PM, while in lamellum myosin II bundles bind and cross-link actin filaments, generating pulling forces. Coordinate balance between these mechanisms leads to persistent centripetal flow of the actomyosin network.

\*Figure adapted from Yam et al., 2007



chain (MLC) at S19 and inhibits myosin II filament assembly (Ueda et al., 2002). Surprisingly, T cells pretreated with Y-27632 continued to show retrograde F-actin flow with unchanged rate (Figures 2.5 A and B and Movie 2G). The drug successfully inhibited MLC phosphorylation, based upon immune-blotting with a phospho-specific antibody (Figure 2.5 B, bottom). As a more direct test of myosin II function, we generated Jurkat T cells expressing the F-actin sensor F-tractin labeled with Td-Tomato (Johnson and Schell, 2009), and measured actin dynamics in cells treated with blebbistatin, a specific inhibitor of myosin II ATPase activity (Straight et al., 2003). As shown in Movie 2H and quantified in Figure 2.5 C, the rates of retrograde flow were unaffected by blebbistatin pre-treatment. Finally, siRNA was used to suppress expression of myosin IIA heavy chain (Myh9). We could suppress protein levels by 75% without any effect on the rate of actin retrograde flow (Figure 2.5 D). Taken together with the results above, these studies show that myosin II exerts contractile forces on the T cell actin network, but these forces are dispensable for actin retrograde flow at the IS.

T cells responding to stimulatory surfaces exhibit initial expansion of the contact area, followed by a steady-state period during which the area remains constant, and a

---

**Figure 2.4. F-actin stabilization leads to contraction of the actomyosin network.**

(A-C) Time-lapse series of T cells spreading on OKT3-coated coverslips. Arrowheads indicate time when 1  $\mu$ M Jas was added. Scale bars represent 10  $\mu$ m. (A) Jurkat T cells stably expressing GFP-actin. (B) Human primary T cell blasts transiently transfected with GFP-actin. (C) E6.1 Jurkat T cells transiently transfected with GFP-NMHC-IIA. (D, E) Kymographs of F-actin and myosin IIA dynamics, generated along the dashed lines in (A) and (C), respectively. Arrowheads indicate the addition of 1  $\mu$ M Jas into the media. Scale brackets represent 10  $\mu$ m  $\times$  1 min.

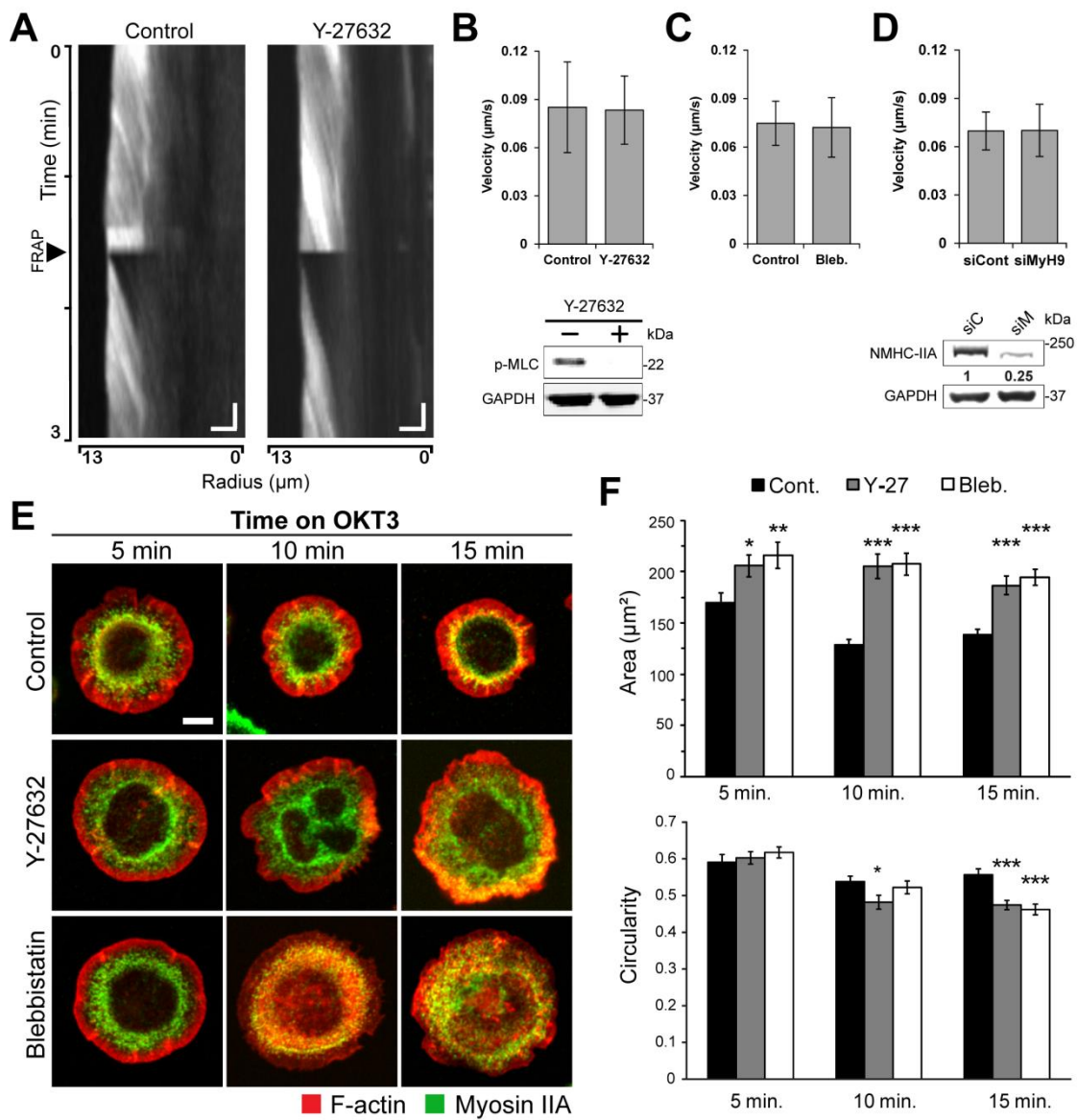


**Figure 2.5. Myosin IIA is not required for F-actin flow but is necessary for long-term maintenance of the IS.**

(A) GFP-actin expressing Jurkat T cells were pre-treated for 15 minutes with vehicle or 25 $\mu$ M Y27632, and imaged while spreading on anti-CD3 coated coverslips. Kymographs were generated along the radii of fully spread cells. Arrowhead indicates the time when photo-bleaching of lamellipodia was induced. Scale bars represent 2  $\mu$ m  $\times$  15 s. (B) Top, analysis of velocities calculated from kymographs as in (A), (mean  $\pm$  SD, n = 15 cells). Bottom, to verify inhibitory activity of Y-27632, Jurkat T cells were pre-treated with Y-27632 as in (A), and stimulated with OKT3 (1  $\mu$ g/ml) for 5 min. Cells were lysed and analyzed by Western blot analysis with antibodies to phosphorylated myosin light chain (pMLC) or GAPDH. (C) Jurkat T cells were transiently transfected with F-Tractin tdTomato, and pre-treated with 50 $\mu$ M blebbistatin or vehicle for 30 min. Actin retrograde flow was analyzed as in (B). Values are mean  $\pm$  SD of 80-90 kymographs from 14-20 cells. (D) GFP-actin expressing Jurkat T cells were transfected with oligonucleotides specific for myosin IIA heavy chain (SiM) or control oligonucleotides (SiC), and cultured for 48 h, at which time suppression was found to be optimal. Top panel, retrograde flow was analyzed as in (B). Bottom panel, lysates were analyzed by Western blot to assess efficiency of suppression. Values represent relative NMHC-IIA levels, normalized to GAPDH. (E) Jurkat T cells were untreated or pretreated with 25  $\mu$ M Y-27632 or 50  $\mu$ M blebbistatin, and allowed to spread for the indicated times on anti-CD3 coated coverslips prior to fixation and labeling with phalloidin and anti-NMHC-IIA. Scale bar, 5  $\mu$ m. (F) Morphometric analysis of cells prepared as in E. Data represent mean  $\pm$  SEM, n = 67-125 cells per condition). \* p < 0.05, \*\* p < 0.01, \*\*\* p < 0.001. Similar results were obtained in two independent experiments.



contraction phase. Time course analysis of IS organization showed that control and myosin-inhibited cells looked comparable during the expansion and steady-state phases of the response. After 10-15 minutes, however, myosin-inhibited cells failed to contract normally and became irregularly shaped (Figures 2.5 E and F). Moreover, the F-actin network looked thinner and more disorganized. Thus, although myosin II activity is dispensable for F-actin flow, it limits cell spreading and maintains synaptic integrity over time.

#### *Inhibition of myosin IIA and F-actin turnover arrests cytoskeletal retrograde flow*

Having analyzed F-actin and myosin II inhibitors separately, we next evaluated their cumulative effect on cytoskeletal dynamics. T cells were pretreated with Y-27632 and allowed to interact with the anti-CD3-coated glass to allow spreading. Jas was then added to the chamber, resulting in arrest of F-actin retrograde flow within ~30 seconds (Figure 2.6 A and Movie 2I). The “frozen” network persisted for several minutes but then thinned and eventually dissipated (data not shown). To verify the complete lack of dynamics, we bleached a region within the LP. Cells treated with Y-27632 and Jas showed no fluorescence recovery, while control cells recovered normally (Figure 2.6 B). Similar results were observed in primary T cell blasts treated with Y-27632 and Jas (Movie 2J), and in Jurkat T cells treated with blebbistatin and Jas (data not shown). In T cells suppressed for myosin IIA by siRNA, Jas treatment did not result in complete loss of actin dynamics; instead a slow, partial collapse of the actin network was observed (Figure 2.7 A and Movie 2K). This may reflect the activity of residual myosin IIA (~25%); or

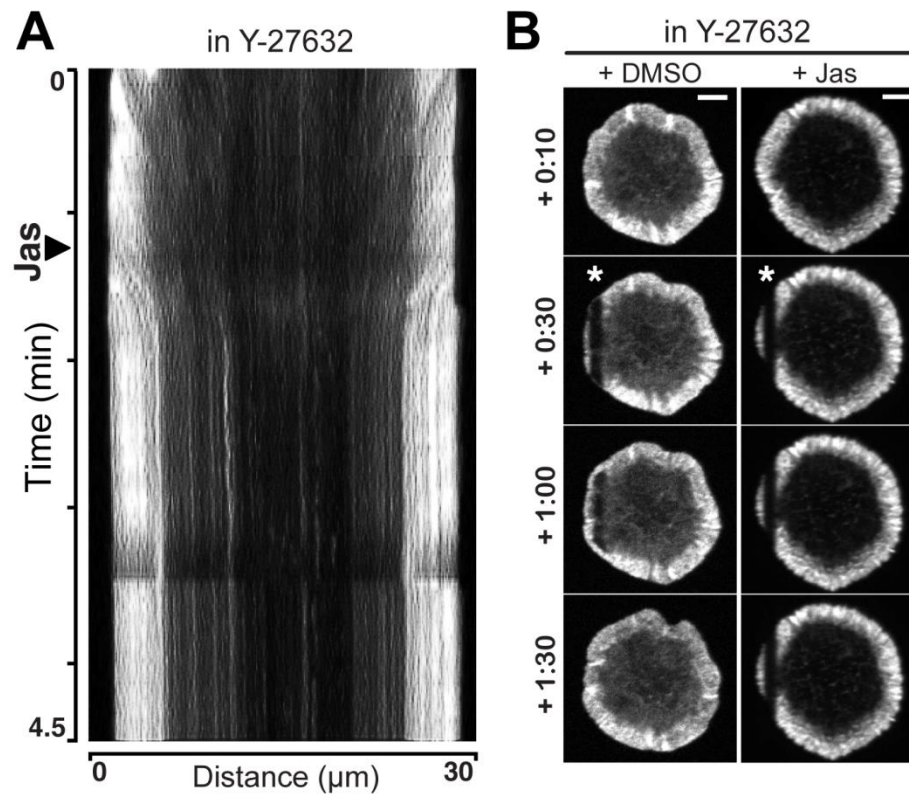


**Figure 2.6. Inhibition of myosin IIA and F-actin stabilization arrests retrograde flow.**

(A) Kymograph was generated along the diameter of a cell pretreated with 25  $\mu\text{M}$  Y-27632 and spreading on OKT3-coated coverglass. Arrowhead along the time axis indicates the addition of 1  $\mu\text{M}$  Jas to the well. The kymograph was sharpened in Photoshop to accentuate F-actin features. (B) Time-lapse series of cells pretreated with 25  $\mu\text{M}$  Y-27632 and allowed to interact with the stimulatory surface for 5 minutes before addition of either DMSO or 1  $\mu\text{M}$  Jas. 30 seconds after the treatment a portion of F-actin, marked with asterisk (\*), was photo-bleached and fluorescence recovery was recorded. Scale bars, 5  $\mu\text{m}$ .

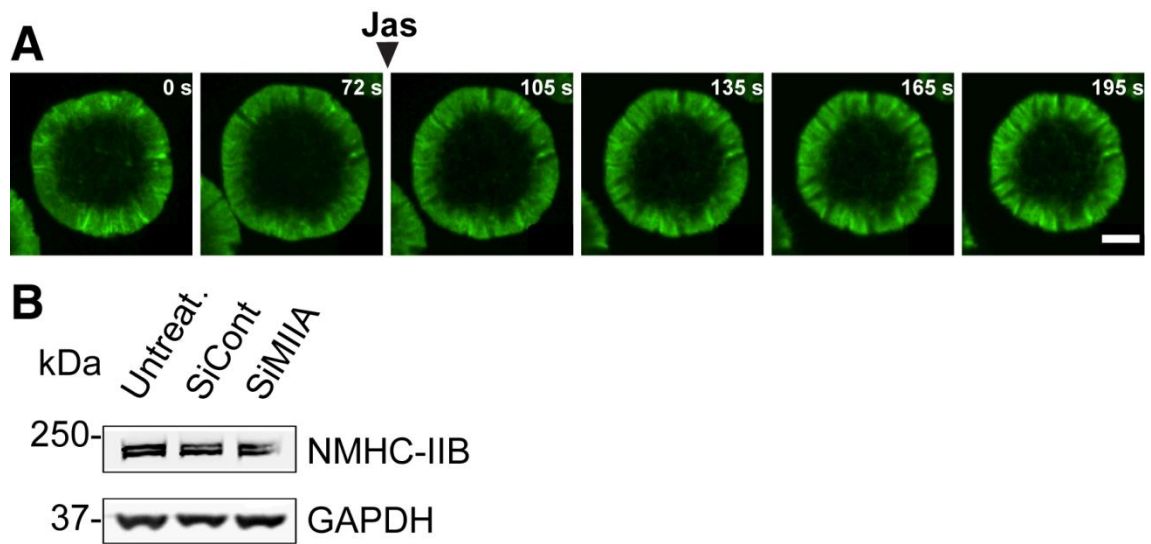


**Figure 2.7. Assessment of F-actin dynamics in response to Jas treatment of cells suppressed for myosin IIA.**

(A) Time-lapse series of Jurkat T cell spreading on OKT3-coated coverglass. At the indicated time, 1  $\mu$ M Jas was added to the imaging well. Scale bars, 5  $\mu$ m. (B) Western blot analysis of myosin IIB expression in Jurkat T cells suppressed for Myosin IIA (same lysates as in Figure 2.5 D, bottom).

the function of myosin IIB, which is also expressed in these cells (Figure 2.7 B). Taken together, these studies show that actin polymerization is the primary engine for retrograde F-actin flow in T cells. Continuous F-actin flow is driven by ongoing assembly of actin filaments in the LP, coupled to disassembly in the LM, with overall organization provided by myosin II motors.

*Depletion of actin-capping protein IQGAP1 accelerates the F-actin network flow*

As a corollary to our studies of F-actin immobilization, we wondered if the network can instead be accelerated in some way. Because F-actin retrograde flow is the net result of polymerization-depolymerization kinetics, we decided to take the cell biological approach to assess the effects of perturbing the F-actin turnover balance on network centralization. IQGAP1 is an actin-binding protein with barbed end-capping activity (Pelikan-Conchaudron et al., 2011). We thus hypothesized that IQGAP1 may regulate F-actin dynamics during TCR signaling. Jurkat T cells expressing GFP-actin were depleted of IQGAP1 using shRNA. Knockdown of IQGAP1 routinely resulted in a nearly complete loss of protein (data not shown). T cells were then imaged while spreading on OKT3-coated coverglass. Confocal imaging showed that IQGAP1-deficient T cells spread to a greater extent and the network was denser as indicated by the increased fluorescence at the IS (Figure 2.8 A and Movie 2L). Furthermore, kymography analysis showed that T cells lacking IQGAP1 had faster F-actin retrograde flow relative to that of the control cells (Figure 2.8 B) The lamellipodia also occupied a larger portion of the synapse area than those in control counterparts. Taken together with the above

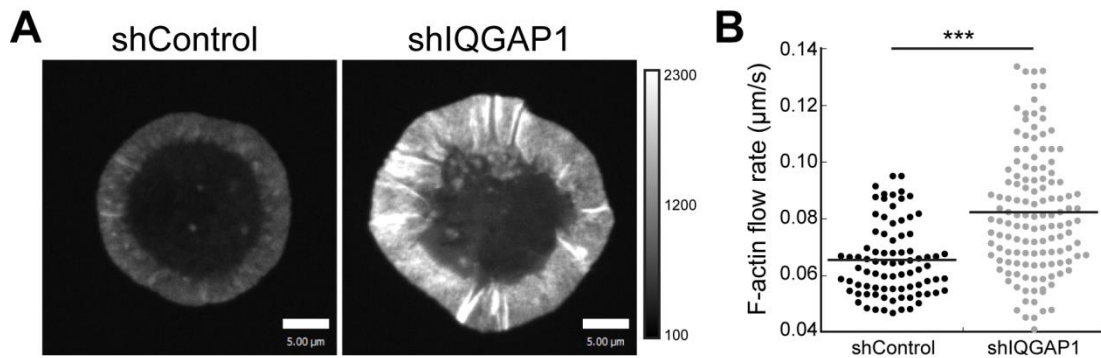


**Figure 2.8. IQGAP1 knockdown in Jurkat T cells accelerates F-actin dynamics at the IS\*.**

(A) Jurkat T cells stably expressing GFP-actin were transfected with empty vector or shIQGAP1 plasmid. Cells were imaged 72 hr. post transfection, while spreading on OKT3-coated coverglass. 0.5  $\mu\text{m}$ -thick Z stacks were collected just above the glass, using the same exposure settings for all cells and representative images are shown as extended projections. Scale bars, 5  $\mu\text{m}$ . (B) F-actin flow rates were analyzed using kymographs drawn along the radii of spreading cells. Data represent mean  $\pm$  SD of at least 140 kymographs from at least 36 cells, pooled from two independent experiments. \*\*\* $p < 0.001$ .

\* These data were published in the manuscript titled:

The Cytoskeletal Adaptor Protein IQGAP1 Regulates TCR-Mediated Signaling and Filamentous Actin Dynamics.

Journal of Immunology. June 2012; Volume 188, pp. 6135-6144.

With the following list of authors: Gorman JA, Babich A, Dick CJ, Schoon RA, Koenig A, Gomez TS, Burkhardt JK, and Billadeau DD.

observations, these data suggest that F-actin network dynamics can be modulated to accelerate or to arrest the retrograde flow.

*F-actin retrograde flow governs SLP-76 MC centralization*

The mechanisms linking MC movement and signaling to F-actin dynamics are poorly understood. Furthermore, recent studies show that microtubules can direct MC movement (Bunnell et al., 2002; Hashimoto-Tane et al., 2011; Lasserre et al., 2010). We took advantage of our ability to manipulate actin flow to examine the relationship between the actomyosin network and SLP-76 MC dynamics. Since we were unsuccessful in raising a stable cell line expressing fluorescently tagged actin and SLP-76, we imaged a mixture of GFP-SLP-76 and GFP-actin expressing T cells to conduct side-by-side analysis of these proteins in response to pharmacological intervention. As expected, treatment with Y-27632 did not perturb F-actin flow (Figure 2.9, before Jas injection). SLP-76 MCs also continued to centralize normally in the presence of Y-27632, indicating that myosin II activity is dispensable for their dynamics (Figure 2.9 B). After addition of Jas, however, MC centralization was arrested concomitantly with the arrest of F-actin (Figure 2.9 A, after Jas, Movie 2M). Interestingly, even MCs close to the center, where F-actin was sparse, stopped their movement. This result is also shown in maximum-over-time projections of movie sequences (Figure 2.9 C). In these images, moving SLP-76 MCs, seen as radial streaks, are readily apparent in cells treated with Y-27632 alone, but only stationary SLP-76 MCs, projected as dots, are evident after the “freeze” of the F-actin

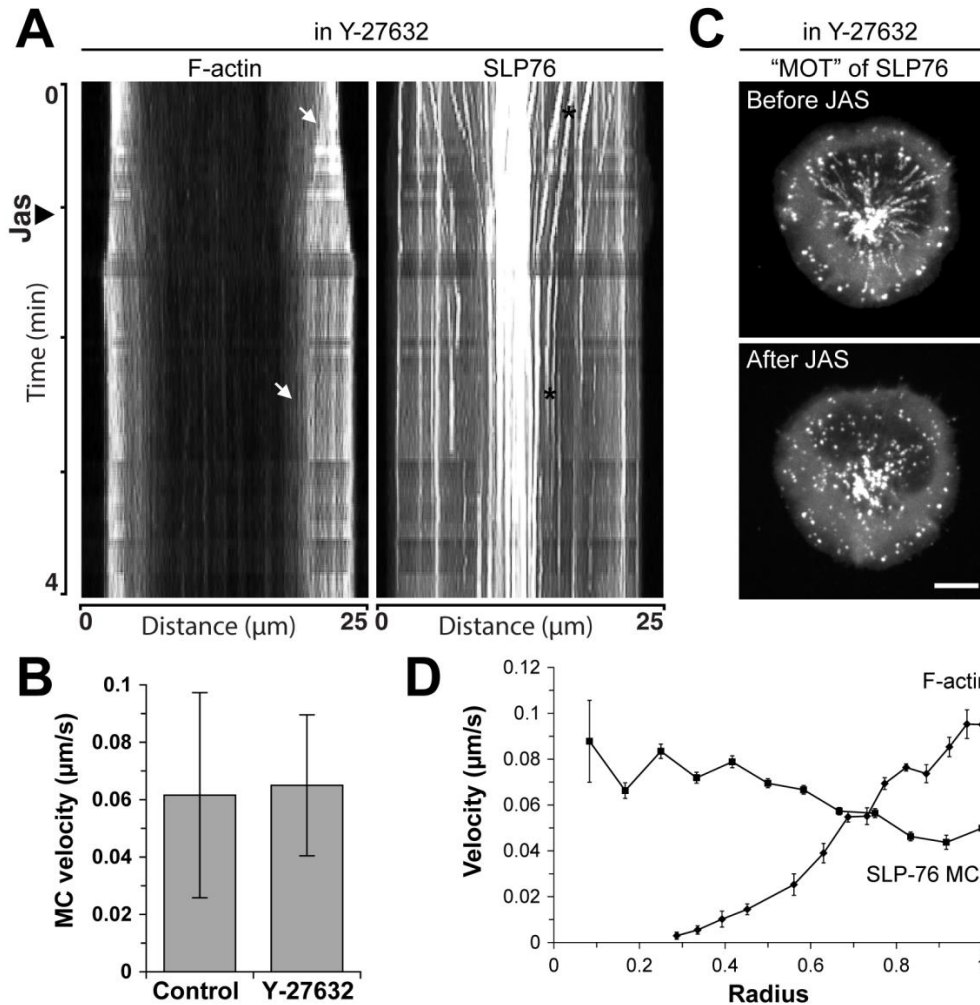


**Figure 2.9. F-actin governs MC dynamics but has different velocity distribution across the IS.**

(A) Kymographs were generated along the diameter of cells expressing GFP-actin and GFP-SLP-76, and sharpened in Photoshop. Arrowhead along the time axis indicates the addition of 1  $\mu\text{M}$  Jas. (B) Jurkat T cells expressing GFP-SLP76 were pretreated with either vehicle control or Y-27632 and allowed to spread on OKT3-coated coverglass. Velocities of SLP-76 MCs were analyzed by kymography (mean  $\pm$  SD,  $n = 40$ -150 MCs from 10-19 cells). (C) "Maximum-over-time" images GFP-SLP-76 Jurkat T cells were compiled from the images acquired before or after the addition of Jas. Scale bars represent 10  $\mu\text{m}$ . Images are representative of three independent experiments. (D) Comparative analysis of SLP-76 MC centripetal velocity from a single cell overlaid with F-actin dynamics from Figure 2.1 E. Mean  $\pm$  SEM.

network. Finally, it is important to note that no new MCs formed in the absence of F-actin retrograde flow (data not shown). Taken together, these observations suggest that dynamic F-actin, and not simply F-actin accumulation at the IS, is required for SLP-76 MC nucleation and centripetal movement.

*SLP-76 MC dynamics do not correlate with F-actin behavior*

Qualitatively, SLP-76 MC centralization did not resemble actomyosin movement, e.g. MCs often gathered at the center of the IS where little F-actin was present to facilitate their movement (Figure 2.10 A and Movie 2N). We therefore performed careful quantitative measurements of MC velocity, to seek clues to the driving mechanism. Particle tracking and kymography analysis yielded very similar results. Both techniques revealed that SLP-76 MC centralized with relatively constant velocity, averaging  $0.065 \pm 0.059 \mu\text{m/s}$  based on particle tracking and  $0.059 \pm 0.034 \mu\text{m/s}$  based on kymography (Figure 2.10). This differs dramatically from the behavior of F-actin, which decelerated with inward movement. F-actin and SLP-76 MC centripetal velocity distributions are overlaid in Figure 2.9 D. From this analysis, it is evident that although F-actin retrograde flow could drive SLP-76 MC movement in the periphery of the IS, SLP-76 MCs actually move faster than the F-actin network in the LM and CB regions. Thus, a second mechanism is needed to account for MC dynamics in these regions.



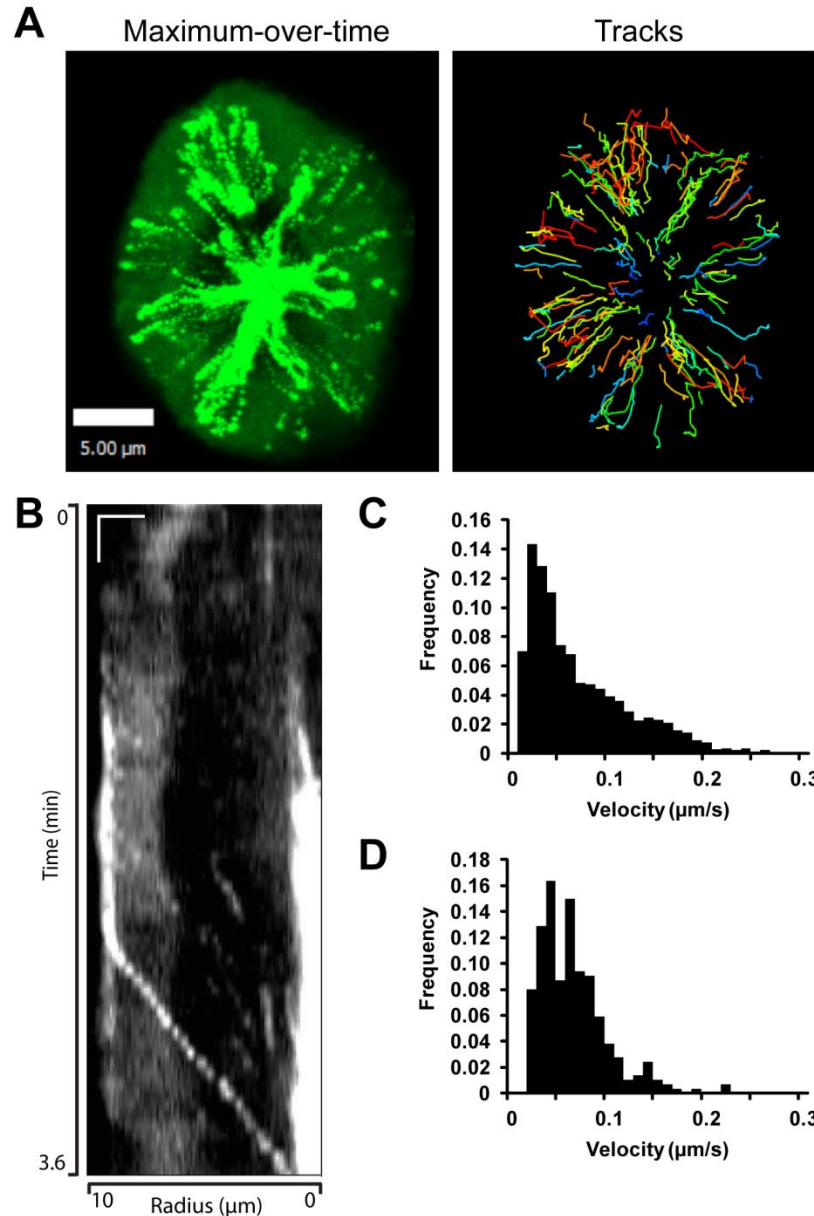


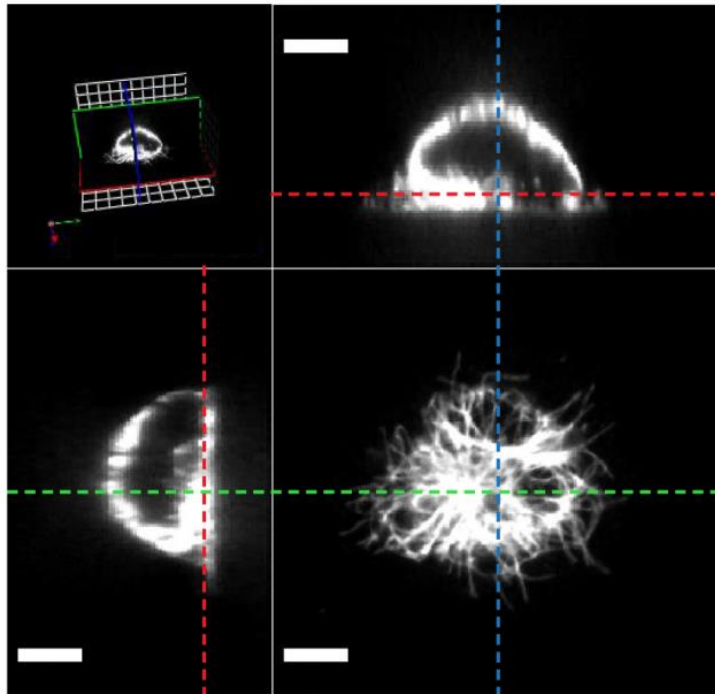
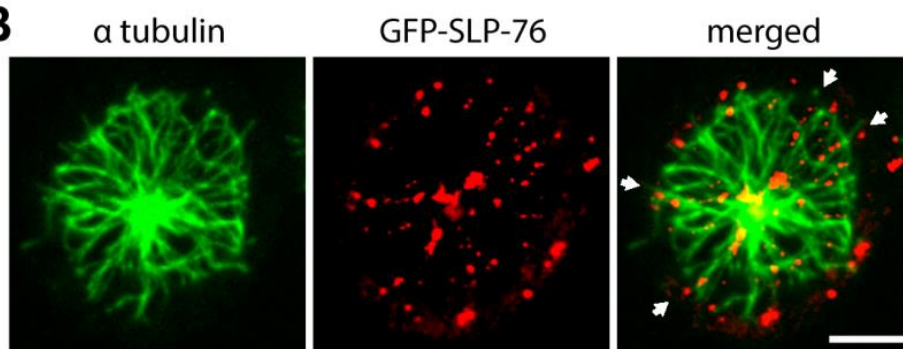
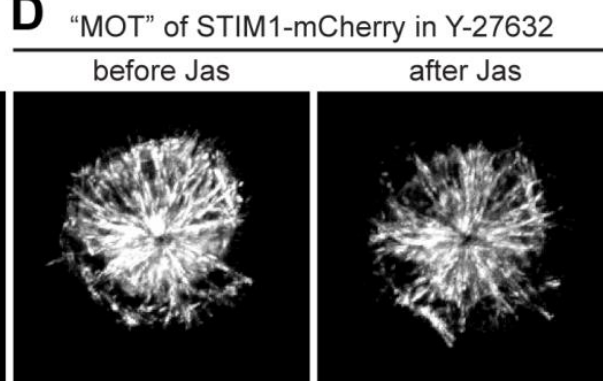
**Figure 2.10. Measurement of SLP-76 MC velocities at the IS**

(A) Left: “Maximum-over-time” projection of a video of SLP-76 MCs centralizing at the IS. Right: Tracks calculated from the same cell as on the left using shortest path algorithm in Velocity. Scale bar, 5  $\mu\text{m}$ . (B) Kymograph generated along the path of a mobile SLP-76 MC. Scale bar represents 2  $\mu\text{m} \times 15$  s. (C) Histogram of apparent instantaneous velocity distribution from the cell in (A),  $n = 6407$ . (D) Histogram of average velocity distribution from a cell population ( $n = 287$  measurements) found using kymography analysis.

*Dynamic microtubule network translocates to the IS in close proximity to SLP-76 MCs*

The discrepancy between the rates of F-actin and SLP-76 MC centralization pointed us in the direction of a microtubule-dependent mechanism. Indeed, multiple reports implicated microtubules and microtubule-dependent motor cytoskeletal dynein in the organization of signaling complexes at the IS (Hashimoto-Tane et al., 2011; Lasserre et al., 2010; Schnyder et al., 2011). Yet, to date, the verdict on the microtubule function in MC dynamics remains controversial. This undoubtedly reflects the complexity of signaling machinery in question. We, therefore, wanted to investigate further the role of microtubules in the organization of the synaptic architecture. Confocal imaging and 3D reconstruction of Jurkat T cells spreading on OKT3-coated glass and immunostained for  $\alpha$  tubulin revealed that microtubules polarized towards the IS and assumed a radial distribution resembling the maximum-over-time projections of MC dynamics (Figure 2.11 A, compare with Figure 2.10 A). While live-cell imaging of SLP-76 and microtubules was less than conclusive, fixed-cell imaging of GFP-SLP-76 cells stained for  $\alpha$  tubulin revealed that microtubules were found in close proximity to GFP-SLP76 MCs, especially in the center of the IS (Figure 2.11 B). Thus we confirm the current notion that microtubules are positioned closely to the MCs to facilitate their movement in the central region of the IS.

We then wondered whether the drug treatment that induces F-actin immobilization could perturb microtubule assembly and dynamics. A convenient way to evaluate microtubule turnover is to look at dynamics of microtubule-plus-end-tracking proteins (+TIPs) such as EB1 or STIM1, which binds directly to EB1 and thus also serves as a marker of growing microtubule ends (Grigoriev et al., 2008). We transfected GFP-actin

**A****B****C****D**

**Figure 2.11. Dynamic microtubule network translocates to the IS proximally to SLP-76 MCs.**

(A) E6.1 Jurkat T cells were dropped on OKT3-coated coverglass and allowed to spread for 15 min. Cells were fixed and stained for microtubules. 3D reconstruction of confocal Z-stacks was performed to assess recruitment of microtubule network to the IS. Scale bar, 5  $\mu\text{m}$ . (B) Jurkat T cells stably expressing GFP-SLP-76 were stained as in (A) and imaged just above the glass. Arrows point to streaks of SLP-76 MCs that lie in close contact with the microtubules. Scale bar, 10  $\mu\text{m}$ . (C) GFP-actin Jurkat T cells were transiently transfected with STIM1-mCherry and stimulated as above. Live-cell confocal imaging was performed just above the glass interface. A single frame from a movie sequence is shown. (D) ‘‘Maximum-over-time’’ projections of STIM1-mCherry were compiled from the images sequences acquired before (left) and after (right) the addition of Jas to cells pretreated with Y-27.

Jurkat T cells with STIM1 fluorescently labeled with mCherry at C terminus and allowed these cells to interact with the stimulatory coverglass. T cells pretreated with Y-27 (Figure 2.11 C) did not show changes in STIM1 distribution and turnover compared to the untreated cells (data not shown). During cell spreading, STIM1 localized to the IS and generally moved in clusters resembling comets, which emanated from a single point, likely MTOC (Figure 2.11 D and Movie 2O). Upon F-actin immobilization by addition of Jas STIM1 continued to move at seemingly unchanged rate and frequency. We conclude that F-actin remodeling is not required to maintain microtubule turnover at the IS.

#### *Dynamic F-actin network maintains microtubules close to the PM*

The dominant role of F-actin flow in SLP-76 MC movement suggested that dynamic F-actin facilitates a global interaction between MCs and microtubules, and that upon F-actin immobilization this interaction is abrogated. Hashimoto-Tane et al. (2011) demonstrated that in activated T cells microtubules are in close proximity to the PM and associate with the membrane-bound MCs through cytoplasmic dynein-dynactin complex. We thus hypothesized that F-actin polymerization may induce local pushing forces on microtubule filaments and press them tightly against the membrane, thereby enabling MC-microtubule association. To test this possibility we resorted to TIRF microscopy, which illuminates the glass slide at an obtuse angle, creating an evanescent wave that penetrates the sample only a short distance of about 70 to 250 nm (Millis, 2012). GFP-actin Jurkat T cells were allowed to spread on OKT3-coated coverglass for 10 minutes with or without Y-27. Cells inhibited for myosin II contraction were then further subjected to Jas treatment for 5 additional minutes. After that, cells were fixed and

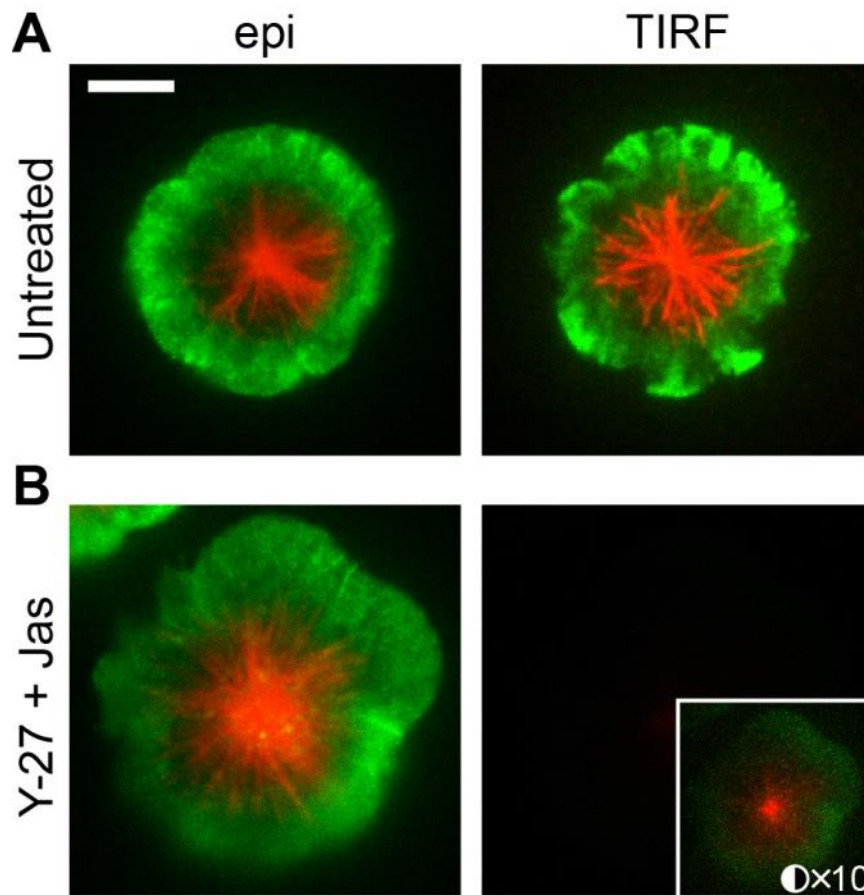


**Figure 2.12. Dynamic F-actin network presses microtubules against plasma membrane at the IS.**

(A and B) GFP-actin Jurkat cells were pretreated with Y-27 for 15 min or left untreated and then allowed to spread on OKT3-coated glass for 10 minutes. Y-27 treated cells were then further treated with Jas so stop the actin flow for 5 min. Cells were then fixed and stained for alpha-tubulin. Untreated (A) and flow-inhibited (B) cells were imaged in widefield and in TIRF (90 nm depth of view). The inset in B shows the same cell in TIRF but with contrast increased 10-fold. Scale bar, 10  $\mu$ m.

stained for microtubules. Widefield imaging confirmed previous observations that microtubules assume an asterisk-like pattern at the IS (Figure 2.12 A, left). This distribution was even more pronounced in the TIRF plane with evanescent wave penetration depth of 90 nm (Figure 2.12 A, right). “Freezing” the F-actin flow did not reduce the amount of microtubules as observed by epifluorescence imaging (Figure 2.12 B, left), however, these microtubules were completely gone from the TIRF plane ( $n > 50$  cells) (Figure 2.12 B, right). Interestingly, immobilized F-actin network also moved away from the PM. Dim fluorescence for both cytoskeletal networks was observed only when the contrast ratio was increased 10-fold (Figure 2.12 B, inset). Collectively, these results indicate that F-actin and microtubules function as a complex unit, whereby F-actin dynamics regulate tight positioning of the microtubule tracks at the IS.

#### *F-actin dynamics are necessary for sustained $Ca^{2+}$ signaling*

Retention of MCs in the IS periphery by integrin ligands, genetic perturbations or physical barriers correlates with enhanced T cell activation (Hashimoto-Tane et al., 2011; Mossman et al., 2005; Nguyen et al., 2008). To assess the effect of MC arrest in the context of F-actin immobilization, we first examined the effects on sustained  $Ca^{2+}$  entry, a hallmark of T cell activation (reviewed in Chapter 1) (Negulescu et al., 1994; Oh-hora, 2009). Cells were loaded with the ratiometric dye fura-2, AM and imaged while spreading on the stimulatory coverslips (Figure 2.13 A). Despite previous reports that myosin IIA contraction is essential for  $Ca^{2+}$  entry (Ilani et al., 2009), we found no difference in  $Ca^{2+}$  levels in cells pretreated with Y-27632 and control cells. Both showed a rapid increase in intracellular  $Ca^{2+}$ , with levels declining gradually over the next 15-30

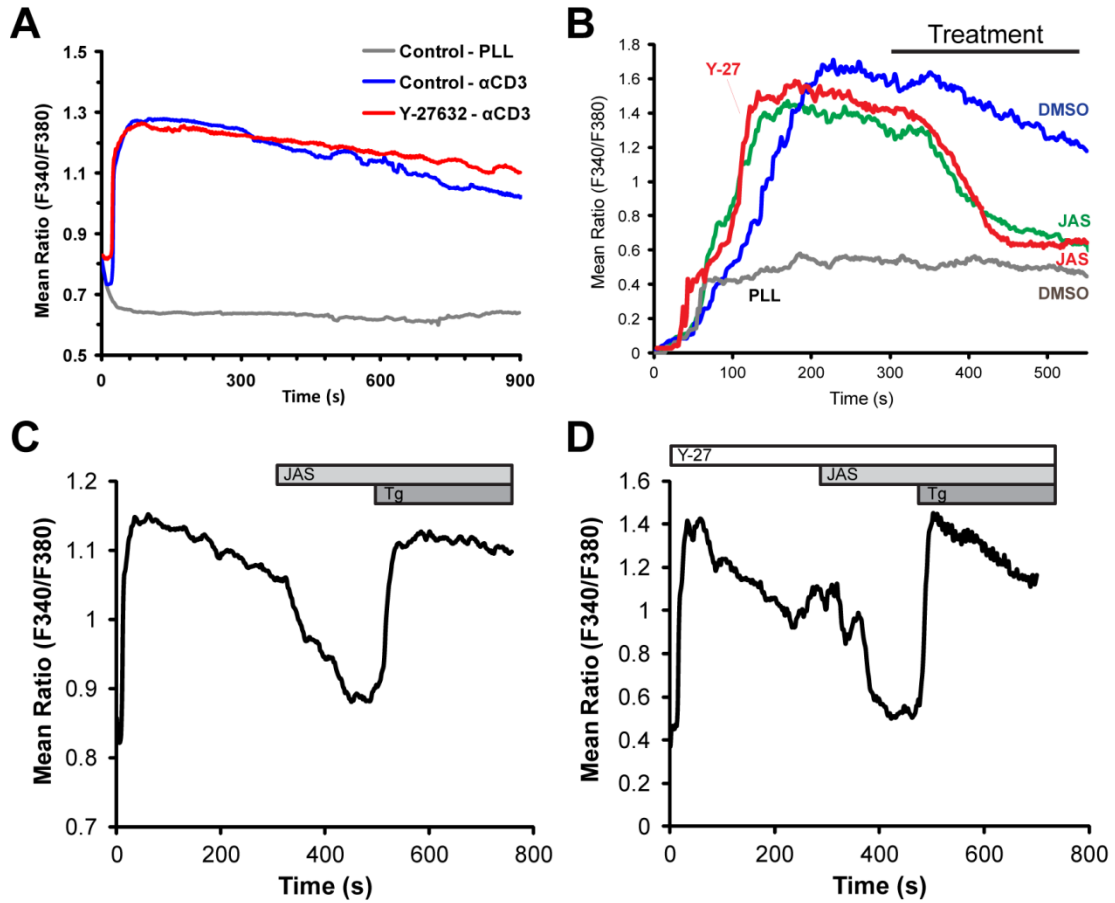


**Figure 2.13. Loss of F-actin dynamics abrogates sustained  $\text{Ca}^{2+}$  signaling by perturbing  $\text{Ca}^{2+}$  release from ER stores.**

(A) GFP-actin Jurkat T cells were pretreated with 25  $\mu\text{M}$  Y-27632 or left untreated and loaded with fura-2 before plating on OKT3- or PLL-coated coverglass in 2 mM  $\text{Ca}^{2+}$ . (B) Cells were pretreated as in (A) and allowed to interact with the stimulatory surfaces for 5 minutes. DMSO or Jas was then added to the imaging chamber and the response was measured for another 5 minutes. Similar results were obtained from three independent experiments. (C and D) Cells were pretreated as in (B). 1  $\mu\text{M}$  Tg was added to the dishes to induce  $\text{Ca}^{2+}$  release from ER stores.



minutes. To assess the “freeze” condition, we pretreated cells with Y-27632 and allowed them to spread on OKT3 for 5 minutes before application of Jas (Figure 2.13 B, red line). Intracellular  $\text{Ca}^{2+}$  levels began to drop within 30 seconds of Jas addition, roughly the same lag period observed for F-actin arrest (Figure 2.6 A). Within 3 minutes,  $\text{Ca}^{2+}$  had diminished to baseline levels, as defined by cells interacting with poly-L-lysine alone. A similar loss of sustained intracellular  $\text{Ca}^{2+}$  was observed when cells were treated with Jas alone (Figure 2.13 B, green line), indicating that F-actin turnover is essential for sustained  $\text{Ca}^{2+}$  signaling.

Loss of intracellular  $\text{Ca}^{2+}$  could result from changes in  $\text{Ca}^{2+}$  release from ER stores or from inhibition of  $\text{Ca}^{2+}$  entry through CRAC channels in the PM. To test if the defect was at the level of ER store release, we treated cells with either Jas alone (Figure 2.13 C) or Y-27632+Jas (Figure 2.13 D) to inhibit  $\text{Ca}^{2+}$  signaling, and then added the SERCA pump inhibitor thapsigargin (Tg) to pharmacologically empty ER stores. In both cases, Tg treatment restored intracellular  $\text{Ca}^{2+}$  to normal levels, indicating that CRAC activity remains intact when F-actin is immobilized. Taken together, these data show that F-actin retrograde flow maintains sustained  $\text{Ca}^{2+}$  signaling by regulating  $\text{Ca}^{2+}$  release from ER stores.

#### *F-actin retrograde flow maintains activation of PLC $\gamma$ 1 in MCs*

$\text{Ca}^{2+}$  store release is regulated by signaling through PLC $\gamma$ 1-dependent cleavage of PIP<sub>2</sub> to generate IP<sub>3</sub>, which stimulates receptors in the ER membrane (Zhang et al., 1999). To ask if PLC $\gamma$ 1 activation is intact in T cells under conditions where F-actin dynamics

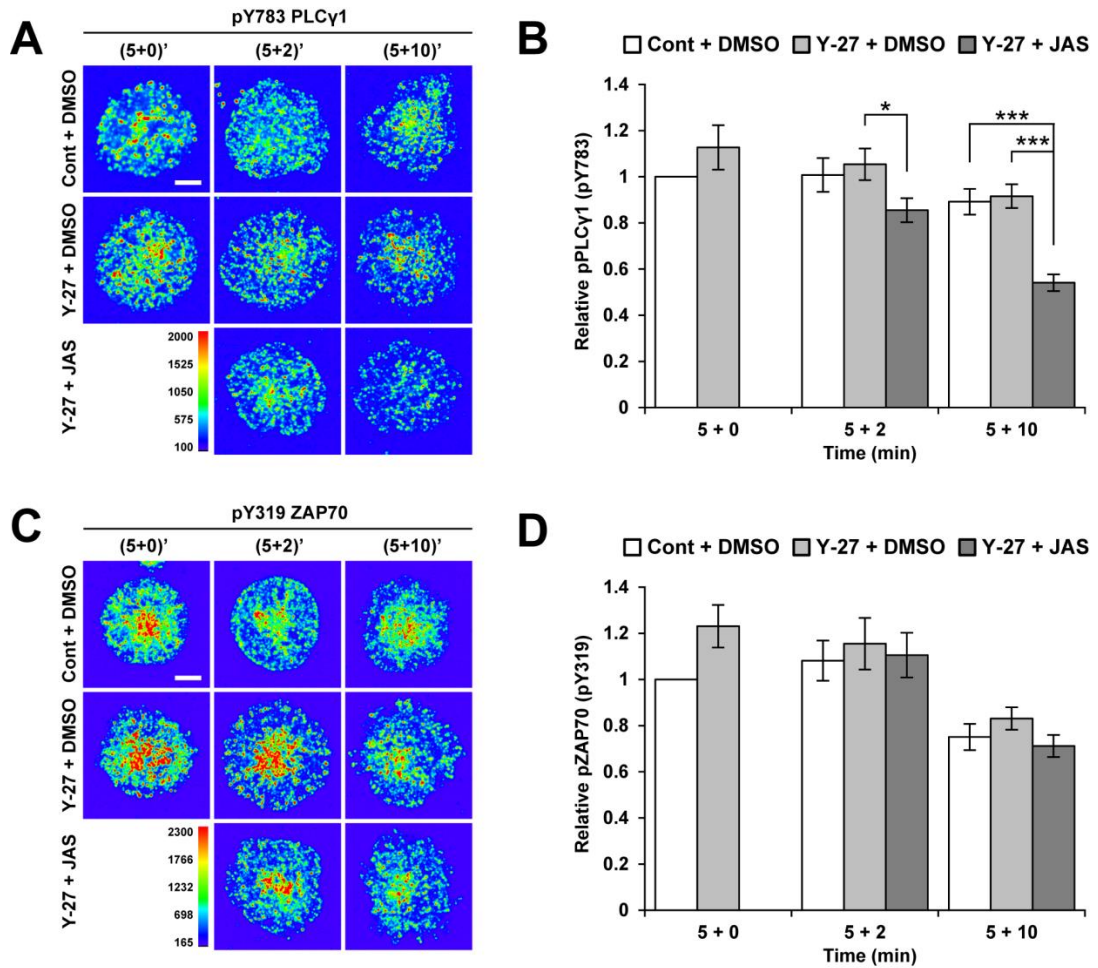


**Figure 2.14. F-actin immobilization selectively inhibits PLC $\gamma$ 1 phosphorylation.**

(A and B) GFP-actin Jurkat T cells were either pretreated with 25  $\mu$ M Y-27632 or left untreated, and plated on OKT3-coated coverglass. After 5 min, cells were treated with DMSO or Jas, then fixed at the indicated times and stained for phospho-Y783 of PLC $\gamma$ 1 (A) or phospho-Y319 of Zap70 (B). Intensity of antibody staining is pseudo-colored. Scale bars, 5  $\mu$ m. (C and D) Analysis of fluorescence intensities from phospho-PLC $\gamma$ 1 (A) or phospho-Zap70 (B) staining. The IS boundaries were gauged by F-actin intensity; phospho-Y intensity per IS was calculated by integrating pixel intensity over IS area. Mean  $\pm$  SEM, \*  $p < 0.05$ , \*\*\*  $p < 0.001$ .

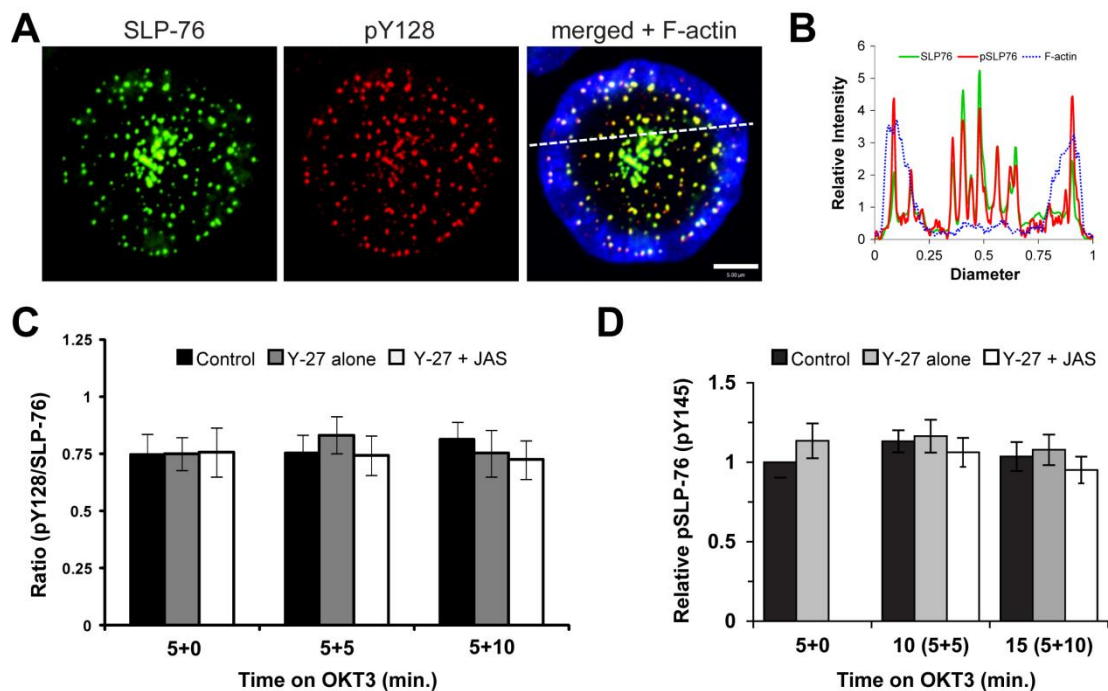


**Figure 2.15. Assessment of SLP-76 phosphorylation in response to F-actin immobilization.**

(A) Jurkat T cells expressing GFP-SLP-76 were allowed to interact with the stimulatory surface. Cells were fixed after 5 minutes and stained for F-actin and phospho-Y128 of SLP-76; a sample cell is shown. Scale bar represents 5  $\mu$ m. (B) Relative fluorescence intensities along the dashed line in (A). (C) Average ratios of fluorescence intensities of phospho-Y128 SLP-76 and total GFP-SLP-76. Cells were pretreated with Y-27632 or left untreated, then allowed to spread for 5 min. Jas was added where indicated and cells allowed to spread further for the indicated times. Mean  $\pm$  SEM (average n = 3410 MCs from average of 23 cells per condition). (D) Relative total fluorescence intensities of phospho-SLP-76 (pY145) obtained from synapses of GFP-actin-expressing Jurkat T cells fixed and stained as in (A). Mean  $\pm$  SEM, average of 30 cells per condition.

have been perturbed, cells were incubated in the presence or absence of Y-27632 and allowed to spread on OKT3-coated surfaces. After 5 minutes, cells were treated with vehicle alone or with Jas to “freeze” the actin network. Cells were fixed at either early times of treatment (5 min + 2 min) or late times (5 min + 10 min), and labeled for PLC $\gamma$ 1 phosphorylated at Y783, which represents the active enzyme pool (Kim et al., 1991). Control T cells formed numerous MCs containing pPLC $\gamma$ 1, and these became more prevalent within the central regions of the IS at the later time points (Figure 2.14 A). Treatment of cells with Y-27 alone had little effect on the intensity of pPLC $\gamma$ 1 staining or in the distribution of pPLC $\gamma$ 1 MCs, consistent with our finding that Ca<sup>2+</sup> signaling is intact in these cells. In contrast, treatment with Y-27 together with Jas resulted in a loss of pPLC $\gamma$ 1 signal at the IS. Loss of pPLC $\gamma$ 1 intensity was detectable by 2 minutes after Jas treatment and further decreased over time; by 10 minutes the pPLC $\gamma$ 1 signal was only 59% of control (Figure 2.14 B). Interestingly, loss of F-actin dynamics did not affect phosphorylation of Zap70 at Y319 (Figures 2.14 C and D). Furthermore, SLP-76 phosphorylation at positions Y128 or Y145 showed no dependence on myosin IIA or F-actin dynamics (Figure 2.15). These results indicate that F-actin dynamics selectively maintain IS-associated PLC $\gamma$ 1 activation, leading to sustained Ca<sup>2+</sup> signaling.

#### **IV. Discussion**

The central role of the actin cytoskeleton in T cell activation was recognized in the 1980s, but exactly how actin orchestrates T cell signaling has remained enigmatic. Early studies relying on actin depolymerizing agents could demonstrate a requirement for actin, but could not define whether actin functions as a static scaffold or whether dynamic processes such as turnover and motility were involved. More recent studies have

successfully addressed the role of individual actin regulatory proteins, but this approach does not provide a sense of the coordinated behavior of the cytoskeletal network. In this study, we took a pharmacological approach combined with genetic intervention to systematically study the roles of actin polymerization and myosin II contraction in controlling protein dynamics and signaling at the IS. Our findings demonstrate that the actomyosin network is a complex functional unit, with retrograde flow driven primarily by actin polymerization, and organizing contractile forces provided by myosin II. We show that ongoing actin polymerization is required for centralization of signaling MCs, for positioning of microtubule network and for tyrosine phosphorylation events leading to sustained  $\text{Ca}^{2+}$  mobilization.

The actomyosin network in spreading T cells exhibits an actin-rich periphery, an actomyosin-rich ring, and central actomyosin poor region corresponding to the LP, LM and CB regions of other cell types (Cai et al., 2006). In particular, IS cyto-architecture bears a striking resemblance to that of fish keratocytes (Yam et al., 2007), cells used as a model of protrusion-based motility. In keratocytes, as in T cells, actin retrograde flow is very fast [40-100 nm/s, vs. 5-8 nm/s in some epithelial cells (Ponti et al., 2004)]. Our estimates of actin retrograde flow rates within the LP are in good agreement with values in the literature (Nguyen et al., 2008; Yu et al., 2010a). However, we find that actin flow slows with movement toward the CB. This behavior has been previously noted in T cells (Yu et al., 2010a), and is also observed in keratocytes (Yam et al., 2007). Based upon studies pioneered in keratocytes (Wilson et al., 2010), we used a panel of pharmacological inhibitors to dissect the roles of actin polymerization and myosin II contraction in driving overall flow of the T cell actomyosin network. We show that actin

polymerization generates most of the force in this system. Previous work shows that this polymerization is carried out by the Arp2/3 complex in response to activation by WAVE2, HS1 and WASp (Gomez et al., 2007; Gomez et al., 2006; Nolz et al., 2006). While we did not find a role for myosin IIA in driving F-actin flow, we did find that myosin II activity maintains the radial symmetry and overall organization of the IS, presumably by cross-linking antiparallel actin filaments and creating a meshed network that functions as a synchronous unit. Moreover, as in non-hematopoietic cells (Cai et al., 2006), myosin IIA activity limits T cell spreading, and promotes a contraction phase during IS maturation. This contraction phase is similar to, albeit more modest than, the response in B cells during antigen gathering (Schnyder et al., 2011). Interestingly, Jurkat T cells also express myosin IIB (Figure 2.7 B and (Jbireal et al., 2010)). Partial contraction was observed in cells suppressed for myosin IIA and treated with Jas, suggesting that either residual myosin IIA (~25%) or myosin IIB contribute to contractile forces in these cells.

Quantitative comparison of F-actin and SLP-76 MC velocities yielded surprising results. Within the LP region, we found that SLP-76 MC centralization was slower than actin retrograde flow by a factor of approximately 0.7. This effect was reported previously by Nguyen et al. (2008), and was interpreted as a “duty ratio”, representing intermittent attachment/detachment of MCs to the continuously moving F-actin network. Similar observations were reported for integrin and TCR MCs, where the duty ratio with actin was ~0.4 (Kaizuka et al., 2007). Strikingly, however, we show that while actin flow slows with centripetal movement, SLP-76 MCs exhibit relatively uniform velocity, and ultimately outpace the actomyosin network. We conclude that actin retrograde flow

cannot be the sole driver of MC centralization, and that other forces must be at play. It seems likely that microtubules are involved, since recent studies show that cytoplasmic dynein drives TCR MC movement into the cSMAC (Hashimoto-Tane et al., 2011). While a “hand-off” from actin in the IS periphery to microtubules in the IS center could be envisioned, there is evidence for a more complex mechanism. First, MCs do not collapse onto the MTOC after F-actin depolymerization (Nguyen et al., 2008; Varma et al., 2006). Second, we find that virtually all MC movement is arrested under conditions that “freeze” actin flow, even within the actin-poor cSMAC region. Furthermore, we and others present evidence of alteration of the microtubule network in response to perturbation of actin binding proteins such as ezrin (Lasserre et al., 2010). These observations, together with our finding that ongoing F-actin polymerization-derived force is required to maintain the microtubule cytoskeleton in close opposition to the PM, point to an intimate crosstalk between the F-actin and microtubule networks, and to simultaneous interaction of MCs with both networks (Lasserre and Alcover, 2010).

The pharmacological approach used here sheds new light on the role of actin scaffolding, actin turnover, and myosin II contraction on specific aspects of T cell signaling. The requirement for myosin II in TCR signaling has been debated (Hammer and Burkhardt, 2013). Jacobelli et al. (2004) found that myosin IIA suppression or inhibition in mouse primary T cells (which express only myosin IIA isoform) affected T cell polarity and migration but not IS formation. However, Ilani et al. (2009) reported that inhibition of myosin II or suppression of Myh9 diminished tyrosine phosphorylation and ablated  $\text{Ca}^{2+}$  signaling. In our hands, myosin II activity was not needed for cell spreading or F-actin retrograde flow in Jurkat or human primary T cells. Moreover, in Jurkat T

cells, we found that myosin II inhibition did not affect MC centralization, tyrosine phosphorylation or  $\text{Ca}^{2+}$  flux. The explanation for these conflicting results is not clear but may involve differences in experimental approaches. In particular, while we used glass coverslips coated with immobilized anti-CD3, Ilani et al used supported lipid bilayers coated with anti-CD3 and ICAM-1. It will be interesting to examine whether the requirement for myosin IIA depends on ligand mobility or on integrin-mediated firm adhesion, which enhances T cell spreading on bilayers (Grakoui et al., 1999).

The Hammer lab had published a study that is closely related to the work in this chapter, describing the actomyosin network in Jurkat T cells (Yi et al., 2012). Our findings support and extend those of Yi et al., and the areas where our results differ are informative. We observed lamellipodial, lamellar, and actin-poor regions of the IS, in excellent agreement with the regions described by Yi et al. Two comparatively minor differences exist between the two studies with respect to cyto-architecture. First, Yi et al. emphasize the presence of actomyosin arcs within the lamellar region. We, too, observe these structures, although in our hands they are rarely obvious, and only become prominent in cells expressing high levels of F-tractin or myosin IIA heavy chain. Second, Yi et al. reported a sharp LP/LM boundary, like that found in tightly adherent migrating cells (Ponti et al., 2004), however we have analyzed retrograde flow rates with 1-2  $\mu\text{m}$  resolution across this region, and find that actin deceleration is a linear function of IS radius. Moreover we observe that actin speckles traverse this boundary. Thus, we conclude that actin flow at the LP/LM boundary undergoes a gradual transition similar to that found in loosely adherent cells such as keratocytes (Yam et al., 2007). Another area where our results differ from those of Yi et al. concerns the contribution of myosin II to



driving actin retrograde flow. Both studies show that actin polymerization provides a large component of the force driving retrograde flow of the actomyosin network, while myosin II contraction imposes radial organization on the network. However, we observed no effect of myosin II inhibition or suppression on actin retrograde flow, while Yi et al. show slowing of the actin network in blebbistatin-treated cells to about 60% of controls. This difference may be due to the stimulatory surfaces used (immobilized anti-CD3 vs. mobile anti-CD3 and ICAM-1).

Probably the most informative difference between our work and Yi et al. involves the relationship of the actomyosin network to MC movement. In both cases, arresting actomyosin flow with a combination of inhibitors arrests centripetal MC movement. However, under steady-state conditions, Yi et al. show that centripetal movement TCR MCs tracks with F-actin flow, while we observed a striking disconnect between the rates of SLP-76 MC movement and actin flow. This is almost certainly due to differences in the proteins under investigation. SLP-76 MCs are known to be mobile under conditions where TCR MCs are not, and we recently showed in collaboration with the Baumgart lab that the velocity of Zap70 MCs (which presumably report on TCR localization) is affected by altered ligand mobility, while SLP-76 MCs are independent of this variable (Hsu et al., 2012). As discussed above, both types of MCs are likely to interact with both the actin and microtubule cytoskeletons, but these data point to fundamental differences in the nature or extent of these interactions.

While Yi et al. focused on describing actomyosin dynamics, we took advantage of our ability to manipulate those dynamics to probe T cell signaling under conditions that “freeze” actomyosin flow, but leave the network intact. This is a powerful technique, as it

allows us to ask for the first time if the presence of an actin scaffold is sufficient to support signaling, or if actin turnover and flow is required. Our results clearly show that ongoing F-actin dynamics are required to sustain TCR signaling. We observed a drop in intracellular  $\text{Ca}^{2+}$  almost immediately after F-actin polymerization was inhibited, regardless of whether the F-actin network was allowed to collapse inward, or was immobilized by pretreatment with myosin II inhibitors. The decrease in intracellular  $\text{Ca}^{2+}$  could be rescued by Tg treatment, indicating that CRAC channels operate normally under conditions where actin turnover is blocked. This finding is consistent with work by Mueller et al. (2007), who showed that CRAC channels function independently of cortical actin in T cells. It is currently unclear how to reconcile these findings with our previous work showing that expression of WAVE2, a key actin nucleation promoting factor, interferes with coupling of ER store release to CRAC channel opening (Nolz et al., 2006). One possibility is that the requirement for WAVE2 does not involve its actin polymerizing activity. The ability of Tg to rescue  $\text{Ca}^{2+}$  influx in actin-immobilized T cells points to a defect in  $\text{Ca}^{2+}$  release from ER stores. In keeping with this, we found diminished levels of phosphorylated  $\text{PLC}\gamma 1$  at the IS under conditions of F-actin immobilization. Phosphorylation of Zap70 and its substrate SLP-76, which lie upstream of  $\text{PLC}\gamma 1$  in the TCR signaling cascade, are intact, indicating that actin immobilization affects a specific  $\text{PLC}\gamma 1$ -proximal signaling event, possibly involving its activating kinase Itk. In keeping with this idea, both Itk and  $\text{PLC}\gamma 1$  interact with actin, and our lab previously observed defects in  $\text{PLC}\gamma 1$  function in T cells deficient for the actin regulatory protein HS1 (Carrizosa et al., 2009; Gomez et al., 2006).

Our ability to “freeze” actomyosin flow is also informative with respect to the mechano-biology of MC signaling. Retention of MCs in the IS periphery induced by integrin engagement, genetic perturbations or physical barriers correlates with enhanced T cell activation, and it has been proposed that this reflects the fact that active signaling takes place in peripheral MCs, while signal extinction takes place in the cSMAC (Hashimoto-Tane et al., 2011; Lasserre et al., 2010; Mossman et al., 2005; Nguyen et al., 2008). However, we find that peripheral MC arrest under F-actin “freeze” condition is not sufficient to enhance signaling; on the contrary, signaling is lost under these conditions. Two models are compatible with our data. First, F-actin flow could promote signaling by generating tension on receptors or signaling complexes. Such tension would be released by inhibiting F-actin flow, but enhanced by restraining ligand or MC movement. The TCR is a mechano-sensor that interacts with the actin cytoskeleton (Kim et al., 2012; Kim et al., 2009; Li et al., 2010), and actin flow could induce conformational change in the TCR. Given our results showing phosphorylation defects downstream of Zap70, however, molecules such as I $\kappa$ B or PLC $\gamma$ 1 might be the relevant, tension-sensitive molecules. Consistent with the idea that F-actin dynamics may modulate TCR function by exerting physical forces on the signaling complexes, our findings show that upon IQGAP1 depletion, T cells exhibit stronger retrograde flow of F-actin at the IS. This highlights that augmented F-actin dynamics correlate with enhanced T cell activation. Although this is not the only possible explanation for the functional effects of IQGAP1 suppression, this paradigm implicates IQGAP1 in the mechanical aspects of the TCR signaling (Gorman et al., 2012).

An alternative explanation of the necessity of retrograde flow is that signaling requires ongoing MC biogenesis. F-actin depletion blocks MC formation without perturbing older MCs and leads to loss of signaling (Campi et al., 2005; Varma et al., 2006). Similarly, interruption of TCR-pMHC interactions prevents MC formation and induces loss of intracellular  $\text{Ca}^{2+}$  without affecting MC centralization (Varma et al., 2006). Our work extends these findings: under our “freeze condition” no new MCs are formed, demonstrating that the presence of F-actin is not sufficient for MC formation; instead, ongoing polymerization is required.

Models based on tension and on new MC formation are not mutually exclusive. Indeed, we hypothesize that the two processes are mechanistically linked. We propose that peripheral F-actin-rich sites nucleate assembly of signaling complexes, which are initially associated with both extracellular ligands and the flowing cytoskeleton. Tension-induced signaling would be maximal immediately prior to initiation of MC movement, and movement would partially relieve tension and dampen signaling. This model has significant physiological implications. For example, ligand mobility on the surface of APCs is predicted to be an important parameter for modulating T cell responses, and molecules that link signaling intermediates to the cytoskeletal network should be interesting therapeutic targets. The scientific community should concentrate the efforts to address these questions and carefully test the predictions of the model.

**CHAPTER 3: ONGOING FLOW OF THE F-ACTIN NETWORK DRIVES  
AFFINITY MATURATION AND SPATIAL ORGANIZATION OF LFA-1 AT  
THE IMMUNOLOGICAL SYNAPSE<sup>56</sup>**

**I. Summary**

Integrin-dependent interactions between T cells and APCs are vital for proper T-cell activation, effector function, and memory formation. Regulation of integrin function occurs via conformational change, which modulates affinity for ligand, and molecular clustering, which modulates receptor valency. Here, we show for the first time that conformational intermediates of LFA-1 are organized in a concentric array at the IS. Using an inhibitor cocktail to arrest F-actin dynamics, we show that formation of this array depends on F-actin flow and ligand mobility. Furthermore, F-actin flow is critical for maintaining the high affinity conformation of LFA-1, and for enhancing valency through recruitment of LFA-1 to the cell-cell interface. Our data provide direct support for a model in which the T cell F-actin network generates mechanical forces that regulate LFA-1 activity at the IS.

---

<sup>5</sup> A version of this chapter has been submitted for publication, as a manuscript titled: Comrie WA, Babich A, Burkhardt JK. Ongoing flow of the F-actin network drives affinity maturation and spatial organization of LFA-1 at the immunological synapse.

<sup>6</sup> WC and AB contributed equally to the project; JB oversaw the work, contributed discussion, and provided critical revision of the manuscript

## II. Introduction

T-cell activation and specific effector function require the formation of a regulated cell-cell contact with an APC bearing cognate pMHC termed the IS. In mature IS, a distinct molecular pattern forms in which an outer ring of LFA-1 and the LFA-1 regulatory protein talin surrounds an inner region enriched in TCR and associated signaling molecules (Monks et al., 1998). These respective regions have been termed the peripheral (p-) and central (c-) SMACs. A third region distal SMAC (dSMAC) region, enriched in CD45, lies at the edge of the IS (Freiberg et al., 2002; Sims et al., 2007). This region corresponds roughly to the F-actin rich lamellipodium of migratory cells (see Figure 2.1 in Chapter 2). Signaling from the TCR occurs in microclusters that form in the IS periphery and undergo F-actin- and microtubule-dependent movement to the IS center (Campi et al., 2005; Hashimoto-Tane et al., 2011; Yokosuka et al., 2005). Most active signaling is associated with newly-formed MCs, while signal extinction occurs in the center of the IS (Varma et al., 2006).

The actin cytoskeletal network plays a central role in IS formation, and ongoing F-actin polymerization is required for TCR signaling (Billadeau et al., 2007; Burkhardt et al., 2008; Campi et al., 2005; Varma et al., 2006; Yu et al., 2013). F-actin dynamics at the IS are characterized by polymerization in the lamellipodium, with centripetal flow and filament disassembly in the central region of the IS. This process is primarily dependent on F-actin polymerization, with minor contributions from myosin IIA contractility (Chapter 2 and (Yi et al., 2012)). Simultaneous inhibition of myosin IIA contraction and F-actin polymerization results in the arrest of F-actin dynamics at the IS, with concomitant loss of  $\text{Ca}^{2+}$  signaling (Chapter 2). Conversely, conditions that increase F-

actin polymerization and retrograde flow correlate with enhanced T-cell activation and cytokine production (Gorman et al., 2012). The molecular basis for the requirement of a dynamic F-actin network has not been elucidated. One possibility is that certain signaling events proceed only under application of physical force, a process termed mechanotransduction. Recent studies indicate that TCR triggering may be sensitive to application of force along the TCR–pMHC bond (Li et al., 2010; Ma et al., 2008b). Moreover, there is evidence that TCR tension-sensing at the IS depends in part on myosin II contraction, and also on F-actin centripetal flow (Kumari et al., 2012). Despite the accumulating evidence for mechanotransduction in TCR signaling, the precise role of F-actin dynamics remains unclear. Furthermore, the role of F-actin-dependent mechanical force in regulating other molecules needed for T cell activation has largely been unaddressed.

Integrins are heterodimeric transmembrane proteins that are critical for the formation and maintenance of cell–cell interactions. In humans, there are 24 known integrin  $\alpha\beta$  dimers consisting of different combinations of the 18  $\alpha$  and 8  $\beta$  chains. The  $\alpha L\beta 2$  integrin LFA-1 is expressed exclusively in leukocytes and is essential for T-cell trafficking and IS formation. In general, integrins are regulated at two distinct levels, valency, or integrin density at the cell–cell interface, and affinity, or the strength of interaction between each individual integrin molecule and its ligand. Both valency and affinity contribute to firm adhesion (Yu et al., 2010b). Therefore, the collective strength of the interaction, which is referred to as avidity, is a product of valency, affinity and relative contact area (Kinashi, 2005).

In resting T cells, LFA-1 is maintained in an inactive, bent conformation with very low ligand binding capacity. TCR stimulation recruits the actin binding protein talin to the  $\beta$  chain of LFA-1. Talin binding to the NPXY/F motif relieves interactions between the transmembrane and cytoplasmic domains of the  $\alpha$  and  $\beta$  chains that are required to maintain the bent conformation, allowing unfolding of LFA-1 and the adoption of an intermediate conformation (Calderwood et al., 1999; Hughes et al., 1996; Kim et al., 2003; Li et al., 2003; Luo et al., 2005; Partridge et al., 2005; Tadokoro et al., 2003). This “switch-blade”-like unfolding occurs in the presence of activating antibodies or ligand-mimetic peptides, and exposes epitopes that report integrin activation (Figure 1A) (Nishida et al., 2006; Takagi et al., 2002). Signaling events, such as talin binding, that result in the modulation of LFA-1 activation are generally termed inside-out signaling (reviewed in (Hogg et al., 2011; Kim et al., 2011; Kinashi, 2005)).

In a reciprocal process termed outside-in signaling, the actual binding of ligand can also induce the activation of LFA-1 through induced fit of the high affinity form. The structural changes that take place upon integrin activation have been characterized using activating mutations and activation-inducing antibodies (Shimaoka et al., 2003; Takagi et al., 2002; Weitz-Schmidt et al., 2011; Zhu et al., 2008). Typically, integrin activation and ligand binding are associated with a lateral swing-out of the hybrid domain, resulting in a downward movement of the  $\alpha 7$  helix in the  $\beta I$  domain, thus inducing the high affinity, extended open conformation of the  $\beta I$  domain. In  $\alpha I$  domain-containing integrins, such as LFA-1, the activated  $\beta I$  domain binds an invariant glutamate residue in the C-linker region between the  $\alpha I$  and  $\beta$ -propeller region. This results in downward movement of the  $\alpha I$  domain  $\alpha 7$  helix and adoption of the extended open, high affinity,  $\alpha I$  domain (Figure



3.1 A). Importantly, it has been shown that antibodies that stabilize the extended conformation or ones that stabilize hybrid domain swing-out greatly increase the affinity of LFA-1 for ligand (Chen et al., 2010b; Schurpf and Springer, 2011). Incubation of cells with antibody TS1/18, which stabilizes the closed  $\beta$ I domain, decreases baseline affinity by half. Conversely, induction of the extended conformation with the activating antibody CBR LFA 1/2 results in a 4-fold increase in affinity from baseline levels, while induction of hybrid domain swing-out with antibody MEM-148 increases the affinity 100-fold over the extended conformation. Thus, conformational change of LFA-1 can regulate its affinity for ICAM-1 by over three orders of magnitude. These data imply that an external force applied to LFA-1 that results in hybrid domain swing-out can greatly enhance LFA-1 affinity for ligand. In support of this idea, molecular modeling has suggested that a tensile force applied parallel to the membrane on the  $\beta$  tail can result in hybrid domain swing-out and affinity modulation (Zhu et al., 2008).

Consistent with the prediction that force can enhance LFA-1 affinity, it has been demonstrated that integrins engage in catch-bond interactions, in which force on the bonds increases the strength and longevity of the interaction (Chen et al., 2012; Chen et al., 2010a; Kong et al., 2009). Bond lifetime increases as tensile normal force is applied, until a threshold is reached where bonds are rapidly ruptured. Importantly, it was found that blocking binding of the  $\alpha$ I internal ligand by the open  $\beta$ I domain with the allosteric inhibitor XVA143 perturbs catch bond behavior, suggesting that conformational change is required to initiate catch-bond interactions. Furthermore, it has been shown that  $\alpha$ 5 $\beta$ 1 and LFA-1 can undergo a process termed cyclic mechanical reinforcement, whereby a short application of high tensile force can induce a state under which bond lifetime is

greatly extended after the original force is removed or decreased (Kong et al., 2013). For LFA-1–ICAM-1 interactions, force cycling increased the average bond lifetime from 1.5 seconds over 35 seconds.

In naïve T cells the integrin LFA-1 is essential for proper T-cell trafficking, conjugate stability and IS maturation. Recently it has been shown that LFA-1–mediated adhesion is critical for the formation of immunological memory (Parameswaran et al., 2005; Scholer et al., 2008). Although it is clear that integrins play a central role in T cell function, major questions remain about the mechanisms that regulate integrin activation at the IS. It has been proposed that tensile force on the  $\beta$  chain of LFA-1 can be produced through linkage to the dynamic F-actin network (Schurpf and Springer, 2011; Springer and Dustin, 2012), but this model has not been directly tested. We have now investigated the function of the T-cell actin cytoskeleton in regulating conformational change and organization of LFA-1 at the IS. Our data suggest that mechanical forces provided by the flow of the T cell actomyosin II network are critical for the recruitment of LFA-1 to the IS and its organization at the interface. Moreover, F-actin dynamics were required for the maintenance of the high affinity conformation of LFA-1; LFA-1 affinity could be modulated through slowing of the F-actin network by VLA-4 co-engagement. We propose that the mechanical force provided by F-actin centripetal flow maintains LFA-1 density and conformational state at the IS, thus regulating LFA-1-mediated adhesiveness and costimulatory potency.

### III. Results

#### *Extended and extended open conformations of LFA-1 display distinct patterns of organization at the IS*

T cell activation by APCs involves clustering of LFA-1 at the cell-cell interface and conformational changes associated with affinity modulation, but the distribution of the activated forms of the molecule in this context has not been well-characterized. To address this question, we labeled conjugates formed between human *ex vivo* CD4<sup>+</sup> T cells and SEE-pulsed Raji B cells with a panel of antibodies specific for different conformations of LFA-1, associated with well-defined changes in ligand binding affinity as depicted in Figure 3.1 A. TS2/4, which binds the  $\beta$  propeller domain of CD11a, (hereafter  $\alpha$ L) was used to label total LFA-1 on cell surface. Conjugates were rendered in 3D in the IS plane (Movie 3A). TS2/4 labeling showed an even distribution across the pSMAC region of the IS with a slight decrease in intensity in the cSMAC, and was largely absent from the F-actin-rich dSMAC region (Figure 3.1 B). Kim127 binds the extended form of CD18 (hereafter  $\beta$ 2) in the intermediate and high affinity conformations, and was used to mark these ligand-binding forms of LFA-1. Kim127 labeled LFA-1 within the pSMAC region, but was largely absent from the cSMAC (Figure 3.1 B). Finally, m24, which binds  $\beta$ 2 within the  $\beta$ I domain following hybrid domain swing-out, was used to specifically label LFA-1 molecules in the extended open (high affinity) state. m24 labeling concentrated in the inner region of pSMAC relative to Kim127 staining, though labeling was typically very low at the very center of the contact area (Figure 3.1 B). The inner boundary of extended open LFA-1 corresponded to the CD3-rich cSMAC region in conjugates that had a clear cSMAC (Figure 3.2 A); however,

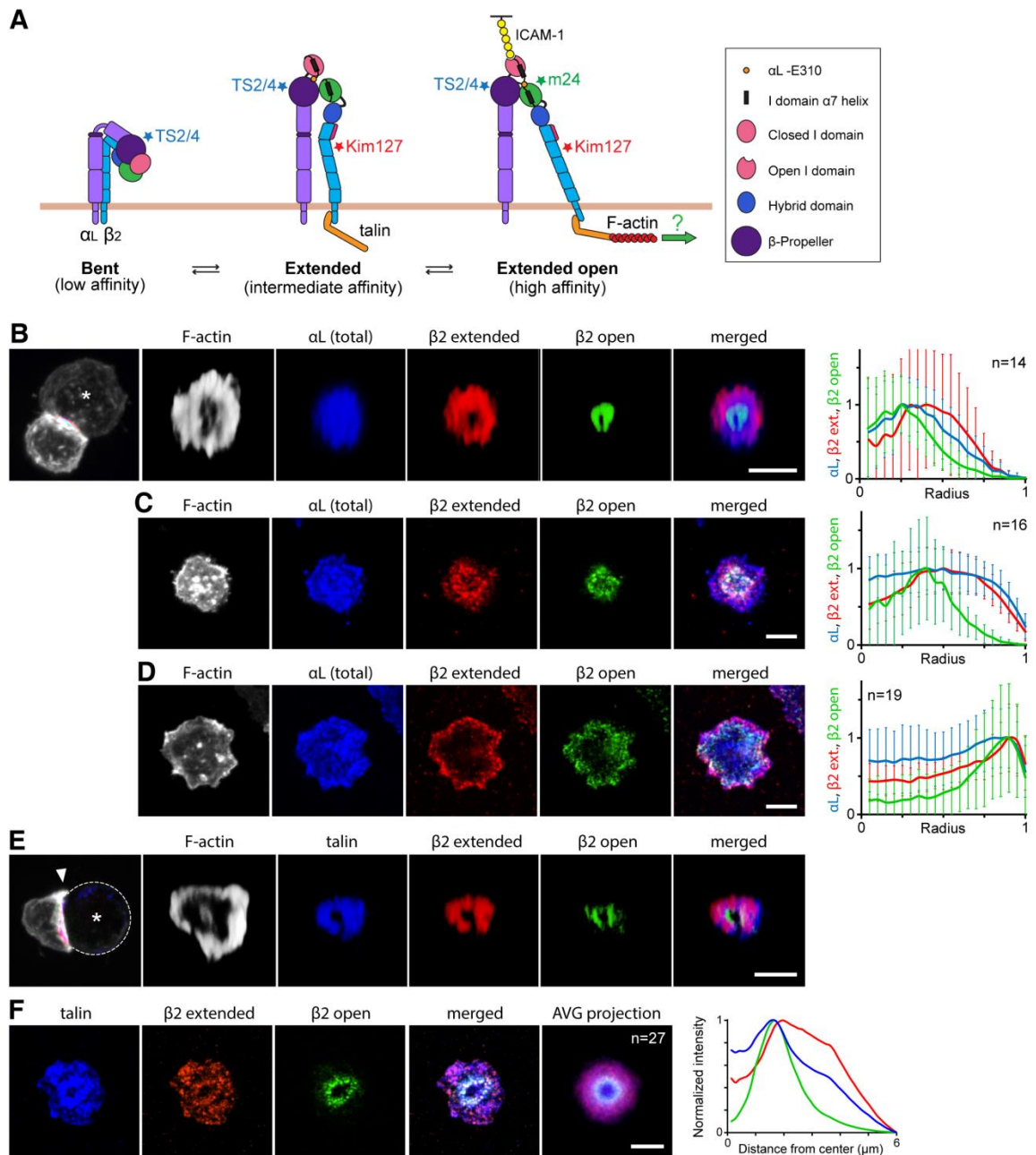


**Figure 3.1. LFA-1 conformational change at the IS is organized into a concentric array via a T-cell intrinsic mechanism.**

(A) LFA-1 conformational states and antibody binding sites. Inactive LFA-1 (low affinity for ligand) exists in bent conformation. Intermediate affinity LFA-1 is induced upon talin binding to the cytoplasmic tail of the  $\beta$  chain. Cytoskeletal interactions and ligand binding further separate the integrin tails and results in extended open conformation of LFA-1, which has high affinity for ligand, ICAM-1. Putative binding sites of monoclonal antibodies are marked with asterisks. (B) Human primary CD4<sup>+</sup> T cells were conjugated to SEE-pulsed Raji B cells (asterisk in first panel) for 25 min, and labeled with CF405M-phalloidin (to detect F-actin) and with antibodies to a conformation-independent epitope on  $\alpha$ L (to detect total LFA-1) and to the  $\beta$ 2 chain in the extended and extended open conformations. Z stacks of whole conjugates were collected and rendered in 3D in the IS plane (arrowhead). Representative rendered images are shown. Right panel, radial intensity profiles of synapses from multiple conjugates were analyzed as described in Chapter 5, Materials and Methods. Data are represented as mean  $\pm$  SD. (C) Cells were allowed to spread on stimulatory bilayers and analyzed as in B. (D) Cells were allowed to spread on stimulatory coverglasses and analyzed as in B. Radial intensity distributions in C and D were obtained as in B. (E) Conjugates were prepared as in B, except that labeling for talin, rather than  $\alpha$ L, was performed. (F) Cells were prepared as in C, except that labeling for talin was performed instead of labeling for  $\alpha$ L and without F-actin staining. Radial intensity distributions in F were obtained from average intensity projections as described in Experimental Procedures. Note that in both E and F, talin colocalizes with the extended and extended open conformations of LFA-1, confirming integrin conformational change. Results are representative of three independent experiments. Where indicated, n represents the number of analyzed synapses per experiment. Scale bars, 5  $\mu$ m.

the overall pattern of LFA-1 and the central clearance was present even in cells where no clear cSMAC accumulation of CD3 was observed (Figure 3.2 B). When superimposed, LFA-1 labeling patterns show a clear concentric distribution, with the extended open conformation distributed more centrally. This observation was confirmed by quantitative analysis of relative signal intensity as function of cell radius in multiple conjugates. As shown in Figure 3.1 B (rightmost panel), this analysis reveals that LFA-1 conformational intermediates form a concentric pattern at the IS, with the bent (low affinity) conformation relatively evenly distributed across the pSMAC and cSMAC regions, a peripheral ring rich in the extended (intermediate affinity) conformation and a more centralized ring enriched in the open headpiece (high affinity) conformation.

The concentric pattern of LFA-1 conformational intermediates was not unique to conjugates. A similar pattern was observed in T cells interacting with stimulatory planar lipid bilayers functionalized with anti-CD3 and ICAM-1 (characterized in Appendix A), except that total LFA-1 was evenly distributed across the entire IS (Figure 3.1 C). Moreover, T cells spreading on glass coverslips coated with anti-CD3 and ICAM-1 also showed a concentric pattern of LFA-1 conformational intermediates (Figure 3.1 D). In this case, cell spreading was more extensive and LFA-1 molecules in the extended conformation formed a thinner ring near the cell periphery. Extended open LFA-1 molecules were also more peripherally localized, accumulating just inside the ring of extended LFA-1. Quantitative analysis of multiple T cells responding to stimulatory bilayers and coverslips (rightmost panels of Figures 3.1 C and 3.1 D, respectively) confirms the generality of these observations, and highlights the shift of the concentric array to the periphery in cells responding to immobilized ligand. We conclude that

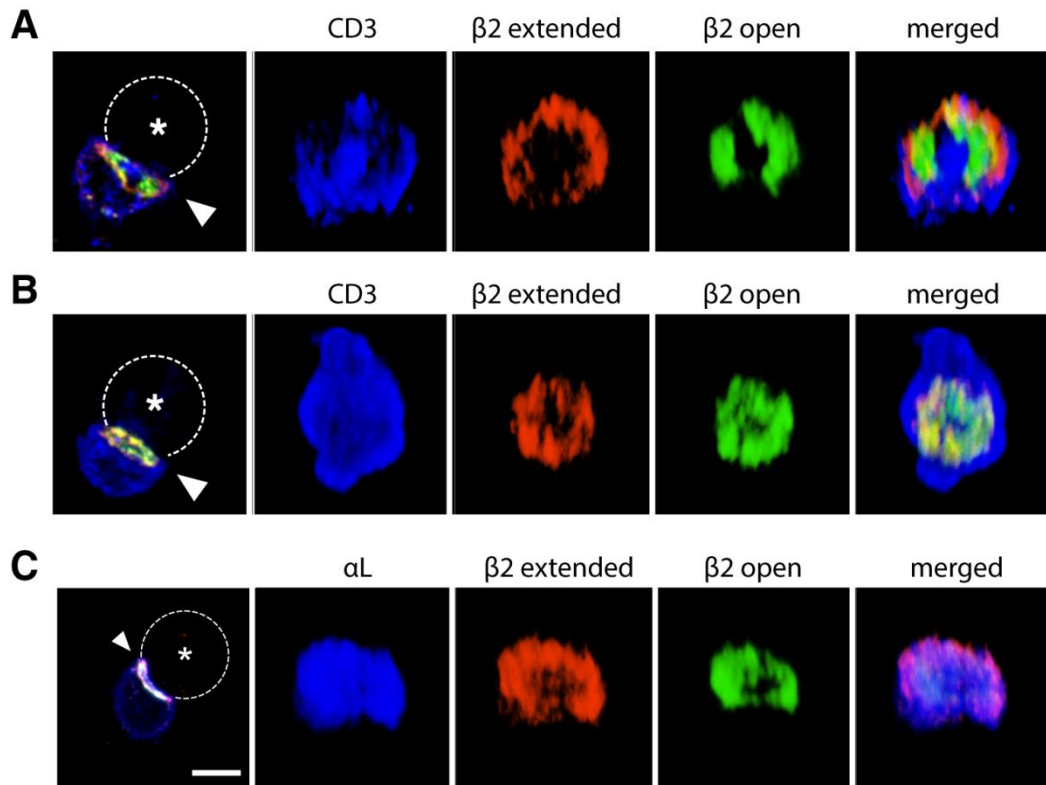


**Figure 3.2. LFA-1 conformational change at the IS is organized into a concentric array regardless of CD3 accumulation in the cSMAC or cell lineage**

(A and B) Human primary CD4<sup>+</sup> T cells were conjugated to SEE-pulsed Raji B cells (dashed outlines and asterisks) for 25 min, and labeled with antibodies to  $\beta 2$  chain in the open and extended conformations and to CD3 $\epsilon$  chain of TCR. Z stacks of whole conjugates were collected and rendered in 3D in the IS plane (arrowhead). Representative rendered images are shown. Activated LFA-1 assumes annular pattern in the presence (A) or absence (B) of CD3  $\epsilon$  enrichment in the cSMAC. (C) Human primary CD8<sup>+</sup> T cells were stimulated as in A and labeled with antibody against  $\beta 2$  open conformation of LFA-1. Cells were then fixed and further stained with antibodies to a conformation-independent epitope on  $\alpha L$  and to the  $\beta 2$  chain in the extended conformation. Cells were imaged and processed as in A. Scale bar, 5  $\mu\text{m}$ .

ligand mobility affects the extent of centralization, but not the tendency toward radial organization of LFA-1 activation intermediates.

As an independent method of assessing integrin conformational change, we used talin, a well-known integrin regulatory protein that binds to the cytoplasmic portion of the  $\beta$  chain upon TCR stimulation, inducing LFA-1 activation (Calderwood et al., 1999; Hogg et al., 2011). Talin co-localized strongly with both the extended and extended open conformations of LFA-1 in conjugates (Figure 3.1 E) and on planar bilayers (Figure 3.1 F). The characteristic distribution of activated LFA-1 was also observed in naïve CD8<sup>+</sup> T cells (Figure 3.2 C), and in CD4<sup>+</sup> T cell blasts (see Figure 3.3). Taken together, these results show that LFA-1 activation intermediates are organized in a radial array at the IS. Since similar patterns are observed in T cells responding to APCs and artificial stimulatory surfaces, we conclude that this process occurs in a T cell intrinsic manner.

*High affinity, extended open conformation of LFA-1 is enriched in areas of low F-actin dynamics*

Since LFA-1 associates with the actin cytoskeleton, it seemed likely that centripetal flow of the F-actin network plays a role in organizing the radial array of LFA-1 activation. In order to better understand the relationship between F-actin dynamics and regulation of LFA-1 affinity, we transduced human primary CD4<sup>+</sup> T lymphoblasts with the F-actin tracer Lifeact-GFP, and analyzed live cells responding to bilayers coated with anti-CD3 and ICAM-1. As shown in Figures 3.3 A and B and Movie 3B, T cells showed a highly dynamic IS characterized by repeated periods of expansion and retraction and an overall inward flow of the F-actin network. The network was generally organized as a



peripheral ring. While some cells exhibited an enrichment of LFA-1-GFP at the IS center (Figure 3.3 A; Movie 3B, left cell), others lacked this central accumulation (Figure 3.3 B; Movie 3B, right cell). In either case, total LFA-1 marked by TS2/4 was present across the IS irrespective of actin intensity, while the extended conformation was present largely in F-actin-poor regions, though absent from the IS center (Figure 3.3 C). Thus, labeling of the extended open conformation did not correlate with F-actin intensity.

Since LFA-1 has been shown to interact with myosin IIA, and myosin IIA is known to mark the actomyosin II network in areas of lower F-actin density in spreading T cells (see Chapter 2), we also evaluated LFA-1 distribution with respect to myosin IIA. As reported previously (Kumari et al., 2012; Yi et al., 2012), T cells spreading on stimulatory planar lipid bilayers exhibited a ring of myosin IIA that overlapped with the inner aspect of the F-actin-rich region (Figure 3.3 D). Interestingly, the ring of myosin IIA accrued between the ring formed by the extended form of LFA-1, which co-localizes with F-actin at the periphery of such cells (see Figure 3.1 C), and the more central ring of extended open LFA-1. The relative localization of myosin IIA and LFA-1 conformational intermediates was somewhat different in T cells responding to SEE-pulsed Raji B cells (Figure 3.3 E). Here, myosin IIA co-localized more tightly with F-actin at the IS periphery, so that peak myosin IIA intensity fell outside the rings of extended and extended open LFA-1. These differences likely involve changes in ligand mobility and the extent of T cell spreading. The important point, however, is that the distribution of myosin IIA does not directly correlate with that of any LFA-1 activation intermediate. Taken together, these data show that high affinity, but not low or intermediate affinity

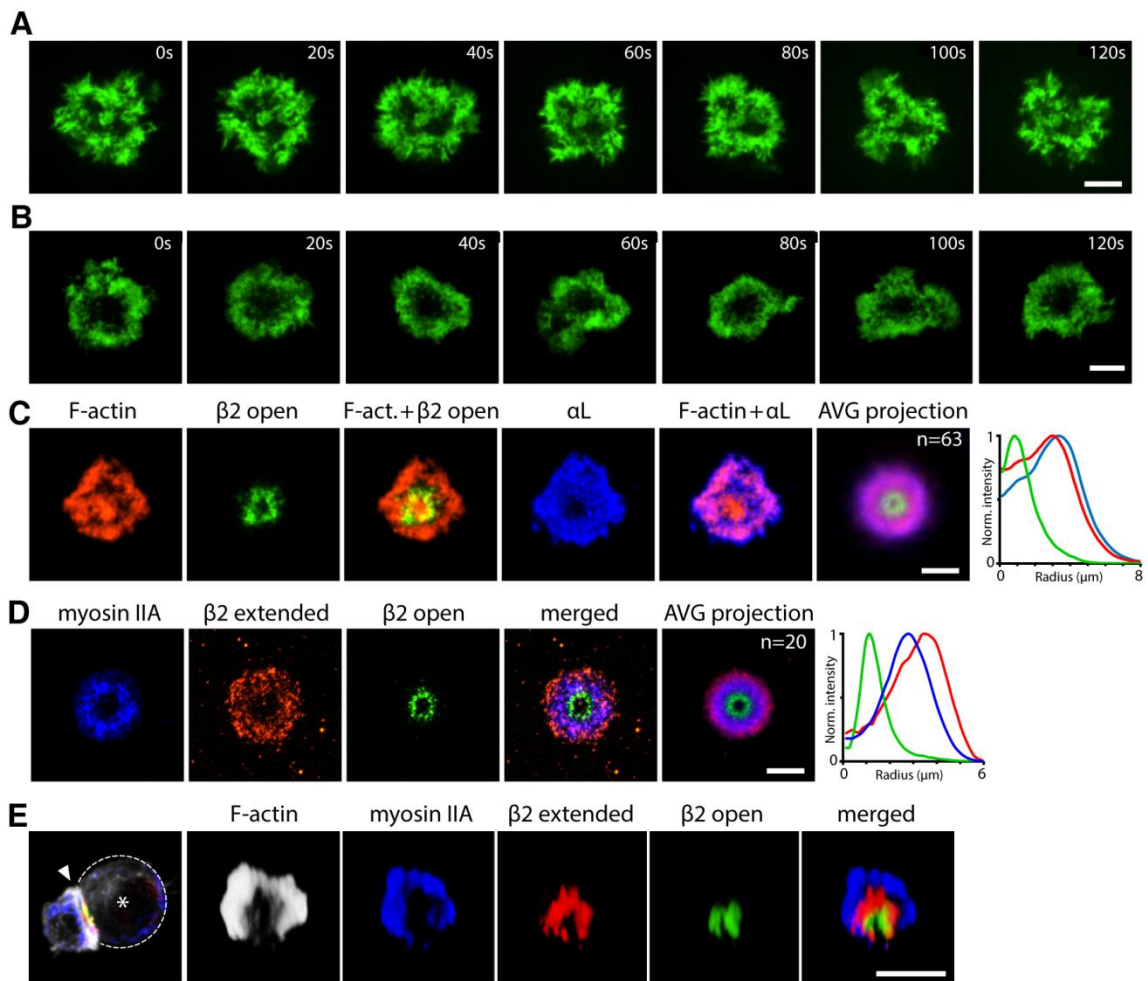


**Figure 3.3. Active LFA-1 is excluded from the zones of high F-actin dynamics**

(**A** and **B**) Time-lapse series of T cells expressing Lifeact-EGFP spreading on the stimulatory bilayers. Imaging was initiated after full spreading was reached. Some cells had a central accumulation of fluorescence (**A**), while others had a central clearance (**B**). (**C**) T cells were allowed to spread on bilayers for 30 minutes and labeled with conformation-specific LFA-1 antibodies and phalloidin as indicated. Right panel, the average intensity distribution at the IS within the cell population was calculated from average intensity projection (AVG projection) of cell population, as described in Chapter 5, Materials and Methods. (**D**) T cells were allowed to spread on bilayers for 30 minutes and labeled with conformation-specific LFA-1 and anti-myosin IIA antibodies as indicated. Right panel, the average intensity distribution at the IS within the cell population was determined as in C. (**E**) T cells were conjugated to SEE-pulsed Raji B cells (dashed outline and asterisk) for 30 minutes and labeled with phalloidin, anti-myosin IIA and conformation specific LFA-1 antibodies as indicated. Z stacks of whole conjugates were collected and rendered in 3D in the IS plane (arrowhead). Representative rendered images are shown. Where indicated, n represents the number of analyzed synapses. Scale bars, 5  $\mu\text{m}$ .

LFA-1 is selectively excluded from regions of high actomyosin II dynamics. Since high affinity LFA-1 is preferentially associated with the F-actin network (Cairo et al., 2006), it seems likely that this pool of the molecule is preferentially pushed to the inner region of the IS and deposited there upon disassembly of actin filaments.

*Ligand mobility influences the magnitude of the retrograde flow rate of F-actin*

An outstanding question in the field is whether ligand mobility influences the rate at which F-actin moves at the synapse. Early studies concentrated either on mobile or on immobile substrates and reports from different labs yielded widely disparate results (DeMond et al., 2008; Kaizuka et al., 2007; Nguyen et al., 2008). The Groves lab (Yu et al., 2010a) had conducted studies in Jurkat T cells spreading on mixed mobility surfaces, and demonstrated that local retardation of F-actin flow occurs upon encountering a barrier in ligand mobility. This observation raised the notion that ligand mobility affects the centripetal movement of the F-actin network. However, in a recent publication (Yi et al., 2012) had shown that in their hands retrograde flow rate was not different between Jurkat cells spreading on stimulatory bilayers or on coverglasses. We also decided to perform a side-by-side analysis of this phenomenon. We dropped GFP-actin Jurkat cells on coverglasses and on bilayers and performed confocal live-cell imaging. Qualitatively, cells spreading on bilayers, which contained OKT3 and ICAM-1, spread less extensively and had much thicker lamellipodia than cells spreading on coverglasses containing the same ligands (Figures 3.4 A and B; Movie 3C). Kymograph analysis showed that cells spreading on mobile OKT3 and ICAM-1 had flow rate of  $87.7 \pm 17.8$  nm/s (mean  $\pm$  SD), which was significantly higher than  $67.8 \pm 16.5$  nm/s (mean  $\pm$  SD) in cells spreading on

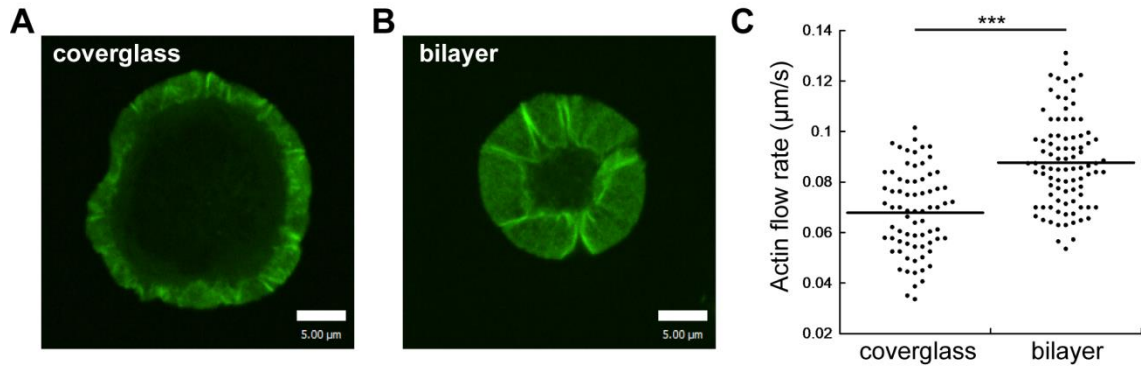


**Figure 3.4. Ligand mobility modulates F-actin retrograde flow rate**

Jurkat T cells expressing low levels of GFP-actin were allowed to spread on the OKT3- and ICAM-1-coated coverglasses (A) or stimulatory bilayers containing the same pair of ligands (B). Representative extent of cell spreading and F-actin organization is depicted. Scale bars, 5 µm. (C) Comparative analysis of F-actin flow rates at the periphery of the IS, as determined by kymography. Each dot represents a single measurement, multiple measurements were made on the same cell; 16 cells were used for measurements on coverglass and 21 cells for measurements on bilayer. \*\*\* $p < 0.001$

immobilized ligands (Figure 3.4 C). Thus, we conclude that ligand mobility does play a role in the extent of cytoskeletal flow rate in stimulated T cells, which may influence the outcome of overall signaling cascade.

*LFA-1 engagement by immobilized ICAM-1 retains high affinity LFA-1 in the periphery of the IS*

We next assessed the role of ligand engagement in defining the organization of LFA-1 activation intermediates with respect to the dynamic actin network. For this, human primary CD4<sup>+</sup> T lymphoblasts were allowed to interact with stimulatory coverslips coated with OKT3 + ICAM-1 or with OKT3 alone, and labeled with conformation-specific antibodies as well as with antibodies against total LFA-1. T cells stimulated with OKT3 + ICAM-1 spread more extensively than cells stimulated with OKT3 alone, but the patterns of total and extended LFA-1 were similar (Figures 3.5 A and B), with a ring of enrichment near periphery of the IS, with intensities at the center reaching ~ 50% of the maximal value (Figure 3.5 A, right panel). In contrast, manipulating ligand engagement had a dramatic effect on the distribution of LFA-1 molecules in the extended open conformation. In these T cell blasts spreading on OKT3 + ICAM-1, staining for the extended open conformation co-localized completely with staining for extended and total LFA-1, whereas in T cells stimulated in the absence of ICAM-1 these high affinity molecules were concentrated at the center of the IS (Figure 3.5 B, right panel). This also showed that ICAM-1 engagement is not absolutely necessary to induce the extended open integrin conformation.

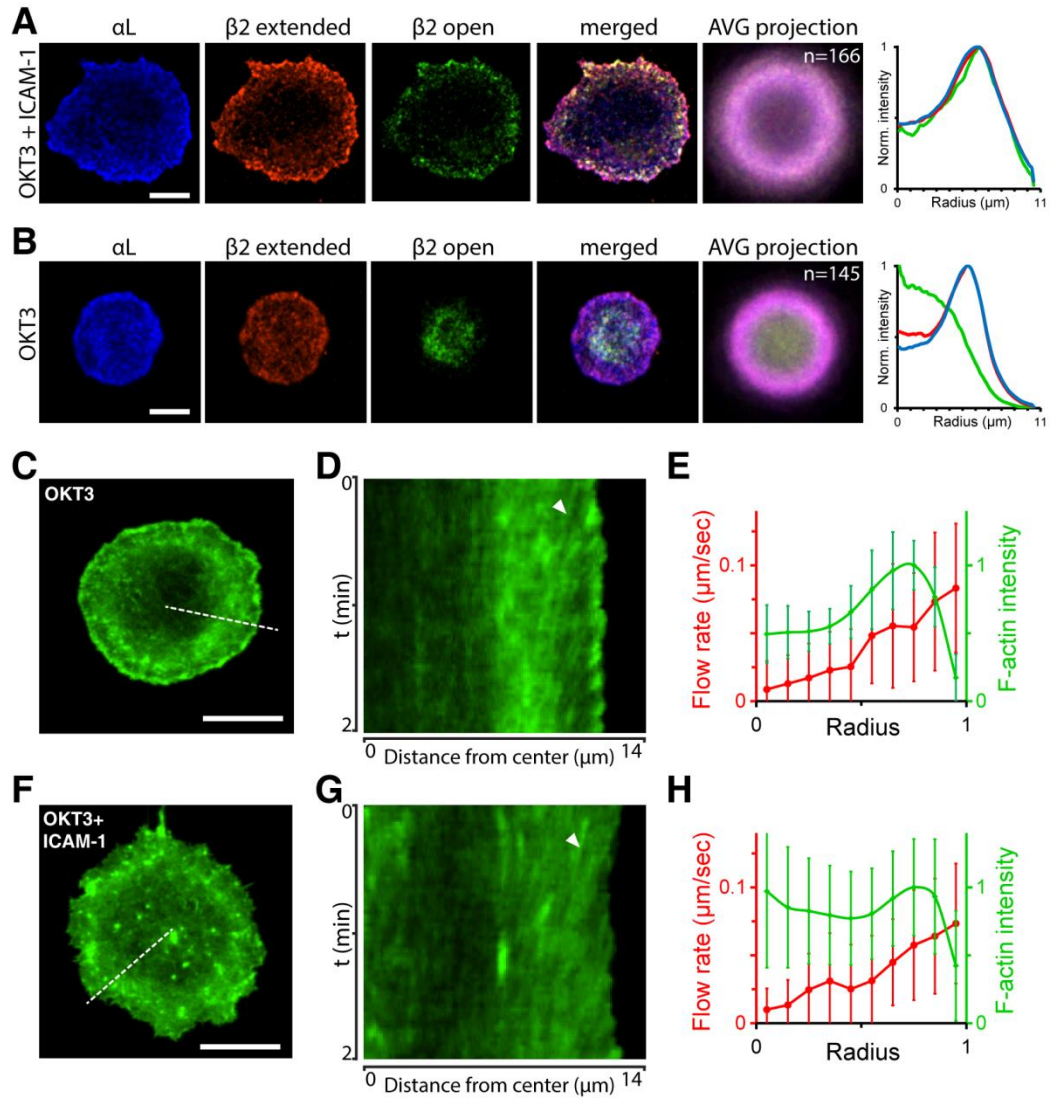


**Figure 3.5. ICAM-1 binding retains the pool of activated LFA-1 in the IS periphery**

(**A** and **B**) Blasted T cells were allowed to interact with coverslips, coated with OKT3+ICAM-1 (**A**) or OKT3 alone (**B**) for 30 minutes, fixed and stained with the indicated antibodies as described in Chapter 5, Materials and Methods. Rightmost panels represent traces of fluorescence intensities obtained from average intensity projections (AVG projection). *n* represents the number of analyzed synapses. (**C**) Blasted T cells expressing Lifeact-EGFP were allowed to interact with the stimulatory coverslips, while being imaged. (**D**) Kymograph of F-actin dynamics generated along the dashed line in C. Arrowhead indicates a mobile fiducial mark in the F-actin network. (**E**) Kymograph analysis of F-actin dynamics along IS radii (663 measurements from 13 cells) superimposed with the normalized radial distribution of F-actin in the same cells. (**F**) Same cells as in C were allowed to interact with the stimulatory coverslips, coated with OKT3+ICAM-1, and imaged for F-actin dynamics. (**G**) Kymograph of F-actin dynamics generated along the dashed line in F. Arrowhead indicates a mobile fiducial mark in the F-actin network. (**H**) Kymograph analysis of F-actin dynamics along IS radii (1180 measurements from 21 cells) superimposed with the normalized radial distribution of F-actin in the same cells. Data are represented as mean  $\pm$  SD. Scale bars in A and B, 5  $\mu$ m and in C and F, 10  $\mu$ m.



The degree of centralization of extended open LFA-1 in T cells stimulated on coverslips without ligand resembled the pattern seen in cells responding to planar bilayers where ICAM-1 is present, but mobile (Figure 3.1 C). The simplest interpretation of these data is that actin-dependent delivery of ICAM-1 to the center of the IS is directly opposed by the immobilized ligand. Alternatively, however, engagement of immobilized ligand could affect the flow of the F-actin network. Evidence for this comes from the work of (Nguyen et al., 2008), who showed that engagement of the  $\beta$ 1 integrin VLA-4 with immobilized VCAM-1 dramatically retards centripetal F-actin flow. To differentiate between these possibilities, we measured F-actin flow rates in T lymphoblasts expressing Lifeact-GFP. T cells spreading on OKT3 alone showed continuous centripetal flow of F-actin (Figures 3.5 C–E; Movie 3D). Kymography analysis revealed flow rate of  $83 \pm 47$  nm/s (mean  $\pm$  SD) in the lamellipodial region, with linear deceleration as the network moved toward the F-actin-low center of the synapse. These results are in good accord with our findings in Jurkat T cells (see Chapter 2).

Importantly, addition of ICAM-1 to the stimulatory coverslips had minimal effect on actin dynamics or the pattern of centripetal deceleration, although we noticed that there was more F-actin at the center of the synapse (Figures 3.5 F–H; Movie 3E). F-actin flow in the very periphery slowed down to  $73 \pm 44$  nm/s but in general, the differences between the two conditions were not statistically significant across the IS radius (Figure 3.12). Taken together, these data favor a model, in which pre-activated (transient intermediate, Step 3 in model in Figure 3.13 B) LFA-1 first binds to ICAM-1 in the periphery of the IS, and then high affinity, ligand-bound molecules are pulled inward by centripetal flow of the F-actin network. If ICAM-1 is present and immobilized, high affinity LFA-1 is

physically retained in the periphery of the contact, whereas if ICAM-1 is absent, or highly mobile, pre-activated LFA-1 can accumulate at the center of the contact area.

*F-actin flow regulates the valency of LFA-1 at the IS*

In order to directly determine the relationship between forces exerted by F-actin flow and LFA-1 conformational change and organization, we used an inhibitor cocktail containing the F-actin-stabilizing agent jasplakinolide (Jas) together with either the myosin II inhibitor blebbistatin (Bleb) or the Rho-kinase inhibitor Y-27632 (Y-27), which indirectly inhibits myosin IIA activity. We and others have shown previously that this treatment stops F-actin flow in Jurkat T cells without depleting the network (Chapter 2 and (Yi et al., 2012)). As expected, treatment of Lifeact-GFP-transduced human primary T cells spreading on planar lipid bilayers with myosin II inhibitors alone had little effect on F-actin dynamics (Figures 3.6 A and B; Movie 3F), but cells treated with myosin II inhibitors together with Jas showed complete inhibition of actin dynamics (Figure 3.6 C; Movie 3F). Using the same pharmacological conditions, we tested the effects on LFA-1 conformational change in T cells interacting with SEE-pulsed Raji B cells. In untreated conjugates, total labeling showed that LFA-1 was enriched at the IS where it was relatively uniformly distributed (Figures 3.7 A and B). To quantify this, labeling intensity was measured as detailed in Chapter 5, Materials and Methods. In Figures 3.7 C–H, each data point represents the average value from 33-75 conjugates from one healthy donor; individual measurements from donor 2 (Figure 3.8) highlight the representative range in variability within experiment. To quantify redistribution of total

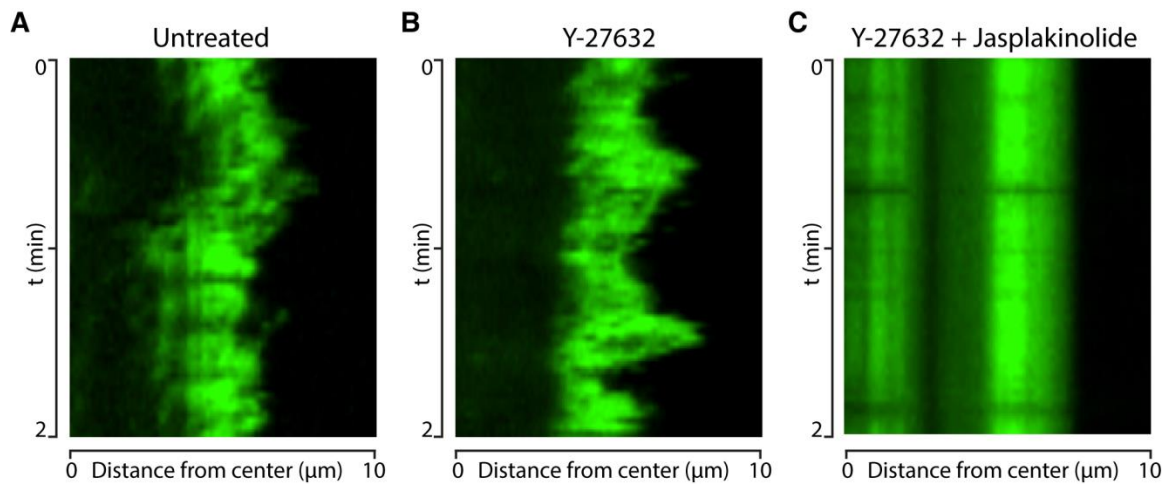


**Figure 3.6. Actin dynamics persist in the under myosin II inhibition alone but cease completely after abrogating F-actin turnover**

(A–C) Kymographs of F-actin dynamics generated from Movie 3F. In untreated cells (A) the peripheral accumulation of F-actin is very dynamic. F-actin dynamics seem unperturbed after pretreatments with Y-27632 (B). Complete “freeze” of the F-actin flow is observed after acute addition of jasplakinolide (C).

LFA-1, TS2/4 labeling intensity was measured at the IS (Figure 3.7 C) and over the entire cell surface (data not shown). The ratio of these two values showed that in untreated cells ~60% of total LFA-1 is present at the IS (Figure 3.7 F). Inhibition of myosin II contraction by treatment with either Bleb or Y-27 had no obvious effect on the distribution of LFA-1 (Figures 3.7 A and B) or the proportion of surface-expressed LFA-1 at the IS (Figure 3.7 F). Unlike cells treated only with myosin II inhibitors, cells treated with inhibitor cocktails (Bleb + Jas or Y-27 + Jas) showed a dramatic depletion of LFA-1 from the IS (Figures 3.7 A–C). Much of this decrease was due to changes in the distribution of cell surface molecules, since cells treated with the inhibitor cocktail showed a 25–30% decrease in the proportion of cell surface LFA-1 localized at the cell-cell contact (Figure 3.7 F). Similar results were obtained in T cells spreading on stimulatory bilayers. In that system, freezing the F-actin network resulted in an overall loss of LFA-1 from the synaptic region, with TS2/4 labeling intensity decreasing to the levels found in bilayers that lacked ICAM-1 (Figure 3.10 B). Here, too, no change in the distribution of total LFA-1 within the plane of the IS was observed (Figures 3.9 A and B). Taken together, these results indicate that F-actin flow continuously shuttles LFA-1 toward the IS, thereby greatly increasing LFA-1 valency (see model in Figure 3.13 A).

*Myosin II contraction and F-actin flow regulate affinity maturation of LFA-1 at the IS*

We next asked whether in addition to regulating LFA-1 valency at the IS, the actin cytoskeletal network controls conformational changes associated with affinity maturation. For this, conjugates were labeled with conformation-specific LFA-1

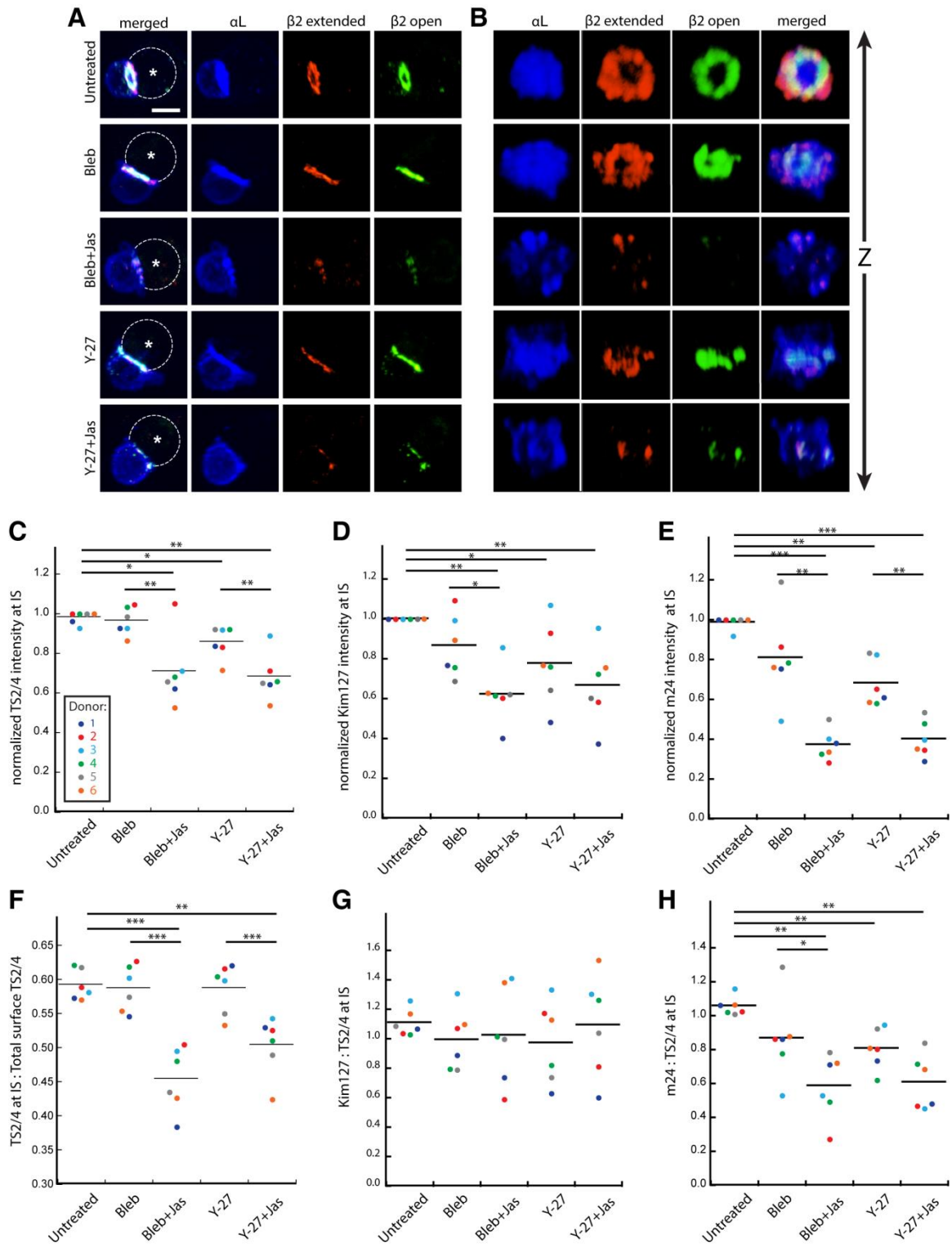


**Figure 3.7. Centripetal flow of the actomyosin II network regulates valency and affinity of LFA-1**

(A) T cells from donor 2 were conjugated with SEE-pulsed Raji B cells (dashed outlines with asterisks) for 10 min. and then either left untreated or treated to inhibit myosin II contraction with Bleb or Y-27 for an additional 15 min. Some myosin II-inhibited conjugates were then treated with Jas for 5 min to arrest the actomyosin II network dynamics. Cells were then fixed and labeled with conformation-specific LFA-1 antibodies. Representative conjugates are shown. Scale bar, 5  $\mu$ m. (B) Rendered IS images from Z stacks are shown *en face*. (C–E) The effects of drug treatments on normalized intensities of total (C), extended (D) and extended open (E) LFA-1 staining at the IS. Data from six independent human donors are shown; at least 33 conjugates were analyzed per condition for each donor. (F) The effects of drug treatments on maintenance of overall LFA-1 recruitment at the IS. Individual donors are color-coded as in C. (G, H) The effects of drug treatments on the efficiency of maintenance of LFA-1 in extended (G) or extended open (H) conformations. Individual donors are color-coded as in C. \* $p < 0.05$ , \*\* $p < 0.01$ , \*\*\* $p < 0.001$

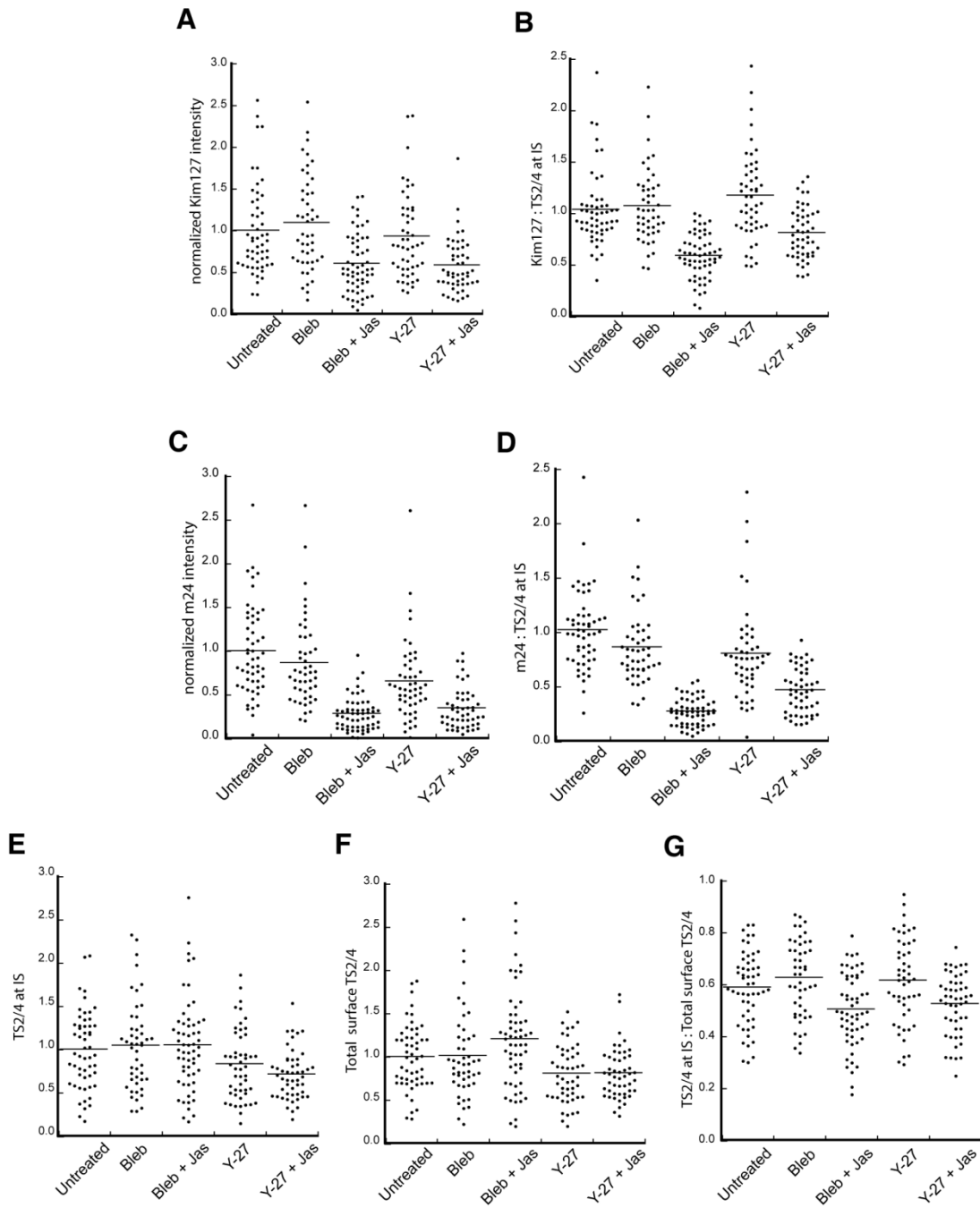


**Figure 3.8. Data from individual conjugates from a single donor in Figure 3.7**

(A–G) Fluorescence intensity values from cells of a single donor (Donor 2) in Figure 3.7. Note the representative range in variation between conjugates. Data are represented as mean within variation range.

antibodies and absolute signal intensities at the IS were measured and normalized to untreated control cells (Figures 3.7D and E). In addition, to control for changes in levels of LFA-1 at the IS and focus analysis on conformational change, Kim127 and m24 intensity values were normalized to TS2/4 intensity (Figures 3.7 G and H). As shown in Figure 3.7 D, treatment with myosin II inhibitors alone resulted in a decrease in the amount of extended LFA-1 at the IS, and a further decrease, when cells were treated with myosin II inhibitors in combination with Jas (Figures 3.7 A, B, and D). However, normalization of Kim127 values to total LFA-1 at the IS revealed that there was no statistical difference in the proportion of IS-associated LFA-1 in the extended conformation after either treatment (Figure 3.7 G). Labeling with m24 also showed a modest decrease in active LFA-1 at the IS after inhibition of myosin II contraction and a profound diminution after the freeze of the F-actin network, reaching approximately 40% of the control values (Figure 3.7 E). In contrast to the results obtained for the extended conformation, we found that the loss of m24 labeling was statistically significant, even after correction for changes in levels of total LFA-1 in the plane of the IS. Inhibition of myosin II contraction alone resulted in a 20% decrease in the proportion of extended open LFA-1, while freezing the F-actin network resulted in a 42% decrease from control cells (Figure 3.7 H).

The effects of inhibition of F-actin dynamics were verified in T cells responding to stimulatory planar bilayers. As in conjugates, we found that both the intermediate and high affinity epitopes decreased upon inhibition of F-actin flow (Figures 3.10 C and D), but when corrected for changes in total LFA-1 at the IS (Figure 2.10 B), we found no change in the proportion of extended LFA-1 at the IS (Figure 3.9 C). We observed a



decrease in proportion of extended open LFA-1 with myosin II inhibition, and a further decrease upon total inhibition of F-actin flow (Figure 3.9 D). On bilayers, freezing the F-actin network decreased the amount of high affinity LFA-1 to the levels observed in the absence of ICAM-1 (Figures 3.9 D and 3.10 D). Taken together, these data show that myosin II contraction and F-actin dynamics at the IS do not play an appreciable role in the maintenance of the intermediate form of LFA-1, but are indispensable for maintaining the extended open conformation of LFA-1.

*F-actin dynamics regulate the localization and distribution of extended open conformation LFA-1*

In addition to analyzing LFA-1 affinity modulation, we asked whether F-actin dynamics organize the radial distribution of LFA-1 activation intermediates. As shown in Figure 3.9 A for individual cells and Figure 3.9 B for population averages (see Chapter 5, Materials and Methods for details), treatment of T cells with the myosin II inhibitors alone had minimal effect on the distribution molecules in either the extended or the extended open conformations. In the experiment shown, Bleb induced an outward shift of the ring of active LFA-1, while Y-27 induced an inward shift; however these effects were modest and were not reproducible between multiple donors (data not shown). In contrast, freezing the F-actin network led to a clear redistribution of the molecules remaining in the intermediate and high affinity conformations. Both intermediate and high affinity LFA-1 became randomly distributed across the IS, and the central clearance region was

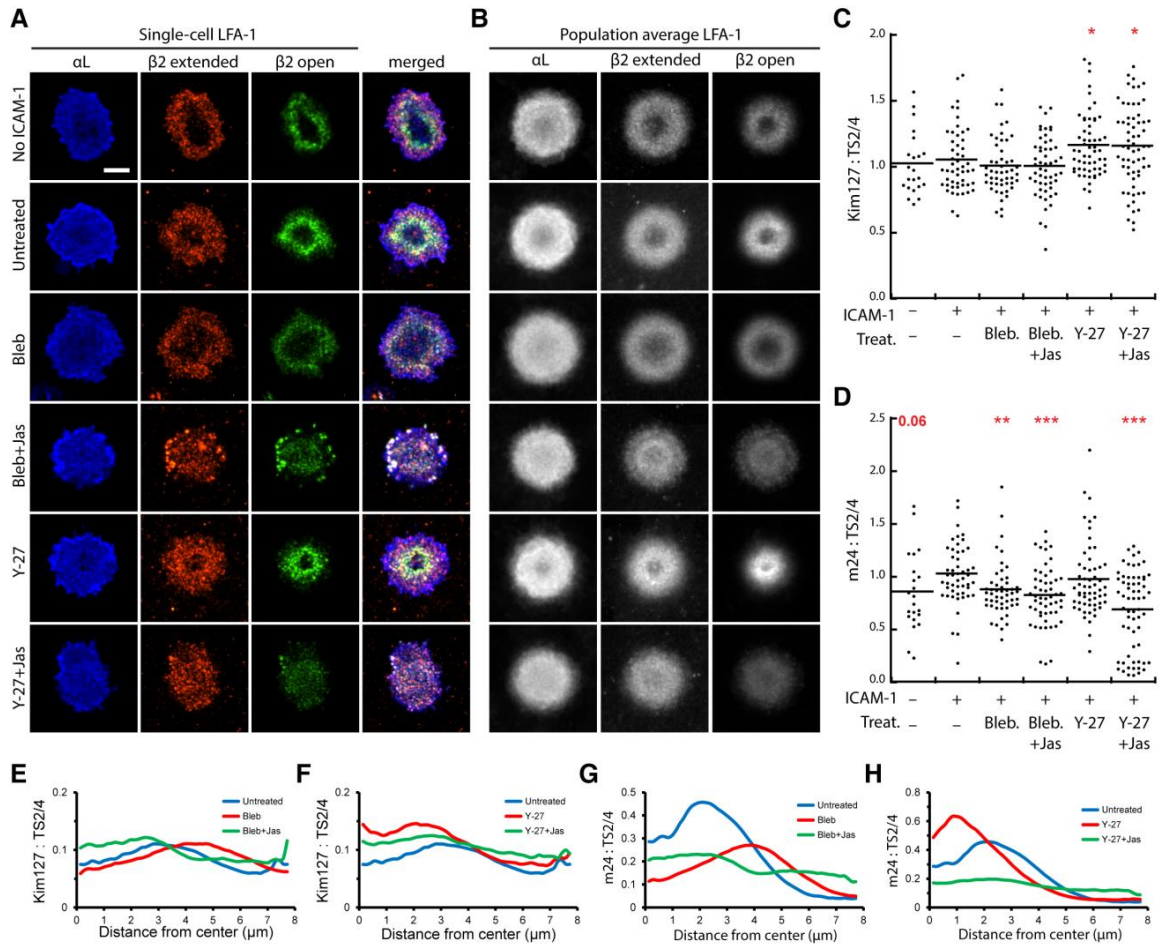
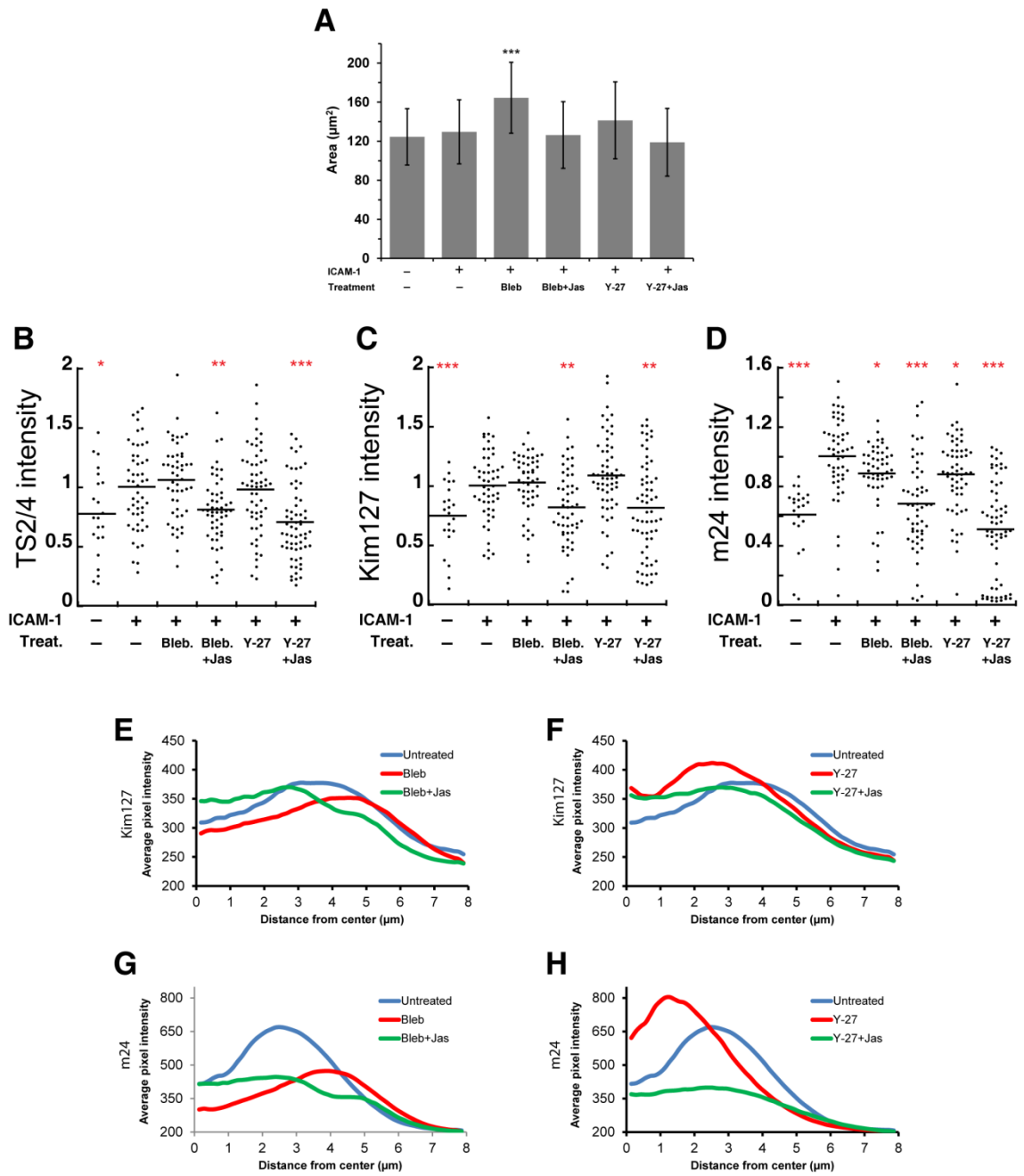


**Figure 3.9. F-actin dynamics regulates the localization and distribution of extended open conformation of LFA-1**

(A) CD4<sup>+</sup> T cells were allowed to spread on stimulatory bilayers for 10 minutes and then either left untreated or treated to inhibit myosin II contraction with Bleb or Y-27 for additional 15 minutes. Some myosin II-inhibited conjugates were then treated with jasplakinolide for 5 min. to arrest flow of the actomyosin II network. Cells were then fixed and labeled with conformation-specific LFA-1 antibodies. Representative synapses were selected within 0.5 SD of the mean. Scale bar, 5  $\mu$ m. (B) Average fluorescence intensity distributions for cell populations (n = 20–58 cells). (C, D) Total intensities of  $\beta$ 2 extended conformation (C) or  $\beta$ 2 extended open conformation (D) staining at the IS were normalized to total  $\alpha$ L staining in the same area. All values were normalized to the mean of the untreated T cells spreading on ICAM-1 and OKT3. Data are represented as mean within the distribution range. Statistical significance relative to untreated T cells spreading on OKT3 and ICAM-1, \*p<0.05, \*\*p<0.01, \*\*\*p<0.001. (E and F) Effects of drug treatments on the distribution of the extended conformation of LFA-1. Similar results are obtained using either Bleb (E) or Y-27 (F) to inhibit myosin II contraction. (G and H) Effects of drug treatments on the distribution of the extended open conformation of LFA-1. Similar results are obtained using either Bleb (G) or Y-27 (H) to inhibit myosin II contraction.



lost (Figures 3.9 A and 3.9 B, rows 4 and 6). In some cells treated with Bleb and Jas, small puncta of high affinity LFA-1 were observed at the cell periphery, but Y-27 + Jas treatment did not have this effect. Quantitative analysis of radial intensity profiles showed that the most dramatic change is the near complete loss of the peak of extended open conformation relative to total LFA-1 under conditions that abrogate F-actin flow (Figures 3.9 E–H). Taken together, these data demonstrate that the concentric pattern of LFA-1 activation intermediates is maintained by continuous F-actin centripetal flow.

*Co-ligation of  $\beta 1$  integrins slows the F-actin network and dampens LFA-1 activation*

Since pharmacological approaches always carry the risk of off-target artifacts, we sought a more physiological context, in which T cell actin flow can be perturbed. In Jurkat T cells, it has been previously shown that co-engagement of VLA-4 with TCR slows actin flow at the IS (Nguyen et al., 2008). We, therefore, asked whether co-ligation of VLA-4 has the same effect in primary T cells responding to TCR stimuli in the context

---

**Figure 3.10. Myosin IIA contraction and F-actin flow maintain high affinity conformation of LFA-1 and its localization at the IS**

(A) Synapse area of CD4<sup>+</sup> T cells after spreading on the stimulatory bilayers for a total of 30 minutes and subjected to the indicated conditions. Data are represented as mean $\pm$ SD. (B and C) Fluorescence intensities from individual synapses presented in figure 5. Statistical significance relative to untreated T cells spreading on ICAM-1 and OKT3, \*p<0.05, \*\*p<0.01, \*\*\*p<0.001. (E and F) Effects of drug treatments on the distribution of the extended conformation of LFA-1. Similar results are obtained using either blebbistatin (E) or Y-27632 (F). (G and H) Effects of drug treatments on the distribution of the extended open conformation of LFA-1. Similar results are obtained using either blebbistatin (G) or Y-27632 (H).

of LFA-1 engagement. T cells spreading on coverslips coated with a combination of OKT3, ICAM-1 and VCAM-1 spread to about the same extent as cells spreading on OKT3 and ICAM-1 alone (data not shown). As shown in Figures 3.11 A–C and Movie 3G, in T cells stimulated with both integrin ligands F-actin flow rates reached  $60 \pm 35$  nm/s (mean  $\pm$  SD) at the periphery of the IS, with a 6-fold decrease in rate near the IS center. Within the outer 40% of the IS radius, where most F-actin dynamics occur, the flow rate was significantly lower than that observed in cells spreading on OKT3 and ICAM-1 (Figure 3.12). Correlating with this decrease in flow rate, VCAM-1 co-ligation resulted in a 34% decrease in the labeling intensity for extended open LFA-1 at the IS (Figure 3.11 D). Most of this decrease was due to changes in affinity modulation; after normalization to total LFA-1 levels, the proportion of LFA-1 molecules in the extended open conformation was reduced by 20%. Since VLA-4 and LFA-1 use many common adapters to link the  $\beta$  chain to the actin cytoskeleton, we considered the possibility that this effect reflects competition between  $\beta 1$  and  $\beta 2$  integrins for these proteins. However, binding of these adapters is required to reach the extended conformation of integrins and, since there was no loss of LFA-1 in the extended conformation, we do not believe that adapter molecules were limiting in this context of stimulation. Indeed, the proportion of LFA-1 molecules in the extended conformation increased significantly upon  $\beta 1$  integrin engagement (Figure 3.11 D). Thus, we conclude that  $\beta 1$ -integrin engagement, like pharmacological treatment, modulates  $\beta 2$ -integrin affinity maturation by slowing centripetal flow of the F-actin network. This result also demonstrates that the F-actin network can serve as a mechanical intermediary between distinct integrins, and possibly between integrins and other cell surface receptors.

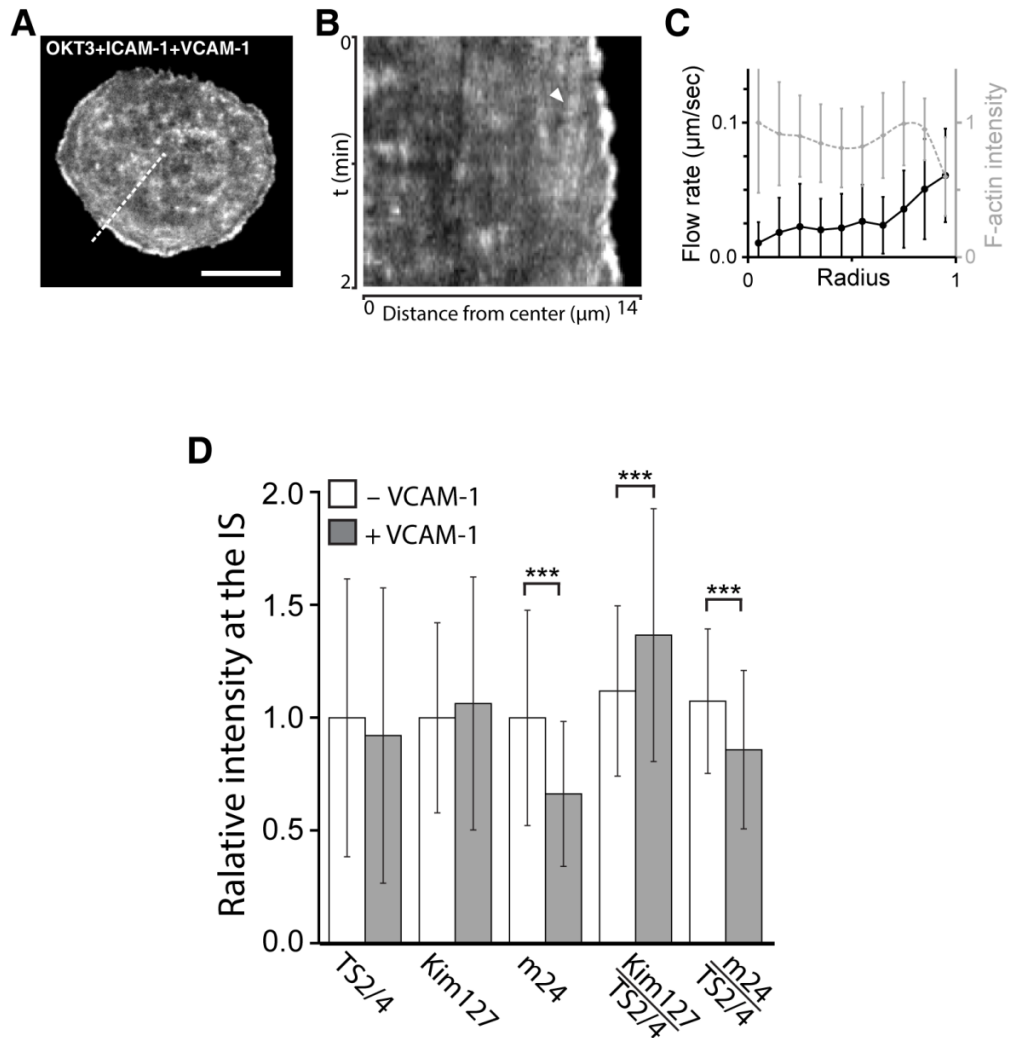


**Figure 3.11. Co-ligation of VLA-4 slows F-actin flow and dampens LFA-1 activation**

(A) Blasted T cells expressing Lifeact-EGFP were allowed to interact with the stimulatory coverslips, while being imaged. Scale bar, 10 μm. (B) Kymograph of F-actin dynamics generated along the dashed line in A. Arrowhead indicates a mobile fiducial mark in the F-actin network. (C) Kymograph analysis of F-actin dynamics (817 measurements from 11 cells) superimposed with the normalized radial distribution of F-actin in the same cells. Data are represented as mean±SD. (D) T cells spreading on OKT3+ICAM-1 (– VCAM-1) or on OKT3+ICAM-1+VCAM-1 (+VCAM-1) coated coverglasses were stained with the indicated antibodies and analyzed for fluorescence intensity in the IS plane. Results are representative of three independent experiments. Data are represented as mean±SD, \*\*\*p<0.001.

#### **IV. Discussion**

Our results establish that LFA-1 conformational intermediates are differentially distributed at the T-cell IS, and that this pattern, along with the adoption of the high affinity conformation, is regulated by actomyosin network flow. These findings are consistent with a mechanotransduction model of LFA-1 affinity maturation, in which force derived from cytoskeletal dynamics enhances LFA-1 affinity (see Figure 3.13 B).

In keeping with previous reports (Monks et al., 1998), we found that total LFA-1 was present across the IS, though sometimes with a minor diminution at the center of the interface. Intermediate affinity LFA-1 in the extended conformation was concentrated in the outermost (pSMAC) region of the IS, whereas high affinity LFA-1 in the extended-open conformation was concentrated more centrally, in a region just outside the cSMAC. This pattern suggests that in T cell–APC conjugates, adhesion is strongest towards the center of the IS where LFA-1 is in its high affinity form, and weaker in the periphery where LFA-1 is present only in the intermediate and low affinity forms.

We find a strict requirement for F-actin flow in the maintenance of LFA-1 organization and affinity regulation at the IS. Since this requirement was observed even in T cells responding to artificial stimulatory surfaces, our data indicate that cell-intrinsic forces are enough to produce large scale separation of the integrin  $\alpha$  and  $\beta$  tails, thereby producing the conformational changes associated with affinity maturation (Fig.7) (Springer and Dustin, 2012). Furthermore, since we see an almost complete loss of ligand dependent LFA-1 activation upon inhibition of actin dynamics, our data suggest that the high affinity, ligand bound state requires ongoing tension. This behavior is



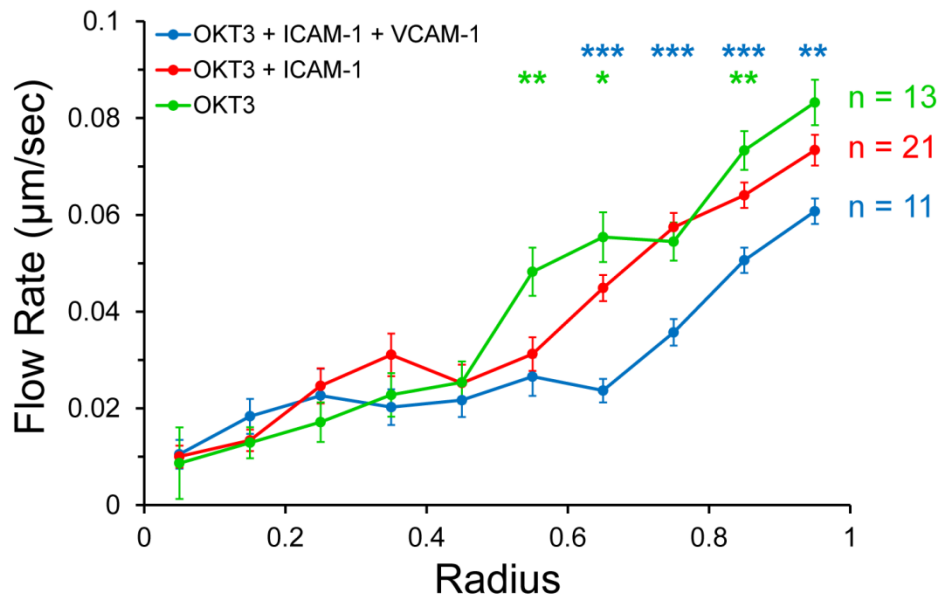


**Figure 3.12. Comparative analysis of F-actin dynamics of T cells responding to various combinations of stimulatory and adhesive ligands**

Radial distributions of F-actin flow rates from Figures 3C, F and Figure 6C were superimposed for comparison. Statistical analysis was performed relative to data from cells spreading on OKT3 + ICAM-1. n represents the number of cells imaged per condition. Data are represented as mean±SEM.

consistent with known properties of catch-bond molecular interactions (Kong et al., 2009). While ligand-induced outside-in signaling enhances LFA-1 activation, it is insufficient to maintain activation in the absence of force. Force is therefore critical not just for the initial priming of LFA-1 for ligand binding, but also for the subsequent maintenance of the high affinity, ligand-bound form.

We show that myosin II function is not necessary for recruitment of LFA-1 to the IS or for long-term maintenance of organizational patterns of the activated integrin pool. Myosin II contraction also does not affect the intermediate affinity pool of LFA-1; however, it promotes adoption of the high affinity extended open conformation. This effect is independent of changes in actin flow rates, since this parameter is unaltered in cells treated with myosin II inhibitors (see Chapter 2). The role of myosin IIA contraction at the IS remains unclear (Hammer and Burkhardt, 2013). However, myosin IIA interacts with LFA-1 during T cell migration, and provides contractile forces required to break LFA-1-ICAM-1 bonds in the trailing end of a migrating T cell (Morin et al., 2008). Additionally, myosin IIA is required for focusing of ICAM-1 microclusters into an annular pattern similar to the pattern we observe for high affinity LFA-1 (Kumari et al., 2012; Yi et al., 2012). This suggests that myosin IIA can exert a direct force on LFA-1, triggering hybrid domain swing-out and affinity maturation of LFA-1 at the IS. This reasoning is in line with evidence that myosin IIA maintains T cell-APC conjugate formation and stability (Ilani et al., 2009).

Interestingly, although high affinity LFA-1 conformation depends on F-actin dynamics, we did not observe a direct spatial correlation between LFA-1 activation and F-actin density or flow rate. A likely explanation for this is that nascent LFA-1-ICAM-1

microclusters originate in the F-actin rich periphery and undergo flow-dependent centralization and compaction (Kaizuka et al., 2007). High affinity LFA-1 is more tightly linked to the actin cytoskeleton than low affinity LFA-1 (Cairo et al., 2006). Thus, centripetal actin flow would drive high affinity LFA-1 further toward the IS center (Hartman et al., 2009). This mechanism requires ICAM-1 to be mobile, and is supported by the fact that the ring of high affinity LFA-1 molecules is distributed more peripherally in T cells responding to coverglasses coated with immobilized ligand, and more centrally in cells responding to bilayers or APCs.

The relative contribution of valency and affinity of LFA-1 in the formation and maintenance of T cell–APC contacts has been a subject of ongoing debate (Bazzoni and Hemler, 1998; Carman and Springer, 2003; Kim et al., 2004). We show here that T cell actin flow drives both aspects of avidity modulation. While flow is required to maintain the high affinity conformation of LFA-1 independently of changes in valency, it also maintains the accumulation of LFA-1 of all affinities at the synapse (Figure 3.13). If the total amount of high affinity form of LFA-1 at the IS represents the total avidity of the system, we observed a 60% reduction following inhibition of actin dynamics. Normalization to total LFA-1 at the IS reveals that changes in affinity account for 70% of this loss, while valency modulation accounts for the other 30%. Thus, while actin flow regulates both valency and affinity, the primary effector of firm adhesion is likely to be the regulation of affinity.

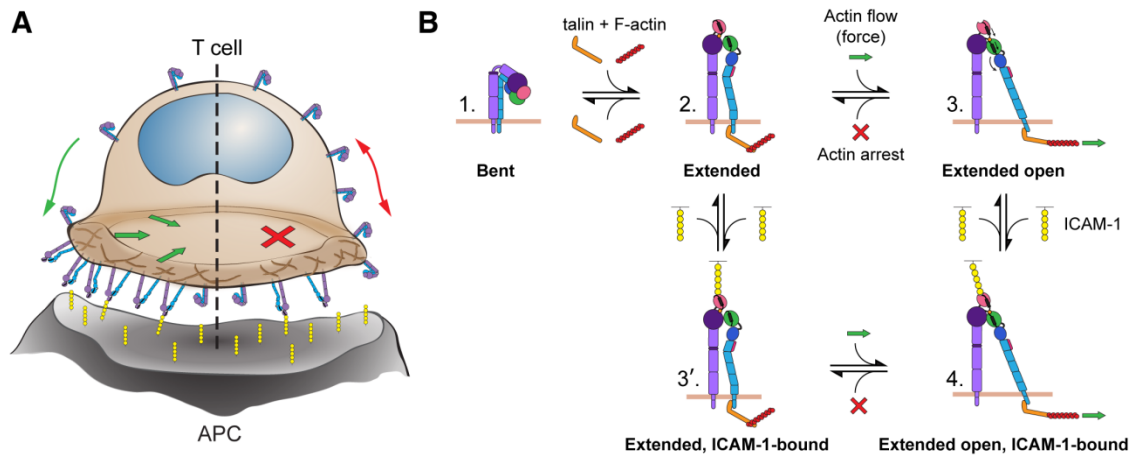


**Figure 3.13. Model of avidity regulation of LFA-1 at the IS**

(A) Ongoing F-actin flow (left) in T cells responding to polarized TCR stimuli actively drives accumulation of LFA-1 at the cell-cell interface. Loss of F-actin dynamics (right) abrogates active recruitment of LFA-1 to the IS and instead leads to passive diffusion of LFA-1 away from the contact site. (B) Inactive LFA-1 exists in a bent conformation (1) on the T-cell surface. Inside-out signaling events downstream of TCR engagement lead to recruitment of talin and F-actin to the integrin  $\beta$  tail. This allows for the segregation of the  $\alpha$  and  $\beta$  tails, and the “switch-blade” unbending of LFA-1 (2). Subsequent application of F-actin-generated tensile force along the talin-LFA-1 interaction facilitates a greater separation of the integrin chains, resulting in swing-out of the hybrid domain and induction of the open headpiece (high affinity) form of LFA-1 (3). The open  $\alpha$ I domain allows for binding of ICAM-1, which through induced fit and resistance of the facilitating force stabilizes LFA-1 activation (4). Alternatively, LFA-1 affinity maturation can proceed through an ICAM-1-bound, intermediate affinity conformation (3'), in which ICAM-1 interacts first with the extended conformation and induces the open head domain prior to application of force; force then stabilizes this interaction.

It is interesting to note that engagement of different integrins by immobilized ligands has distinct effects on F-actin dynamics at the IS. In Jurkat T cells, VLA-4 ligation of VCAM-1 has been shown to decelerate F-actin flow nearly to a halt (Nguyen et al., 2008). We have reproduced this finding, but did not see a similar effect in Jurkat T cells responding to ICAM-1 (data not shown). In primary T cells, we find that engagement of LFA-1 induces a very modest slowing of the actin network. However, we observed significant slowing in primary T cells responding to a combination of VLA-4 and LFA-1 ligands. The reasons for this difference are unclear; one plausible idea is that the  $\beta 1$  chain provides tight anchorage to the actin cytoskeleton, while the  $\beta 2$  chain allows slippage and continued actin flow. This could be achieved through differential interactions with actin-binding adapter molecules. If slippage of LFA-1 – actin interactions is occurring, the transient interactions must be sufficient to maintain LFA-1 conformational change. Consistent with the observed slowing of the actin network, we observed diminished LFA-1 activation with the addition of VCAM-1. This has important functional implications, since upregulation of VLA-4 during T cell activation could not only enhance binding to VCAM-1, but also effectively down-regulate LFA-1 dependent interactions.

Our data suggest that force provided by the T cell F-actin network is critical for integrin affinity maturation and maintenance of catch-bond interactions between LFA-1 and ICAM-1. While loss of LFA-1 affinity is likely to be a direct effect of loss of force following inhibition of F-actin dynamics, it is possible that other molecules involved in LFA-1 signaling are also affected by cytoskeletal immobilization. In fact, talin and vinculin, two cytoskeletal proteins involved in regulation of integrin activation and

adhesive strengthening, depend on force transmission for proper function (del Rio et al., 2009). Talin, as previously mentioned, is required for the initial unbending of inactive integrins, thus producing the intermediate affinity conformation. Subsequently, talin functions as one of the key molecules linking the  $\beta$  chain to the actin cytoskeleton, thereby transducing force between the cytoskeleton and the integrin. Talin itself is regulated by mechanotransduction, and can stretch by up to 160 nm under tension (del Rio et al., 2009). Stretching of talin is dependent on myosin II contraction and is transient in nature, with multiple stretching and relaxation events occurring over time (Margadant et al., 2011). Unfolding of the rod domain in talin reveals 11 vinculin binding sites; vinculin in turn stabilizes talin stretching in a feedback loop and also binds to F-actin, reinforcing the connection to the cytoskeleton (Ciobanasu et al., 2013; Hirata et al., 2014; Margadant et al., 2011). Vinculin interaction with talin is reversible and mechano-sensitive, thus, loss of tension would most likely result in talin dissociation from the F-actin network. While knowledge about talin and vinculin mechano-sensitivity comes from research done on focal adhesions in other cell types, it is known that vinculin is delivered to the T cell IS in a WAVE2-dependent manner, and is required for talin recruitment and conjugate stability, but not for recruitment of LFA-1 (Nolz et al., 2007). These observations indicate that vinculin stabilization of the interaction between F-actin and talin specifically enhances LFA-1 affinity maturation at the IS.

Synapse formation is only a single step in an immune response. Prior to antigen-dependent stimulation, T cells continuously migrate in the lymph nodes searching for ligands. Once cognate peptides are found, T cells stop and form a stable conjugate with an APC to receive information about intruding pathogens. Once appropriate stimulation

has been achieved, T cells release the APCs and regain migratory characteristics. The regulation of “stop and go” signals is not entirely understood, and how T cells can disengage from the firm attachments with APCs is currently unknown. Our findings suggest that LFA-1 would naturally disengage ICAM-1 on APCs if the symmetric F-actin flow dissipates. Over time, if signals from the TCR diminish, either through loss of antigen or increase in negative regulators, such as CTLA-4, F-actin flow would also diminish. This would reduce the amount of force on the integrin bonds and cause relaxation of the contact. Such a model postulates a self-regulated timing mechanism for proper T cell activation.

Besides their function in adhesion, integrins are also potent costimulatory molecules. The pathways downstream of integrin activation are termed “outside-in” signaling. Naïve T cells require activation of LFA-1 through “inside-out” signaling downstream of TCR, which in turn depends on adhesion downstream of integrins. This “catch 22” scenario has made “outside-in” signaling notoriously hard to study. However, a few studies have successfully separated integrin outside-in signaling from integrin mediated adhesion. LFA-1 engagement has been shown to lead to SLP-76 microcluster formation and T cell polarization in an ADAP-dependent fashion (Baker et al., 2009; Wang et al., 2009). T cells lacking  $\beta 2$  chain were unable to respond potently to TCR stimulation even in the context of CD28 costimulation, resulting in reduced ERK phosphorylation and inflammatory cytokine production at later time points (Li et al., 2009; Varga et al., 2010). Importantly, it has been shown that “outside-in” signaling in the integrin  $\alpha$ IIB $\beta$ 3 is completely dependent on the segregation of  $\alpha$  and  $\beta$  tails and does not occur in the extended conformation (Zhu et al., 2007). If LFA-1 functions similarly to  $\alpha$ IIB $\beta$ 3 in this

respect, it is likely that maintenance of the extended open conformation of LFA-1 represents the signaling competent pool at the IS. Therefore, F-actin dynamics may not only regulate “inside–out” mediated adhesion, but also affect “outside–in” side of signaling by LFA-1.

Given the critical role of cytoskeletal dynamics in maintaining the high affinity conformation of LFA-1, and the effects of ligand mobility on the extent of integrin centralization, it is likely that ICAM-1 mobility on the surface of APCs has a role in modulating the extent of LFA-1 activation. Highly mobile molecules would provide little resistance to the T cell cytoskeletal flow and thus be less effective in inducing high affinity state of LFA-1. In agreement with this, soluble ICAM-1 does not induce the extended open integrin conformation. Furthermore, immobilized ICAM-1 was able to induce LFA-1 activation when TCR was stimulated with either soluble or immobile ligands (Feigelson et al., 2010). It is also known that Natural Killer cells are highly to the mobility of ICAM-1 on target surfaces (Gross et al., 2010). When ICAM-1 mobility was increased by depleting F-actin in target cells, conjugates with NK cells became unstable and lytic granule polarization was diminished. Conversely, overexpression of actin-binding protein ezrin to anchor ICAM-1 to the cytoskeleton strengthened conjugates and enhanced lytic granule polarization. This evidence highlights modulation of ligand mobility as a potential way of regulating T-cell–APC interactions.

Overall, our results demonstrate the importance of F-actin dynamics at the IS in the mechanotransduction of intracellular signaling events leading LFA-1 activation. Interestingly, integrins may not be the only mechano-sensitive molecules on T cell surface, as recent findings implicate the TCR in mechanotransduction as well (Kim et al.,



2009). The emerging paradigm is that of a clock mechanism, whereby the F-actin flow sets the spatio-temporal parameters of signaling cascades at the IS, which ultimately result in effective T cell activation.

## CHAPTER 4: DISCUSSION

### Summary

Cytoskeletal remodeling is a crucial aspect in regulation of numerous T cell functions. Early studies highlighted the degree of importance of actin filaments in signaling events that take place at the IS. However, those studies were inconclusive regarding the exact role of the filamentous network. Recent approaches aim to investigate whether F-actin-generated forces contribute to the molecular rearrangements in early T cell activation. In the present work, we demonstrate that propagation of signaling at the level of  $\text{Ca}^{2+}$  mobilization and integrin triggering is dependent upon ongoing F-actin dynamics at the IS.

By using a combination of inhibitors that perturb F-actin turnover and myosin IIA activity, we have established that the retrograde flow of the actomyosin network is a consequence of actin polymerization, rather than myosin IIA contraction. Consistent with previous reports, we showed that myosin IIA accumulates at the IS upon TCR engagement and associates with F-actin into tight bundles in the lamellum. Under conditions that stabilize F-actin, myosin IIA is able to exert tension of the network, but this tension is dispensable for the overall centripetal flow when F-actin polymerization proceeds normally. Although the exact role of myosin IIA in T cell activation is disputed, we found that myosin IIA contraction limits cell spreading and provides symmetrical organization of the interface. We showed that F-actin remodeling sustains  $\text{Ca}^{2+}$  mobilization by managing TCR-proximal signaling events. In our hands, the activation of Zap70 kinase was not altered by inhibition of F-actin dynamics, while PLC $\gamma$ 1

phosphorylation was significantly diminished in the absence of cytoskeletal retrograde flow.

We also researched the role of F-actin-generated flow in triggering activation of the  $\beta 2$  integrin LFA-1, which is an essential mediator in T cell adhesion and co-stimulation. Careful analysis of the localization of LFA-1 conformational intermediates revealed that the high-affinity conformation of LFA-1 is enriched in the inner zone of the pSMAC. The activated LFA-1 was largely excluded from the cSMAC and the dSMAC regions. The recruitment of LFA-1 to the IS, as well as induction of the high-affinity state largely depends on F-actin retrograde flow and partially on myosin IIA contraction. Unlike the  $\beta 1$  integrin VLA-4, which was previously shown to slow down F-actin retrograde flow (Nguyen et al., 2008), engagement of LFA-1 does not significantly retard actin centralization across the IS, although partial deceleration was observed. Additionally, co-engagement of VLA-4 attenuates LFA-1 activation most likely through modulation of F-actin dynamics. The above results cumulatively emphasize the contribution of persistent F-actin remodeling in the organization of signaling dynamics and integrin triggering during T cell activation. In this chapter, I discuss the significance of these findings and provide insight into future directions for research.

### **The architecture of actomyosin and microtubule networks at the IS**

In Chapter 2, I carefully investigated the organization of cytoskeletal networks at the IS. Live-cell analysis of fluorescently labeled molecules and fixed-cell immunofluorescence imaging revealed that actin filaments polymerize at the periphery of the IS and move centripetally. This peripheral accumulation of branched actin filaments

defines the lamellipodium , and is generated by the Arp2/3 complex in response to activation by WAVE2, HS1 and WASp (Gomez et al., 2007; Gomez et al., 2006; Nolz et al., 2006). Myosin IIA localizes behind the actin-rich ring and colocalizes with low levels of bundled F-actin. This zone is analogous to the lamellum in fibroblasts and keratocytes and is regulated by ROCK activity and myosin IIA contraction (Cai et al., 2006; Yam et al., 2007). Finally, the cell body (CB) region is mainly depleted of actomyosin network and serves as the site of MTOC docking. Microtubules accumulate throughout the CB and LM zones but they are sparse, albeit not absent, in the LP, mainly because ongoing F-actin flow pushes them out of the region (Waterman-Storer and Salmon, 1997). The cooperation between these two cytoskeletal networks facilitates efficient transport of signaling MCs, secretory vesicles and cellular organelles (Figure 4.1). The cyto-architecture of primary T cell bears resemblance with that of Jurkat T cells; however, the boundaries between the regions are less clear and there is significant accumulation of diffuse F-actin in the CB, which may reflect the extent of activation of NPFs in these cells.

I found that F-actin flow slows down inwardly along the radius of the IS. The deceleration has also been observed by other labs (Yi et al., 2012; Yu et al., 2010a) as well as in other cell types (Cai et al., 2006; Yam et al., 2007). While there are differences in the cytoskeletal organization between Jurkat cells and primary T cells, we report that their actin flow rates are comparable. Peripheral F-actin moves at an average of  $95 \pm 28$  nm/s in Jurkat cells, while in blasted primary T cells the flow averages  $83 \pm 47$  nm/s with gradual centripetal deceleration in both cell types. Indeed, the deceleration behavior may be a ubiquitous paradigm in nature, as suggested by mathematical

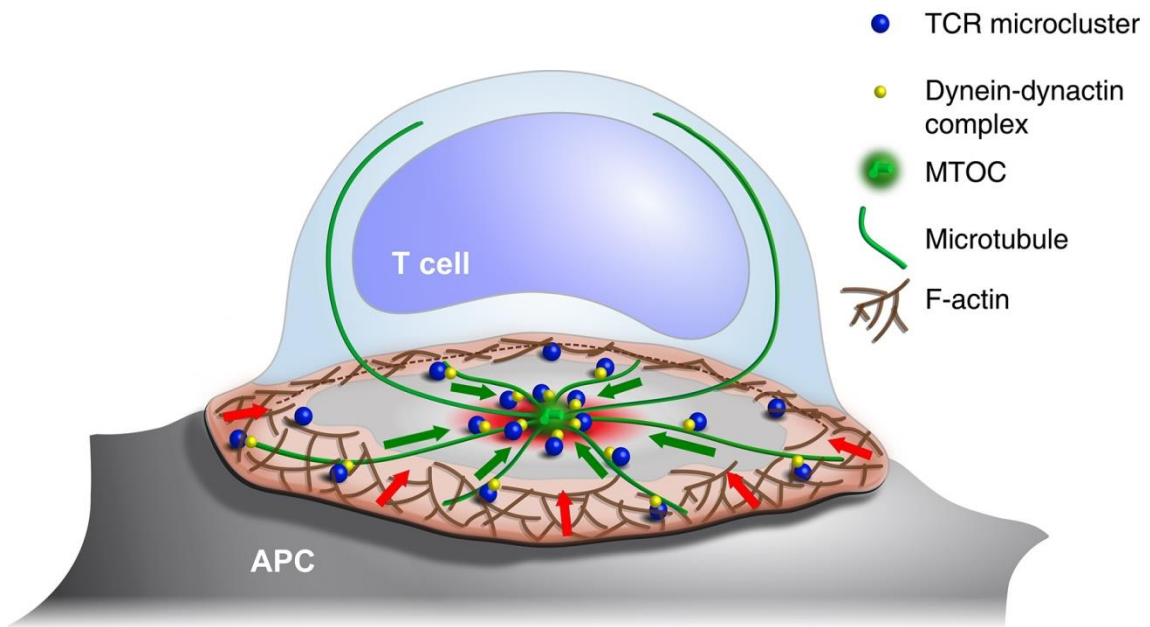


**Figure 4.1. Cytoskeleton-dependent organization of signaling machinery at the T cell immunological synapse**

A T lymphocyte interacting with an antigen presenting cell develops an immunological synapse, where T cell receptors and associated proteins assemble into membrane-bound microclusters that translocate continuously towards the center of the interface. F-actin retrograde flow initiates microcluster formation and movement in the periphery (red arrows), while microtubule-dependent transport by cytoplasmic dynein drives microcluster coalescence in the center of the immunological synapse (green arrows). The ongoing flow of F-actin also pushes the MTOC close to the membrane to facilitate the transport of MCs along microtubules. The delivery of signaling molecules to the central zone (red gradient) is associated with extinction of signaling.

Figure modified from:

Babich A and Burkhardt JK, *Lymphocyte signaling converges on microtubules*. *Immunity*. June 2011; Volume 34, pp. 825-827.

modeling (Zhu et al., 2010). Additionally, our finding that F-actin flow rates are higher on bilayers than on glass (Figure 3.4) indicate that ligand mobility can modulate F-actin flow, as has been shown for T cells spreading on mixed-mobility surfaces (Yu et al., 2010a).

Recently, a controversy has been raised regarding the nature of the actomyosin network at the IS. The issue is whether the network is a single unit or a combination of two independent networks. Yi et al. (2012) have proposed that actomyosin-rich LM originates downstream of formins, which polymerize linear actin filaments, while the extensive branched F-actin in LP, nucleated by Arp2/3 complex, presents a separate population of filaments. Although we agree that there is significant difference between LP and LM regions in terms of architecture and dynamics, we do not believe that those differences signify two independent networks. Indeed, closer examination reveals that GFP-actin speckles transverse the two zones as they move along the radius. Thus, we propose that the whole network is polymerized downstream of Arp2/3, and that branched actin filaments become progressively more parallel as more and more myosin IIA accumulates and bundles them. This is consistent with reports that formin activity is largely dispensable for actin polymerization at the IS (Gomez et al., 2007). Future experiments should be directed to visualize the F-actin cytoskeleton at high resolution using electron microscopy and super-resolution techniques such as PALM and STEDM.

### **The function (or lack thereof) of myosin IIA at the IS**

In the past decade, more than half a dozen papers have addressed the function of myosin IIA at the IS. Surprisingly, there is a great range of conclusions regarding the

importance of the motor in T cell activation. Early studies from the Krummel lab demonstrated that myosin IIA is dispensable for conjugate formation and molecular recruitment to the IS (Jacobelli et al., 2004). Subsequent work by Ilani et al. (2009) revealed that myosin II was essential for maintenance of T cell–APC contact and MC dynamics at the IS. These disparate findings have incited a number of follow-up studies, which attempted to iron out the inconsistencies. Yi et al. (2012) investigated IS formation in Jurkat T cells spreading on stimulatory bilayers. Although they did not find myosin II function as essential in F-actin retrograde flow, they did demonstrate that F-actin and TCR MCs move more slowly and haphazardly in T cells with inhibited myosin II activity. A parallel study by Yu et al. (2012) showed that treatment of cells with MLCK inhibitor ML-7 resulted in loss of  $\text{Ca}^{2+}$  mobilization and phospho-Zap70. In addition, (Kumari et al., 2012) showed that myosin IIA knockdown blunted  $\text{Ca}^{2+}$  flux and prevented of cSMAC coalescence. The disagreements about the extent of myosin IIA involvement in the cytoskeletal remodeling at the IS may reflect the various contexts of stimulation of T cells, however, that remains to be demonstrated.

The investigation in Chapter 2 also addresses the role of myosin IIA in T cell signaling. Using inhibitors of myosin II function (blebbistatin or Y-27632) or genetic intervention (Myh9 siRNA), we showed that F-actin flow is not perturbed in cells that lack myosin IIA contraction. Furthermore, stabilization of F-actin by jasplakinolide completely abrogates the flow in myosin IIA-inhibited cells, unlike in uninhibited cells, where jasplakinolide addition results in a collapse of the actomyosin ring to the center. T cells lacking myosin IIA function also show normal  $\text{Ca}^{2+}$  mobilization response and phosphorylation of TCR-proximal molecules, such as Zap70, SLP-76 and PLC $\gamma$ 1. In our

hands, lack of myosin IIA function in retrograde flow at the IS cannot be attributed to cell type or stimulatory conditions as we have recapitulated our findings in primary cells and on planar lipid bilayers. We do observe increased cell spreading and asymmetric oscillations in the actomyosin network in the absence of myosin II contraction, which suggests that myosin II exerts some influence on the network, but in most cases this influence is not necessary to sustain dynamics and signaling at the IS. Moreover, we have successfully used myosin II inhibitors to investigate the role of myosin II function in LFA-1 integrin activation (Chapter 3). Here, too, we see at best a blunting of LFA-1 activation upon myosin II inhibition, with the main role in the process falling on actin polymerization-derived dynamics.

The fact that we see actomyosin collapse to the center of the IS upon F-actin stabilization indicates that under some conditions myosin II is able to exert force on the network. It is important to keep in mind that myosin IIA is not an independent contributor to the retrograde flow, rather the motor moves along a continually moving track, analogous to a runner on a treadmill. Thus, the extent of myosin II contraction may be overshadowed by robust actin polymerization at the interface. Indeed, T cells have exceptionally fast retrograde flow, analogous to that in keratocytes (40-100 nm/s), and an order of magnitude higher than that in some epithelial cells (5-8 nm/s) (Ponti et al., 2004). This may reflect hyper-activation of machinery that drives network turnover at the IS, i.e. cofilin, profilin, HS1 and Arp2/3 among others. On the other hand, stabilization of F-actin filaments may exaggerate myosin IIA contraction by straining the whole network. In agreement with this notion, our unpublished observations indicate that



treatment with Calyculin A boosts myosin IIA contraction and causes a rapid collapse of the actomyosin network towards the center of the IS.

Studies *in vitro* and in keratocytes demonstrate that myosin II motor activity can sever actin filaments and thus contribute to retrograde flow (Haviv et al., 2008; Wilson et al., 2010). This is not the likely function in T cells as we do not see the accumulation of actin filaments in the center of the IS when myosin IIA function is abrogated. The severing activity may be unique to keratocytes because of their peculiar crescent shape. In these cells, myosin IIA accumulates in two foci behind the cell body, in zones of highest torsion in the network. However, T cells do not have such privileged sites of network disassembly and myosin IIA filaments are not positioned to tear the network apart. The apparent lack of myosin II contribution in retrograde flow or filament disassembly does not rule out its function in the organization of IS symmetry and spreading. Myosin II can cross-link anti-parallel filaments and assemble them into a coherent network that would function as a synchronous unit. This bundling activity would enable the cells to “feel” local fluctuations and minimize symmetry-breaking. In support of this idea, the Dustin lab reported that ablation of myosin IIA increases the percentage of cells that spontaneously initiate random migration of the stimulatory bilayers (Kumari et al., 2012).

### **What role do F-actin dynamics play in T cell signaling?**

The early models of T cell activation concentrated on the spatial distribution of molecular complexes but failed to explain the temporal progression of signaling (Grakoui et al., 1999). The simplistic understanding was that the accumulation of TCR in the

cSMAC would lead to efficient signaling. However, subsequent research has pointed out that early signaling begins before SMACs take shape (Lee et al., 2002). The modified models began to take the dynamic nature of the IS into account and postulated that active cytoskeletal flow contributes to molecular rearrangements required for proper signaling (Yokosuka et al., 2010). The data in Chapter 2 further solidify the notion that mere positioning of signaling complexes along the radius of the IS does not determine their signal potential. While peripheral retention of MCs augments signaling in the presence of F-actin retrograde flow (Mossman et al., 2005; Nguyen et al., 2008), retention of MCs in the absence of F-actin dynamics is insufficient to enhance activation. Peripheral localization of MCs may be necessary for signaling because machinery that determines signaling output is most efficient in the periphery of the IS. Once the machinery is shut down, however, the localization becomes irrelevant. In agreement with this explanation, we show in Chapter 3 that upon immobilization of F-actin flow, the remaining activated LFA-1 loses highly organized peripheral localization and becomes randomly distributed at the IS.

Varma et al. (2006) showed that the MCs that persist upon the depletion of F-actin are not sufficient to sustain signaling, since  $\text{Ca}^{2+}$  was reduced to baseline levels within minutes of Latrunculin A treatment. Consistent with this observation, we reported that Rho kinase inhibition (with Y-27) to inhibit myosin II activity and actin stabilization (with Jas) in T cells resulted in complete F-actin immobilization with a concomitant drop in intracellular  $\text{Ca}^{2+}$  levels (Chapter 2). In addition to immobilizing the F-actin network, this pharmacological manipulation inhibited new MC formation and immobilized existing MCs. Thus, two interpretations are possible: either ongoing actin-dependent

assembly of new MCs or application of actin-dependent mechanical force on existing MCs is needed to sustain  $\text{Ca}^{2+}$  signaling. While our original data implied that cytoskeletal forces and/or dynamic scaffold is required for signaling and nucleation of MCs, subsequent TIRF imaging of the “frozen” network revealed that F-actin filaments are lifted away from the membrane – something that could not be readily addressed by confocal microscopy. This novel finding leaves room for the possibility that a static scaffold may be sufficient for nucleation of *de novo* MCs, but upon F-actin immobilization the scaffold is physically displaced from the PM, creating a gap, which precludes signaling. Thus it is unclear whether actin polymerization sustains  $\text{Ca}^{2+}$  mobilization downstream of TCR by generating forces on the signaling molecules or by maintaining the F-actin scaffold in close proximity to the PM. While these two possibilities would be technically challenging to tease apart, it is clear that the existence of a static actin scaffold is insufficient to support  $\text{Ca}^{2+}$  signaling. Rather, a dynamic actin network is needed, reflecting a requirement either for continued actin polymerization or for centripetal flow of the actomyosin II network. Currently, we favor the need of direct forces on the signaling molecules.

Assuming that the cytoskeleton is capable of exerting direct forces on the signaling machinery at the IS, there are two plausible explanations for the data. First, force, which is a direct consequence of network remodeling, could propagate signaling. Force may be necessary to activate the TCR itself and/or some of its downstream effectors and also induce high-affinity state of LFA-1. Loss of F-actin dynamics would consequently relax the tension at the IS; conversely, engagement of receptors by immobilized ligands would increase the tension. There is support for this idea, as recent studies implicate force in

TCR and integrin signaling (Kim et al., 2009; Kong et al., 2009; Li et al., 2010). Current thinking is that actin flow induces conformational changes in receptors exposing moieties required for signaling (discussed below). Interestingly, we found that immobilization of the F-actin network did not affect tyrosine phosphorylation of Zap70 or SLP-76, suggesting that at least in Jurkat cells this phenomenon does not stem from effects on the TCR *per se*; whether this is true in primary T cells remains to be determined. However, we did find that PLC $\gamma$ 1 phosphorylation was diminished. This finding is in agreement with our studies on HS1-deficient T cells, where defects in lamellipodial actin and MC dynamics correlated with diminished association of PLC $\gamma$ 1 with the insoluble cytoskeletal fraction and unstable recruitment of pPLC $\gamma$ 1 to the IS (Carrizosa et al., 2009), see also (Patsoukis et al., 2009). Given that the active, phosphorylated pool of PLC $\gamma$ 1 preferentially associates with the cytoskeleton (Carrizosa et al., 2009; Patsoukis et al., 2009), it is interesting to speculate that PLC $\gamma$ 1 is a relatively direct point of intersection between the T cell cytoskeleton and the signaling cascade leading to ER store release.

An alternative explanation is that sustained signaling could require ongoing MC biogenesis. While many phosphorylation events have been correlated with enhanced signaling, it is not clear which events are causally linked to T cell activation. It is possible that only nascent MCs are capable of relevant signaling (e.g. production of IP<sub>3</sub> and DAG), in which case, the phosphorylation observed in the mature MCs may be a by-product of transient initial signaling. This model is supported by evidence that F-actin depletion blocks MC formation without diffusing mature MCs, yet signaling is abruptly lost (Campi et al., 2005; Varma et al., 2006). Similarly, interruption of TCR-pMHC

interactions prevents MC formation and induces loss of intracellular  $\text{Ca}^{2+}$  without affecting MC centralization (Varma et al., 2006).

The above-mentioned models are not mutually exclusive and could be mechanically linked. The assembly of MCs in the presence of a flowing cytoskeleton suggests that the cytoskeleton can provide a transient scaffold, a conveyor belt of sorts, to deliver MC components to the PM. Actin-rich sites nucleate complexes which mature with continual delivery of additional molecules until MCs become auto-stabilized. The simultaneous interaction with the cytoskeleton and extracellular ligands would create tension within MCs and induce conformational changes in interacting molecules. The tension would be maximal immediately prior to initiation of MC movement. If this is indeed the case, then one would expect that ligand mobility and clustering are important parameters that regulate the extent of T cell activation. Additionally, clutch molecules that transduce force from the cytoskeleton onto MCs are critical regulatory points for modulation of signaling. As discussed later in this chapter, future studies should evaluate the above predictions by employing force mapping techniques, coupled with genetic knockdown screens and correlative microscopy.

### **Mechanotransduction at the IS**

Actin dynamics may promote early steps of T cell activation by exerting forces on the TCR and its MC components and on integrins and their associated complexes. While key points of intersection have been identified, many mechanistic questions remain. Does mechanotransduction occur at the level of the TCR? If so, how is force transmitted to the TCR, and what, if any, is the contribution of the APC cytoskeleton? Why is the

activation of PLC $\gamma$ 1 sensitive to perturbation of actin dynamics – is there mechanotransduction at the level of signaling MCs? How exactly force induces high-affinity conformation of LFA-1? And which adaptor molecules are involved in force transduction for mechanical activation of integrins at the IS? In addition to these molecular questions, there are many unanswered questions about higher order interactions and feedback events. Here I will discuss the evidence that addresses these questions and provide the current paradigm in the field of how T cells test local extracellular environment and transduce the information across the PM.

### TCR triggering

Studies done in the 90's showed that TCR ligation induces the association of ITAM motifs with actin cytoskeleton (Rozdzial et al., 1995; Rozdzial et al., 1998). More recently Nck was suggested to mediate the interaction between the CD3 complex and F-actin (Kesti et al., 2007). While current literature agrees that actin at least in part drives TCR dynamics (Barda-Saad et al., 2005; DeMond et al., 2008; Hartman et al., 2009), to date, there is no clear understanding of how TCR connects to the actomyosin network. This question has important implications, since evidence exists for mechano-sensitivity within TCR (Kim et al., 2012; Kim et al., 2009). A likely explanation is that cytoskeletal forces may be transduced along the TCR and countered by ligand binding in the extracellular space (Feigelson et al., 2010; Hsu et al., 2012; Tseng et al., 2005). To test the mechanical triggering model, the Finkel lab showed that effective TCR triggering, as indicated by efficient Ca<sup>2+</sup> mobilization, depends on T cell adhesion to surrogate stimulatory surfaces and an intact cytoskeleton (Ma et al., 2008b). Whether force is required to expose ITAM motifs for cytoskeletal interactions is the subject of ongoing

debate (van der Merwe and Dushek, 2011). We find that Zap70 phosphorylation and accumulation at the IS persists in the absence of cytoskeletal flow. If mechanical triggering of the TCR was absolutely required for T cell signaling, then one would expect that such proximal kinase as Zap70 would be diminished at the IS once the flow is “frozen”. Therefore, at least in Jurkat T cells spreading on immobilized stimulatory antibody, mechano-sensitivity of the TCR is not required to maintain exposed ITAM motifs for Zap70 recruitment and phosphorylation. This, however, does not preclude the importance of this mechanism in other circumstances. Additional support for mechanical tension in T cell signaling comes from studies of T cells interacting with TCR stimulatory beads, where  $Ca^{2+}$  mobilization is enhanced by moving the attached bead away from the IS (Li et al., 2010). Current efforts should be made to measure and map forces exerted on the extracellular environment by the T cell cytoskeleton. Here too, the predictions are that the nature of stimulatory ligands, along with their mobility and clustering, should affect force-dependent signal propagation.

### Mechano-sensing in MCs

Using PALM imaging to visualize MCs containing different signaling molecules, the Baumgart lab has reported that MCs exhibit various morphologies and that the morphology is modulated by the F-actin cytoskeleton (Hsu and Baumgart, 2011). Furthermore, the report demonstrated that mobile SLP-76 MCs become progressively more segregated from the immobile Zap70 MCs in Jurkat T cells spreading on the anti-CD3-coated coverslips. It remains to be determined if this spatial segregation occurs on mobile stimulatory surfaces, or if molecular dissociation is a side-effect of ligand immobilization. These observations support a plausible explanation that the cytoskeletal

forces can be harvested at the level of multi-molecular complexes. While this concept is a fairly novel in the field, there is circumstantial evidence suggesting that MCs may be mechano-sensitive. Whether MCs reside on the PM or on vesicular compartments is a subject of ongoing debate. Nonetheless, MCs should not be regarded simply as endosomal vesicles, neither are they spontaneous aggregates of signaling molecules; rather, findings from the Samelson lab indicate that MCs possess highly organized nano-scale spatial organization (Sherman et al., 2011). Many protein interactions in MCs have been mapped using biochemical assays (Houtman et al., 2006; Kuhne et al., 2003; Yablonski et al., 2001). It is known that phosphorylation of LAT leads to recruitment of GADS/SLP-76 module to the PM and subsequent signaling events bring PLC $\gamma$ 1 to the complex (Braiman et al., 2006; Yablonski et al., 1998). In the MCs, PLC $\gamma$ 1 is wedged between LAT and SLP-76, with GADS serving as a hinge. One can envision that tension generated along the LAT/SLP-76 axis could be absorbed by PLC $\gamma$ 1. Interestingly, the activating tyrosine 783 lies in the region of PLC $\gamma$ 1 that would experience stretching if force was applied to SLP-76. ITK binds to SLP76 and is closely positioned to phosphorylate PLC $\gamma$ 1 (Bogin et al., 2007). Additionally, previous research from our lab demonstrated that loss of HS1, an effector of ITK, disrupts the spatio-temporal organization of PLC $\gamma$ 1-containing complexes at the IS (Carrizosa et al., 2009).

Further evidence that MC structure is critically important for signaling came from the Yablonski lab, where it was shown that length rather than the sequence of the P-I region of SLP76 is important for sustained signaling. Deletion of this region abrogated signaling but substitution of a scrambled sequence of the same length fully rescued signaling. Thus, the investigators argued that the P-I region of SLP-76 serves a structural role that is not



dependent on immediate protein-protein interactions (Gonen et al., 2005). Taken together, these results imply that proteins within MCs downstream of TCR can respond to mechanical forces and that force vectors may induce conformational changes in MC-associated signaling complexes.

### LFA-1 activation

LFA-1 can be regulated at the single molecule level, via affinity maturation, or at the population level (via valency). Our work in Chapter 3 shows that ongoing F-actin flow controls both mechanisms. Both LFA-1 and its binding partner talin exhibit mechanosensitivity and can respond to applied tension. In line with dependence of LFA-1 on mechanical stimulation, we find that actomyosin dynamics play a crucial role in LFA-1 recruitment to the IS and subsequent induction of the high-affinity conformation of integrin. While maintenance of the intermediate affinity conformation did not depend on F-actin flow, the proportion of molecules in the high-affinity conformation was significantly diminished upon F-actin immobilization. Moreover, organization of activated integrin into a ring pattern was maintained by F-actin flow, regardless of the context of stimulation. Interestingly, inhibition of myosin IIA alone reduced the efficiency of LFA-1 activation, even though we did not notice substantial effects on F-actin dynamics. Possibly, myosin IIA participates in bond-formation between F-actin and LFA-1, since myosin IIA has been found in integrin-associated complexes (Morin et al., 2008). The ongoing requirement for cytoskeletal dynamics reflects the catch-bond type binding of LFA-1, where tension strengthens the interaction and loss of tension relieves the bond with ligand (Thomas, 2008). Our data highlight the necessity of actin

polymerization-derived force in maintenance of firm adhesion through LFA-1–ICAM-1 binding.

#### Force-sensing by talin and vinculin

The link between LFA-1 and actomyosin is likely indirect and requires intermediates that can bind integrin and F-actin. The most prominent of these are talin and vinculin. In T cells vinculin is recruited to the IS downstream of WAVE2 and facilitates recruitment of talin to the interface (Nolz et al., 2007). Studies of focal adhesions demonstrated that talin is a mechano-sensitive molecule that stretches upon experiencing tension (del Rio et al., 2009). As described above, talin binding triggers extension of integrin chains and increases affinity for ligand (Simonson et al., 2006). Talin can also bind directly to F-actin, creating a physical link between integrins and the flowing actomyosin network. Accordingly, we find a high degree of co-localization of talin with high-affinity LFA-1. The presumption is that tension exerted along this axis kinetically tests the stability of the integrin interaction by using talin as a stretch sensor. In other systems, it has been shown that stretching of talin rod domain reveals 11 binding sites for vinculin, an adaptor protein that binds to Arp2/3 and F-actin, thus reinforcing the bond with the cytoskeleton. In turn, loss of tension on talin reverses vinculin binding and weakens the bonds (Hirata et al., 2014). Thus, in T cells talin and vinculin may comprise a module that feeds back on force to strengthen the interaction between LFA-1 and actin cytoskeleton, as has been shown for focal adhesions in other cell types (Ciobanasu et al., 2013).

### Ligand mobility and clustering

Tension that is an essential component in mechanotransduction must come from application of force and concomitant resistance of engaged molecules. Thus, an important area of investigation is mobility of ligands on the surface of APCs and how this parameter influences the spatio-temporal organization of signaling dynamics at the IS. Currently there are reports that surface stiffness and ligand mobility affect TCR signaling (Hsu et al., 2012; Judokusumo et al., 2012; O'Connor et al., 2012; Tseng et al., 2005). Furthermore, mobility of integrin ligands is also critical in adhesion and costimulation, as affinity maturation of LFA-1 occurs only in the presence of surface-bound, but not soluble ICAM-1 (Feigelson et al., 2010). Going forward, the challenge for the field is to understand this integrated complexity, a task that will require novel approaches ranging from protein conformational biosensors to multi-photon analysis of signaling dynamics during an *in vivo* immune response. The mechanisms that determine ligand mobility and clustering on APCs may prove to be great therapeutic targets to modulate the immune response.

### Putting the mechanotransduction model to the test

Although the mechanotransduction model can account for the requirement of ongoing F-actin flow at the IS, it is not the only plausible explanation. F-actin remodeling could participate in the recruitment and spatial organization of signaling complexes independently of force transduction at the molecular level. More careful analysis is needed to determine the production of force at the IS, and whether that force can be utilized by the receptors and/or receptor-associated molecules to initiate and sustain signaling. Here I will present a few directions to test the specific aspects of the

mechanotransduction model as well as consider the alternative hypotheses for the role of cytoskeletal rearrangements in at the IS.

Currently, forces exerted by the T cell cytoskeleton are poorly characterized. Multiple aspects of T cell biology impede the progress on this front. T cells are relatively small, spreading to an average of 100-200  $\mu\text{m}^2$  (Chapter 3), while other cell types, such as fibroblasts, in which forces have been successfully mapped, spread to a 15-fold larger area (Cai et al., 2010). Also, unlike the firmly adherent cells, T cells do not form focal adhesions or stress fibers, indicating that the forces in this cell type are much lower in magnitude. Despite these caveats, numerous efforts are being made to track cytoskeletal forces during T cell activation. The Milone lab has recently engineered high-density pillar arrays that can report forces based on the deflection of individual pillars (M. Milone, personal communication). Analogous substrates had been used previously to track forces in other cell types (Cai et al., 2006), however, the densely-packed arrays will facilitate the precise mapping of forces at the T cell IS. Additionally, acrylamide gels with embedded beads have been used to measure force vectors in Jurkat T cells responding to anti-CD3-coated surfaces (A. Upadhyaya, personal communication). Although these measurements are relatively crude, they provide evidence that tension along the TCR correlates with F-actin retrograde flow rate (unpublished data).

To test the necessity of force in TCR and LFA-1 activation one could supply external forces on T cells with the immobilized F-actin network. In chemokine signaling LFA-1 activation has been shown to rely on shear stress produced by blood flow *in vivo* (Shamri et al., 2005). Thus, shear flow is predicted to create the tension that may be necessary for receptor activation and signaling. Closed-chamber systems, which regulate the fluid flow

rate, could rescue the TCR and integrin signaling even without ongoing F-actin centralization at the IS. Alternatively, stretchable surfaces can be used to introduce strain on the receptors (Tamada et al., 2004). Stretching of T cells after “freezing” the F-actin network would provide the force, which may be required for sustained  $\text{Ca}^{2+}$  mobilization and induction of high-affinity conformation in LFA-1.

The pharmacological treatments used in this thesis cannot readily differentiate between the role of the F-actin polymerization and retrograde flow, since stopping one precludes the other. Thus, at this time it is not possible to determine whether signaling is maintained essentially by the network flow or by the ongoing production of filaments. Local bursts of F-actin polymerization throughout the IS plane may generate forces orthogonal to the membrane; this would allow for tension-dependent activation of the receptors even in the context of freely mobile ligands, as seen on the stimulatory bilayers. The differential roles of F-actin polymerization and retrograde flow could be governed by two related NPFs: WASp and WAVE2. These molecules differ in their localization at the IS; while WAVE2 localizes to the LP region (Nolz et al., 2006), WASp is preferentially recruited to the MCs (Barda-Saad et al., 2005). Moreover, ablation of WAVE2 has detrimental effects on the F-actin network flow at the IS, though WASp seems dispensable for this process (Nolz et al., 2006). Current research from the Dustin lab indicates that WASp and HS1 orchestrate TCR signaling (M. Dustin, personal communication), pointing to the functional importance of WASp-dependent F-actin polymerization in the TCR MCs.

We show that the F-actin reorganization is needed to recruit the LFA-1 integrin to the T cell–APC contact site, promoting the role of F-actin dynamics in valency regulation.

This paradigm can be extended to other membrane receptors and cytoplasmic adapter molecules. Newly polymerized actin filaments may provide a specialized dynamic scaffold for the recruitment of signaling molecules to the PM. In line with this idea, new MC formation is abrogated upon F-actin “freeze”. Furthermore, retrograde flow can increase local concentration of signaling molecules at the IS and facilitate their subsequent activation. Thus, it has been shown that in migratory cells the spatial persistence of Rac activity specifically depends of F-actin remodeling and not simply on F-actin accumulation at the leading edge (Peng et al., 2011).

Recently, the Baumgart lab demonstrated by super-resolution microscopy that Zap70, LAT and SLP-76 complexes exhibit a variety of cluster morphologies at the IS, which may reflect transmission of forces along MC components (Hsu and Baumgart, 2011). MC shape was shown to be partially regulated by the presence of actin filaments at the IS, since depletion of F-actin destabilized MC shape leading to a loss in circularity, indicating that F-actin plays a scaffolding function in the organization of signaling molecules within MCs. This, however, does not eliminate the role of flow-generated force in signaling, as the deformations in MC morphology could result from other factors, for example microtubule-dependent motility, and may not be relevant in signaling.

Even though our original observation that F-actin flow sustains signaling at the IS pointed to mechanotransduction, recent TIRF imaging of T cells with the immobilized F-actin revealed that the acto-myosin II network is lifted off the PM. This result leaves room for a possibility that force is not crucial for signaling. Rather, the presence of a static F-actin scaffold in close proximity to the PM could facilitate signal transduction. In this case, ongoing F-actin remodeling is required to continually push the network against

the membrane and thus maintain the interaction of F-actin with the membrane-associated components of the TCR and integrin signaling pathways. This evidence also reveals that the polymerization exerts pushing forces parallel as well as normal to the PM. Thus, a T cell not only spreads on the stimulatory surface, but also actively pushes itself into the APC. This mode of behavior can facilitate a more efficient discovery of pMHCs and enable mechanotransduction independently of the centripetal flow at the T cell IS.

### **What are the clutch molecules that couple signaling molecules to cytoskeletal flow?**

Just like an automobile requires a clutch to modulate transduction of force between the engine and transmission, T cells rely on adaptor molecules that couple signaling receptors and receptor-associated proteins to F-actin flow. Simplistically, these “clutch proteins” should be regulated in an activation-dependent manner and should be able to bind F-actin and MC components. Loss of a “clutch” should diminish signaling efficiency (e.g.  $\text{Ca}^{2+}$  mobilization) and possibly MC dynamics. Multiple proteins have been found that fit these criteria; however, the redundancy on one hand and the cooperative nature of interactions on the other make the investigation of individual components a cumbersome task. To name a few putative “clutches”: HS1 (Gomez et al., 2006), Vav1 (Sylvain et al., 2011), ADAP (Pauker et al., 2011), WASp (Barda-Saad et al., 2005), talin (Wernimont et al., 2011) and ezrin (Lasserre et al., 2010) amongst others. These proteins have been shown to localize to the IS and modulate various aspects of TCR signaling. I propose that future investigations should involve a broad shRNA screen to discover which “clutch” molecules play dominant roles in MC assembly, dynamics and signaling.

## **Cross-talk between TCR and integrin signaling complexes**

Some of the early studies of IS formation concentrated on stimulation through the TCR alone (Bunnell et al., 2002; Bunnell et al., 2001). Subsequent work compared synapse architecture downstream of TCR or integrin ligation (Baker et al., 2009). Side-by-side comparison showed that SLP-76 MCs exhibit differential assembly kinetics and dynamics under the two stimulatory conditions. Thus, MCs formed by TCR ligation assembled quickly and underwent centralization to the cSMAC, while MCs generated by integrin ligation showed up later during cell spreading and were largely long-lived and immobile. Baker and colleagues implicated different binding partners of SLP-76 in the formation of different MCs. The interaction with LAT turned out to be essential for formation of SLP-76 MCs downstream of TCR, while binding to ADAP was crucial for MCs downstream of integrins. Remarkably, it took almost a decade since the first report from the Kupfer lab regarding the molecular patterns at the IS (Monks et al., 1998) to conduct careful high-resolution imaging of synapse formation in the costimulatory setting (Kaizuka et al., 2007; Nguyen et al., 2008). Studies on bilayers demonstrated that integrin clusters and TCR MCs reside in spatially distinct yet adjacent micro-domains within the IS. Furthermore, findings on stimulatory coverglasses indicated that in the context of stimulation by anti-CD3 antibody and VLA-4 ligand, MCs do not centralize at the IS but instead exhibit stronger signaling in the periphery. The homogeneity of behavior suggests that in that setting all MCs have the same properties, which means that when stimulated by both ligands, T cells make hybrid clusters that contain signaling molecules associated with TCR and with integrins. Unpublished work from our lab shows that on patterned



surfaces, *de novo* MCs preferentially form at the interface between TCR and integrin ligands, suggesting that MC nucleation is a cooperative process that involves both axes of signaling. It would be informative to investigate the molecular make-up of these MCs by surface micro-patterning techniques combined with super-resolution imaging and correlative microscopy.

### **Actin-microtubule cross-talk in synaptic organization and dynamics**

The newly-formed IS exhibits extensive actin polymerization towards the APC, followed by efficient polarization of MTOC to the center of the contact zone. Studies in Jurkat T cells stimulated on glass have shown that microtubules are dispensable for the initial burst of F-actin at the IS (Bunnell et al., 2001). However, microtubules are required to maintain long-term cell spreading and molecular dynamics. It is thought that microtubules provide tracks for delivery of signaling molecules that are required for proper signaling (Lasserre and Alcover, 2010).

Using TIRF imaging that enables visualization of cytoskeletal structures within 90 nm from PM, we show that inhibition of F-actin turnover leads to lifting of the F-actin and microtubule networks away from the synapse. Our finding that precise positioning of MTOC at the membrane depends on actin dynamics indicates that there is ongoing interplay between the two networks during sustained phase of signaling. To determine whether F-actin actively pushes microtubules towards the IS, one should depolymerize the F-actin network and examine the presence of microtubules in the TIRF plane. I postulate that in the absence of an F-actin scaffold, microtubules will not be able to associate tightly with the PM. This poses a question about how microtubules and

branched actin filaments are organized with respect to each other. Whether microtubules grow below or above the actin flow remains to be answered by careful 3-D reconstruction of super-resolution images and/or electron tomography.

Given that the F-actin network continuously flows away from the PM, actin-dependent pushing of microtubules towards the PM is possible only if microtubules associate with the growing ends of actin filaments. To date, there is no evidence that microtubules and actin filaments bind directly to each other. Therefore, the interaction is likely facilitated by auxiliary proteins that have dual affinity for F-actin and microtubules. Formins, such as mDia and FMNL1, fit well within this profile. Recent work from the Billadeau lab showed that formin-dependent actin polymerization is dispensable for formation of peripheral lamellipodia (Gomez et al., 2007). Furthermore, it was also found that depletion of formins abrogated efficient translocation of the MTOC to the IS. Immunofluorescence staining revealed that mDia and FMNL1 colocalize with F-actin and also with the MTOC. This observation is consistent with earlier findings that mDia mediates formation and organization of stable microtubules (Palazzo et al., 2001). Evidence that mDia associates directly with microtubules (Bartolini et al., 2008) or with the +TIP tracking protein EB1 (Wen et al., 2004) further corroborates involvement of formins in microtubule organization and stability. The recently identified formin inhibitor SMIFH2 could be used to shed new light on this area of research (Rizvi et al., 2009). The prediction is that acute loss of formin activity during the sustained phase of spreading would enhance signaling by preventing efficient MTOC anchoring at the IS and disrupting centralization of TCR-mediated MCs. Additionally, co-localization and

immune-precipitation experiments should help identify the interactions that mediate crosstalk between the two cytoskeletal networks.

Another protein that is known to coordinate cytoskeletal crosstalk at the IS is ezrin (Roumier et al., 2001; Shaffer et al., 2009). Knockdown of ezrin in T cells altered organization of microtubules and apposition of MTOC to the PM (Lasserre et al., 2010). Furthermore, ezrin silencing disrupted movement of SLP-76-containing MCs, leading to hyper-activation of signaling molecules, such as PLC $\gamma$ 1 and Erk1/2. Ezrin is recruited to the IS and our unpublished observations indicate that while ezrin clusters in the periphery of the interface, it does not colocalize with SLP-76 MCs (data not shown). Since ezrin does not bind microtubules directly, it relies on binding partners, such as Disk Large 1 (Dlg1), to mediate the interplay between F-actin and microtubules. Furthermore, ezrin FERM domain can bind to phospholipids (Jayasundar et al., 2012), opening the possibility that ezrin-Dlg1 complexes recruit microtubules directly to PM.

Microtubules and microtubule-dependent motor cytoplasmic dynein have been linked to processive MC centralization (Figure 4.1). Colchicine treatment disrupts microtubules and prevents movement of SLP-76 MC to the cSMAC region (Bunnell et al., 2002). Additionally, dynein is recruited to the IS (Combs et al., 2006) and its silencing abolishes MC coalescence and prolongs signaling in the pSMAC (Hashimoto-Tane et al., 2011). We find that the relatively uniform centralization rate of SLP76 MCs is consistent with the power output of a cytoskeletal motor such as cytoplasmic dynein. Although in other cell types cytoplasmic dynein has been reported to move nearly 20 times faster than SLP-76 MCs (Ma and Chisholm, 2002) (1.7  $\mu$ m/s for dynein vs. 80 nm/s for SLP-76 MCs), we believe that the apparent MC rate is the result of simultaneous engagement of the

microtubule and the F-actin networks. Interestingly, MCs do not collapse onto the MTOC after F-actin depletion (Nguyen et al., 2008; Varma et al., 2006), suggesting that ongoing F-actin turnover is necessary to maintain their interaction with microtubules. Subsequent studies should investigate this peculiar phenomenon.

The role of F-actin flow in MC dynamics is undisputed and numerous labs show that depletion of F-actin halts MC movement (Nguyen et al., 2008; Varma et al., 2006). We also show that immobilization of F-actin stops SLP-76 MCs from reaching the center of the IS (Figure 2.9 and Movie 2M). The Krummel lab had reported that in migrating T cells TCR MCs move to the F-actin-poor region rather than to the cSMAC (Beemiller et al., 2012). Their conclusion was that MCs are transported by actin centripetal flow into the zone of actin depolymerization. While this is a likely explanation, it may not be complete. I postulate that during cell migration, the microtubule network is constantly remodeled by F-actin flow. Buckling of microtubules may deflect MC trajectories away from the MTOC. As described above, there is enough evidence supporting the notion that MCs simultaneously associate with F-actin and with microtubules and that both networks participate in their centripetal movement.

### **Concluding comments – the big picture of the IS**

Here we have shown that ongoing remodeling of the F-actin cytoskeleton is required to sustain signaling and choreograph spatio-temporal organization of receptors and associated complexes at the IS during early phases of T-cell activation. In the past one and a half decades we have learned a lot about the structure and function of the IS. New imaging techniques and biological assays have significantly advanced our understanding

of the mechanisms that drive T cell activation. However, our current knowledge represents but a sliver of all the secrets hidden in T cells. Redundancy and complexity in the system have significantly slowed down our progress and have often led to erroneous conclusions. A major caveat in research is that pathways are studied in isolation, often without deep regard to how other pathways may be affected by feed-back and feed-forward loops. The F-actin cytoskeleton, while a major player, is only one contributor in an immensely integrated network. In order to make headway in our understanding of T cell activation, we must see the IS as an irreducibly complex matrix, where each variable to some extent affects all the others. Future studies should be geared to provide a holistic view of the IS structure and function in space and time.

## CHAPTER 5: MATERIALS AND METHODS

### *Reagents and Antibodies*

Unless otherwise noted, reagents were from Sigma Aldrich. Y-27632 and (-)-blebbistatin were from EMD Chemicals. Jasplakinolide, Neutravidin, fura-2, AM, goat anti-mouse IgG-Alexa Fluor 680, Alexa Fluor 594 phalloidin, Alexa Fluor 488 and Alexa Fluor 594 labeling kits were from Life Technologies. CF405M phalloidin was from Biotium, and streptavidin DyLight 650 and DyLight 650 labeling kits were from Thermo Scientific. Leaf-purified anti-CD3 antibody OKT3 and biotinylated SK7 were from BioLegend and biotinylated OKT3 was from eBioscience. Mouse monoclonal antibodies TS2/4 (anti-CD11a) and Kim127 (anti-CD18) were harvested from hybridomas (ATCC). Mouse monoclonal antibody m24 (anti-CD18) was from Abcam. Goat polyclonal antibody against talin was from Santa Cruz. Rabbit polyclonal antibody against myosin IIA heavy chain was from Covance. Rabbit polyclonal antibodies against phospho-myosin light chain (pS19), phospho-PLC $\gamma$ 1 (pY783) and phospho-Zap70 (pY319) and rabbit polyclonal antibody specific for myosin IIB heavy chain were from Cell Signaling Technology. Rat monoclonal anti-alpha tubulin antibody was from Serotec. Mouse anti-GAPDH was from Millipore and goat anti-rabbit IgG-IRDye800 was from Rockland. Anti-phospho-SLP-76 (pY145) was from Epitomics and Alexa Fluor 647 anti-phospho-SLP-76 (pY128) was from BD Phosflow. Human VCAM-1-Fc chimera was from R&D Systems. 293T cells expressing his-tagged mouse ICAM-1 were generously provided by Dr. Eric Long, National Institutes of Health, and ICAM-1-His was purified from these cells as previously described (March and Long, 2011), also see below).

### *Plasmids and RNAi*

Unless otherwise noted, standard molecular biology protocols were used for molecular cloning. A construct expressing full-length heavy chain of non-muscle myosin IIA (NMHC IIA) N-terminally tagged with EGFP (Wei and Adelstein, 2000) was obtained from Addgene. A plasmid encoding NMHC IIA tagged with mKate2 was constructed in our lab. 5'-

tcgaggatccaccggtcgccaccATGGTGAGCGAGCTGATTAAGGAG-3' and 5'-

gccataagcttccggaacctctccaccTCTGTGCCCCAG-3' were used to PCR amplify mKate2 tag from the pmKate2- $\beta$ -actin vector (Evrogen). Capital letters indicate the tag and underlines indicate AgeI and HindIII restriction sites. The PCR product was digested with AgeI and HindIII and swapped with EGFP in the pEGFP-NMHC IIA-C3 plasmid.

F-Tractin (ITPKA-9-40) tagged with tdTomato was a gift from M. Schell (Johnson and Schell, 2009). cDNA encoding the 17 amino acid F-actin binding peptide Lifeact (a gift from the Sixt lab) was tagged with EGFP on the C-terminus using linker sequence 5'-GGGGATCCACCGGTCGCCACC-3'. Lifeact-EGFP was then cloned into the pDONR221 donor vector, and subsequently into pLX301 destination vector (Addgene) using Gateway Technology. Lentivirus was generated as described below.

For myosin IIA knock-down, ON-TARGETplus SMARTpool of siRNA duplexes against the heavy chain of human myosin IIA (Myh9) and siGENOME non-Targeting siRNA control #2 were purchased from Dharmacon. 500 pmol of oligonucleotides were used for transfection, as described below. For IQGAP1 knock-down, the shIQGAP1-targeting sequence (5' -GTCCTGAACATAATCTCAC-3'), which corresponds to nucleotides 1318–1336 using National Center for Biotechnology Information Genbank

accession number NM\_003870 was cloned into pFRT.H1p vector, which was described elsewhere (Gomez et al., 2006).

#### *Transfection of Jurkat and primary T cells*

We have found that transfection efficiency works best when cells are electroporated in antibiotic-free media. This is crucial to optimal yields. Growing the cultures in antibiotic-free media for 16-24 hours before electroporation enhances the growth of the cells, but is not as crucial of a factor as electroporating them in antibiotic-free media and culturing the cells after electroporation in antibiotic-free media. It is also crucial for the cells to be in log phase.

Cells were seeded at  $2.0 \times 10^5$  cells/ml cultured in antibiotic-free 10% FBS RPMI 1640 for 16-24 hours before electroporation. The next day cells were harvested and resuspended at  $2.0 \times 10^7$  cells/ml in antibiotic-free RPMI 1640 supplemented with 10% FBS. 500  $\mu$ l of cell suspension was transferred to a 4-mm BTX cuvette and a desired amount of DNA plasmid or RNA oligonucleotides (usually 20-40  $\mu$ g for DNA constructs and 1.5  $\mu$ g (~500 pmol) for siRNA) was added. Cells in cuvettes were then electroporated using BTX Electro Square Porator ECM 830 (Harvard Apparatus BTX) with a single pulse using 310V for 10ms. Immediately after that, cells were incubated on ice for 5 min and then transferred to antibiotic-free RPMI 1640 with 10% FBS. For expression studies cells were used 6-16 hours later. For RNAi-mediated knockdown cells were used 24-72 hours later. If it was necessary live cells were enriched using a Ficoll Paque gradient.

Transfection of primary human T cells was performed using electroporation of *in vitro* transcribed mRNA. To prepare mRNA, the EGFP-actin fusion protein coding



sequence was cloned 3' to the T7 promoter of the pGEM-64A plasmid (provided by Y. Zhao, University of Pennsylvania) (Zhao et al., 2006). *In vitro* transcription of 7-mG(ppp)G-capped and polyadenylated EGFP-actin mRNA was performed using the mScript mRNA kit (Epicentre Biotechnologies) in accordance with the manufacturer's instructions. Following purification, GFP-actin mRNA was evaluated for polyadenylation and overall RNA quality by electrophoresis using a 1% agarose gel and ethidium bromide staining.  $5.0 \times 10^6$  CD4<sup>+</sup> T cell blasts were washed once with PBS and resuspended in 100  $\mu$ l of RPMI 1640 medium (Lonza) without additives. 10  $\mu$ g of the *in vitro* transcribed EGFP-actin mRNA was added to the cell suspension and the cell/mRNA mixture was transferred to a 2 mm cuvette (BTX). Electroporation with a single 500 V pulse of 720  $\mu$ s duration was performed using an electroporator as above. Electroporated cells were transferred to a culture flask containing 10ml RPMI-1640 medium, 10% fetal bovine serum (Hyclone) and 10 mM HEPES and incubated for 17-20 hours prior to use.

#### *Lentiviral transduction of primary T cells*

To generate recombinant lentivirus,  $1.8 \times 10^7$  293T cells were seeded in 15-cm plates the day prior to transfection, and then co-transfected using the calcium phosphate method with 48  $\mu$ g of the DNA of interest (PLX301 backbone), 36.3  $\mu$ g of psPAX2 and 12.1  $\mu$ g of pDM2.G. Supernatant was harvested 30 hr. after transfection and used immediately to transduce T cells. T cells were transduced by spin infection with lentivirus on day 3 post activation.  $2.0 \times 10^6$  blasting T cells were seeded per well of a 6-well culture plate containing 2 ml of lentiviral supernatant along with 8  $\mu$ g/ml Polybrene. Cells were centrifuged at 2,000 rpm and 37°C for 2 hr. at which point, the media was replaced with



### *Cell Culture and T cell-B cell conjugation*

Jurkat cells stably expressing low levels of GFP-actin (Gomez et al., 2006) were primarily used for Chapter 2. J14 (SLP-76-deficient) Jurkat cells stably reconstituted with GFP-SLP-76 (Baker et al., 2009), were from Dr. G. Koretzky, Univ. of Pennsylvania.

Human peripheral blood CD4<sup>+</sup> T cells were obtained from the University of Pennsylvania's Human Immunology Core under an Institution Review Board (IRB)-approved protocol. T cells were activated with 4.5  $\mu$ m human T-Activator CD3/CD28 magnetic beads (Dynabeads, Life Technologies) in RPMI 1640 (Invitrogen) supplemented with 10% FBS (Atlanta Biologicals), GlutaMAX (Invitrogen) and 50 U/ml of human rIL-2. T cell blasts were cultured in a humidified 37°C incubator with 5% CO<sub>2</sub>. Beads were removed from T-cell cultures on day 6 after initial stimulation, and cells were then cultured for an additional day to allow for surface re-expression of CD3.

The human B cell line Raji was cultured in RPMI 1640 culture medium supplemented with 1% penicillin G and streptomycin, 1% GlutaMAX, 10%FBS. For conjugation experiments Raji B cells were pulsed with 2  $\mu$ g/ml staphylococcal enterotoxin E (SEE, Toxin Technologies) for 1 hour at 37°C and allowed to interact with equal number of T cells for 30 minutes.

### *Western blotting*

To verify Y-27632 activity in Chapter 2, Jurkat T cells were pretreated for 15 min with DMSO alone or 25  $\mu$ M Y-27632 and stimulated with soluble OKT3 (1  $\mu$ g/ml) for 5

min. Cells were then washed in cold PBS and lysed at 4°C in 50 mM Tris-HCl (pH 7.5), 150 mM NaCl, 5 mM EDTA, 1% Triton X-100, 10 mM NaF, 1 mM Na<sub>3</sub>VO<sub>4</sub>, and protease inhibitors. For western blotting, lysates were separated on a NuPAGE gel (Invitrogen), transferred to nitrocellulose, probed with the indicated primary antibodies in 3% BSA in TBST, followed by incubation with secondary antibodies diluted in 3% dry milk in TBST. Membranes were imaged on a LI-COR Odyssey fluorescence scanner within the linear range.

#### *Preparation of supported planar lipid bilayers<sup>7</sup>*

Lipids DOPC, DSPE-PEG(2000)-biotin and DGS-NTA(Ni) (Avanti Polar Lipids) were reconstituted in chloroform at 98:1:1 mol %, respectively. The mixture was then dried under a gentle stream of air and desiccated in a vacuum chamber for 1 hour. The dried lipid cake was hydrated in PBS, sonicated using a tabletop sonication bath (Branson) for 15 min to generate multilamellar vesicles, and then passed through a 50 nm pore membrane using a mini-extruder (Avanti Polar Lipids). The resulting small unilamellar vesicles were stored at 4°C for 2-3 months.

25×75 mm glass slides (# 1.5, Thermo Scientific) were cleaned for 15 minutes using Piranha solution (3:1 ratio of sulfuric acid and 30% hydrogen peroxide) (Dustin et al., 2007) and then washed thoroughly with distilled water. Slides were then air-dried and adhered to Sticky-Slide I<sup>0.2</sup> Luer closed chambers (Ibidi). Small unilamellar vesicles in PBS were added to the chambers to cover the exposed glass surface for 15 min. After

---

<sup>7</sup> For a comprehensive version of this protocol refer to Appendix A.

thorough rinsing with PBS, the chambers were incubated with Neutravidin (Life Technologies) and 1 mM NiSO<sub>4</sub> for 15 minutes, then thoroughly rinsed again with PBS and incubated with excess OKT3-biotin and ICAM1-His. Chambers were rinsed and left in phenol red-free L-15 imaging medium (Invitrogen) supplemented with 2 mg/ml D-glucose. Lipid bilayer surfaces were used for imaging studies on the same day.

#### *Single-cell Ca<sup>2+</sup> assays*

Jurkat T cells were loaded with 3 μM fura-2, AM in RPMI for 15 min at 37°C, washed in L-15 medium supplemented with 2 mM CaCl<sub>2</sub> and resuspended at 2x10<sup>6</sup>/ml. Cells were dropped on OKT3-coated and heated delta-T dishes (Biotechs) and imaged every 3 seconds by sequential illumination with 340 and 380 nm lasers. Acquisition was done on Leica DMI6000 microscope using Orca-03G camera (Hamamatsu) and 40X oil objective, and images were analyzed with Metafluor (Molecular Devices). For inhibitor studies, cells were pretreated with 25 μM Y-27632 concomitant with fura-2, AM incubation, washed in L-15 medium with Y-27632 and imaged in drug-containing medium. Jasplakinolide or DMSO were added after the cells had reached a plateau in Ca<sup>2+</sup> response (5 minutes into spreading). In some experiments, 1 μM Tg was added to block Ca<sup>2+</sup> uptake into ER stores. Ca<sup>2+</sup> mobilization was analyzed by plotting 340 nm/380 nm ratios from individual cells over time and average traces from cell population were shown.

### *Fixed-cell fluorescence microscopy*

For imaging of fixed cells in Chapter 2, coverslips were coated with poly-(L-lysine) as described (Bunnell et al., 2003), followed by 10 µg/ml OKT3 (2 hr. at 37°C or overnight at 4°C), and washed with PBS. Cells were harvested and resuspended at  $5 \times 10^5$ /ml in L-15 medium. Coverslips were equilibrated at 37°C, and  $1.0 \times 10^5$  cells were allowed to interact with the surface for the indicated times. Cells were fixed in 3% paraformaldehyde and labeled as in (Dehring et al., 2011). Cells were imaged on a Zeiss Axiovert 200 equipped with a PerkinElmer Ultraview ERS6 spinning disk confocal system and a 63× planapo 1.4 NA oil objective. Images were collected using an Orca ER camera (Hamamatsu) and analyzed using Volocity versions 5.5 to 6.3 (Perkin Elmer). Unless indicated, 1 µm-thick Z stacks of three images were collected at the T cell-coverglass interface and displayed as extended projections.

Acquisition in TIRF was done on Leica DMI6000 microscope using 100X planapo 1.46 NA oil objective (Leica) and Evolve 512 EMCCD camera (Photometrics). TIRF and widefield images were acquired sequentially by switching between TIRF (90 nm penetration depth) and epifluorescence microscopy. Images were collected in LAS AF software (Leica).

For imaging of fixed cells in Chapter 3, coverslips (12 mm, #1.0, Bellco) were directly coated with 10 µg/ml OKT3 for 2 hr. at 37°C or overnight at 4°C, followed by washing with PBS and incubation with 1 µg/ml ICAM-1. Where indicated, coverslips were subsequently incubated with VCAM-1 at 1 µg/ml for 2 hr. at 37°C. LFA-1 monoclonal antibodies were directly labeled as follows: m24 was labeled with Alexa

Fluor 488, Kim127 was labeled with Alexa Fluor 594 and TS2/4 was labeled with DyLight 650. Other permutations of labeling yielded less than optimal staining results.

T cells were harvested and resuspended at  $5 \times 10^5$ /ml in L-15 medium. Coverslips or chambers were equilibrated at  $37^\circ\text{C}$ , and  $\sim 5.0 \times 10^4$  cells (for coverslips) or  $\sim 1.5 \times 10^5$  cells (for lipid bilayers) were allowed to interact with the surfaces for the indicated times. Wherever m24 antibody was used, live cells were labeled with m24 5 min. before fixation (as this antibody does not label fixed cells). Cells were then fixed in 3% paraformaldehyde and labeled with other antibodies as described previously (Dehring et al., 2011), except that 50 mM  $\text{NH}_4\text{Cl}$  was used as a quenching reagent. 0.5- $\mu\text{m}$  thick stacks consisting of three planes (0.25  $\mu\text{m}$  apart) were collected at the T cell-coverglass interface and displayed as extended projections. Alternatively, T cell-B cell conjugates (see above) were imaged as 10- $\mu\text{m}$  thick stacks were collected with planes spaced 0.5  $\mu\text{m}$  apart. 25–50 spread T cells or conjugates were selected per condition and used for further analysis.

#### *Live-cell fluorescence microscopy*

For live cell imaging in Chapter 2, eight-well Lab-Tek II chambered cover glasses (Nunc) were coated with OKT3 as for fixed-cell experiments. Immediately before imaging, chambers were covered with 400  $\mu\text{l}$  of imaging medium (phenol red-free RPMI 1640, 25  $\mu\text{M}$  HEPES) and equilibrated to  $37^\circ\text{C}$  on the microscope stage within a Solent environmental chamber. Cells were harvested, resuspended in imaging medium at  $2 \times 10^6$ /ml, and 5–10  $\mu\text{l}$  of cell suspension was added to the well. Time-lapse images were collected at 63X using the microscope described above. 1  $\mu\text{m}$  thick Z stacks of three

images were collected every 3s for 5–7 min. Emission discrimination filters were used for multi-color imaging. 20–40 randomly selected cells were analyzed per condition.

For live-cell imaging on coverglass in Chapter 3, eight-well Lab-Tek II chambered cover glasses (Nunc) were coated with OKT3 as described above. Immediately before imaging, wells were covered with 400  $\mu$ l of L-15 medium and equilibrated to 37°C on the microscope stage. Cells were harvested, resuspended in L-15 medium at  $2 \times 10^6$ /ml, and 5–10  $\mu$ l of cell suspension was added to the well. Time-lapse images (0.5- $\mu$ m thick Z stacks of three images) were collected every 2 s for 1-2 min. Emission discrimination filters were used for multi-color imaging. 10–20 spread T cells per condition were selected for image analysis.

For live-cell imaging of T cells on planar lipid bilayers, surfaces were prepared as described above and T cell suspension was injected into the opening of the closed chamber assembly. Cells were allowed to settle onto bilayers at 37°C and imaging was initiated after full spreading has been reached, at least 10 cells were imaged per experiment.

#### *Image processing and quantitative analysis*

Retrograde flow of the actin network was measured in two ways. First, movies of spreading T cells expressing GFP-actin were processed using the Smart Sharpen filter in Adobe Photoshop, with 300% amplification of local maxima within a 3 pixel radius. This facilitated identification of individual GFP-actin speckles, which were used as fiduciary marks for analysis. Analysis of sharpened and unprocessed movies yielded similar results, and unprocessed images are shown unless otherwise specified. As an alternative



approach, a portion of the F-actin network was photo-bleached to induce a synchronous wave of bleached GFP-actin propagating towards the center of the IS. In both cases, a ray was struck from the center of the IS to the periphery, and vertical kymographs were generated in Volocity 5.5 and analyzed in ImageJ 1.45k (NIH). Actin flow rate was calculated based on the angle of deflection from the vertical direction. Instantaneous velocities were plotted as a function of relative position along the IS radius.

SLP76 MC tracking analysis was done using custom algorithms written in Volocity and Microsoft Excel. Objects with intensities 1.5 standard deviations above the average intensity of the IS were identified and filtered by size; objects were then tracked using the shortest path algorithm in Volocity. Instantaneous velocities and relative (x, y) coordinates of each MC were exported into Microsoft Excel, and the distance from the IS centroid was calculated for each MC at each time point. Instantaneous MC velocities within each 1  $\mu\text{m}$  segment along the IS radius were averaged, and plotted as a function of radius. Kymography was used to confirm the findings from particle tracking for individual MCs. For this, maximum over time projections were generated from movie sequences, and used to define the tracks of MC movement. Kymographs were generated along these tracks, and MC velocity was calculated based on the angle of deflection from the vertical direction.

To measure the distribution of cytoskeletal components across the IS, a 0.5  $\mu\text{m}$  thick line was drawn along the diameter of spreading cells, and fluorescence intensity profiles were measured. To assess IS area and shape, custom built algorithms in Volocity software were used to identify the cells based on the intensity of the F-actin network. IS

area was calculated automatically by integrating the pixels within the identified objects. IS shape (circularity) was calculated using the following equation,

$$S = \frac{P^2}{4\pi A},$$

where S represents IS shape and P and A are perimeter and area of the IS, respectively.

To assess PLC $\gamma$ 1 activation, spreading GFP-actin expressing cells were fixed and labeled with anti-phospho-PLC $\gamma$ 1, and cell boundaries were defined based on actin intensity as described above. For each cell profile, background signal was subtracted, and total phospho-PLC $\gamma$ 1 signal intensity was quantified. Values from 80 cells were averaged for each experimental condition.

In Chapter 3, movies of T cells expressing Lifeact-GFP were analyzed for retrograde flow of the actin network using the kymography module in Volocity 6.3. A ray was struck from the center of the IS to the cell periphery, and the generated kymograph was inspected for deflections in the flow. Instantaneous velocities were plotted as a function of relative position along the IS radius to generate a plot of F-actin flow rate distribution across the IS radius. For publication purposes, all kymographs were digitally enhanced using the Smart Sharpen filter in Adobe Photoshop, with 150% amplification of local maxima within a 2-pixel radius.

Measurements of distributions of LFA-1 and other molecules across the IS were done in two ways. First, images of T cells were cropped to the same size, aligned based on the centroid for each cell and imported as a stack into ImageJ 1.46r (NIH). The stack of all images was projected as average intensity to generate a pattern of fluorescence distribution in cell population, and the Radial Profile plug-in was used to obtain average

intensity values along the radius of the projected IS. Second, radial fluorescence intensities from images of individual cells were imported into Microsoft Excel and all radii were normalized. Fluorescence intensity values were binned according to their relative position along the normalized IS radius. All values within a particular bin were used to determine the mean and standard deviation.

To assess spreading area and total fluorescence intensity, custom algorithms in Volocity were used to identify T cell IS boundaries based on thresholds for total LFA-1 (TS2/4) or F-actin intensity (if TS2/4 staining was not available). The IS area was calculated automatically by integrating pixels within the identified objects. Total fluorescence intensity from the IS area was determined after background-correction based on fluorescence of unoccupied stimulatory surface.

#### *Statistical evaluation*

Statistical analysis was performed using Microsoft Excel. In individual experiments, statistical significance was determined using a two-tailed Student's t test for unpaired samples with equal variances. When comparing changes in donor population, a two-tailed Student's t test for paired samples was performed. Outliers were discounted as being 2 standard deviations away from the mean.

## **APPENDIX A: PREPARATION OF MIXED-MOBILITY SURFACES**

Mixed-mobility surfaces are the stimulatory surfaces with a combination of mobile and immobile ligands that can be used to test the role of ligand mobility and patterning on cellular responses. Below I present a number of protocols that should be used to generate these specialized surfaces. These protocols may be optimized for each particular context of research.

### *Preparation of glass surfaces*

Note: Wear personal protective equipment (lab coat, apron, goggles and heavy gauntlets) at all times while working with Piranha solution.

1. Set up a clean Coplin jar or a tall narrow beaker in a secondary container in the hood.
2. Add 50 ml of Sulfuric acid to the jar
3. Carefully add 16.6 ml of fresh Hydrogen peroxide to the jar. (If cleaning 25x75 mm coverslips, make sure that they can be fully submerged in the solution, otherwise find a container of suitable dimensions.)
4. Mix the solution with long glass rod. Care during this step is critical as the exothermic reaction quickly heats up the solution to above 100°C. (For optimal cleaning, use the solution shortly after preparation as it wears off within a few hours.)
5. Clip the coverslips into locking polypropylene forceps and dunk them into Piranha solution. Do not take off the forceps but instead, leave them on the glass throughout the cleaning procedure. Evolution of gas on glass surface should

ensue. Piranha solution activates surface by exposing negatively charged  $\text{-OH}$  groups.

6. Incubate the glass coverslips for 20-30 minutes.
7. Prepare two 250 ml beakers of distilled, deionized water, which will be used to remove the residual sulfuric acid off of the coverslips after the incubation.
8. Carefully pick up the coverglasses one at a time and transfer them into one of the beakers with water prepared in the previous step. (The used Piranha solution remains highly corrosive for a few hours. It should be left in the hood and disposed of the next day. Special vented amber bottle placed in a secondary container should be used for temporary Piranha waste collection.) Swirl the glass slips lightly in water to allow most of the acid to come off the glass. The pH of this rinse solution is about 2.0. This waste should be collected by the Safety Department according to the protocol, but practically can be discarded in the drain with copious amounts of water.
9. Transfer the glass to the other beaker and swirl repeatedly again. Optionally, sonicate the glass in a tabletop sonication bath for a minute.
10. To dry the glass, insert the forceps with coverslips into FACs tube rack, pointing up. Allow the glass to dry by air and gravity. Aspirate the large droplets of water, which accumulate at the bottom of the glass slips.
11. Do not leave the glass exposed to air for a long time, as contaminants will quickly settle on the surface and inactivate the hydroxyl groups, reducing the quality of the mixed-mobility surfaces.

### *Preparation of small unilamellar vesicles*

Note: The critical issues in this protocol are the quality of lipids and small unilamellar vesicles. These factors will directly influence the mobility of bilayers. The lipid solutions should be stored under inert gas (Argon or Nitrogen) in special Avanti vials with Teflon seals and at  $-20^{\circ}\text{C}$ ; chloroform will freeze at  $-80^{\circ}\text{C}$ . Work with chloroform and acetone solution should be conducted in the fume hood. Wear protective equipment.

1. Prepare lipid solutions in chloroform in a desired mol% ratio. We use 100 mM DOPC:DSPE-PEG(2000) biotin:DGS-NTA (nickel salt) in a 98:1:1 mol% ratio. Alternatively, make separate solutions of DOPC:DSPE-PEG(2000) biotin (98:2 mol%) and DOPC:DGS-NTA (nickel salt) (98:2 mol%) and mix them immediately before making vesicles. Chloroform evaporation can cause inaccuracy in measurement, thus the volumes of lipid solutions should be noted and losses in volume should be replenished before mixing different lipid solutions.
2. Set up a 10 ml glass test tube in the hood and rinse it with chloroform, using glass pipette.
3. Using glass syringe, transfer 200  $\mu\text{l}$  of lipid solution to the test tube.
4. Dry the chloroform using gentle stream of inert gas or air. The dried lipid layer is called lipid cake.
5. Further, dry the lipid cake in a vacuum chamber for 1-2 hours.
6. Add 1 ml of PBS solution to the lipid cake and sonicate it for 20 minutes to rehydrate the lipids. This results in a spontaneous formation of multilamellar

vesicles that have many layers analogous to an onion. The turbidity in the solution will make it appear milky.

7. Assemble the mini-extruder as per Avanti instructions, use 50 nm pore membrane for vesicle extrusion. Pass pure water through it a few times to ensure that the assembly does not leak. If leakage is discovered, re-assemble the extruder.
8. Pass the lipid vesicles back and forth at least 11 times to make sure that all unilamellar vesicles are homogeneous in size. This will partially clear the solution. Make sure to pass the vesicles through the membrane an odd number of times so that the final mixture is not in the original syringe.
9. The resulting small unilamellar vesicles are stable at 4°C for 2-3 months. If aggregation occurs, centrifuge the vesicle solution at top speed for 1-2 minutes.

#### *Preparation of supported planar bilayers*

1. Attach the cleaned and dried glass (see the protocol above) on the bottom of Ibidi Sticky-Slide I<sup>0.2</sup> Luer.
2. Dilute lipid vesicle mixture 5-fold in PBS before addition to glass; oversaturation of glass surface with lipid vesicles will result in partial fusion of vesicles to glass and diminish the mobility of the bilayers.
3. Add about 100 µl of diluted solution to each chamber. Mark the intake well of the chamber with an arrow; this will guide subsequent additions to the same side of the chamber to create flow in one direction.
4. Incubate the chamber assembly with lipids for about 15 minutes.

5. Rinse the chamber thoroughly with PBS to remove the excess vesicles. This should be done by sequential addition of PBS to the intake well and removal of flow-through on the other side. About 150  $\mu$ l of PBS can be added at a time for a total of 6 to 8 times.
6. Incubate the bilayers with excess fluorescent Neutravidin or Streptavidin (1  $\mu$ g per chamber) and 1 mM NiSO<sub>4</sub> for 15 minutes.
7. Rinse thoroughly as before.
8. Incubate the chambers with the desired stimulatory and adhesion ligands. (Biotinylated and his-tagged ligands should be added in excess to cover the surface completely. We use 1  $\mu$ g of OKT3-biotin and 2  $\mu$ g of ICAM-1–His per chamber. Optimal concentrations of ligands should be determined empirically)
9. Incubate the surfaces for 15 minutes and rinse as previously. Replace PBS with L-15 imaging media in the final rinse.
10. Bilayer surfaces should be tested for ligand mobility (Figure X.1) and used within 2 days after preparation. Ligand mobility and surface quality may decrease with longer storage.

### *Preparation of the PDMS stamps*

#### Making “hard” PDMS (hPDMS)

1. Mix 3.4 g of VDT-731 (Gelest) with 1 g of HMS-301 (Gelest) in 50 ml tube and vortex to ensure even mixing.
2. Add 4 drops of modulator, 2,4,6,8-Tetramethyl-2,4,6,8-tetravinylcyclotetrasiloxane (Sigma), and mix thoroughly.



3. Add 4 drops of platinum catalyst platinum(0)-2,4,6,8-tetramethyl-2,4,6,8-tetravinylcyclotetrasiloxane complex solution (Sigma), and mix thoroughly.
4. Gently spread hPDMS on the silicon master wafer (which must be manufactured beforehand elsewhere) using either the Parafilm spatula. Cover the micro pattern area thoroughly.
5. Bake the master with hPDMS layer at 60C for 20-40 minutes.

#### Making “soft” PDMS (sPDMS)

1. Mix 45 g of PDMS base (Sylgard) with 5 g of supplied curing agent thoroughly in the plate or in the disposable paper cup until it becomes milky.
2. Centrifuge the mixed PDMS at 1000 rpm for 2 minutes to remove the air bubbles.

#### Making the composite stamp

1. Put the hPDMS-covered master face up into the tin-foiled large Petri dish to contain the regular PDMS from the contact with the dish. Make sure the hPDMS is properly cured after the baking. Pour the regular PDMS onto the master to cover it with 5-10 mm layer of regular PDMS.
2. Bake it at 60C for more than 1 hour, until the surface is stiff to touch. (The unpeeled cured stamp on the master can be stored at room temperature for few weeks.)
3. Gently peel the stamp from the master. Keep in mind, that the master is a fragile silicone mono-crystal and can crack easily; before peeling, make sure the non-patterned side of the master is completely free from the regular PDMS that got underneath the master during the curing.

### *Micro-contact printing*

1. Cut the stamp with paperknife or razor blade gently into the 5x5 or 10x10 mm blocks. Make sure the printing surface is not damaged. Avoid contact with the patterned side.
2. Coat the stamp with the protein of interest. Keep in mind that the protein concentration is a factor for the quality of stamping. Keep protein concentration in the coating solution around 20  $\mu\text{g/ml}$  and do not exceed 100  $\mu\text{g/ml}$ . Excess protein will aggregate and reduce the quality of patterning.
3. For coating, put the stamping PDMS blocks with the stamping surface pointing face up in a small Petri dish. Put 100  $\mu\text{l}$  of coating solution onto the stamping surface and cover the liquid bead with 15 mm glass coverslip to spread the liquid evenly on PDMS. Incubate at room temperature for 30 minutes.
4. During this incubation, clean the glass coverslips as described above.
5. Dip the incubated PDMS stamps into deionized water a few times and dry the stamp completely using a jet of air. Ideally, inert gas (such as nitrogen) should be used to avoid oxidation and hydrolysis.
6. Gently place the PDMS stamp on the cleaned coverslip face down with plastic or slightly wetted tweezers. It is critical to prevent shifting or jumping of the stamp on the glass.
7. Carefully place a 10-15 g weight (we use a wrench socket) on the top of the stamp and wait 1 minute to ensure the proper contact between the stamp and glass coverslip.

8. Swiftly remove the weight and the stamp from the glass with tweezers by one quick uplifting motion. Do not reuse the stamps as that will result in cross-contamination of ligands.
9. Attach the glass to the bottom of the Ibidi Sticky-Slide I<sup>0.2</sup> Luer and rinse a few times with distilled water to remove weakly-bound ligands. Multiple patterns can be used that are suitable for T cell stimulation (Figure X.2)

*Preparation of mixed-mobility surfaces*

1. To generate surfaces that have mobile and immobile ligands, pattern the glass as described above then add lipid vesicles as described above.
2. For studies of T cell activation, a potential combination would be OKT3-biotin in the mobile phase of the mixed mobility surface and ICAM-1 in the immobile phase (pattern anti-human IgG1 antibody and then incubate with ICAM-1-Fc chimera when the surface undergoes incubations with ligand. We do not recommend printing ICAM-1 directly on glass, as we have found out that ICAM-1 is easily denatured upon drying and will not stimulate cells.)
3. Characterization of mixed-mobility surface is provided in Figure X.3 and Movie XA.

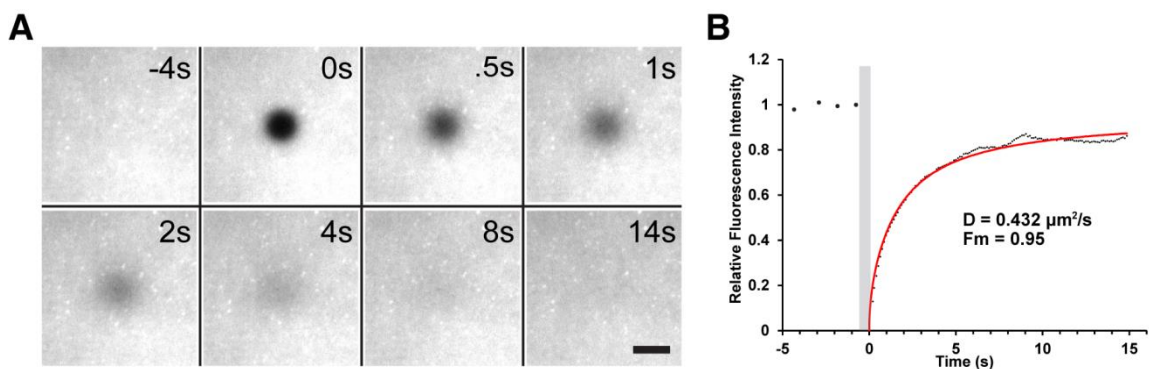


**Figure X.1. Preparation and characterization of supported planar lipid bilayers**

(A). Planar lipid bilayers were generated by incubation of small unilamellar vesicles in glass bottom chambers. SUVs contained DOPC, DSPE-PEG(2000)-biotin and DGS-NTA(Ni) (98:1:1 mol%). Bilayers were incubated with streptavidin DyLight 650, and subsequently with OKT3-biotin and his-tagged ICAM-1 (not shown). Time-lapse imaging of fluorescence recovery after photo-bleaching of fluorescent streptavidin loaded with OKT3-biotin is shown as a series. Scale bar, 5  $\mu\text{m}$ . (B) Fluorescence recovery of a region bleached in A. Gray bar represents the time when photo-bleaching was applied. The diffusion coefficient ( $D$ ) and the mobile fraction ( $F_m$ ) are indicated.

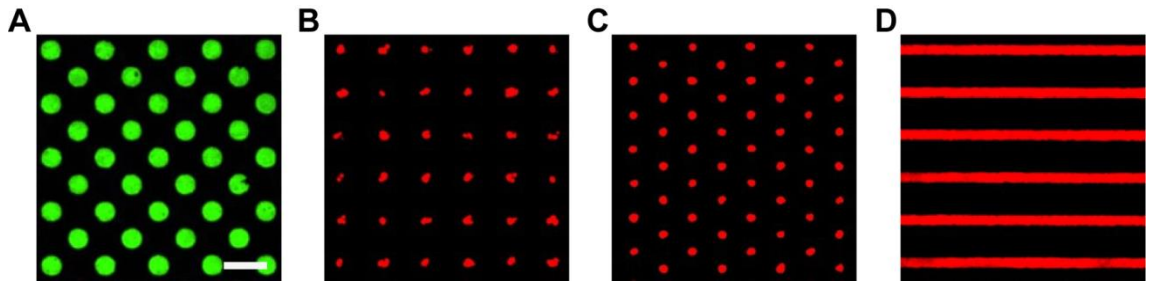


**Figure X.2. Characterization of patterned surfaces prepared by means of micro-contact printing**

(A) 2  $\mu\text{m}$  dots, 4  $\mu\text{m}$  center-to-center square packing. Scale bar, 4  $\mu\text{m}$ . (B) 1  $\mu\text{m}$  dots, 4  $\mu\text{m}$  center-to-center square packing. (C) 1  $\mu\text{m}$  dots, 4  $\mu\text{m}$  center-to-center, hexagonal packing. (D) 1  $\mu\text{m}$  thick lines, 5  $\mu\text{m}$  center-to-center.

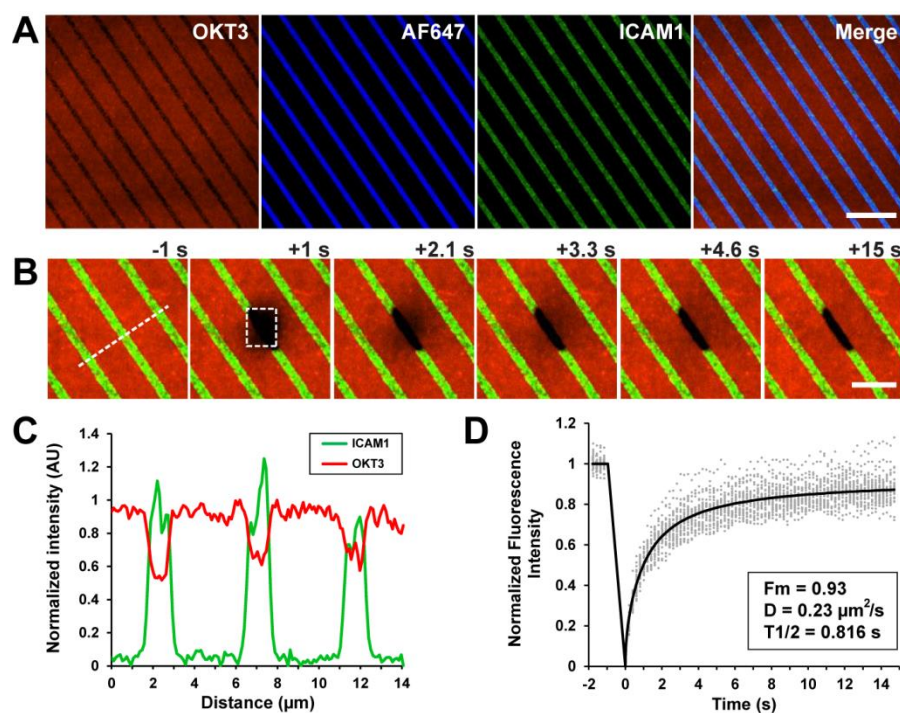


### Figure X.3. Characterization of mixed-mobility surfaces

(A) Human ICAM1-Fc was mixed with an unspecific anti-IgG AF647 and printed onto glass using PDMS stamp with 1  $\mu\text{m}$  wide lines, 5  $\mu\text{m}$  center-to-center. DOPC lipid vesicles containing 1% DSPE-PEG2000-Biotin were then deposited onto the patterned surface to form lipid bilayers. Mixed-mobility surfaces were then incubated with NTA-TexasRed and anti-human IgG AF488 to label ICAM-Fc. Mono-biotinylated OKT3 was finally added to the bilayers. Surface images are shown, scale bar: 10  $\mu\text{m}$ . (B) Mobility of lipid portion of mixed-mobility surfaces was checked using FRAP. A region depicted by dashed lines at +1 s was photo-bleached. Scale bar, 5  $\mu\text{m}$ . (C) Fluorescence intensity profile of mixed-mobility surface was acquired along the dashed line in B from the panel at -1 s. (D) Fluorescence recovery after photo-bleaching (FRAP) of the lipid portion of the mixed mobility surfaces.

## **APPENDIX B: SUPPLEMENTAL MOVIE LEGENDS**

### **Movie 2A. Myosin IIA localizes to the IS and accumulates behind the lamellipodium, related to Figure 2.1.**

Jurkat T cells stably expressing GFP-actin were transiently transfected with mKate2-NMHC IIA (myosin IIA heavy chain). After 16 hours, cells were allowed to spread on OKT3-coated coverglass. Confocal image sequences were acquired every 3 seconds for 5 minutes. Scale bar represents 5  $\mu\text{m}$ .

### **Movie 2B. F-actin features at the IS slow down towards the center of the IS, related to Figure 2.2.**

Jurkat E6.1 cells stably expressing GFP-actin were allowed to interact with OKT3-coated coverglass. Confocal 1- $\mu\text{m}$  thick Z-stacks were acquired every 6 seconds for 12.5 minutes. Movie sequence of a spreading cell is shown as “raw” extended projection (left) or as “enhanced” extended projection (right), and corresponds to still images and kymograph in Figure 2.1 A and B. Scale bar represents 10  $\mu\text{m}$ .

### **Movie 2C. Bleaching of GFP-actin prominently reveals F-actin velocity at the IS, related to Figure 2.2.**

GFP-actin Jurkat T cells were allowed to spread on OKT3 for 5 minutes before image acquisition was initiated. Confocal images were acquired every 3 seconds for 1-2 minutes. Left panel shows a spread T cell subjected to high intensity laser to bleach GFP-actin in the cytosol. The corresponding time series is in Figure 2.2 C. Right panel shows

an enlarged view of the boxed region on the left and corresponds to the kymograph shown in Figure 2.2 C. Scale bars represent 5  $\mu\text{m}$  (left) and 2  $\mu\text{m}$  (right).

**Movie 2D. The F-actin ring collapses to the center of the IS in Jurkat cells upon stabilization of actin filaments, related to Figure 2.4.**

Jurkat T cells stably expressing GFP-actin were allowed to contact OKT3-coated coverglasses and imaged after full spreading was reached. Jasplakinolide was added to the wells when indicated. Confocal 1  $\mu\text{m}$ -thick Z-stacks were acquired every 3 seconds for 7 minutes and are shown as extended projections. Scale bars, 10  $\mu\text{m}$ .

**Movie 2E. The actomyosin network collapses to the center of the IS in human primary T cells upon stabilization of actin filaments, related to Figure 2.4.**

Human primary CD4<sup>+</sup> T cell blasts expressing GFP-actin were dropped onto OKT3-coated coverglass and allowed to spread for 3 minutes. After full spreading was reached, 0.5- $\mu\text{m}$  thick z stack projections were collected every 3 seconds. Jasplakinolide was added to the imaging chamber when indicated. Similar results were obtained in 2 independent experiments. Scale bar represents 5  $\mu\text{m}$ .

**Movie 2F. The myosin IIA network collapses to the center of the IS in Jurkat cells upon stabilization of actin filaments, related to Figure 2.4.**

Jurkat E6.1 cells transiently transfected with GFP-NMHC IIA were allowed to contact OKT3-coated coverglass and imaged after full spreading was reached. Jasplakinolide was



added to the wells when indicated. Confocal 1  $\mu\text{m}$ - thick Z-stacks were acquired every 3 seconds for 7 minutes and are shown as extended projections. Scale bars, 5  $\mu\text{m}$ .

**Movie 2G. F-actin retrograde flow is unperturbed in cells pretreated with Y-27632, related to Figure 2.5.**

Jurkat T cells stably expressing GFP-actin were pretreated with Y-27632 for 15 minutes to inhibit myosin II activity. Cells were then allowed to spread on OKT3-coated coverglass and imaged to assess the dynamics of the F-actin network. Confocal 1  $\mu\text{m}$ -thick Z-stacks were acquired every 3 seconds for 7 minutes and are shown as extended projections. Scale bar represents 10  $\mu\text{m}$ .

**Movie 2H. Myosin II inhibition with blebbistatin does not affect F-actin retrograde flow, related to Figure 2.5.**

Jurkat T cells transiently transfected with F-Tractin tdTomato were pretreated with blebbistatin for 30 minutes to inhibit myosin II activity. Cells were then allowed to spread on OKT3-coated coverglass and imaged to assess the dynamics of the F-actin network. Confocal 1  $\mu\text{m}$ -thick Z-stacks were acquired every 3 seconds for 1-5 minutes and are shown as extended projections. Scale bar, 5  $\mu\text{m}$ .

**Movie 2I. Pre-treatment with Y-27632 and acute treatment with Jas arrests F-actin retrograde flow in Jurkat T cells, related to Figure 2.6.**

Jurkat T cells stably expressing GFP-actin were pretreated with Y-27632 for 15 minutes to inhibit myosin IIA activity. Cells were then allowed to spread on OKT3-coated

coverglass and imaged to assess the dynamics of the F-actin network. During imaging, cells were treated with jasplakinolide when indicated. Confocal 1  $\mu\text{m}$ -thick Z-stacks were acquired every 3 seconds for 7 minutes and are shown as extended projections. Scale bar, 10  $\mu\text{m}$ .

**Movie 2J. Pre-treatment with Y-27632 and acute treatment with Jas arrests F-actin retrograde flow in human primary T cells, related to Figure 2.6.**

Human CD4<sup>+</sup> T cell blasts expressing GFP-actin were pre-treated with Y-27632 for 15 minutes. Cells were then allowed to spread on OKT3-coated coverglass for 3 minutes before imaging. 0.5- $\mu\text{m}$  thick Z-stack projections were acquired every 3 seconds. When indicated, 1  $\mu\text{M}$  Jas was added to the imaging well. Similar results were obtained in 2 independent experiments. Scale bar, 5  $\mu\text{m}$ .

**Movie 2K. Myosin IIA suppression with siRNA does not affect actin retrograde flow, related to Figure 2.7.**

Jurkat T cells expressing GFP-actin were transfected with siRNA against the heavy chain of myosin IIA and used 48 hours later. Cells were allowed to spread on OKT3-coated coverglass, and 1  $\mu\text{m}$ -thick Z-stack projections were collected every 3 seconds. When indicated, 1  $\mu\text{M}$  jasplakinolide was added to the imaging well. Scale bar, 5  $\mu\text{m}$ .

**Movie 2L. T cells suppressed for IQGAP1 exhibit accelerated F-actin flow at the IS, related to Figure 2.8.**

Jurkat T cells stably expressing GFP-actin were transfected with vector DNA (left) or shIQGAP1 plasmid (right). Cells were harvested 72 hours post transfection and stimulated on glass surfaces coated with OKT3. 0.5  $\mu\text{m}$ -thick Z-stacks just above the glass interface were collected every 3 seconds for 3.5 minutes and are shown as extended projections. Scale bar, 5  $\mu\text{m}$ .

**Movie 2M. F-actin dynamics govern SLP-76 MC movement, related to Figure 2.9.**

Jurkat T cells stably expressing GFP-actin (left) or GFP-SLP-76 (right) were mixed in culture and pretreated with Y-27632 for 15 minutes. The cell mixture was then dropped onto OKT3-coated coverglass to initiate spreading. Fields of view were scanned for cells that had dynamic GFP-actin and SLP-76. Confocal 1  $\mu\text{m}$ -thick Z-stacks were acquired every 3 seconds for 2.5 minutes and are shown as extended projections. Jasplakinolide was added to the imaging chamber when indicated. After acquisition, movie sequences of individual cells were cropped and tiled for side-by-side comparison. Scale bar, 5  $\mu\text{m}$ .

**Movie 2N. SLP-76 MCs move to the center of the IS at constant velocity, related to Figure 2.10.**

Jurkat T cells stably expressing GFP-SLP-76 were dropped onto OKT3-coated coverglass and imaged after full spreading was reached. Confocal 1  $\mu\text{m}$ -thick Z-stacks were acquired every 3.2 seconds for 4 minutes and are shown as extended projections. Scale bar, 5  $\mu\text{m}$ .

**Movie 2O. F-actin retrograde flow is dispensable for microtubule assembly and dynamics, related to Figure 2.11.**

Jurkat T cells stably expressing GFP-actin were transiently transfected with STIM1-mCherry, pretreated with Y-27632 for 15 minutes dropped onto OKT3-coated coverglass for stimulation. Confocal 1  $\mu\text{m}$ -thick Z-stacks were acquired every 6 seconds for 3 minutes and are shown as extended projections. Jasplakinolide was added to the imaging chamber at 1 min 30 s. Scale bar, 5  $\mu\text{m}$ .

**Movie 3A. LFA-1 conformational change at the IS is organized into a concentric array in T cell-B cell conjugates, related to Figure 3.1.**

Human primary CD4<sup>+</sup> T cells were conjugated to SEE-pulsed Raji B cells for 25 min, and labeled with phalloidin (gray) and with antibodies to total LFA-1 (blue) as well as conformation-specific antibodies to extended (red) and extended open (green) LFA-1. Z stacks of whole conjugates were collected and rendered in 3D in the IS plane.

**Movie 3B. F-actin dynamics in human CD4<sup>+</sup> lymphoblasts spreading on stimulatory bilayers, related to Figure 3.3.**

Human *ex vivo* primary T cells were blasted and transduced with Lifeact-GFP lentivirus. Upon protein expression, cells were allowed to interact with the stimulatory planar lipid bilayers and F-actin dynamics in the IS plane were assessed by live-cell confocal microscopy. Left cell shows an accumulation of Lifeact-GFP in the central region, while right cell does not have that enrichment.

**Movie 3C. F-actin dynamics in Jurkat cells spreading on stimulatory bilayers, related to Figure 3.4.**

GFP-actin Jurkat T cells were allowed to spread on stimulatory bilayers containing OKT3 and ICAM-1. Imaging was initiated after full spreading has been reached. Note the extensive lamellipodial protrusions. Cells were imaged every 3 seconds right above the interface. Scale bar, 5  $\mu\text{m}$ .

**Movie 3D. F-actin dynamics in human CD4+ lymphoblasts spreading on OKT3-coated coverglass, related to Figure 3.5**

Human *ex vivo* primary T cells were blasted and lentivirally transduced with Lifeact-GFP. Upon protein expression, cells were allowed to interact with the stimulatory coverglass coated with OKT3. F-actin dynamics in the IS plane were assessed by live-cell confocal microscopy. Cells were imaged every 2 seconds. Scale bar, 10  $\mu\text{m}$ .

**Movie 3E. F-actin dynamics in human CD4+ lymphoblasts spreading on OKT3- and ICAM-1-coated coverglass, related to Figure 3.5**

Human *ex vivo* primary T cells were blasted and transduced with Lifeact-GFP lentivirus. Upon protein expression, cells were allowed to interact with the stimulatory coverglass coated with OKT3 and ICAM-1. F-actin dynamics in the IS plane were assessed by live-cell confocal microscopy. Cells were imaged every 2 seconds. Scale bar, 10  $\mu\text{m}$ .

**Movie 3F. F-actin dynamics persist in human T cells under myosin II inhibition but cease completely after abrogating F-actin turnover, related to Figure 3.7.**

Human *ex vivo* primary T cells were blasted and transduced with Lifeact-GFP lentivirus. Cells were then pretreated with Y-27 or left untreated and allowed to interact with the stimulatory bilayers. After full spreading had been reached, Jas was added to imaging chamber. Cells were imaged every 2 seconds. Scale bar, 5  $\mu\text{m}$ .

**Movie 3G. F-actin dynamics in human CD4+ lymphoblasts spreading on OKT3-coated coverglass in the presence of immobilized ICAM-1 and VCAM-1, related to Figure 3.11.**

Human *ex vivo* primary T cells were blasted and transduced with Lifeact-GFP lentivirus. Upon protein expression, cells were allowed to interact with the stimulatory coverglass coated with OKT3, ICAM-1 and VCAM-1. F-actin dynamics in the IS plane were assessed by live-cell confocal microscopy. Cells were imaged every 2 seconds. Scale bar, 10  $\mu\text{m}$ .

**Movie XA. Characterization of ligand mobility on mixed-mobility surfaces**

Alexa Fluor 488-labeled secondary antibody was micro-contact printed onto glass using PDMS stamp with 2- $\mu\text{m}$  dots. Subsequently, the space surrounding the patterns was coated with lipid bilayer containing 1% biotinylated lipid (see Appendix A for details). The surfaces were then incubated with Alexa Fluor 594-conjugated Streptavidin to label the bilayer. The resulting mixed-mobility surfaces were imaged by confocal microscopy every 2 seconds. A region of the pattern was photo-bleached at 10 seconds into the movie to test the mobility of ligands. Scale bar, 5  $\mu\text{m}$ .

## REFERENCES

- Abraham, C., and Miller, J. (2001). Molecular mechanisms of IL-2 gene regulation following costimulation through LFA-1. *J Immunol* *167*, 5193-5201.
- Al-Alwan, M.M., Liwski, R.S., Haeryfar, S.M., Baldrige, W.H., Hoskin, D.W., Rowden, G., and West, K.A. (2003). Cutting edge: dendritic cell actin cytoskeletal polarization during immunological synapse formation is highly antigen-dependent. *J Immunol* *171*, 4479-4483.
- Alon, R., and Dustin, M.L. (2007). Force as a facilitator of integrin conformational changes during leukocyte arrest on blood vessels and antigen-presenting cells. *Immunity* *26*, 17-27.
- Alonso, M.T., Manjarres, I.M., and Garcia-Sancho, J. (2012). Privileged coupling between Ca(2+) entry through plasma membrane store-operated Ca(2+) channels and the endoplasmic reticulum Ca(2+) pump. *Mol Cell Endocrinol* *353*, 37-44.
- Arrieumerlou, C., Randriamampita, C., Bismuth, G., and Trautmann, A. (2000). Rac is involved in early TCR signaling. *J Immunol* *165*, 3182-3189.
- Babich, A., Li, S., O'Connor, R.S., Milone, M.C., Freedman, B.D., and Burkhardt, J.K. (2012). F-actin polymerization and retrograde flow drive sustained PLCgamma1 signaling during T cell activation. *J Cell Biol* *197*, 775-787.
- Bachmann, M.F., McKall-Faienza, K., Schmits, R., Bouchard, D., Beach, J., Speiser, D.E., Mak, T.W., and Ohashi, P.S. (1997). Distinct roles for LFA-1 and CD28 during activation of naive T cells: adhesion versus costimulation. *Immunity* *7*, 549-557.
- Badour, K., Zhang, J., Shi, F., McGavin, M.K., Rampersad, V., Hardy, L.A., Field, D., and Siminovitch, K.A. (2003). The Wiskott-Aldrich syndrome protein acts

- downstream of CD2 and the CD2AP and PSTPIP1 adaptors to promote formation of the immunological synapse. *Immunity* 18, 141-154.
- Baixauli, F., Martin-Cofreces, N.B., Morlino, G., Carrasco, Y.R., Calabia-Linares, C., Veiga, E., Serrador, J.M., and Sanchez-Madrid, F. (2011). The mitochondrial fission factor dynamin-related protein 1 modulates T-cell receptor signalling at the immune synapse. *EMBO J* 30, 1238-1250.
- Baker, R.G., Hsu, C.J., Lee, D., Jordan, M.S., Maltzman, J.S., Hammer, D.A., Baumgart, T., and Koretzky, G.A. (2009). The adapter protein SLP-76 mediates "outside-in" integrin signaling and function in T cells. *Mol Cell Biol*.
- Barda-Saad, M., Braiman, A., Titerence, R., Bunnell, S.C., Barr, V.A., and Samelson, L.E. (2005). Dynamic molecular interactions linking the T cell antigen receptor to the actin cytoskeleton. *Nat Immunol* 6, 80-89.
- Barda-Saad, M., Shirasu, N., Pauker, M.H., Hassan, N., Perl, O., Balbo, A., Yamaguchi, H., Houtman, J.C., Appella, E., Schuck, P., and Samelson, L.E. (2010). Cooperative interactions at the SLP-76 complex are critical for actin polymerization. *EMBO J*.
- Barr, V.A., Bernot, K.M., Srikanth, S., Gwack, Y., Balagopalan, L., Regan, C.K., Helman, D.J., Sommers, C.L., Oh-Hora, M., Rao, A., and Samelson, L.E. (2008). Dynamic movement of the calcium sensor STIM1 and the calcium channel Orai1 in activated T-cells: puncta and distal caps. *Mol Biol Cell* 19, 2802-2817.
- Barreiro, O., Vicente-Manzanares, M., Urzainqui, A., Yanez-Mo, M., and Sanchez-Madrid, F. (2004). Interactive protrusive structures during leukocyte adhesion and transendothelial migration. *Front Biosci* 9, 1849-1863.



- Bartolini, F., Moseley, J.B., Schmoranzner, J., Cassimeris, L., Goode, B.L., and Gundersen, G.G. (2008). The formin mDia2 stabilizes microtubules independently of its actin nucleation activity. *J Cell Biol* 181, 523-536.
- Bazzoni, G., and Hemler, M.E. (1998). Are changes in integrin affinity and conformation overemphasized? *Trends Biochem Sci* 23, 30-34.
- Beemiller, P., Jacobelli, J., and Krummel, M.F. (2012). Integration of the movement of signaling microclusters with cellular motility in immunological synapses. *Nat Immunol*.
- Beemiller, P., and Krummel, M.F. (2010). Mediation of T-Cell Activation by Actin Meshworks. *Cold Spring Harb Perspect Biol*.
- Ben-Aissa, K., Patino-Lopez, G., Belkina, N.V., Maniti, O., Rosales, T., Hao, J.J., Kruhlak, M.J., Knutson, J.R., Picart, C., and Shaw, S. (2012). Activation of moesin, a protein that links actin cytoskeleton to the plasma membrane, occurs by phosphatidylinositol 4,5-bisphosphate (PIP<sub>2</sub>) binding sequentially to two sites and releasing an autoinhibitory linker. *J Biol Chem* 287, 16311-16323.
- Bhakta, N.R., Oh, D.Y., and Lewis, R.S. (2005). Calcium oscillations regulate thymocyte motility during positive selection in the three-dimensional thymic environment. *Nat Immunol* 6, 143-151.
- Billadeau, D.D., Nolz, J.C., and Gomez, T.S. (2007). Regulation of T-cell activation by the cytoskeleton. *Nat Rev Immunol* 7, 131-143.
- Bivona, T.G., Wiener, H.H., Ahearn, I.M., Silletti, J., Chiu, V.K., and Philips, M.R. (2004). Rap1 up-regulation and activation on plasma membrane regulates T cell adhesion. *J Cell Biol* 164, 461-470.

- Bleijs, D.A., van Duijnhoven, G.C., van Vliet, S.J., Thijssen, J.P., Figdor, C.G., and van Kooyk, Y. (2001). A single amino acid in the cytoplasmic domain of the beta 2 integrin lymphocyte function-associated antigen-1 regulates avidity-dependent inside-out signaling. *J Biol Chem* 276, 10338-10346.
- Bogin, Y., Ainey, C., Beach, D., and Yablonski, D. (2007). SLP-76 mediates and maintains activation of the Tec family kinase ITK via the T cell antigen receptor-induced association between SLP-76 and ITK. *Proc Natl Acad Sci U S A* 104, 6638-6643.
- Braiman, A., Barda-Saad, M., Sommers, C.L., and Samelson, L.E. (2006). Recruitment and activation of PLCgamma1 in T cells: a new insight into old domains. *EMBO J* 25, 774-784.
- Bubb, M.R., Senderowicz, A.M., Sausville, E.A., Duncan, K.L., and Korn, E.D. (1994). Jasplakinolide, a cytotoxic natural product, induces actin polymerization and competitively inhibits the binding of phalloidin to F-actin. *J Biol Chem* 269, 14869-14871.
- Bunnell, S.C., Barr, V.A., Fuller, C.L., and Samelson, L.E. (2003). High-resolution multicolor imaging of dynamic signaling complexes in T cells stimulated by planar substrates. *Sci STKE* 2003, PL8.
- Bunnell, S.C., Hong, D.I., Kardon, J.R., Yamazaki, T., McGlade, C.J., Barr, V.A., and Samelson, L.E. (2002). T cell receptor ligation induces the formation of dynamically regulated signaling assemblies. *J Cell Biol* 158, 1263-1275.

- Bunnell, S.C., Kapoor, V., Tribble, R.P., Zhang, W., and Samelson, L.E. (2001). Dynamic actin polymerization drives T cell receptor-induced spreading: a role for the signal transduction adaptor LAT. *Immunity* 14, 315-329.
- Bunnell, S.C., Singer, A.L., Hong, D.I., Jacque, B.H., Jordan, M.S., Seminario, M.C., Barr, V.A., Koretzky, G.A., and Samelson, L.E. (2006). Persistence of cooperatively stabilized signaling clusters drives T-cell activation. *Mol Cell Biol* 26, 7155-7166.
- Bunting, M., Harris, E.S., McIntyre, T.M., Prescott, S.M., and Zimmerman, G.A. (2002). Leukocyte adhesion deficiency syndromes: adhesion and tethering defects involving beta 2 integrins and selectin ligands. *Current opinion in hematology* 9, 30-35.
- Burkhardt, J.K., Carrizosa, E., and Shaffer, M.H. (2008). The actin cytoskeleton in T cell activation. *Annu Rev Immunol* 26, 233-259.
- Bustelo, X.R. (2001). Vav proteins, adaptors and cell signaling. *Oncogene* 20, 6372-6381.
- Butler, B., Kastendieck, D.H., and Cooper, J.A. (2008). Differently phosphorylated forms of the cortactin homolog HS1 mediate distinct functions in natural killer cells. *Nat Immunol* 9, 887-897.
- Cai, Y., Biais, N., Giannone, G., Tanase, M., Jiang, G., Hofman, J.M., Wiggins, C.H., Silberzan, P., Buguin, A., Ladoux, B., and Sheetz, M.P. (2006). Nonmuscle myosin IIA-dependent force inhibits cell spreading and drives F-actin flow. *Biophys J* 91, 3907-3920.
- Cai, Y., Rossier, O., Gauthier, N.C., Biais, N., Fardin, M.A., Zhang, X., Miller, L.W., Ladoux, B., Cornish, V.W., and Sheetz, M.P. (2010). Cytoskeletal coherence requires myosin-IIA contractility. *J Cell Sci* 123, 413-423.

- Cairo, C.W., Mirchev, R., and Golan, D.E. (2006). Cytoskeletal regulation couples LFA-1 conformational changes to receptor lateral mobility and clustering. *Immunity* 25, 297-308.
- Calderwood, D.A., Yan, B., de Pereda, J.M., Alvarez, B.G., Fujioka, Y., Liddington, R.C., and Ginsberg, M.H. (2002). The phosphotyrosine binding-like domain of talin activates integrins. *J Biol Chem* 277, 21749-21758.
- Calderwood, D.A., Zent, R., Grant, R., Rees, D.J., Hynes, R.O., and Ginsberg, M.H. (1999). The Talin head domain binds to integrin beta subunit cytoplasmic tails and regulates integrin activation. *J Biol Chem* 274, 28071-28074.
- Calvez, R., Lafouresse, F., De Meester, J., Galy, A., Valitutti, S., and Dupre, L. (2011). The Wiskott-Aldrich syndrome protein permits assembly of a focused immunological synapse enabling sustained T-cell receptor signaling. *Haematologica* 96, 1415-1423.
- Campi, G., Varma, R., and Dustin, M.L. (2005). Actin and agonist MHC-peptide complex-dependent T cell receptor microclusters as scaffolds for signaling. *J Exp Med* 202, 1031-1036.
- Cannon, J.L., and Burkhardt, J.K. (2004). Differential roles for Wiskott-Aldrich syndrome protein in immune synapse formation and IL-2 production. *J Immunol* 173, 1658-1662.
- Cao, Y., Janssen, E.M., Duncan, A.W., Altman, A., Billadeau, D.D., and Abraham, R.T. (2002). Pleiotropic defects in TCR signaling in a Vav-1-null Jurkat T-cell line. *EMBO J* 21, 4809-4819.

- Carman, C.V., and Springer, T.A. (2003). Integrin avidity regulation: are changes in affinity and conformation underemphasized? *Current opinion in cell biology* 15, 547-556.
- Carrizosa, E., Gomez, T.S., Labno, C.M., Klos Dehring, D.A., Liu, X., Freedman, B.D., Billadeau, D.D., and Burkhardt, J.K. (2009). Hematopoietic lineage cell-specific protein 1 is recruited to the immunological synapse by IL-2-inducible T cell kinase and regulates phospholipase Cgamma1 Microcluster dynamics during T cell spreading. *J Immunol* 183, 7352-7361.
- Chen, E.J., Shaffer, M.H., Williamson, E.K., Huang, Y., and Burkhardt, J.K. (2013). Ezrin and moesin are required for efficient T cell adhesion and homing to lymphoid organs. *PLoS One* 8, e52368.
- Chen, W., Lou, J., Evans, E.A., and Zhu, C. (2012). Observing force-regulated conformational changes and ligand dissociation from a single integrin on cells. *The Journal of cell biology* 199, 497-512.
- Chen, W., Lou, J., and Zhu, C. (2010a). Forcing switch from short- to intermediate- and long-lived states of the alphaA domain generates LFA-1/ICAM-1 catch bonds. *The Journal of biological chemistry* 285, 35967-35978.
- Chen, X., Xie, C., Nishida, N., Li, Z., Walz, T., and Springer, T.A. (2010b). Requirement of open headpiece conformation for activation of leukocyte integrin alphaXbeta2. *Proceedings of the National Academy of Sciences of the United States of America* 107, 14727-14732.

- Ciobanasu, C., Faivre, B., and Le Clainche, C. (2013). Integrating actin dynamics, mechanotransduction and integrin activation: the multiple functions of actin binding proteins in focal adhesions. *European journal of cell biology* 92, 339-348.
- Combs, J., Kim, S.J., Tan, S., Ligon, L.A., Holzbaaur, E.L., Kuhn, J., and Poenie, M. (2006). Recruitment of dynein to the Jurkat immunological synapse. *Proc Natl Acad Sci U S A* 103, 14883-14888.
- Contento, R.L., Campello, S., Trovato, A.E., Magrini, E., Anselmi, F., and Viola, A. (2010). Adhesion shapes T cells for prompt and sustained T-cell receptor signalling. *EMBO J* 29, 4035-4047.
- Cotta-de-Almeida, V., Westerberg, L., Maillard, M.H., Onaldi, D., Wachtel, H., Meelu, P., Chung, U.I., Xavier, R., Alt, F.W., and Snapper, S.B. (2007). Wiskott Aldrich syndrome protein (WASP) and N-WASP are critical for T cell development. *Proceedings of the National Academy of Sciences of the United States of America* 104, 15424-15429.
- de la Fuente, M.A., Sasahara, Y., Calamito, M., Anton, I.M., Elkhali, A., Gallego, M.D., Suresh, K., Siminovitch, K., Ochs, H.D., Anderson, K.C., *et al.* (2007). WIP is a chaperone for Wiskott-Aldrich syndrome protein (WASP). *Proc Natl Acad Sci U S A* 104, 926-931.
- Dehring, D.A., Clarke, F., Ricart, B.G., Huang, Y., Gomez, T.S., Williamson, E.K., Hammer, D.A., Billadeau, D.D., Argon, Y., and Burkhardt, J.K. (2011). Hematopoietic lineage cell-specific protein 1 functions in concert with the Wiskott-Aldrich syndrome protein to promote podosome array organization and chemotaxis in dendritic cells. *J Immunol* 186, 4805-4818.

- del Rio, A., Perez-Jimenez, R., Liu, R., Roca-Cusachs, P., Fernandez, J.M., and Sheetz, M.P. (2009). Stretching single talin rod molecules activates vinculin binding. *Science* *323*, 638-641.
- Delon, J., Bercovici, N., Liblau, R., and Trautmann, A. (1998). Imaging antigen recognition by naive CD4<sup>+</sup> T cells: compulsory cytoskeletal alterations for the triggering of an intracellular calcium response. *Eur J Immunol* *28*, 716-729.
- Delon, J., Kaibuchi, K., and Germain, R.N. (2001). Exclusion of CD43 from the immunological synapse is mediated by phosphorylation-regulated relocation of the cytoskeletal adaptor moesin. *Immunity* *15*, 691-701.
- DeMond, A.L., Mossman, K.D., Starr, T., Dustin, M.L., and Groves, J.T. (2008). T cell receptor microcluster transport through molecular mazes reveals mechanism of translocation. *Biophys J* *94*, 3286-3292.
- Dombroski, D., Houghtling, R.A., Labno, C.M., Precht, P., Takesono, A., Caplen, N.J., Billadeau, D.D., Wange, R.L., Burkhardt, J.K., and Schwartzberg, P.L. (2005). Kinase-independent functions for Itk in TCR-induced regulation of Vav and the actin cytoskeleton. *J Immunol* *174*, 1385-1392.
- Dumont, C., Corsoni-Tadzak, A., Ruf, S., de Boer, J., Williams, A., Turner, M., Kioussis, D., and Tybulewicz, V.L. (2009). Rac GTPases play critical roles in early T-cell development. *Blood* *113*, 3990-3998.
- Dupre, L., Aiuti, A., Trifari, S., Martino, S., Saracco, P., Bordignon, C., and Roncarolo, M.G. (2002). Wiskott-Aldrich syndrome protein regulates lipid raft dynamics during immunological synapse formation. *Immunity* *17*, 157-166.

- Dushek, O. (2011). Elementary steps in T cell receptor triggering. *Frontiers in immunology* 2, 91.
- Dustin, M.L., and Groves, J.T. (2012). Receptor signaling clusters in the immune synapse. *Annu Rev Biophys* 41, 543-556.
- Dustin, M.L., Starr, T., Varma, R., and Thomas, V.K. (2007). Supported planar bilayers for study of the immunological synapse. *Curr Protoc Immunol Chapter 18*, Unit 18 13.
- Evans, R., Lellouch, A.C., Svensson, L., McDowall, A., and Hogg, N. (2011). The integrin LFA-1 signals through ZAP-70 to regulate expression of high-affinity LFA-1 on T lymphocytes. *Blood* 117, 3331-3342.
- Feigelson, S.W., Grabovsky, V., Manevich-Mendelson, E., Pasvolsky, R., Shulman, Z., Shinder, V., Klein, E., Etzioni, A., Aker, M., and Alon, R. (2011). Kindlin-3 is required for the stabilization of TCR-stimulated LFA-1:ICAM-1 bonds critical for lymphocyte arrest and spreading on dendritic cells. *Blood* 117, 7042-7052.
- Feigelson, S.W., Pasvolsky, R., Cemerski, S., Shulman, Z., Grabovsky, V., Ilani, T., Sagiv, A., Lemaitre, F., Laudanna, C., Shaw, A.S., and Alon, R. (2010). Occupancy of lymphocyte LFA-1 by surface-immobilized ICAM-1 is critical for TCR- but not for chemokine-triggered LFA-1 conversion to an open headpiece high-affinity state. *J Immunol* 185, 7394-7404.
- Fooksman, D.R., Vardhana, S., Vasiliver-Shamis, G., Liese, J., Blair, D.A., Waite, J., Sacristan, C., Victora, G.D., Zanin-Zhorov, A., and Dustin, M.L. (2010). Functional anatomy of T cell activation and synapse formation. *Annu Rev Immunol* 28, 79-105.



- Freeley, M., O'Dowd, F., Paul, T., Kashanin, D., Davies, A., Kelleher, D., and Long, A. (2012). L-plastin regulates polarization and migration in chemokine-stimulated human T lymphocytes. *J Immunol* *188*, 6357-6370.
- Freiberg, B.A., Kupfer, H., Maslanik, W., Delli, J., Kappler, J., Zaller, D.M., and Kupfer, A. (2002). Staging and resetting T cell activation in SMACs. *Nature immunology* *3*, 911-917.
- Friedman, R.S., Beemiller, P., Sorensen, C.M., Jacobelli, J., and Krummel, M.F. (2010). Real-time analysis of T cell receptors in naive cells in vitro and in vivo reveals flexibility in synapse and signaling dynamics. *J Exp Med* *207*, 2733-2749.
- Fuller, C.L., Braciale, V.L., and Samelson, L.E. (2003). All roads lead to actin: the intimate relationship between TCR signaling and the cytoskeleton. *Immunol Rev* *191*, 220-236.
- Goksoy, E., Ma, Y.Q., Wang, X., Kong, X., Perera, D., Plow, E.F., and Qin, J. (2008). Structural basis for the autoinhibition of talin in regulating integrin activation. *Mol Cell* *31*, 124-133.
- Gomez, T.S., and Billadeau, D.D. (2008). T cell activation and the cytoskeleton: you can't have one without the other. *Adv Immunol* *97*, 1-64.
- Gomez, T.S., Kumar, K., Medeiros, R.B., Shimizu, Y., Leibson, P.J., and Billadeau, D.D. (2007). Formins regulate the actin-related protein 2/3 complex-independent polarization of the centrosome to the immunological synapse. *Immunity* *26*, 177-190.
- Gomez, T.S., McCarney, S.D., Carrizosa, E., Labno, C.M., Comiskey, E.O., Nolz, J.C., Zhu, P., Freedman, B.D., Clark, M.R., Rawlings, D.J., *et al.* (2006). HS1 functions as

- an essential actin-regulatory adaptor protein at the immune synapse. *Immunity* *24*, 741-752.
- Gonen, R., Beach, D., Ainey, C., and Yablonski, D. (2005). T cell receptor-induced activation of phospholipase C-gamma1 depends on a sequence-independent function of the P-I region of SLP-76. *J Biol Chem* *280*, 8364-8370.
- Gorman, J.A., Babich, A., Dick, C.J., Schoon, R.A., Koenig, A., Gomez, T.S., Burkhardt, J.K., and Billadeau, D.D. (2012). The Cytoskeletal Adaptor Protein IQGAP1 Regulates TCR-Mediated Signaling and Filamentous Actin Dynamics. *J Immunol* *188*, 6135-6144.
- Govern, C.C., Paczosa, M.K., Chakraborty, A.K., and Huseby, E.S. (2010). Fast on-rates allow short dwell time ligands to activate T cells. *Proceedings of the National Academy of Sciences of the United States of America* *107*, 8724-8729.
- Grakoui, A., Bromley, S.K., Sumen, C., Davis, M.M., Shaw, A.S., Allen, P.M., and Dustin, M.L. (1999). The immunological synapse: a molecular machine controlling T cell activation. *Science* *285*, 221-227.
- Grasis, J.A., Browne, C.D., and Tsoukas, C.D. (2003). Inducible T cell tyrosine kinase regulates actin-dependent cytoskeletal events induced by the T cell antigen receptor. *J Immunol* *170*, 3971-3976.
- Grigoriev, I., Gouveia, S.M., van der Vaart, B., Demmers, J., Smyth, J.T., Honnappa, S., Splinter, D., Steinmetz, M.O., Putney, J.W., Jr., Hoogenraad, C.C., and Akhmanova, A. (2008). STIM1 is a MT-plus-end-tracking protein involved in remodeling of the ER. *Curr Biol* *18*, 177-182.

- Gross, C.C., Brzostowski, J.A., Liu, D., and Long, E.O. (2010). Tethering of intercellular adhesion molecule on target cells is required for LFA-1-dependent NK cell adhesion and granule polarization. *Journal of immunology* *185*, 2918-2926.
- Hammer, J.A., 3rd, and Burkhardt, J.K. (2013). Controversy and consensus regarding myosin II function at the immunological synapse. *Curr Opin Immunol*.
- Han, J., Luby-Phelps, K., Das, B., Shu, X., Xia, Y., Mosteller, R.D., Krishna, U.M., Falck, J.R., White, M.A., and Broek, D. (1998). Role of substrates and products of PI 3-kinase in regulating activation of Rac-related guanosine triphosphatases by Vav. *Science* *279*, 558-560.
- Hartgroves, L.C., Lin, J., Langen, H., Zech, T., Weiss, A., and Harder, T. (2003). Synergistic assembly of linker for activation of T cells signaling protein complexes in T cell plasma membrane domains. *J Biol Chem* *278*, 20389-20394.
- Hartman, N.C., Nye, J.A., and Groves, J.T. (2009). Cluster size regulates protein sorting in the immunological synapse. *Proc Natl Acad Sci U S A* *106*, 12729-12734.
- Hashimoto-Tane, A., Yokosuka, T., Sakata-Sogawa, K., Sakuma, M., Ishihara, C., Tokunaga, M., and Saito, T. (2011). Dynein-driven transport of T cell receptor microclusters regulates immune synapse formation and T cell activation. *Immunity* *34*, 919-931.
- Haviv, L., Gillo, D., Backouche, F., and Bernheim-Groswasser, A. (2008). A cytoskeletal demolition worker: myosin II acts as an actin depolymerization agent. *J Mol Biol* *375*, 325-330.

- Heng, T.S., Painter, M.W., and Immunological Genome Project, C. (2008). The Immunological Genome Project: networks of gene expression in immune cells. *Nat Immunol* 9, 1091-1094.
- Higgs, H.N., and Pollard, T.D. (1999). Regulation of actin polymerization by Arp2/3 complex and WASp/Scar proteins. *J Biol Chem* 274, 32531-32534.
- Higgs, H.N., and Pollard, T.D. (2000). Activation by Cdc42 and PIP(2) of Wiskott-Aldrich syndrome protein (WASP) stimulates actin nucleation by Arp2/3 complex. *J Cell Biol* 150, 1311-1320.
- Hirao, M., Sato, N., Kondo, T., Yonemura, S., Monden, M., Sasaki, T., Takai, Y., Tsukita, S., and Tsukita, S. (1996). Regulation mechanism of ERM (ezrin/radixin/moesin) protein/plasma membrane association: possible involvement of phosphatidylinositol turnover and Rho-dependent signaling pathway. *J Cell Biol* 135, 37-51.
- Hirata, H., Tatsumi, H., Lim, C.T., and Sokabe, M. (2014). Force-dependent vinculin binding to talin in live cells: a crucial step in anchoring the actin cytoskeleton to focal adhesions. *American journal of physiology. Cell physiology*.
- Hogg, N., Patzak, I., and Willenbrock, F. (2011). The insider's guide to leukocyte integrin signalling and function. *Nat Rev Immunol* 11, 416-426.
- Hoth, M., Fanger, C.M., and Lewis, R.S. (1997). Mitochondrial regulation of store-operated calcium signaling in T lymphocytes. *J Cell Biol* 137, 633-648.
- Houtman, J.C., Higashimoto, Y., Dimasi, N., Cho, S., Yamaguchi, H., Bowden, B., Regan, C., Malchiodi, E.L., Mariuzza, R., Schuck, P., *et al.* (2004). Binding

- specificity of multiprotein signaling complexes is determined by both cooperative interactions and affinity preferences. *Biochemistry* 43, 4170-4178.
- Houtman, J.C., Yamaguchi, H., Barda-Saad, M., Braiman, A., Bowden, B., Appella, E., Schuck, P., and Samelson, L.E. (2006). Oligomerization of signaling complexes by the multipoint binding of GRB2 to both LAT and SOS1. *Nat Struct Mol Biol* 13, 798-805.
- Hsu, C.J., and Baumgart, T. (2011). Spatial association of signaling proteins and F-actin effects on cluster assembly analyzed via photoactivation localization microscopy in T cells. *PLoS One* 6, e23586.
- Hsu, C.J., Hsieh, W.T., Waldman, A., Clarke, F., Huseby, E.S., Burkhardt, J.K., and Baumgart, T. (2012). Ligand mobility modulates immunological synapse formation and T cell activation. *PLoS One* 7, e32398.
- Huang, J., Zarnitsyna, V.I., Liu, B., Edwards, L.J., Jiang, N., Evavold, B.D., and Zhu, C. (2010). The kinetics of two-dimensional TCR and pMHC interactions determine T-cell responsiveness. *Nature* 464, 932-936.
- Hughes, P.E., Diaz-Gonzalez, F., Leong, L., Wu, C., McDonald, J.A., Shattil, S.J., and Ginsberg, M.H. (1996). Breaking the integrin hinge. A defined structural constraint regulates integrin signaling. *The Journal of biological chemistry* 271, 6571-6574.
- Huppa, J.B., Axmann, M., Mortelmaier, M.A., Lillemeier, B.F., Newell, E.W., Brameshuber, M., Klein, L.O., Schutz, G.J., and Davis, M.M. (2010). TCR-peptide-MHC interactions in situ show accelerated kinetics and increased affinity. *Nature* 463, 963-967.

- Huse, M., Le Floch, A., and Liu, X. (2013). From lipid second-messengers to molecular motors: microtubule-organizing center reorientation in T cells. *Immunological Reviews*.
- Ilani, T., Khanna, C., Zhou, M., Veenstra, T.D., and Bretscher, A. (2007). Immune synapse formation requires ZAP-70 recruitment by ezrin and CD43 removal by moesin. *J Cell Biol* 179, 733-746.
- Ilani, T., Vasiliver-Shamis, G., Vardhana, S., Bretscher, A., and Dustin, M.L. (2009). T cell antigen receptor signaling and immunological synapse stability require myosin IIA. *Nat Immunol* 10, 531-539.
- Irvine, D.J., Purbhoo, M.A., Krogsgaard, M., and Davis, M.M. (2002). Direct observation of ligand recognition by T cells. *Nature* 419, 845-849.
- Jacobelli, J., Chmura, S.A., Buxton, D.B., Davis, M.M., and Krummel, M.F. (2004). A single class II myosin modulates T cell motility and stopping, but not synapse formation. *Nat Immunol* 5, 531-538.
- Jayasundar, J.J., Ju, J.H., He, L., Liu, D., Meilleur, F., Zhao, J., Callaway, D.J., and Bu, Z. (2012). Open conformation of ezrin bound to phosphatidylinositol 4,5-bisphosphate and to F-actin revealed by neutron scattering. *J Biol Chem* 287, 37119-37133.
- Jbireal, J.M., Strell, C., Niggemann, B., Zanker, K., and Entschladen, F. (2010). The selective role of myosin VI in lymphoid leukemia cell migration. *Leuk Res* 34, 1656-1662.

- Johnson, H.W., and Schell, M.J. (2009). Neuronal IP3 3-kinase is an F-actin-bundling protein: role in dendritic targeting and regulation of spine morphology. *Mol Biol Cell* 20, 5166-5180.
- Judokusumo, E., Tabdanov, E., Kumari, S., Dustin, M.L., and Kam, L.C. (2012). Mechanosensing in T lymphocyte activation. *Biophysical journal* 102, L5-7.
- Kaizuka, Y., Douglass, A.D., Varma, R., Dustin, M.L., and Vale, R.D. (2007). Mechanisms for segregating T cell receptor and adhesion molecules during immunological synapse formation in Jurkat T cells. *Proc Natl Acad Sci U S A* 104, 20296-20301.
- Kandula, S., and Abraham, C. (2004). LFA-1 on CD4+ T cells is required for optimal antigen-dependent activation in vivo. *J Immunol* 173, 4443-4451.
- Katagiri, K., and Kinashi, T. (2012). Rap1 and integrin inside-out signaling. *Methods Mol Biol* 757, 279-296.
- Katagiri, K., Maeda, A., Shimonaka, M., and Kinashi, T. (2003). RAPL, a Rap1-binding molecule that mediates Rap1-induced adhesion through spatial regulation of LFA-1. *Nat Immunol* 4, 741-748.
- Kesti, T., Ruppelt, A., Wang, J.H., Liss, M., Wagner, R., Tasken, K., and Saksela, K. (2007). Reciprocal regulation of SH3 and SH2 domain binding via tyrosine phosphorylation of a common site in CD3epsilon. *J Immunol* 179, 878-885.
- Kim, C., Ye, F., and Ginsberg, M.H. (2011). Regulation of integrin activation. *Annual review of cell and developmental biology* 27, 321-345.

- Kim, H.K., Kim, J.W., Zilberstein, A., Margolis, B., Kim, J.G., Schlessinger, J., and Rhee, S.G. (1991). PDGF stimulation of inositol phospholipid hydrolysis requires PLC-gamma 1 phosphorylation on tyrosine residues 783 and 1254. *Cell* 65, 435-441.
- Kim, M., Carman, C.V., and Springer, T.A. (2003). Bidirectional transmembrane signaling by cytoplasmic domain separation in integrins. *Science* 301, 1720-1725.
- Kim, M., Carman, C.V., Yang, W., Salas, A., and Springer, T.A. (2004). The primacy of affinity over clustering in regulation of adhesiveness of the integrin  $\alpha$ L $\beta$ 2. *J Cell Biol* 167, 1241-1253.
- Kim, S.T., Shin, Y., Brazin, K., Mallis, R.J., Sun, Z.Y., Wagner, G., Lang, M.J., and Reinherz, E.L. (2012). TCR Mechanobiology: Torques and Tunable Structures Linked to Early T Cell Signaling. *Frontiers in immunology* 3, 76.
- Kim, S.T., Takeuchi, K., Sun, Z.Y., Touma, M., Castro, C.E., Fahmy, A., Lang, M.J., Wagner, G., and Reinherz, E.L. (2009). The alphabeta T cell receptor is an anisotropic mechanosensor. *J Biol Chem* 284, 31028-31037.
- Kinashi, T. (2005). Intracellular signalling controlling integrin activation in lymphocytes. *Nature reviews. Immunology* 5, 546-559.
- Kong, F., Garcia, A.J., Mould, A.P., Humphries, M.J., and Zhu, C. (2009). Demonstration of catch bonds between an integrin and its ligand. *J Cell Biol* 185, 1275-1284.
- Kong, F., Li, Z., Parks, W.M., Dumbauld, D.W., Garcia, A.J., Mould, A.P., Humphries, M.J., and Zhu, C. (2013). Cyclic mechanical reinforcement of integrin-ligand interactions. *Molecular cell* 49, 1060-1068.



- Kuhne, M.R., Lin, J., Yablonski, D., Mollenauer, M.N., Ehrlich, L.I., Huppa, J., Davis, M.M., and Weiss, A. (2003). Linker for activation of T cells, zeta-associated protein-70, and Src homology 2 domain-containing leukocyte protein-76 are required for TCR-induced microtubule-organizing center polarization. *J Immunol* 171, 860-866.
- Kumari, S., Vardhana, S., Cammer, M., Curado, S., Santos, L., Sheetz, M.P., and Dustin, M.L. (2012). T Lymphocyte Myosin IIA is Required for Maturation of the Immunological Synapse. *Frontiers in immunology* 3, 230.
- Kupfer, A., Dennert, G., and Singer, S.J. (1985). The reorientation of the Golgi apparatus and the microtubule-organizing center in the cytotoxic effector cell is a prerequisite in the lysis of bound target cells. *The Journal of molecular and cellular immunology : JMCI* 2, 37-49.
- Kupfer, A., and Singer, S.J. (1989). Cell biology of cytotoxic and helper T cell functions: immunofluorescence microscopic studies of single cells and cell couples. *Annu Rev Immunol* 7, 309-337.
- Labno, C.M., Lewis, C.M., You, D., Leung, D.W., Takesono, A., Kamberos, N., Seth, A., Finkelstein, L.D., Rosen, M.K., Schwartzberg, P.L., and Burkhardt, J.K. (2003). Itk functions to control actin polymerization at the immune synapse through localized activation of Cdc42 and WASP. *Current Biology* 13, 1619-1624.
- Lasserre, R., and Alcover, A. (2010). Cytoskeletal cross-talk in the control of T cell antigen receptor signaling. *FEBS Lett* 584, 4845-4850.
- Lasserre, R., Charrin, S., Cuche, C., Danckaert, A., Thoulouze, M.I., de Chaumont, F., Duong, T., Perrault, N., Varin-Blank, N., Olivo-Marin, J.C., *et al.* (2010). Ezrin tunes

- T-cell activation by controlling Dlg1 and microtubule positioning at the immunological synapse. *EMBO J*.
- Lee, H.S., Lim, C.J., Puzon-McLaughlin, W., Shattil, S.J., and Ginsberg, M.H. (2009). RIAM activates integrins by linking talin to ras GTPase membrane-targeting sequences. *J Biol Chem* 284, 5119-5127.
- Lee, K.H., Holdorf, A.D., Dustin, M.L., Chan, A.C., Allen, P.M., and Shaw, A.S. (2002). T cell receptor signaling precedes immunological synapse formation. *Science* 295, 1539-1542.
- Li, D., Molldrem, J.J., and Ma, Q. (2009). LFA-1 regulates CD8+ T cell activation via T cell receptor-mediated and LFA-1-mediated Erk1/2 signal pathways. *The Journal of biological chemistry* 284, 21001-21010.
- Li, R., Mitra, N., Gratkowski, H., Vilaire, G., Litvinov, R., Nagasami, C., Weisel, J.W., Lear, J.D., DeGrado, W.F., and Bennett, J.S. (2003). Activation of integrin alphaIIb beta3 by modulation of transmembrane helix associations. *Science* 300, 795-798.
- Li, S.Y., Du, M.J., Wan, Y.J., Lan, B., Liu, Y.H., Yang, Y., Zhang, C.Z., and Cao, Y. (2013). The N-terminal 20-amino acid region of guanine nucleotide exchange factor Vav1 plays a distinguished role in T cell receptor-mediated calcium signaling. *J Biol Chem* 288, 3777-3785.
- Li, Y.C., Chen, B.M., Wu, P.C., Cheng, T.L., Kao, L.S., Tao, M.H., Lieber, A., and Roffler, S.R. (2010). Cutting Edge: mechanical forces acting on T cells immobilized via the TCR complex can trigger TCR signaling. *J Immunol* 184, 5959-5963.

- Liu, S.J., Hahn, W.C., Bierer, B.E., and Golan, D.E. (1995). Intracellular mediators regulate CD2 lateral diffusion and cytoplasmic Ca<sup>2+</sup> mobilization upon CD2-mediated T cell activation. *Biophys J* *68*, 459-470.
- Liu, X., Kapoor, T.M., Chen, J.K., and Huse, M. (2013). Diacylglycerol promotes centrosome polarization in T cells via reciprocal localization of dynein and myosin II. *Proc Natl Acad Sci U S A*.
- Lowin-Kropf, B., Shapiro, V.S., and Weiss, A. (1998). Cytoskeletal polarization of T cells is regulated by an immunoreceptor tyrosine-based activation motif-dependent mechanism. *J Cell Biol* *140*, 861-871.
- Luik, R.M., Wang, B., Prakriya, M., Wu, M.M., and Lewis, R.S. (2008). Oligomerization of STIM1 couples ER calcium depletion to CRAC channel activation. *Nature* *454*, 538-542.
- Luo, B.H., Carman, C.V., Takagi, J., and Springer, T.A. (2005). Disrupting integrin transmembrane domain heterodimerization increases ligand binding affinity, not valency or clustering. *Proceedings of the National Academy of Sciences of the United States of America* *102*, 3679-3684.
- Ma, S., and Chisholm, R.L. (2002). Cytoplasmic dynein-associated structures move bidirectionally in vivo. *J Cell Sci* *115*, 1453-1460.
- Ma, Z., and Finkel, T.H. (2010). T cell receptor triggering by force. *Trends Immunol* *31*, 1-6.
- Ma, Z., Janmey, P.A., and Finkel, T.H. (2008a). The receptor deformation model of TCR triggering. *FASEB J* *22*, 1002-1008.

- Ma, Z., Sharp, K.A., Janmey, P.A., and Finkel, T.H. (2008b). Surface-anchored monomeric agonist pMHCs alone trigger TCR with high sensitivity. *PLoS Biol* 6, e43.
- Marangoni, F., Murooka, T.T., Manzo, T., Kim, E.Y., Carrizosa, E., Elpek, N.M., and Mempel, T.R. (2013). The transcription factor NFAT exhibits signal memory during serial T cell interactions with antigen-presenting cells. *Immunity* 38, 237-249.
- March, M.E., and Long, E.O. (2011). beta2 integrin induces TCRzeta-Syk-phospholipase C-gamma phosphorylation and paxillin-dependent granule polarization in human NK cells. *J Immunol* 186, 2998-3005.
- Margadant, F., Chew, L.L., Hu, X., Yu, H., Bate, N., Zhang, X., and Sheetz, M. (2011). Mechanotransduction in vivo by repeated talin stretch-relaxation events depends upon vinculin. *PLoS biology* 9, e1001223.
- Menasche, G., Kliche, S., Chen, E.J., Stradal, T.E., Schraven, B., and Koretzky, G. (2007). RIAM links the ADAP/SKAP-55 signaling module to Rap1, facilitating T-cell-receptor-mediated integrin activation. *Mol Cell Biol* 27, 4070-4081.
- Millis, B.A. (2012). Evanescent-wave field imaging: an introduction to total internal reflection fluorescence microscopy. *Methods Mol Biol* 823, 295-309.
- Monks, C.R., Freiberg, B.A., Kupfer, H., Sciaky, N., and Kupfer, A. (1998). Three-dimensional segregation of supramolecular activation clusters in T cells. *Nature* 395, 82-86.
- Morin, N.A., Oakes, P.W., Hyun, Y.M., Lee, D., Chin, Y.E., King, M.R., Springer, T.A., Shimaoka, M., Tang, J.X., Reichner, J.S., and Kim, M. (2008). Nonmuscle myosin

- heavy chain IIA mediates integrin LFA-1 de-adhesion during T lymphocyte migration. *J Exp Med* 205, 195-205.
- Morley, C. (2013). The actin-bundling protein L-plastin supports T cell motility and activation. *Immunological Reviews*.
- Moser, M., Legate, K.R., Zent, R., and Fassler, R. (2009). The tail of integrins, talin, and kindlins. *Science* 324, 895-899.
- Mossman, K.D., Campi, G., Groves, J.T., and Dustin, M.L. (2005). Altered TCR signaling from geometrically repatterned immunological synapses. *Science* 310, 1191-1193.
- Mueller, P., Quintana, A., Griesemer, D., Hoth, M., and Pieters, J. (2007). Disruption of the cortical actin cytoskeleton does not affect store operated Ca<sup>2+</sup> channels in human T-cells. *FEBS Lett* 581, 3557-3562.
- Namba, Y., Ito, M., Zu, Y., Shigesada, K., and Maruyama, K. (1992). Human T cell L-plastin bundles actin filaments in a calcium-dependent manner. *J Biochem* 112, 503-507.
- Negulescu, P.A., Shastri, N., and Cahalan, M.D. (1994). Intracellular calcium dependence of gene expression in single T lymphocytes. *Proc Natl Acad Sci U S A* 91, 2873-2877.
- Nguyen, K., Sylvain, N.R., and Bunnell, S.C. (2008). T cell costimulation via the integrin VLA-4 inhibits the actin-dependent centralization of signaling microclusters containing the adaptor SLP-76. *Immunity* 28, 810-821.

- Nishida, N., Xie, C., Shimaoka, M., Cheng, Y., Walz, T., and Springer, T.A. (2006). Activation of leukocyte beta2 integrins by conversion from bent to extended conformations. *Immunity* 25, 583-594.
- Nolz, J.C., Gomez, T.S., Zhu, P., Li, S., Medeiros, R.B., Shimizu, Y., Burkhardt, J.K., Freedman, B.D., and Billadeau, D.D. (2006). The WAVE2 complex regulates actin cytoskeletal reorganization and CRAC-mediated calcium entry during T cell activation. *Curr Biol* 16, 24-34.
- Nolz, J.C., Medeiros, R.B., Mitchell, J.S., Zhu, P., Freedman, B.D., Shimizu, Y., and Billadeau, D.D. (2007). WAVE2 regulates high-affinity integrin binding by recruiting vinculin and talin to the immunological synapse. *Mol Cell Biol* 27, 5986-6000.
- Nolz, J.C., Nacusi, L.P., Segovis, C.M., Medeiros, R.B., Mitchell, J.S., Shimizu, Y., and Billadeau, D.D. (2008). The WAVE2 complex regulates T cell receptor signaling to integrins via Abl- and CrkL-C3G-mediated activation of Rap1. *J Cell Biol* 182, 1231-1244.
- O'Connor, R.S., Hao, X., Shen, K., Bashour, K., Akimova, T., Hancock, W.W., Kam, L.C., and Milone, M.C. (2012). Substrate rigidity regulates human T cell activation and proliferation. *Journal of immunology* 189, 1330-1339.
- Oh-hora, M. (2009). Calcium signaling in the development and function of T-lineage cells. *Immunological Reviews* 231, 210-224.
- Ostergaard, H., and Clark, W.R. (1987). The role of Ca<sup>2+</sup> in activation of mature cytotoxic T lymphocytes for lysis. *J Immunol* 139, 3573-3579.

- Palazzo, A.F., Cook, T.A., Alberts, A.S., and Gundersen, G.G. (2001). mDia mediates Rho-regulated formation and orientation of stable microtubules. *Nat Cell Biol* 3, 723-729.
- Parameswaran, N., Suresh, R., Bal, V., Rath, S., and George, A. (2005). Lack of ICAM-1 on APCs during T cell priming leads to poor generation of central memory cells. *Journal of immunology* 175, 2201-2211.
- Partridge, A.W., Liu, S., Kim, S., Bowie, J.U., and Ginsberg, M.H. (2005). Transmembrane domain helix packing stabilizes integrin alphaIIb beta3 in the low affinity state. *The Journal of biological chemistry* 280, 7294-7300.
- Pathak, D., Sepp, K.J., and Hollenbeck, P.J. (2010). Evidence that myosin activity opposes microtubule-based axonal transport of mitochondria. *The Journal of neuroscience : the official journal of the Society for Neuroscience* 30, 8984-8992.
- Patsoukis, N., Lafuente, E.M., Meraner, P., Kim, J., Dombkowski, D., Li, L., and Boussiotis, V.A. (2009). RIAM regulates the cytoskeletal distribution and activation of PLC-gamma1 in T cells. *Sci Signal* 2, ra79.
- Pauker, M.H., Reicher, B., Fried, S., Perl, O., and Barda-Saad, M. (2011). Functional cooperation between the proteins Nck and ADAP is fundamental for actin reorganization. *Mol Cell Biol* 31, 2653-2666.
- Pelikan-Conchaudron, A., Le Clainche, C., Didry, D., and Carlier, M.F. (2011). The IQGAP1 protein is a calmodulin-regulated barbed end capper of actin filaments: possible implications in its function in cell migration. *J Biol Chem* 286, 35119-35128.
- Peng, G.E., Wilson, S.R., and Weiner, O.D. (2011). A pharmacological cocktail for arresting actin dynamics in living cells. *Mol Biol Cell* 22, 3986-3994.

- Phatak, P.D., and Packman, C.H. (1994). Engagement of the T-cell antigen receptor by anti-CD3 monoclonal antibody causes a rapid increase in lymphocyte F-actin. *J Cell Physiol* *159*, 365-370.
- Pilling, A.D., Horiuchi, D., Lively, C.M., and Saxton, W.M. (2006). Kinesin-1 and Dynein are the primary motors for fast transport of mitochondria in *Drosophila* motor axons. *Mol Biol Cell* *17*, 2057-2068.
- Pollard, T.D., and Berro, J. (2009). Mathematical models and simulations of cellular processes based on actin filaments. *J Biol Chem* *284*, 5433-5437.
- Ponti, A., Machacek, M., Gupton, S.L., Waterman-Storer, C.M., and Danuser, G. (2004). Two distinct actin networks drive the protrusion of migrating cells. *Science* *305*, 1782-1786.
- Porter, J.C., Bracke, M., Smith, A., Davies, D., and Hogg, N. (2002). Signaling through integrin LFA-1 leads to filamentous actin polymerization and remodeling, resulting in enhanced T cell adhesion. *J Immunol* *168*, 6330-6335.
- Quann, E.J., Merino, E., Furuta, T., and Huse, M. (2009). Localized diacylglycerol drives the polarization of the microtubule-organizing center in T cells. *Nature immunology* *10*, 627-635.
- Quintana, A., Kummerow, C., Junker, C., Becherer, U., and Hoth, M. (2009). Morphological changes of T cells following formation of the immunological synapse modulate intracellular calcium signals. *Cell Calcium* *45*, 109-122.
- Raab, M., Wang, H., Lu, Y., Smith, X., Wu, Z., Strebhardt, K., Ladbury, J.E., and Rudd, C.E. (2010). T Cell Receptor "Inside-Out" Pathway via Signaling Module SKAP1-RapL Regulates T Cell Motility and Interactions in Lymph Nodes. *Immunity*.



- Rao, A. (2009). Signaling to gene expression: calcium, calcineurin and NFAT. *Nat Immunol* *10*, 3-5.
- Ratner, S., Sherrod, W.S., and Lichlyter, D. (1997). Microtubule retraction into the uropod and its role in T cell polarization and motility. *J Immunol* *159*, 1063-1067.
- Reicher, B., Joseph, N., David, A., Pauker, M.H., Perl, O., and Barda-Saad, M. (2012). Ubiquitylation-dependent negative regulation of WASp is essential for actin cytoskeleton dynamics. *Mol Cell Biol* *32*, 3153-3163.
- Rizvi, S.A., Neidt, E.M., Cui, J., Feiger, Z., Skau, C.T., Gardel, M.L., Kozmin, S.A., and Kovar, D.R. (2009). Identification and characterization of a small molecule inhibitor of formin-mediated actin assembly. *Chemistry & biology* *16*, 1158-1168.
- Robert, V., Triffaux, E., Savignac, M., and Pelletier, L. (2012). [Calcium signaling in T lymphocytes]. *Medecine sciences : M/S* *28*, 773-779.
- Roumier, A., Olivo-Marin, J.C., Arpin, M., Michel, F., Martin, M., Mangeat, P., Acuto, O., Dautry-Varsat, A., and Alcover, A. (2001). The membrane-microfilament linker ezrin is involved in the formation of the immunological synapse and in T cell activation. *Immunity* *15*, 715-728.
- Rozdzial, M.M., Malissen, B., and Finkel, T.H. (1995). Tyrosine-phosphorylated T cell receptor zeta chain associates with the actin cytoskeleton upon activation of mature T lymphocytes. *Immunity* *3*, 623-633.
- Rozdzial, M.M., Pleiman, C.M., Cambier, J.C., and Finkel, T.H. (1998). pp56Lck mediates TCR zeta-chain binding to the microfilament cytoskeleton. *J Immunol* *161*, 5491-5499.

- Saxton, W.M., and Hollenbeck, P.J. (2012). The axonal transport of mitochondria. *J Cell Sci* 125, 2095-2104.
- Schnyder, T., Castello, A., Feest, C., Harwood, N.E., Oellerich, T., Urlaub, H., Engelke, M., Wienands, J., Bruckbauer, A., and Batista, F.D. (2011). B cell receptor-mediated antigen gathering requires ubiquitin ligase Cbl and adaptors Grb2 and Dok-3 to recruit dynein to the signaling microcluster. *Immunity* 34, 905-918.
- Scholer, A., Hugues, S., Boissonnas, A., Fetler, L., and Amigorena, S. (2008). Intercellular adhesion molecule-1-dependent stable interactions between T cells and dendritic cells determine CD8<sup>+</sup> T cell memory. *Immunity* 28, 258-270.
- Schurpf, T., and Springer, T.A. (2011). Regulation of integrin affinity on cell surfaces. *EMBO J* 30, 4712-4727.
- Schwindling, C., Quintana, A., Krause, E., and Hoth, M. (2010). Mitochondria positioning controls local calcium influx in T cells. *J Immunol* 184, 184-190.
- Sebzda, E., Bracke, M., Tugal, T., Hogg, N., and Cantrell, D.A. (2002). Rap1A positively regulates T cells via integrin activation rather than inhibiting lymphocyte signaling. *Nat Immunol* 3, 251-258.
- Shaffer, M.H., Dupree, R.S., Zhu, P., Saotome, I., Schmidt, R.F., McClatchey, A.I., Freedman, B.D., and Burkhardt, J.K. (2009). Ezrin and moesin function together to promote T cell activation. *J Immunol* 182, 1021-1032.
- Shamri, R., Grabovsky, V., Gauguier, J.M., Feigelson, S., Manevich, E., Kolanus, W., Robinson, M.K., Staunton, D.E., von Andrian, U.H., and Alon, R. (2005). Lymphocyte arrest requires instantaneous induction of an extended LFA-1 conformation mediated by endothelium-bound chemokines. *Nat Immunol* 6, 497-506.

- Shcherbina, A., Bretscher, A., Kenney, D.M., and Remold-O'Donnell, E. (1999). Moesin, the major ERM protein of lymphocytes and platelets, differs from ezrin in its insensitivity to calpain. *FEBS Lett* 443, 31-36.
- Shen, W.W., Frieden, M., and Demaurex, N. (2011). Remodelling of the endoplasmic reticulum during store-operated calcium entry. *Biology of the cell / under the auspices of the European Cell Biology Organization* 103, 365-380.
- Sherman, E., Barr, V., Manley, S., Patterson, G., Balagopalan, L., Akpan, I., Regan, C.K., Merrill, R.K., Sommers, C.L., Lippincott-Schwartz, J., and Samelson, L.E. (2011). Functional Nanoscale Organization of Signaling Molecules Downstream of the T Cell Antigen Receptor. *Immunity*.
- Shimaoka, M., Xiao, T., Liu, J.H., Yang, Y., Dong, Y., Jun, C.D., McCormack, A., Zhang, R., Joachimiak, A., Takagi, J., *et al.* (2003). Structures of the alpha L I domain and its complex with ICAM-1 reveal a shape-shifting pathway for integrin regulation. *Cell* 112, 99-111.
- Simonson, W.T., Franco, S.J., and Huttenlocher, A. (2006). Talin1 regulates TCR-mediated LFA-1 function. *J Immunol* 177, 7707-7714.
- Sims, T.N., Soos, T.J., Xenias, H.S., Dubin-Thaler, B., Hofman, J.M., Waite, J.C., Cameron, T.O., Thomas, V.K., Varma, R., Wiggins, C.H., *et al.* (2007). Opposing effects of PKCtheta and WASp on symmetry breaking and relocation of the immunological synapse. *Cell* 129, 773-785.
- Singleton, K.L., Gosh, M., Dandekar, R.D., Au-Yeung, B.B., Ksionda, O., Tybulewicz, V.L., Altman, A., Fowell, D.J., and Wulfig, C. (2011). Itk controls the spatiotemporal organization of T cell activation. *Sci Signal* 4, ra66.

- Skokos, D., Shakhar, G., Varma, R., Waite, J.C., Cameron, T.O., Lindquist, R.L., Schwickert, T., Nussenzweig, M.C., and Dustin, M.L. (2007). Peptide-MHC potency governs dynamic interactions between T cells and dendritic cells in lymph nodes. *Nat Immunol* 8, 835-844.
- Smirnova, E., Griparic, L., Shurland, D.L., and van der Blik, A.M. (2001). Dynamin-related protein Drp1 is required for mitochondrial division in mammalian cells. *Mol Biol Cell* 12, 2245-2256.
- Smyth, J.T., DeHaven, W.I., Bird, G.S., and Putney, J.W., Jr. (2007). Role of the microtubule cytoskeleton in the function of the store-operated Ca<sup>2+</sup> channel activator STIM1. *J Cell Sci* 120, 3762-3771.
- Smyth, J.T., Dehaven, W.I., Bird, G.S., and Putney, J.W., Jr. (2008). Ca<sup>2+</sup>-store-dependent and -independent reversal of Stim1 localization and function. *J Cell Sci* 121, 762-772.
- Springer, T.A., and Dustin, M.L. (2011). Integrin inside-out signaling and the immunological synapse. *Curr Opin Cell Biol*.
- Springer, T.A., and Dustin, M.L. (2012). Integrin inside-out signaling and the immunological synapse. *Current opinion in cell biology* 24, 107-115.
- Stewart, M.P., McDowall, A., and Hogg, N. (1998). LFA-1-mediated adhesion is regulated by cytoskeletal restraint and by a Ca<sup>2+</sup>-dependent protease, calpain. *J Cell Biol* 140, 699-707.
- Straight, A.F., Cheung, A., Limouze, J., Chen, I., Westwood, N.J., Sellers, J.R., and Mitchison, T.J. (2003). Dissecting temporal and spatial control of cytokinesis with a myosin II Inhibitor. *Science* 299, 1743-1747.

- Sun, Y., Dandekar, R.D., Mao, Y.S., Yin, H.L., and Wulfig, C. (2011). Phosphatidylinositol (4,5) bisphosphate controls T cell activation by regulating T cell rigidity and organization. *PLoS One* 6, e27227.
- Suzuki, J., Yamasaki, S., Wu, J., Koretzky, G.A., and Saito, T. (2007). The actin cloud induced by LFA-1-mediated outside-in signals lowers the threshold for T-cell activation. *Blood* 109, 168-175.
- Sylvain, N.R., Nguyen, K., and Bunnell, S.C. (2011). Vav1-Mediated Scaffolding Interactions Stabilize SLP-76 Microclusters and Contribute to Antigen-Dependent T Cell Responses. *Sci Signal* 4, ra14.
- Tadokoro, S., Shattil, S.J., Eto, K., Tai, V., Liddington, R.C., de Pereda, J.M., Ginsberg, M.H., and Calderwood, D.A. (2003). Talin binding to integrin beta tails: a final common step in integrin activation. *Science* 302, 103-106.
- Takagi, J., Petre, B.M., Walz, T., and Springer, T.A. (2002). Global conformational rearrangements in integrin extracellular domains in outside-in and inside-out signaling. *Cell* 110, 599-511.
- Takahashi, K. (2012). WAVE2 Protein Complex Coupled to Membrane and Microtubules. *Journal of oncology* 2012, 590531.
- Takesono, A., Heasman, S.J., Wojciak-Stothard, B., Garg, R., and Ridley, A.J. (2010). Microtubules regulate migratory polarity through Rho/ROCK signaling in T cells. *PLoS One* 5, e8774.
- Tamada, M., Sheetz, M.P., and Sawada, Y. (2004). Activation of a signaling cascade by cytoskeleton stretch. *Dev Cell* 7, 709-718.

- Tamkun, J.W., DeSimone, D.W., Fonda, D., Patel, R.S., Buck, C., Horwitz, A.F., and Hynes, R.O. (1986). Structure of integrin, a glycoprotein involved in the transmembrane linkage between fibronectin and actin. *Cell* 46, 271-282.
- Terasaki, M., Chen, L.B., and Fujiwara, K. (1986). Microtubules and the endoplasmic reticulum are highly interdependent structures. *Journal of Cell Biology* 103, 1557-1568.
- Thomas, W. (2008). Catch bonds in adhesion. *Annual review of biomedical engineering* 10, 39-57.
- Tseng, S.Y., Liu, M., and Dustin, M.L. (2005). CD80 cytoplasmic domain controls localization of CD28, CTLA-4, and protein kinase C $\theta$  in the immunological synapse. *J Immunol* 175, 7829-7836.
- Turner, M., and Billadeau, D.D. (2002). VAV proteins as signal integrators for multi-subunit immune-recognition receptors. *Nat Rev Immunol* 2, 476-486.
- Tybulewicz, V.L., Ardouin, L., Prisco, A., and Reynolds, L.F. (2003). Vav1: a key signal transducer downstream of the TCR. *Immunol Rev* 192, 42-52.
- Ueda, K., Murata-Hori, M., Tatsuka, M., and Hosoya, H. (2002). Rho-kinase contributes to diphosphorylation of myosin II regulatory light chain in nonmuscle cells. *Oncogene* 21, 5852-5860.
- Valitutti, S., Coombs, D., and Dupre, L. (2010). The space and time frames of T cell activation at the immunological synapse. *FEBS Lett.*
- Valitutti, S., Dessing, M., Aktories, K., Gallati, H., and Lanzavecchia, A. (1995). Sustained signaling leading to T cell activation results from prolonged T cell receptor occupancy. Role of T cell actin cytoskeleton. *J Exp Med* 181, 577-584.

- van der Merwe, P.A., and Dushek, O. (2011). Mechanisms for T cell receptor triggering. *Nat Rev Immunol* *11*, 47-55.
- van Rheenen, J., Song, X., van Roosmalen, W., Cammer, M., Chen, X., Desmarais, V., Yip, S.C., Backer, J.M., Eddy, R.J., and Condeelis, J.S. (2007). EGF-induced PIP2 hydrolysis releases and activates cofilin locally in carcinoma cells. *J Cell Biol* *179*, 1247-1259.
- Van Seventer, G.A., Shimizu, Y., Horgan, K.J., and Shaw, S. (1990). The LFA-1 ligand ICAM-1 provides an important costimulatory signal for T cell receptor-mediated activation of resting T cells. *J Immunol* *144*, 4579-4586.
- Varga, G., Nippe, N., Balkow, S., Peters, T., Wild, M.K., Seeliger, S., Beissert, S., Krummen, M., Roth, J., Sunderkotter, C., and Grabbe, S. (2010). LFA-1 contributes to signal I of T-cell activation and to the production of T(h)1 cytokines. *J Invest Dermatol* *130*, 1005-1012.
- Varma, R., Campi, G., Yokosuka, T., Saito, T., and Dustin, M.L. (2006). T cell receptor-proximal signals are sustained in peripheral microclusters and terminated in the central supramolecular activation cluster. *Immunity* *25*, 117-127.
- Wabnitz, G.H., Lohneis, P., Kirchgessner, H., Jahraus, B., Gottwald, S., Konstandin, M., Klemke, M., and Samstag, Y. (2010). Sustained LFA-1 cluster formation in the immune synapse requires the combined activities of L-plastin and calmodulin. *Eur J Immunol* *40*, 2437-2449.
- Wang, H., Wei, B., Bismuth, G., and Rudd, C.E. (2009). SLP-76-ADAP adaptor module regulates LFA-1 mediated costimulation and T cell motility. *Proc Natl Acad Sci U S A* *106*, 12436-12441.

- Wang, X., and Schwarz, T.L. (2009). The mechanism of Ca<sup>2+</sup>-dependent regulation of kinesin-mediated mitochondrial motility. *Cell* 136, 163-174.
- Watanabe, Y., Sasahara, Y., Ramesh, N., Massaad, M.J., Yeng Looi, C., Kumaki, S., Kure, S., Geha, R.S., and Tsuchiya, S. (2013). T-cell receptor ligation causes Wiskott-Aldrich syndrome protein degradation and F-actin assembly downregulation. *The Journal of allergy and clinical immunology*.
- Waterman-Storer, C.M., Desai, A., Bulinski, J.C., and Salmon, E.D. (1998). Fluorescent speckle microscopy, a method to visualize the dynamics of protein assemblies in living cells. *Curr Biol* 8, 1227-1230.
- Waterman-Storer, C.M., and Salmon, E.D. (1997). Actomyosin-based retrograde flow of microtubules in the lamella of migrating epithelial cells influences microtubule dynamic instability and turnover and is associated with microtubule breakage and treadmilling. *J Cell Biol* 139, 417-434.
- Wei, Q., and Adelstein, R.S. (2000). Conditional expression of a truncated fragment of nonmuscle myosin II-A alters cell shape but not cytokinesis in HeLa cells. *Mol Biol Cell* 11, 3617-3627.
- Wei, S.H., Safrina, O., Yu, Y., Garrod, K.R., Cahalan, M.D., and Parker, I. (2007). Ca<sup>2+</sup> signals in CD4<sup>+</sup> T cells during early contacts with antigen-bearing dendritic cells in lymph node. *J Immunol* 179, 1586-1594.
- Weitz-Schmidt, G., Schurpf, T., and Springer, T.A. (2011). The C-terminal alphaI domain linker as a critical structural element in the conformational activation of alphaI integrins. *J Biol Chem* 286, 42115-42122.



- Wen, Y., Eng, C.H., Schmoranzer, J., Cabrera-Poch, N., Morris, E.J., Chen, M., Wallar, B.J., Alberts, A.S., and Gundersen, G.G. (2004). EB1 and APC bind to mDia to stabilize microtubules downstream of Rho and promote cell migration. *Nat Cell Biol* 6, 820-830.
- Wernimont, S.A., Simonson, W.T., Greer, P.A., Seroogy, C.M., and Huttenlocher, A. (2010). Calpain 4 is not necessary for LFA-1-mediated function in CD4+ T cells. *PLoS One* 5, e10513.
- Wernimont, S.A., Wiemer, A.J., Bennin, D.A., Monkley, S.J., Ludwig, T., Critchley, D.R., and Huttenlocher, A. (2011). Contact-dependent T cell activation and T cell stopping require talin1. *J Immunol* 187, 6256-6267.
- Wilson, C.A., Tsuchida, M.A., Allen, G.M., Barnhart, E.L., Applegate, K.T., Yam, P.T., Ji, L., Keren, K., Danuser, G., and Theriot, J.A. (2010). Myosin II contributes to cell-scale actin network treadmilling through network disassembly. *Nature* 465, 373-377.
- Wulfing, C., and Davis, M.M. (1998). A receptor/cytoskeletal movement triggered by costimulation during T cell activation. *Science* 282, 2266-2269.
- Yablonski, D., Kadlecsek, T., and Weiss, A. (2001). Identification of a phospholipase C-gamma1 (PLC-gamma1) SH3 domain-binding site in SLP-76 required for T-cell receptor-mediated activation of PLC-gamma1 and NFAT. *Mol Cell Biol* 21, 4208-4218.
- Yablonski, D., Kuhne, M.R., Kadlecsek, T., and Weiss, A. (1998). Uncoupling of nonreceptor tyrosine kinases from PLC-gamma1 in an SLP-76-deficient T cell. *Science* 281, 413-416.

- Yam, P.T., Wilson, C.A., Ji, L., Hebert, B., Barnhart, E.L., Dye, N.A., Wiseman, P.W., Danuser, G., and Theriot, J.A. (2007). Actin-myosin network reorganization breaks symmetry at the cell rear to spontaneously initiate polarized cell motility. *J Cell Biol* 178, 1207-1221.
- Yi, J., Wu, X.S., Crites, T., and Hammer, J.A., 3rd (2012). Actin Retrograde Flow and Acto-Myosin II Arc Contraction Drive Receptor Cluster Dynamics at the Immunological Synapse in Jurkat T-Cells. *Mol Biol Cell*.
- Yokosuka, T., Kobayashi, W., Takamatsu, M., Sakata-Sogawa, K., Zeng, H., Hashimoto-Tane, A., Yagita, H., Tokunaga, M., and Saito, T. (2010). Spatiotemporal basis of ctla-4 costimulatory molecule-mediated negative regulation of T cell activation. *Immunity* 33, 326-339.
- Yokosuka, T., and Saito, T. (2010). The immunological synapse, TCR microclusters, and T cell activation. *Current topics in microbiology and immunology* 340, 81-107.
- Yokosuka, T., Sakata-Sogawa, K., Kobayashi, W., Hiroshima, M., Hashimoto-Tane, A., Tokunaga, M., Dustin, M.L., and Saito, T. (2005). Newly generated T cell receptor microclusters initiate and sustain T cell activation by recruitment of Zap70 and SLP-76. *Nat Immunol* 6, 1253-1262.
- Yonezawa, N., Nishida, E., Iida, K., Yahara, I., and Sakai, H. (1990). Inhibition of the interactions of cofilin, destrin, and deoxyribonuclease I with actin by phosphoinositides. *J Biol Chem* 265, 8382-8386.
- Yu, C.H., Wu, H.J., Kaizuka, Y., Vale, R.D., and Groves, J.T. (2010a). Altered actin centripetal retrograde flow in physically restricted immunological synapses. *PLoS One* 5, e11878.

- Yu, H., Leitenberg, D., Li, B., and Flavell, R.A. (2001). Deficiency of small GTPase Rac2 affects T cell activation. *J Exp Med* *194*, 915-926.
- Yu, T., Wu, X., Gupta, K.B., and Kucik, D.F. (2010b). Affinity, lateral mobility, and clustering contribute independently to beta 2-integrin-mediated adhesion. *American journal of physiology. Cell physiology* *299*, C399-410.
- Yu, Y., Fay, N.C., Smoligovets, A.A., Wu, H.J., and Groves, J.T. (2012). Myosin IIA Modulates T Cell Receptor Transport and CasL Phosphorylation during Early Immunological Synapse Formation. *PLoS One* *7*, e30704.
- Yu, Y., Smoligovets, A.A., and Groves, J.T. (2013). Modulation of T cell signaling by the actin cytoskeleton. *J Cell Sci* *126*, 1049-1058.
- Zakaria, S., Gomez, T.S., Savoy, D.N., McAdam, S., Turner, M., Abraham, R.T., and Billadeau, D.D. (2004). Differential regulation of TCR-mediated gene transcription by Vav family members. *J Exp Med* *199*, 429-434.
- Zhang, J., Shehabeldin, A., da Cruz, L.A., Butler, J., Somani, A.K., McGavin, M., Kozieradzki, I., dos Santos, A.O., Nagy, A., Grinstein, S., *et al.* (1999). Antigen receptor-induced activation and cytoskeletal rearrangement are impaired in Wiskott-Aldrich syndrome protein-deficient lymphocytes. *J Exp Med* *190*, 1329-1342.
- Zhao, Y., Zheng, Z., Cohen, C.J., Gattinoni, L., Palmer, D.C., Restifo, N.P., Rosenberg, S.A., and Morgan, R.A. (2006). High-efficiency transfection of primary human and mouse T lymphocytes using RNA electroporation. *Mol Ther* *13*, 151-159.
- Zhou, Z., Yin, J., Dou, Z., Tang, J., Zhang, C., and Cao, Y. (2007). The calponin homology domain of Vav1 associates with calmodulin and is prerequisite to T cell

- antigen receptor-induced calcium release in Jurkat T lymphocytes. *J Biol Chem* 282, 23737-23744.
- Zhu, J., Burakov, A., Rodionov, V., and Mogilner, A. (2010). Finding the cell center by a balance of dynein and myosin pulling and microtubule pushing: a computational study. *Mol Biol Cell* 21, 4418-4427.
- Zhu, J., Carman, C.V., Kim, M., Shimaoka, M., Springer, T.A., and Luo, B.H. (2007). Requirement of alpha and beta subunit transmembrane helix separation for integrin outside-in signaling. *Blood* 110, 2475-2483.
- Zhu, J., Luo, B.H., Xiao, T., Zhang, C., Nishida, N., and Springer, T.A. (2008). Structure of a complete integrin ectodomain in a physiologic resting state and activation and deactivation by applied forces. *Molecular cell* 32, 849-861.
- Zipfel, P.A., Bunnell, S.C., Witherow, D.S., Gu, J.J., Chislock, E.M., Ring, C., and Pendergast, A.M. (2006). Role for the abi/wave protein complex in T cell receptor-mediated proliferation and cytoskeletal remodeling. *Curr Biol* 16, 35-46.